THE UNIVERSITY
of EDINBURGH

Identification and characterization of CENP-A^{Cnp1}-associated proteins in *Schizosaccharomyces pombe*

Puneet Prabhakar Singh

Thesis presented for the Degree of Doctor of Philosophy

The University of Edinburgh

2018

THE UNIVERSITY *of* EDINBURGH

Abstract

Centromeres are chromosomal regions on each chromosome crucial for the assembly of the kinetochore which facilitates the binding of the microtubules and subsequently leads to accurate chromosome segregation during mitosis and meiosis. Centromeres are epigenetically defined by exclusive localization of the centromere-specific histone H3-variant CENP-A. Although centromere sequence is neither necessary nor sufficient for centromere function, centromeres are generally associated with particular sequences. The mechanism by which CENP-A is deposited and inherited exclusively at centromeric chromatin is not fully understood.

Schizosaccharomyces pombe provides an excellent model system to dissect the structure and function of a complex eukaryotic centromere due to its epigenetically regulated centromeres that are structurally related to those of metazoa. The main aim of this thesis was to study the proteome of CENP-A^{Cnp1} chromatin and gain insights into potential role of CENP-A^{Cnp1}-associated proteins in CENP-A^{Cnp1} chromatin establishment and maintenance. Affinity purification and mass spectrometry analysis of GFP-CENP-A^{Cnp1} was used to identify centromeric chromatin-enriched proteins based on their relative abundance in GFP-CENP-A^{Cnp1} compared to mock affinity-purifications. The analysis yielded 199 proteins enriched in centromere chromatin preparations and 23 non-essential proteins were selected for further investigation. Here, I investigate the involvement of Hap2 and Dbl5 in CENP-A^{Cnp1} chromatin establishment and maintenance.

Hap2, an Ino80 complex subunit, is enriched over the CENP-A chromatin and is required to maintain normal nucleosome occupancy at centromeres. Cells lacking the *hap2* gene fail to establish CENP-A^{Cnp1} chromatin on a naïve centromeric sequence and show attenuated transcriptional silencing at centromeres. Surprisingly, loss of different Ino80 complex subunits showed an opposing effect on centromere establishment frequency suggesting that some Ino80 subunits could have different effects on de novo centromere establishment. CENP-A^{Cnp1} is deposited at centromeres in late S/early G2 phase of the cell cycle in a replication-independent manner (Lando et al., 2012; Shukla et al., 2017). Eviction of histone H3 is postulated to provide an opportunity for CENP-A^{Cnp1} nucleosome deposition (Allshire and Karpen,

2008; Shukla et al., 2017). Hap2 is required to promote replication-independent histone H3 turnover at ectopically inserted centromere 2 central domain DNA, endogenous centromeres and other genomic regions; this could explain the loss of centromere establishment and maintenance observed in *hap2*Δ.

In budding yeast, the Psh1 E3 ubiquitin ligase regulates CENP-A^{Cse4} levels. Dbl5 is a Psh1 homolog and thus may also regulate CENP-A^{Cse4} levels via ubiquitin-mediated proteolysis. Deletion of the *dbl5* gene partially suppressed a *cnp1-1* mutant and completely suppressed a *mis6-306* mutant temperature sensitivity suggesting a genetic interaction with this kinetochore component. Overexpression of CENP-A^{Cnp1} causes segregation defects and toxicity in *dbl5*Δ with spreading of CENP-A^{Cnp1} into pericentric outer repeat regions. Similar to budding yeast Psh1, deletion of the *dbl5* gene stabilized CENP-A^{Cnp1} protein levels in vivo suggesting a role in CENP-A^{Cnp1} degradation. In budding yeast, CENP-A^{Cse4} was shown to be ubiquitylated, in a Psh1-dependent manner, and targeted for degradation (Hewawasam et al., 2010; Ranjitkar et al., 2010). Human CENP-A is ubiquitylated on lysine 124 by the CUL4A-RBX1-COPS8 complex which has been proposed to be required for the deposition of CENP-A at centromeres (Niikura et al., 2015). In fission yeast CENP-A^{Cnp1} is ubiquitylated in Dbl5-dependent manner. Mass Spectrometric analysis of affinity selected GFP-CENP-A^{Cnp1} reproducibly detected ubiquitylation of CENP-A^{Cnp1} lysine 4 (K4), however its biological function remains to be determined.

Studying non-kinetochore CENP-A chromatin associated proteins is important for understanding the regulatory mechanisms involved in controlling the dynamics of nucleosome assembly and disassembly at centromeres. It remains to be determined whether, as shown here in *S. pombe*, different Ino80 subunits have opposing roles at metazoan centromeres. Further analysis are required to determine the role of Dbl5 and CENP-A^{Cnp1} K4 ubiquitylation in ensuring normal patterns of CENP-A^{Cnp1} deposition.

Lay Summary

DNA is wrapped around an octamer of two of each of the highly conserved histones H2A, H2B, H3 and H4 to make nucleosomes. Nucleosomes are compacted into a condensed structure called chromatin. The centromere is the specialized DNA sequence on every chromosome where histone H3 is fully/partially replaced with a histone H3 variant called centromere protein A (CENP-A). It has been proposed that eviction of histone H3 provides an opportunity for CENP-A nucleosome deposition. Over last few decades, many approaches have been used to identify proteins associated with centromeres.

This study comprises the first mass spectrometric analysis to identify CENP-A^{Cnp1} chromatin-associated proteins in fission yeast. I have developed a protocol to purify CENP-A^{Cnp1} chromatin complex and the role of centromere-associated proteins in the regulation of centromeres. Using this approach, I identified Hap2 which is required for the establishment and maintenance of CENP-A^{Cnp1} chromatin by regulating the exchange of histone H3 onto the chromatin. I also identified Dbl5 which facilitates modification and subsequent degradation of CENP-A^{Cnp1}. These results suggests that regulation of CENP-A^{Cnp1} chromatin in fission yeast is more complex than anticipated.

Declaration

I declare that this thesis was composed by myself and the research presented is my own, with contributions made by others being clearly indicated. I also declare that this work has not been submitted for any other degree or professional qualification.

Puneet Prabhakar Singh

August 2018

Acknowledgement

I would like to thank Prof. Robin Allshire for giving me the opportunity to come and do my PhD in his lab. I am grateful for his outstanding scientific guidance and constant support throughout these years as well as for giving me the freedom to pursue my own ideas. I thank Dr. Alison Pidoux, Dr. Manu Shukla and Dr. Sharon White for endless advice and teaching me everything I know about fission yeast. I would like to thank both Robin and Alison for reading my thesis. I would also like to thank my PhD committee, Dr. Patrick Heun and Dr. Philipp Voigt for their interest in my work and for sharing their knowledge. I also extend my thanks to Dr. Christos Spanos for his expertise, running the mass spectrometry samples and performing MaxQuant analysis. I am indebted to all the past and present laboratory members for their contributions to my project in terms of both ideas and reagents and for creating a pleasant working atmosphere. I also acknowledge all my friends for their support as I wrote this thesis. And last but not least, to my family in India for their understanding and limitless encouragement.

Table of Contents

Abbreviations

5-FOA	5-fluoro-orotic-acid
ade	adenine
arg	arginine
ATP	adenosine triphosphate
bp	base pair
C-terminal	carboxy terminal
CATD	CENP-A targeting domain
cc	central core
CCAN	Constitutive Centromere Associated Network
CENP	centromere protein
ChIP	chromatin Immunoprecipitation
ChIP-qPCR	ChIP coupled to detection by quantitative real-time PCR
dH20	distilled water
DNA	deoxyribonucleic acid
FACT	facilitates chromatin transcription
GFP	green fluorescent protein
HA	haemagglutinin
HDAC	histone deacetylase
HJURP	Holliday junction recognition protein
HP1	heterochromatin protein 1
IgG	immunoglobulin
imr	inner most repeats

IP	immunoprecipitation
Kb	kilobase
kD	kilodalton
LB	Luria Bertani medium
lox	Lox site
ME	malt extract
MNase	micrococcal nuclease
N-terminal	amino-terminal
nmt	no message in thiamine
ORC	Origin Recognition Complex
otr	outer repeats
PBS	Phosphate buffered saline
PCR	polymerase chain reaction
PMG	pombe media glutamate
RNA	ribonucleic acid
RNAi	RNA interference
RNAPII	RNA polymerase II
rpm	rotation per minute
RT-PCR	reverse transcription polymerase chain reaction
SDS	sodium dodecyl sulphate
sim	silencing in the middle
TBE	tris-borate EDTA
TBZ	thiobendazole
tRNA	transfer RNA

ts	temperature sensitive
Tween	polyoxyethylenesorbitan monolaurate
ura	uracile
wt	wild type
YES	yeast extract supplemeted

List of Figures

List of Tables

Chapter 1

Introduction

Cell division is the process where cells, having grown in size and undergone DNA replication, divide their genetic material evenly into daughter cells. Centromeres are specialized chromatin domains found within each chromosome that provide the foundation for the multi-protein complex called the kinetochore (Westhorpe and Straight, 2014). To faithfully segregate the chromosomes, the kinetochore must attach to spindle microtubules emanating from opposite poles that drive chromosome segregation (Pidoux and Allshire 2000). As centromeres and kinetochores are key requirements for proper segregation, their regulation is essential for cell survival (Kops et al., 2005). Thus, the study of the centromere is essential for understanding the biology of cell division.

1.1 Chromatin organization

The diploid human cell has about 6 billion bases or 2 meters of DNA contained within a nucleus of less than 10 microns in diameter. In order to fit, the DNA is coiled and hierarchically compacted into a condensed nucleoprotein structure called chromatin. At the primary level, the 146 bp DNA is wrapped roughly two times around an octamer of two of each of the highly conserved histones H2A, H2B, H3 and H4 to make nucleosomes (Kornberg, 1974, Arents et al., 1991, Luger et al., 1997 and Luger et al., 1998), the fundamental unit of chromatin. Multiple electrostatic interactions between the negatively charged DNA and positively charged histones stabilizes nucleosome structure (Luger and Richmond, 1998). The coiling of DNA around histones form a 10 nm fiber, which is further compacted to form a 30 nm fiber, which is readily observed in *in vitro* experiments, while its existence *in vivo* remains controversial (Woodcock and Ghosh, 2010, Fusser et al., 2011, Hsieh et al., 2015; Zhu and Li, 2016). Further folding of the chromatin fiber is much more obscure. It has been clear that the plasticity and dynamics of the higher order chromatin structure are important determinants of key biological processes inherent to DNA, including control of transcription, attenuation of DNA damage and chromosome segregation (Kornberg and Lorch, 1992, Li et al., 2007, Li and Reinberg, 2011; Gibcus and Dekker, 2013). However,

chromatinized DNA is much less accessible than its naked form. Therefore, the processes that require direct DNA contacts are associated with mechanisms that locally open up chromatin. Chromatin can exist in a relatively open and relaxed state called euchromatin, or a more compact state called heterochromatin. Euchromatin is gene-rich and generally transcriptionally active in contrast to heterochromatin which is gene poor and mostly transcriptionally repressed (Babu and Verma, 1987; Grewal and Jia, 2007). In recent years, developments in microscopy and high-resolution chromosome conformation capture techniques (3C etc) have led to a detailed view of chromatin into several new subtypes based on DNA epigenetic marks (like methylation), histone variants, histone post-translational modifications (PTMs), and their 3D organization (Bickmore and van Steensel, 2013)

1.2 Centromere structure

The centromere is the specialized DNA sequence on every chromosome which is essential for chromosome segregation. Although the mechanism of chromosome segregation is conserved between species, the structure and composition are quite variable and also the centromeric DNA sequence varies greatly between organisms (Allshire and Karpen, 2008). In most species, centromeric chromatin is fully/partially assembled in histone H3 variant called centromere protein A (CENP-A; Cnp1 in *Schizosaccharomyces pombe*, Cse4 in *Saccharomyces cerevisiae*, CID in *Drosophila melanogaster*). CENP-A nucleosomes form the structural and functional foundation for the kinetochore and are essential for proper chromosome segregation. Interestingly, the stable inheritance of centromere location on the chromosomes suggests a strong reliance on specific DNA sequences. However, only the point centromeres in budding yeasts are specified by specific DNA sequence while such high DNA specificity is not observed in other species. Instead, epigenetic mechanisms are implicated in defining the location for CENP-A assembly and kinetochore formation. As centromeres are essential for cell viability, the reason cells have evolved so many different structural organizations for the centromeres while keeping a similar functional mechanism is an interesting question for centromere biology. As discussed below, centromere organization varies hugely between different species - point centromeres, regional centromeres, and holocentric centromeres (Figure 1.1; Allshire and Karpen, 2008; Henikoff et al., 2001; Steiner and Henikoff, 2015).

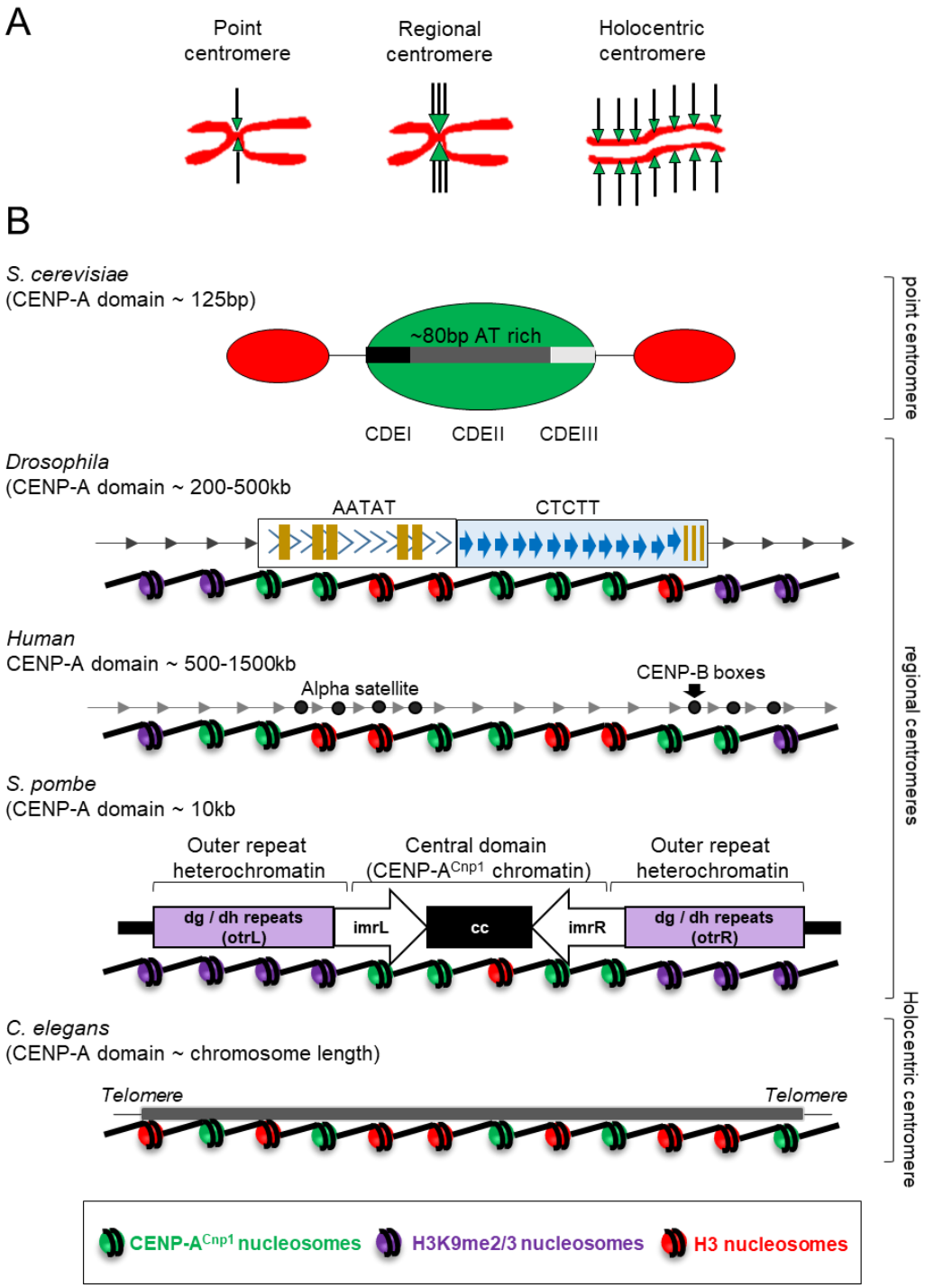

Figure 1.1: Schematic representation of centromere organization

(A) Point centromeres are specified by a consensus DNA sequence and have only a single CENP-A nucleosome at the centromere. Regional centromeres have many CENP-A nucleosomes spread over a region of chromatin rather than a unique consensus DNA sequence. While in holocentric centromeres CENP-A nucleosome are spread along the entire length of the chromosome. (Green – centromere) (B) Organization of centromeric DNA in *Saccharomyces cerevisiae*, *Caenorhabditis elegans*, *Drosophila melanogaster*, *Homo sapiens* and *Schizosaccharomyces pombe* (Adapted from Allshire and Karpen, 2008).

Point centromeres

Centromeres in the budding yeast *Saccharomyces cerevisiae* are specified by 125 bp consensus DNA sequence comprised of three centromeric DNA elements (*CDEI*, *CDEII* and *CDEIII*) which are conserved on each chromosome, over which a single CENP-A nucleosome is assembled (Figure 1.2)(Clark and Carbon, 1985 and Westermann et al., 2007). This 125 bp DNA sequence fragment is sufficient for complete mitotic and meiotic centromere function on circular minichromosomes and also on linear artificial chromosomes (Cottarel et al., 1989). *CDEI* contains an 8 bp recognition site for centromere binding factor 1 (Cbf1) which also functions as a transcription factor (Ohkuni and Kitagawa, 2011). *CDEII* element is an 80 bp AT-rich (~90%) sequence that wraps a single CENP-A^{Cse4} nucleosome (Cse4 is the budding yeast CENP-A homolog). *CDEIII* contains a 25 bp sequence in which the majority of nucleotides are essential for chromosome segregation (McGrew et al., 1986). *CDEIII* is critical for centromere function and serves as a binding site for the Cbf3 complex (Ctf13p, Skp1p, Cep3p and Cbf2p). Mutations in *CDEIII* abolish Cbf3 binding and centromere function (Lechner and Carbon 1991). The Ctf19 complex (Ctf19p, Mcm21p and Okp1p) binds the Cbf3 complex and the Ndc80 complex (Ndc80p, Spc24p, Spc25p, and Nuf2p). The interaction with a single microtubule is mediated by the Dam1 complex which interacts with Ctf3 complex and Ndc80 complex (Cheeseman et al., 2002).

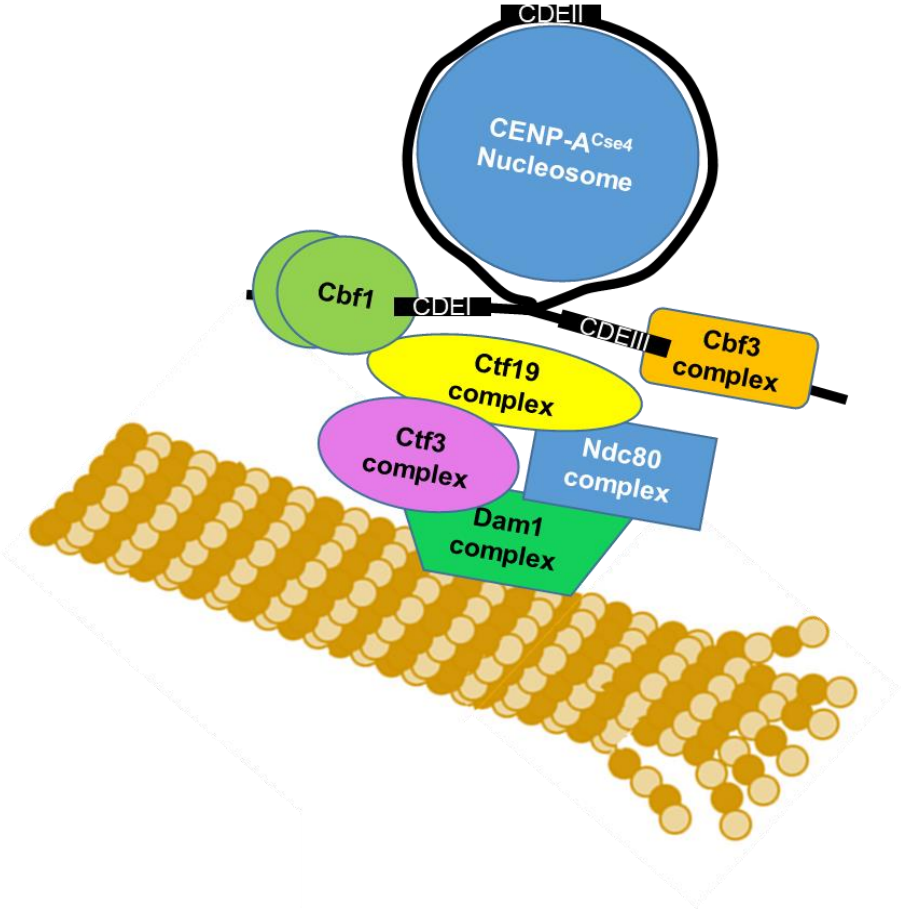

Figure 1.2: Schematic representation of budding yeast centromere

Budding yeast (*S. cerevisiae*) has point centromeres, wherein centromeres are genetically specified by a conserved 125 bp DNA sequence.

Regional centromeres

Regional centromeres are the most common type of centromeres present in many model / highly-studied organisms: *Drosophila, Human*, fission yeast, etc (Figure 1.1)

Drosophila melanogaster: Centromeres are formed upon 420 kb highly AT-rich repeats composed of 85% of AATAT and AAGAG satellites with about 10% of interspersed transposable elements that are not necessarily specific for the centromeres (Sun et al., 1997). Interestingly, AATAT and AAGAG repeats can be found throughout the genome and on their own are incapable of inducing centromere formation. Centromeres are composed of interspersed blocks of CENP-A (CID in *D.*

melanogaster) and histone H3. Overexpression of CENP-A^{CID} leads to mislocalization of CENP-A^{CID} on chromosome arms, thereby forming multicentric chromosomes and causing segregation defects (Heun et al., 2006). Tethering CENP-A^{CID} via CID-GFP-LacI fusion protein to stably integrated *lac* operator (*lacO*) arrays leads to assembly of an ectopic functional kinetochore that allows epigenetic inheritance of centric chromatin even after removal of tethering (Mendiburo et al., 2011). These observations show that CENP-A^{CID} is necessary and sufficient for centromere specification and behaves as a self-propagating epigenetic mark for centromere identity.

Human: Centromeres are composed of ~171 bp highly AT-rich α-satellite tandem repeats. These α-satellite repeats can extend for 3-5 Mb with several long interspersed elements (LINE), short interspersed elements (SINE) and long terminal repeat retrotransposons (LTR) within the same centromere. At almost all centromeres, CENP-B boxes are present within (some) alpha-satellite sequences; CENP-B boxes are recognized by DNA binding centromere protein B (CENP-B). However, insertion of α-satellite at an ectopic locus is not sufficient to drive centromere formation. Interestingly, *de novo* formation of a functional centromere on a human artificial chromosome requires α-satellite repeats that contain CENP-B boxes (Okada et al., 2007). Centromeres are composed of interspersed blocks of CENP-A and histone H3 (Sullivan and Karpen, 2001).

Fission yeast: Regional centromeres with domains of heterochromatin and CENP-A. See section 1.3.

Holocentric centromeres

The nematode *Caenorhabditis elegans* is the most well-studied holocentric organism, wherein kinetochores and microtubule attachments are located at many sites along the entire length of their chromosomes. They also lack the primary constriction in their metaphase chromosomes which is readily observed in monocentric species. Holocentric chromosome are known to have evolved independently at least four times in plants and nine times in animals (Melters et al., 2012). Despite the vast differences in the centromere organization, kinetochore composition remains similar to that in monocentric organisms. CENP-A (HCP-3 in *C. elegans*) localizes along the entire length of the chromosome, occupying about 50% of the genome (Gassmann et al.,

2012). Interestingly, DNA injected into *C. elegans* germline assembles *de novo* centromeres at high frequencies and can autonomously segregate during cell division in a heterochromatin protein 1 (HP1)–independent manner (Yuen et al., 2011).

Unconventional centromeres

In many insect lineages, there are independent transitions from monocentricity to holocentricity with loss of CENP-A and some inner/outer kinetochore proteins (Drinnenberg et al., 2014). Similarly, many kinetoplastid species have been discovered lacking CENP-A, like *Trypanosoma brucei*, *Trypanosoma cruzi*, *Leishmania* species and *Bodo saltans*. *T. brucei* is among the well-studied kinetoplastid species. Interestingly, as well as lacking CENP-A, no conventional kinetochore proteins have been identified to date (reviewed in Akiyoshi and Gull, 2013). The kinetochore-like structure has been observed in *T. brucei* by transmission electron microscopy (Ogbadoyi et al., 2000). Therefore, it is very intriguing how *T. brucei* form kinetochore structures despite the absence of CENP-A homolog. 19 kinetochore proteins have been identified, KKT1 was first identified by microscopy and KKT2-19 by its association with KKT1 using mass spectrometry (Akiyoshi and Gull, 2014). Therefore, these species may have evolved a completely novel way to define centromere identity.

1.3 *Schizosaccharomyces pombe* centromeres

The fission yeast, *Schizosaccharomyces pombe*, is an excellent model organism for studying chromosome/centromere structure and function due to its small genome (13.8 Mb) with only three chromosomes (chromosome I is 5.7 Mb, chromosome II is 4.6 Mb and chromosome III is 3.5 Mb) but still possess large and complex regional centromeres ~35-115 kb in size, whose chromatin/protein composition and structural organization has similarities to those of higher eukaryotes, including humans. *S. pombe* centromeres are composed of two main domains: a central domain with two inverted innermost repeat region (*imr*) that surrounds an AT-rich non-repetitive central core sequence (*cc/cnt*) and flanking outer repeat regions (*otr*). *Imr* repeats are unique to each centromere while all centromeres share *otr* repeats elements that are composed of several *dg* repeats (~4.4 kb) and *dh* repeats (~4.8 kb). CENP-A^{Cnp1} nucleosomes are assembled on the central domain which is associated with the kinetochore proteins while the flanking *otr* repeats are embedded in heterochromatin marked with methylation of histone H3 on lysine K9 (H3K9me), directed by RNA

interference (RNAi) machinery and associated with heterochromatin proteins, such as $HP1^{Swi6}$ and Chp1. RNAi triggers initial recruitment of Clr4 and heterochromatin on outer repeats and is absolutely required for heterochromatin nucleation. However, RNAi is dispensable for the maintenance of heterochromatin on centromeric outer repeats (Buscaino et al., 2013). Centromeric heterochromatin is essential for the recruitment of cohesin over the outer repeats and accurate chromosome segregation (Bernard et al., 2001). Adjacent heterochromatin has also been shown to promote CENP-A^{Cnp1} establishment on naïve central domain DNA to form functional centromeres (Folco et al., 2008; Kagansky et al., 2009)

The two domains are separated by tRNA boundary elements with one or more tRNA genes within *imr* repeats, between different types of chromatin: CENP-A^{Cnp1} chromatin and heterochromatin. tRNA gene clusters that act as boundaries to prevent heterochromatin from spreading (Scott et al., 2006). The kinetochore is assembled onto the central domain chromatin (CENP-A^{Cnp1} chromatin), that bind 2-4 microtubules during cell division (Pidoux and Allshire, 2004) (Figure 1.3).

1.4 Kinetochore architecture and assembly

The kinetochore is the large multi-protein complex that is assembled on centromeric DNA. Despite the differences in centromeric DNA sequences, the divergent N-terminal tail of CENP-A, centromere organization, and kinetochore structure, many kinetochore and centromere proteins are conserved (Malik and Henikoff, 2009). In addition to its structural role, kinetochore also serves an important regulatory role by recruiting spindle assembly checkpoint (SAC) proteins, a surveillance pathway, to delay exit from mitosis upon detection of improper kinetochore-microtubule attachments. Kinetochore can be divided into inner kinetochore and outer kinetochore by conventional electron microscopy.

Inner Kinetochore

The inner kinetochore mediates the direct connection between the kinetochore and the chromosomal DNA. The site of attachment for microtubules on each chromosome is defined by the presence of CENP-A nucleosomes. Interestingly, ectopic deposition of CENP-A by tethering HJURP/CAL1, CENP-C, CENP-I or CENP-T, at a noncentromeric locus leads to assembly of fully functional kinetochores with constitutive centromere-associated network (CCAN) proteins, Ndc80 complex and

stable kinetochore-microtubule attachments (Barnhart et al., 2011; Hori et al., 2013; Chen et al., 2014). Downstream of CENP-A, functional kinetochores require CCAN proteins (Figure 1.4). Many CCAN proteins were originally identified by affinity purification of CENP-K^{Sim4} from *S. pombe* (Liu et al., 2005) and in a subsequent study affinity purification with CENP-A containing nucleosomes from HeLa cells (Foltz et al., 2006) shows that the CCAN complex is conserved. The CCAN is composed of 16 proteins in vertebrates (grouped into five sub-units: CENP-C, CENP-L/N, CENP-O/P/Q/R/U, CENP-H/I/K/M and CENP-S/T/X/W), form the base of the kinetochore linking CENP-A to the outer kinetochore complex (Pesenti et al., 2018).

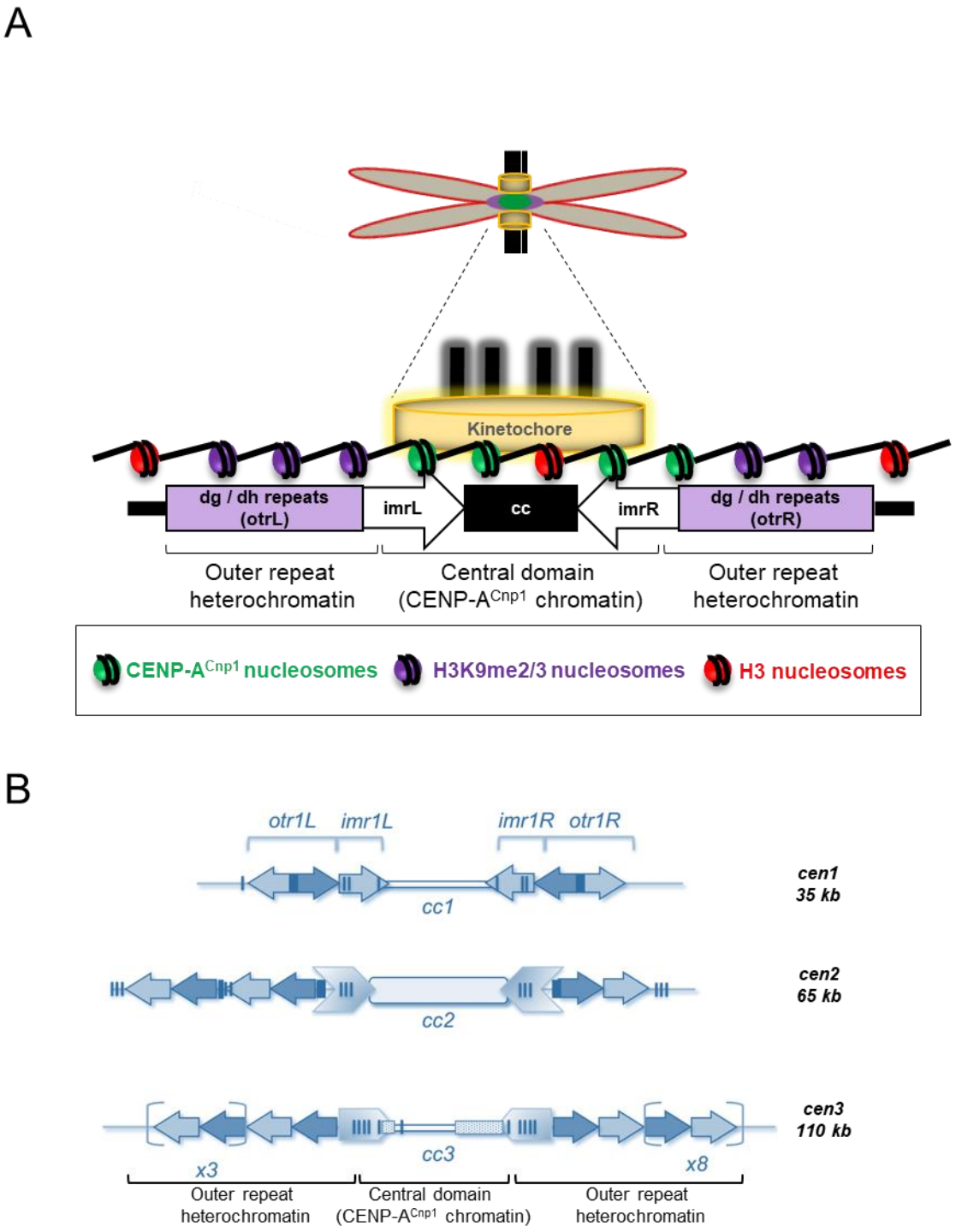

Figure 1.3: Fission yeast centromere
(A) Schematic representation of the fission yeast centromere with central domain and flanking heterochromatin. (B) DNA structure of fission yeast centromeres (adapted from Pidoux and Allshire, 2004). See section 1.3 for more details.

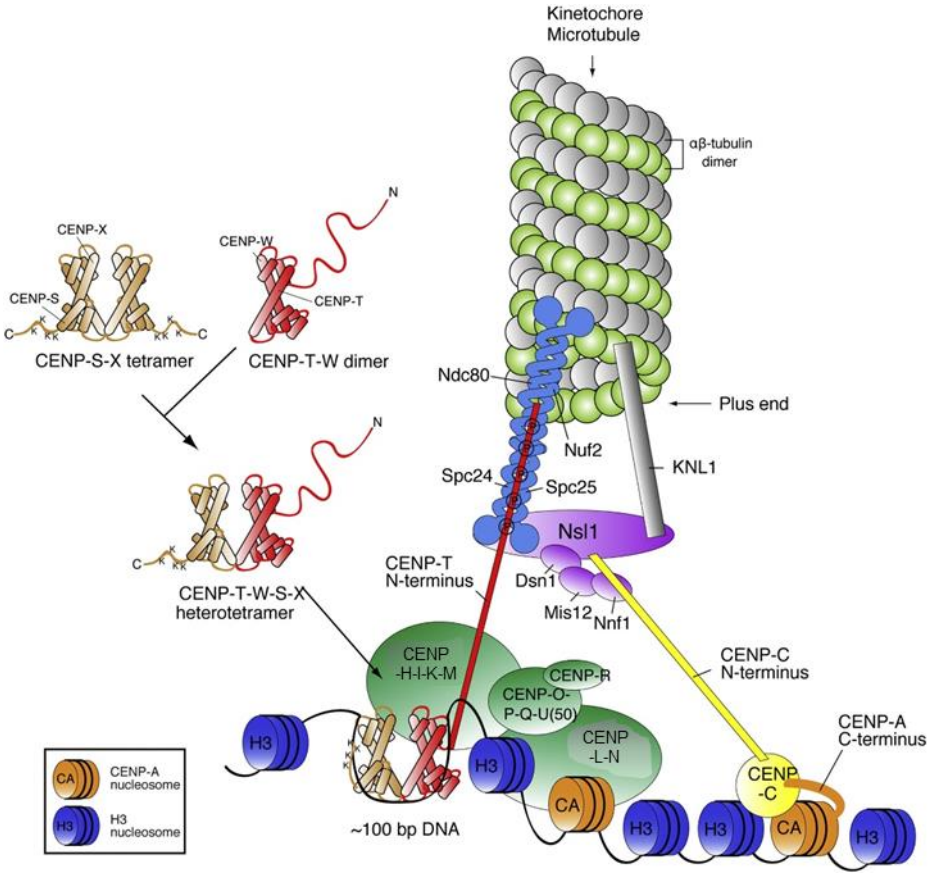

Figure 1.4: Molecular architecture of the vertebrate kinetochore

Schematic representation of the associations of the kinetochore proteins (adapted from Takeuchi and Fukagawa, 2015). See section 1.4 for more details.

CENP-A

CENP-A (centromere protein A; also known as Cnp1 in fission yeast) is an evolutionarily conserved, centromere-specific 17 kD protein, with 60% identity to histone H3, which localize to active centromeres constitutively throughout the cell cycle (Palmer et al., 1991; Sullivan et al., 1994; Warburton et al., 1997). It was first identified as an antigen for anti-centromere autoantibodies (ACA) serum along with CENP-B and CENP-C, from patients with CREST syndrome (Earnshaw and Rothfield, 1985). Inactivation or depletion of CENP-A in most organisms causes chromosome segregation defects. CENP-A null mice exhibit early embryonic lethality, demonstrating that the gene is essential in mammals (Howman et al., 2000) while CENP-A overexpression in *Drosophila* results in induction of ectopic kinetochores (Heun et al., 2006). Despite being an evolutionarily conserved protein, the N terminal

tail (from 20 to 200 amino acids) of CENP-A is highly divergent both in length and amino acid composition, suggesting an organism-specific evolution of CENP-A, CENP-A interacting proteins, centromere sequence and centromere drive (Malik and Henikoff, 2002; Henikoff and Dalal, 2005). Post deposition of CENP-A, additional proteins are recruited to the centromere to form kinetochore. Functional kinetochores require assembly of CCAN/inner kinetochore onto CENP-A nucleosomes. CENP-C and CENP-N binds specifically to CENP-A nucleosomes at different binding sites on CENP-A nucleosomes (Carroll et al., 2009; Carroll et al., 2010). Interestingly, artificial tethering of CENP-A to ectopic locus using LacO/LacI system results in recruitment of CENP-C and CENP-T (Tachiwana et al., 2015).

CENP-C

Using immunoelectron microscopy, CENP-C was first localized in the inner kinetochore plate within human mitotic chromosomes (Saitoh et al., 1992). CENP-C localizes to the centromere via a 60 amino-acid domain and can bind DNA non-specifically (Sugimoto et al., 1994; Yang et al., 1996). CENP-C forms the structural platform for kinetochore assembly and bridges the centromeric chromatin and the microtubules. CENP-C sequence is mostly intrinsically disordered with conserved domains: N-terminal Mis12 binding site, central region and CENP-C motif for CENP-A nucleosome binding and a C terminal region for CENP-C dimerization (Przewloka et al., 2011; Screpanti et al., 2011; Kato et al., 2013; Klare et al, 2015). Interestingly, ectopic targeting of the CENP-C N terminus (1-643 aa) efficiently formed functional kinetochores with KMN network proteins but lacking CCAN proteins (Hori et al, 2013). Disruption of the CENP-C gene results in cell death due to chromosome missegregation and metaphase arrest, while overexpression of CENP-C disrupts mitosis but does not disrupt native centromeres and does not lead to ectopic centromere formation (Fukagawa et al., 1999). Depletion of CENP-C by siRNA abolishes localization of the CCAN to the centromere, and also leads to reduction in the overall levels of CENP-A in the cell and at the centromere (Carroll et al., 2010; Klare et al., 2015). Interestingly, tethering CENP-C to ectopic locus using the LacO/LacI system results in CENP-A-independent kinetochore assembly (Gascoigne et al., 2011). CENP-C binding to HJURP (CENP-A-specific chromatin assembly factor) is required for *de novo* accumulation to CENP-C at synthetic centromeres (Tachiwana et al., 2015). CENP-C binding to CENP-A is required for stability of

centromeric chromatin (Falk et al., 2015). CENP-C interacts with CENP-HKIM via the PEST-sequence-rich region of CENP-C, and *in vitro* localization of CENP-HIKM is dependent on CENP-C (Klare et al., 2015). Cross-linking Mass Spectrometry (XL-MS) revealed a network, with CENP-C contacting CENP-CHIKMLN, histone H4 and histone H2B but not histone H2A; thus emerging as an important kinetochore protein (Weir et al., 2015). In fission yeast, the N-terminal minimal region (26-50 amino acid) of CENP-C is required for Mis12C binding and phosphorylation of Thr28 by aurora-B kinase Ark1 disrupts this interaction, leading to reduced Mis12 localization at the kinetochore (Zhou et al., 2017). Interestingly, Cnp3 (CENP-C orthologue) is not essential in fission yeast, suggesting a different architectural programming of the kinetochore.

CENP-LN

CENP-L and CENP-N were identified as CENP-A-associated proteins in human cells (Obuse et al. 2004; Foltz et al. 2006). CENP-N has been shown to interact directly with CENP-A nucleosomes. Depletion of CENP-N by siRNA leads to decreased binding of CENP-ACHIK to the centromere and caused a reduction in overall CENP-A levels in the cells (Carroll et al., 2009). Both CENP-L and CENP-N interact with CENP-C (McKinley et al., 2015). Moreover, *in vitro* CENP-LN preferentially binds octameric CENP-A nucleosome core particles over histone H3 nucleosome core particles (Weir et al., 2016). CENP-C interacts with CENP-LN and CENP-HIKM, independently (McKinley et al., 2015; Weir et al., 2016).

CENP-OPQRU

CENP-OPQRU forms a discrete stable complex and is not required for the cell viability under normal conditions, although knockout cells (except CENP-R) do have a slow proliferation rate and deficiency in recovering from spindle damage (Hori el al., 2008). CENP-OPQU proteins are conserved in budding and fission yeast (with no apparent CENP-R orthologue) but, in contrast to vertebrates, they are essential in these species. CENP-OP-deficient cells have no defects in localization of CENP-HIKM to the centromere while deficiency of CENP-HIKM abolishes centromeric localization of CENP-HIKM and CENP-OP (Okada et al., 2006), suggesting localization of CENP-OPQRU at the centromere occurs downstream of CENP-HKIM. Interestingly, CENP-

U can interact with Hec1 (a component of Ndc80 complex) *in vitro* and *in vivo* and is required for proper kinetochore-microtubule attachments (Hua et al., 2011).

CENP-HIKM

CENP-H and CENP-K forms a dimer and interacts with CENP-I and this interaction is stabilized by CENP-M (Hoischen et al., 2018; Okada et al., 2006; Basilico et al., 2014). Like CENP-A and CENP-C, CENP-H is only detected at the active centromeres in stable dicentric chromosomes (Sugata et al., 2000). Depletion of CENP-H results in mislocalization of CENP-C at the centromere but not CENP-A (Fukagawa et al., 2001). While depletion of CENP-I results in prometaphase block and diffuse CENP-C and CENP-H (Nishihashi et al., 2002) localisation. CENP-M is a pseudo GTPase but its function at the centromeres remains unknown. Depletion of CENP-M leads to delocalization of CENP-TW and Ndc80 from the centromere, while CENP-C localization remains unperturbed (Basilico et al., 2014). In fission yeast, CENP-I^{Mis6} is required for CENP-K^{Sim4} kinetochore localization (Pidoux et al., 2003)

CENP-TWSX

CENP-TWSX proteins have histone-fold domains associates to form a stable heterotetramer with DNA binding activity. CENP-TWSX binds ~100 bp of DNA compared to the canonical histone octamer which binds ~147 bp of DNA. CENP-TWSX bends DNA to form nucleosome-like structure (Nishino et al., 2012). CENP-T and CENP-W are essential proteins while CENP-S and CENP-X are dispensable. The CENP-T C-terminus is essential for its kinetochore localization while its N-terminus directly binds to Ndc80 which is critical for microtubule associations of the outer kinetochore (Gascoigne et al., 2011; Takeuchi et al., 2014). CENP-TW associates with nucleosomal DNA and histone H3 but not with CENP-A nucleosomes. In CENP-W-deficient cells, kinetochore localization of CCAN proteins are abolished except CENP-C, while CENP-H depletion does not affect localization of CENP-TW. Therefore, the CENP-TW complex functions upstream of the CCAN complex except CENP-C (Hori et al., 2008). However, CENP-TW localization to the centromere depends on CENP-C (Klare et al., 2015). Tethering of CENP-T to an ectopic locus using the LacO/LacI system results in CENP-A- and CENP-C-independent kinetochore assembly (Gascoigne et al., 2011).

Outer Kinetochore

The outer kinetochore is a proteinaceous structure devoid of any detectable DNA by electron microscopy (Cooke et al., 1993). The outer kinetochore KMN network (KNL1/Mis12 complex/Ndc80 complex) acts as a microtubule binding interface at kinetochores (Cheeseman et al., 2006). In *S. pombe*, the equivalent complex is called the NMS (Ndc80-MIND-Spc7) complex (Liu et al., 2005). In *S. pombe*, the NMS complex remains associated with centromeres throughout the cell cycle (Hayashi et al., 2006; Liu et al., 2005; Pidoux et al., 2003). The Ndc80 complex contains: Ndc80/Hec1, Nuf2, Spc24, and Spc25, and the Mis12 complex contains: Mtw1/Mis12, Dsn1/Mis13, Nsl1/Mis14, and Nnf1. In humans, depletion of Dsn1 results in reduced levels of CENP-A and CENP-H at centromeres, suggesting that the complex may contribute to inner kinetochore assembly (Kline et al., 2006). The Mis12 complex is required for mediating proper attachments between kinetochores and microtubules (Kline et al., 2006; Pinsky et al., 2003). Mis12 has been shown to associate with the N terminus of CENP-C (Milks et al., 2009; Gascoigne et al., 2011; Zhou et al., 2017). The Mis12 complex also interacts directly with the C-terminal domain of KNL1 and associates with the Ndc80 complex via the C-terminus of Nsl1 *in vitro* (Petrovic et al., 2010). In *Drosophila*, Ndc80 requires Mis12 and Nsl1 for localization to centromeres (Venkei et al., 2011). In humans, the Mis12 complex has been shown to be recruited at endogenous centromeres by CENP-T (Rago et al., 2015). Thus, CENP-C and CENP-T mediate interactions between the inner kinetochore and the outer kinetochore.

Stoichiometry of Kinetochore Subunits

In *S. cerevisiae*, EM and electron tomography of negatively-stained preparations of budding yeast kinetochore particles were radially surrounded by 5 to 7 globular domains, which possibly represents a single KMS network (Gonen et al., 2012). Biochemical reconstitutions suggest that there are two CENP-CHIKMLN complexes per CENP-A nucleosome in humans (Weir et al., 2016). Lacking from the reconstitution were the CENP-TWSX complex and the CENP-OPQRU complex (Weir et al., 2016). CENP-C and CENP-T act in parallel with two full KMN complexes and CENP-T can recruit two additional NDC80 complexes in CDK1-dependent manner that involves interaction with phosphorylated threonine 11 and threonine 85 (Huis et

al., 2016; Suzuki et al., 2015). Therefore, the current model of human kinetochores consist of two copies of CENP-C and CENP-T associated with a CENP-A nucleosome and they can recruit four Mis12, four KNL1 and eight NDC80 complexes (Figure 1.5). CENP-OPQUR is proposed to self-assemble on kinetochores with varying stoichiometry (Eskat et al., 2012).

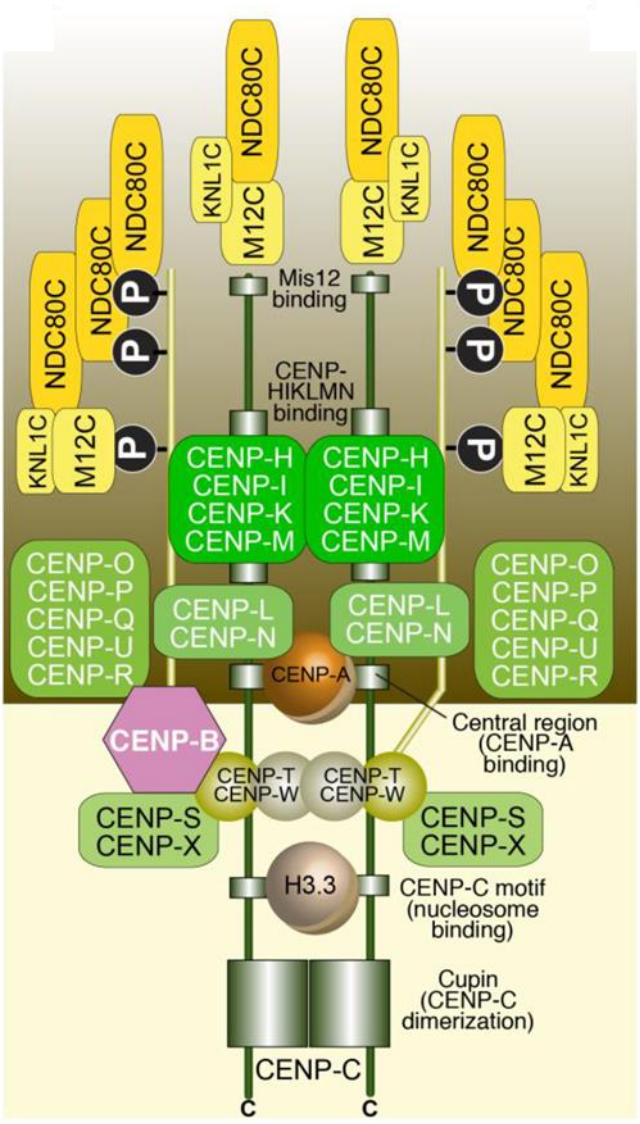

Figure 1.5: Model for the assembly of human kinetochore

Each CENP-A nucleosome has the potential to interact with two CCAN complexes. Both CENP-C and CENP-T each carry two full KMN networks. In addition, CENP-T can recruit two NDC80 complexes. Hence each CENP-A nucleosome is capable of binding to eight NDC80 complexes (adapted from Musacchio and Desai, 2017).

1.5 Epigenetic regulation of centromeres

Understanding how CENP-A is assembled and maintained only at centromeres is of great relevance in centromere biology. In many organisms, centromeres are assembled on preferred sequences (Allshire and Karpen, 2008). Therefore, in early centromere research the concept of a relationship between the centromere DNA and centromere formation was proposed. This idea was redefined after the discovery of mardel(10) chromosome which completely lacks centromeric DNA and possesses a neocentromere capable of normal kinetochore assembly and function (Voullaire et al., 1993). Since then neocentromeres have been found or induced in human, chicken, horse, orang-utan, potato, *Candida albicans* and *S. pombe* chromosomes (Warburton et al., 1997; Shang et al., 2010; Wade et al., 2009; Locke et al., 2011; Gong et al., 2012; Ketel et al., 2009; Ishii et al., 2008). The fact that kinetochores can form on non-centromeric DNA sequence provides support for the epigenetic nature of centromeres. Human CENP-A can associate with neocentromeres lacking any detectable α-satellite DNA, while α-satellite-rich inactive centromeres of dicentric chromosomes lack CENP-A (Warburton et al., 1997). In *C. albicans*, the deletion of *CEN5* does not affect cell growth due to highly efficient neocentromere formation (Ketel et al., 2009). In comparison, in *S. pombe*, the frequency of cells surviving after the deletion of a centromere is very low and the rescue is due to either telomere fusion or neocentromere formation exclusively at the subtelomeric regions (Ishii et al., 2008). Neocentromere formation on non-centromeric DNA indicates that it is CENP-A and not the DNA sequence that regulates the place where centromeres are formed and supports the idea that CENP-A is an epigenetic mark for specification of active centromeres.

In general the centromere DNA is neither necessary nor sufficient for centromere identity and centromere specification is controlled by epigenetic mechanisms (Karpen & Allshire, 1997; Allshire and Karpen, 2008; Westhorpe and Straight, 2014). Centromere formation is also epigenetically regulated in fission yeast. Transformation of plasmid-borne minichromosomes containing portions of centromere DNA adopt either a mitotically stable or unstable segregation states by stochastic establishment of centromere function (Steiner and Clarke, 1994). In *S. pombe*, a forced recombination between two non-homologous chromosomes to induce dicentric chromosome formation that are stabilized by epigenetic inactivation of one of the

centromeres (Sato et al., 2012). CENP-A is only localized at active centromere in human and *Drosophila* dicentric chromosomes (Earnshaw and Migeon, 1985; Earnshaw et al., 1989; Agudo et al., 2000).

Artificial tethering of CENP-A, CENP-C, CENP-T, CENP-I or the CENP-A-specific chaperones, HJURP and CAL1 in vertebrates and *Drosophila* respectively, at non-centromeric loci is sufficient to assemble a functional kinetochore capable of microtubule attachments (Barnhart et al., 2011; Mendiburo et al., 2011; Hori et al., 2013; Chen et al., 2014; Barrey and Heun, 2017). These tethering experiments combined with neocentromere formation and centromere inactivation of one of the centromere in dicentric chromosomes provide evidence that CENP-A is an epigenetic mark for centromere specification independent of DNA sequence.

1.6 CENP-A assembly

During replication of DNA in S phase, histones from the parental strand are randomly divided between the two daughter strands. This process is directly coupled with the replication-dependent incorporation of canonical H3 and H3.3 nucleosomes (Ahmad and Henikoff, 2002; Choi et al., 2005; Dunleavy et al., 2011). The deposition of CENP-A at centromeres occurs during specific phases of the cell cycle which varies between organisms, cell types and developmental stages (Figure 1.6). In human cells, SNAP-tag–based pulse labeling experiments demonstrated incorporation of new CENP-A nucleosomes during late telophase/early G1 (Jansen et al., 2007). Similar cell-cycle timing of CENP-A incorporation was observed using *Xenopus* egg extracts, with assembly occuring shortly after mitotic exit (Bernad et al., 2011). In *Drosophila*, new CENP-A^{CID} is incorporated at centromeres in somatic tissues during late telophase/early G1 (Dunleavy et al., 2012), cultured cells at metaphase (Mellone et al., 2011) and during anaphase in embryos (Schuh et al., 2007). Loading of new CENP-A in *Arabidopsis* occurs mainly in G2 (Lermontova et al., 2007). In fission yeast, new CENP-A^{Cnp1} assembly at the centromere occurs during mid G2 phase of the cell cycle (Dunleavy et al., 2007; Lando et al., 2012; Shukla et al., 2017). In budding yeast both copies of centromeric CENP-A^{Cse4} are replaced during S phase following centromere replication (Wisniewski et al., 2014).

Despite the fact that new CENP-A assembly at centromeres varies between organisms, a highly conserved feature is that CENP-A assembly occurs independently of replication. Following replication, levels of CENP-A at human centromeres drop by half (Jansen et al., 2007). Thus, from S phase onwards, either gaps completely devoid of nucleosomes may be generated at centromeres or a placeholder H3 nucleosome could temporarily fill these gaps until the time of assembly of new CENP-A (Sullivan, 2001; Allshire and Karpen, 2008; Probst et al., 2009). In humans, immunohybridisation analysis on chromatin fibers suggest that both H3.1 and H3.3 are deposited at centromeres following replication, while during G1 the reduction in H3.3 levels and corresponding deposition of CENP-A suggest that H3.3 likely acts as a placeholder for CENP-A at centromeres (Dunleavy et al. 2011). Recent analysis in *S. pombe* using recombination-induced tag exchange (RITE) system demonstrated that histone H3 is deposited as a temporary placeholder during S-phase and in G2 it is replaced with CENP-A^{Cnp1} (Shukla et al., 2017). Thus, H3 placeholder function may be conserved in species where CENP-A assembly is separated from replication.

1.7 Factors affecting CENP-A assembly

The cell cycle timing of deposition of CENP-A results from dynamics of CENP-A loading machinery and cell cycle regulators. In humans, new CENP-A is deposited at centromeres in late telophase/early G1 (Jansen et al., 2007). However, inhibition of cyclin dependent kinases Cdk1 and Cdk2 in any phase of the cell cycle is sufficient to trigger rapid CENP-A assembly (Silva et al., 2012).

CENP-A requires its chaperone HJURP (Holliday junction recognition protein) in mammals or Scm3 (suppressor of chromosome segregation) in yeast, to distinguish it from histone H3 and facilitate its incorporation at centromeres (Dunleavy et al., 2009; Foltz et al., 2009; Pidoux et al., 2009; Williams et al., 2009; Bernad et al., 2011; Barnhart et al., 2011). The *Drosophila* CENP-A^{CID} chaperone Cal1 has no homology to HJURP or Scm3 (Chen et al., 2014) but performs similar functions to HJURP. Recruitment of CENP-A and HJURP to centromeres requires the hMis18 complex, Mis18BP1, Mis18α and Mis18β (Fujita et al., 2007). *S. pombe* contains a single Mis18 protein that display 30% identity with vertebrate paralogs (Nardi et al., 2016). In humans, Cdk1 and Cdk2 negatively regulate CENP-A prior to completion of mitosis,

after which time Plk1 (Polo-like kinase 1) takes over to activate new CENP-A deposition (McKinley and Cheeseman, 2014). CENP-C facilitates the recruitment of M18BP1 to centromeric chromatin, thus allowing a feedback loop where resident CENP-A recruits new CENP-A via CENP-C→Mis18BP→Mis18α/β→HJURP (Moree et al., 2011).

In fission yeast, CENP-A^{Cnp1} loading depends on HJURP^{Scm3}, Mis16 (RbAp46 and RbAp48 in humans) and Mis18 (Hayashi et al., 2004; Pidoux et al., 2009). Mis16 and Mis18 are required for maintaining the hypo-acetylated state of histone H4 in the central domain (Hayashi et al., 2004). CENP-A^{Cnp1} recruitment to the central domain also depends on the conserved kinetochore proteins CENP-I^{Mis6} (Takahashi et al., 2000) and CENP-K^{Sim4} (Pidoux et al., 2003).

In fission yeast, Sim3 (Homologue of histone binding protein NASP in humans and N1/N2 in *Xenopus*) directly interacts with CENP-A^{Cnp1} and required for deposition of newly synthesized CENP-A^{Cnp1} in G2 phase (Dunleavy et al., 2007).

Ams2, a GATA-type zinc finger motif-containing factor, was isolated as a multicopy suppressor of *cnp1-1* (Chen et al., 2003). Ams2 governs the cellular levels of histones in the cell via transcriptional regulation of the core histone genes (Takayama et al., 2016). The relative levels of histone H3 and histone H4 are known to affect CENPA^{Cnp1} deposition at centromeres (Castillo et al., 2007).

1.8 Transcription of centromeric DNA

Despite the fact that centromeres are generally located in poorly transcribed regions, recent studies suggest an important role of centromeric transcription and/or centromeric transcripts in assembly of specialized chromatin at centromeres (Figure 1.6; reviewed in Duda et al., 2017).

In fission yeast, transcription of the outer repeats at centromeres has been well characterized (Volpe et al., 2002; Djupedal et al., 2005; Chen et al., 2008 reviewed in Allshire and Madhani, 2018). Outer repeat transcripts accumulate following deletion of components of the RNA interference (RNAi) machinery such as Dicer (Dcr1), RNA-directed RNA polymerase (Rdp1), and Argonaute (Ago1), accompanied by de-repression of outer repeat transcriptional silencing and loss of histone H3 lysine 9

methylation (Volpe et al., 2002). Recently, heterochromatin has been shown to be required to promote the *de novo* establishment of CENP-A^{Cnp1} chromatin on naïve centromeric sequences and also ensures sister-centromere cohesion to promote proper segregation of chromosomes (Folco et al., 2008, Kagansky et al., 2009; Bernard et al., 2001; Nonaka et al., 2002).

Transcription also plays a role in forming boundaries between outer repeat heterochromatin domain and CENP-A^{Cnp1} central domain at centromeres in fission yeast. tRNA genes separate these distinct domains at endogenous centromeres (Takahashi et al. 1991). Transcription of these tRNA genes by RNAPII is required to maintain the boundary between heterochromatin domain and CENP-A^{Cnp1} domain at centromeres and prevent spreading of H3K9me2 into the central CENP-A^{Cnp1} domain (Scott et al., 2006).

Transcription has been observed at centromeres and is implicated in CENP-A deposition in human (Chan et al., 2012; Molina et al., 2016; McNulty et al., 2017; Quenet and Dalal, 2014), *Xenopus* (Grenfell et al., 2016), maize (Topp et al., 2004), *Drosophila* (Rosic et al. 2014; Chen et al., 201) and *S. pombe* (Choi et al., 2011; Choi et al., 2012; Catania et al., 2015). Interestingly, actively transcribed genes are found within neocentromere regions and their expression does not affect the presence of a functional kinetochore in human and fission yeast (Saffery et al., 2003; Ishii et al., 2008). In humans, the mardel(10) neocentromere is formed over a domain with abundant L1 retrotrasposons and RNAi-mediated knockdown of the RNA transcripts leads to a reduced CENP-A levels and impaired mitotic function of these neocentromeres (Chueh et al., 2009). At the sequence-specified point centromeres of budding yeast, centromeric transcripts are transcribed by RNAPII and contribute to centromere function (Ohkuni and Kitagawa, 2011). In humans, RNAPII inhibition during mitosis leads to a decrease in centromeric α-satellite transcription and lagging chromosomes with reduced CENP-C binding (Chan et al., 2012). Human artificial chromosome (HAC) centromeres are enriched for histone H3 methylations that are associated with active transcription, including H3K4me1 H3K4me2, H3K36me2 and H3K36me3 (Bergmann et al., 2011). In addition, depletion of H3K4me2 leads to rapid loss of transcription of the underlying α-satellite DNA and defective CENP-A incorporation (Bergmann et al., 2011). Targeting a transcriptional activator or a transcriptional repressor to the HAC centromere results in missegregation and loss of

the HAC (Nakano et al., 2008). It has been proposed that transcription of centromeric DNA might facilitate the replacement of histone H3 with CENP-A or facilitate localization of factors required for CENP-A deposition (Figure 1.7; Allshire and Karpen, 2008). In fission yeast, mutants that increase stalling of RNAPII-mediated transcription promote incorporation of CENP-A^{Cnp1} central domain sequences, suggesting a role of transcription in CENP-A^{Cnp1} incorporation (Catania et al., 2015). This suggests that manipulating transcriptional state of the underlying centromere DNA might interfere with the kinetochore assembly (Ohkuni and Kitagawa, 2011).

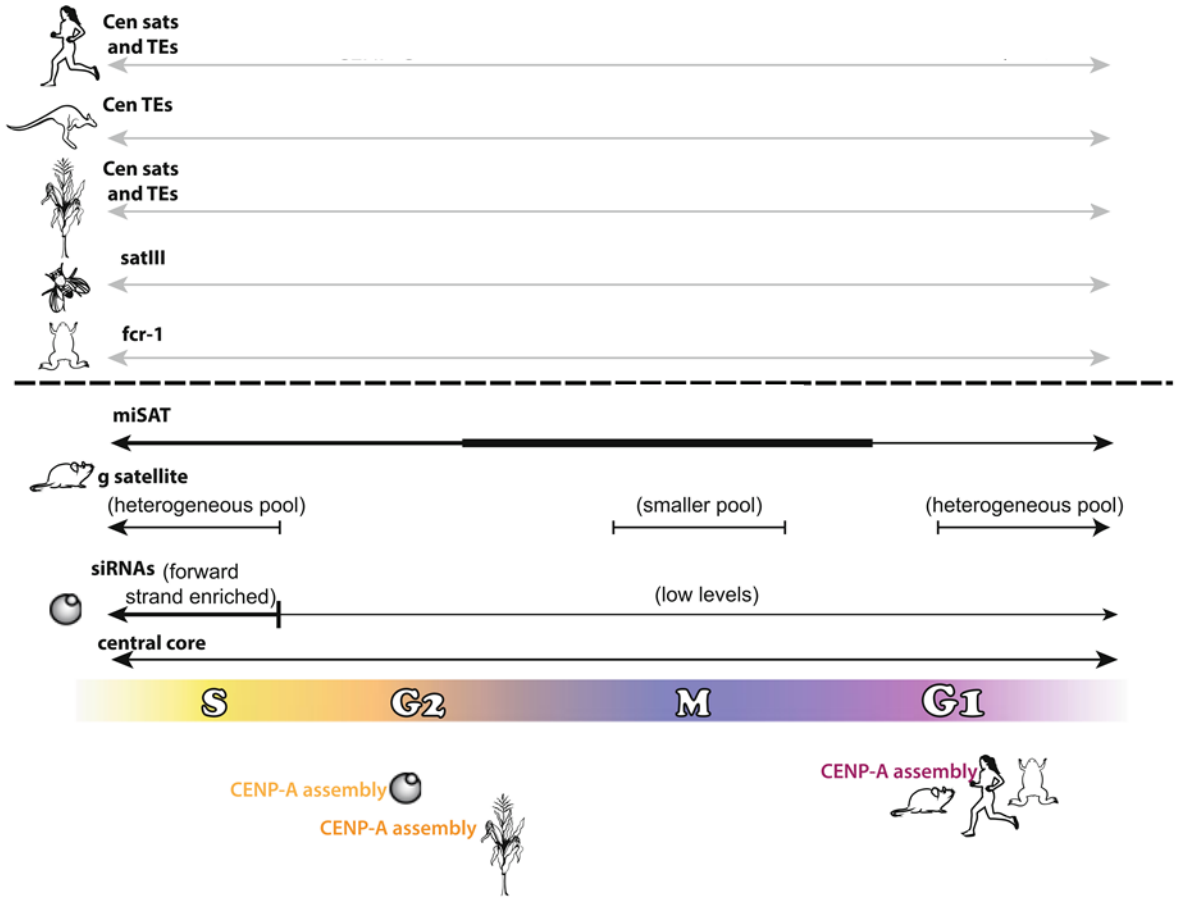

Figure 1.6: Cell cycle variation of centromere transcription

(adapted from Duda et al, 2017). Cell cycle centromeric transcription in human, wallaby, maize, *Drosophila*, frog, mouse and yeast. *Below dashed line:* Timing of transcription is known for these species. The thickness of bars represents the level of transcription. *Above dashed line:* Transcripts have been identified but the timing of transcription is not known in these species. Specific CENP-A assembly times are indicated for each group of species at the bottom.

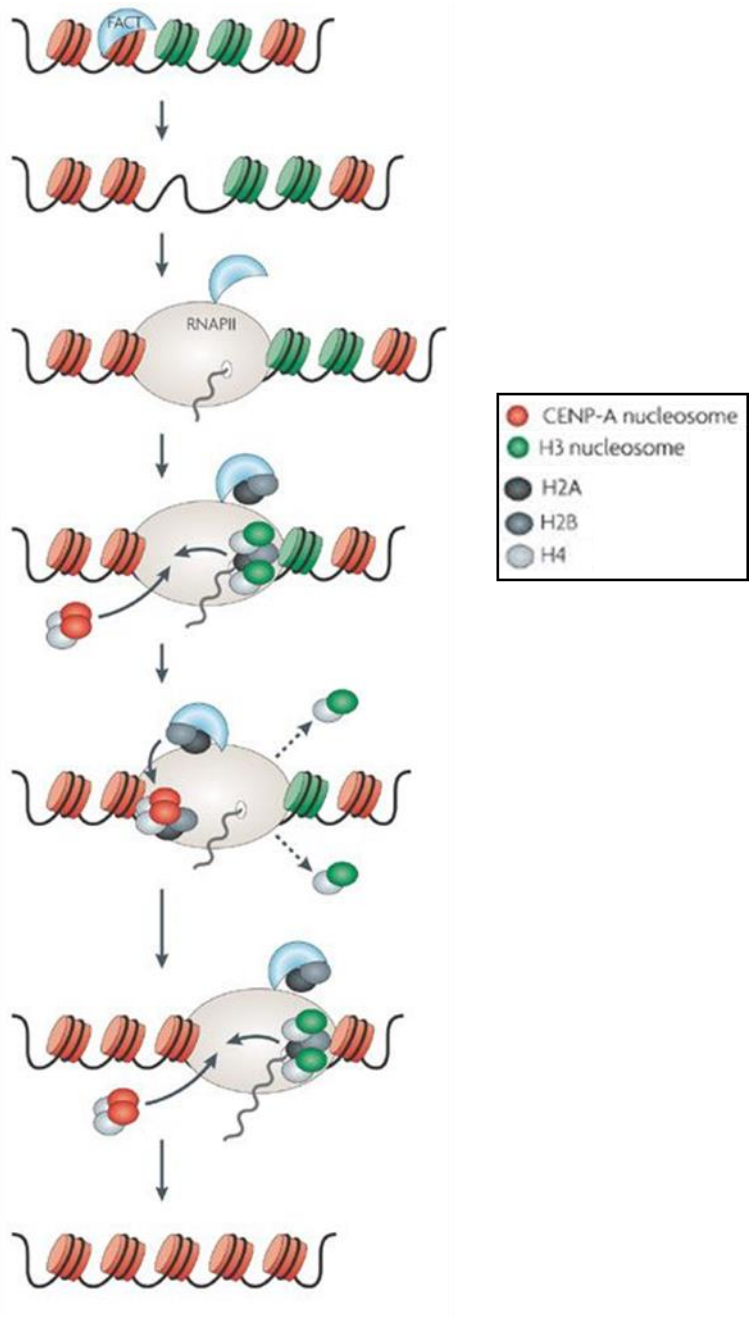

Figure 1.7: Potential role of transcription at centromeres

(adapted from Allshire and Karpen, 2008). The FACT (facilitates chromatin transcription) complex facilitates nucleosome eviction in front of RNAPII and allows nucleosome incorporation behind RNAPII. FACT also associates with CENP-A nucleosomes. FACT-mediated transcription of the central domain DNA could lead to replacement of H3 nucleosome with CENP-A nucleosome.

1.9 Role of chromatin remodeling complexes at centromeres

ATP-dependent chromatin remodelers have been shown to contribute to disassembly and assembly of nucleosomes (Clapier and Cairns, 2009). In humans, the remodeling and spacing factor (RSF) interacts with CENP-A chromatin in mid G1 and depletion of Rsf1 leads to a reduction of the CENP-A levels at centromeres and causes chromosome misalignment (Figure 1.8 A) (Perpelescu et al., 2009). The RSF complex has been shown to reconstitute and regularly space CENP-A nucleosomes *in vitro* (Perpelescu et al., 2009).

In *S. cerevisiae*, the SWI/SNF chromatin remodeling complex has been shown to prevent ectopic localization of CENP-A^{Cse4} (Figure 1.8 B) (Gkikopolus et al., 2011). The SWI/SNF can also dissociate CENP-A^{Cse4} nucleosomes *in vitro* (Gkikopolus et al., 2011). In *S. cerevisiae*, the chromatin remodeling complex RSC also associates with centromeres (Hsu et al., 2003). However, depletion of RSC does not affect recruitment of CENP-A^{Cse4} at centromeres (Hsu et al., 2003). The RSC complex has been shown to facilitate loading of cohesion onto chromosome arms and ensure proper chromosome segregation (Huang et al., 2004).

The Fun30 chromatin remodeler, Fft3, has been shown to associate with the central domain and boundaries of centromeric and telomeric chromatin in fission yeast (Figure 1.8 C) (Stralfors et al., 2011). Deletion of Fft3 leads to reduction of CENP-A^{Cnp1} and an increase in H3, H2A.Z, H3K9Ac and H4K12Ac levels in the *imr* regions at centromeres (Stralfors et al., 2011). However, this does not result in the spreading of H3K9me in the *imr* regions (Stralfors et al., 2011). Therefore, Fft3 is required to prevent accumulation of euchromatin marks into the central domain (imr).

In fission yeast, central domain DNA has also been shown to be transcribed by RNAPII, while the function of this transcription is not very well understood. The transcripts emanating from the central domain are rapidly degraded by the exosome (Choi et al., 2011). Histone chaperone FACT (facilitates chromatin transcription) dissociates histones from the front of elongating RNAPII and reassemble behind it (Belotserkovskaya et al., 2003). FACT and the histone deacetylase (HDAC) complex, Clr6-CII, are required to maintain H3 chromatin integrity during RNAPII transcription and prevent ectopic incorporation of CENP-A^{Cnp1} (Choi et al., 2012).Increased stalling of RNAPII-mediated transcription of central domain sequences promotes

incorporation of CENP-A^{Cnp1}, suggesting a role of transcription in CENP-A^{Cnp1} incorporation (Catania et al., 2015). The ATP-dependent remodeling factor Hrp1 (orthologue of *S. cerevisiae* chromo-helicase DNA-binding protein Chd1) is associated with central domain and required to maintain normal levels of CENP-A^{Cnp1} at centromeres in fission yeast. CENP-A^{Cnp1} localization correlates with Hrp1 occupancy and change in histone H3 density in *hrp1*Δ cells (Walfridsson et al., 2005; Choi et al., 2011). Recently, Choi et al. (2017) also found a correlation between the localization of Ino80 subunits and removal of histone H3 in the *ies6*Δ mutant, implicating the Ino80 complex in eviction of histone H3 nucleosomes and therefore in promoting CENP-A^{Cnp1} incorporation (Choi et al., 2017). Understanding how the combinatorial effect of these chromatin remodeling activities are connected to CENP-A^{Cnp1} chromatin/centromere function in *S. pombe* is intriguing and worth investigating.

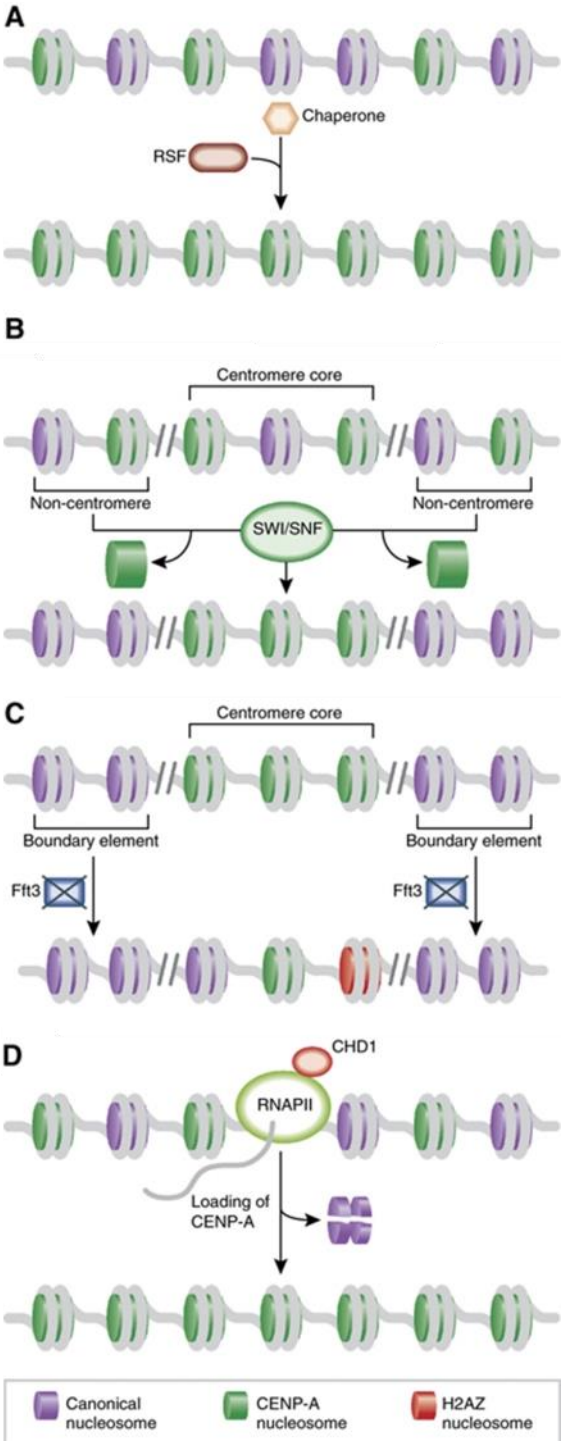

Figure 1.8: The role of chromatin remodeling complexes at the centromeres

(A) In humans, chromatin remodeling complex RSF concerted repositioning of CENP-A nucleosomes (B) In *S. cerevisiae*, chromatin remodelling complex SWI/SNF prevent ectopic localization of CENP-A^{Cse4} (C) In *S. pombe*, action of Fft3 chromatin remodeler is required to maintenance of CENP-A^{Cnp1} and to prevent accumulation of of euchromatic marks at centromeres (D) Chromo-helicase DNA-binding protein CHD1 is required for efficient loading of CEN-A^{Cnp1} nucleosomes by regulating H3 nucleosome dynamics in fission yeast. Adapted from Prasad and Ekwall, 2011. See section 1.9 for more details.

1.10 Post-translational modifications of CENP-A

Post-translational modifications (PTMs) of histones are well known to regulate many biological processes, such as chromatin condensation, gene expression, cell differentiation and apoptosis (Xu et al., 2014; Srivastava and Foltz, 2018; Srivastava et al., 2018). At least 17 different types of PTM on more than 30 amino acid residues of human histone H3 variants have been reported to play a crucial role in diverse cellular processes (Xu et al., 2014). Five types of modifications, methylation, acetylation, phosphorylation, sumoylation and ubiquitylation, have been identified for CENP-A in different species (Table 1.1; Figure 1.9). Consistent with the divergence of the CENP-A N terminus, several modifications have been identified that are unique to individual species.

In humans, trimethylated Gly1 on CENP-A by N-terminal RCC Methyltransferase 1 (NRMT1) is required for the full recruitment of CENP-I and CENP-T at centromeres without affecting CENP-C (Bailey et al. 2013; Sathyan et al., 2017). Interestingly, *S. pombe* shows a similar requirement of CENP-A^{Cnp1} amino terminus in the recruitment of CENP-I^{Mis6} and CENP-T^{Cnp20} (Folco et al., 2015). Phosphorylation of CENP-A on Ser7 is proposed to be involved in loading of CENP-C onto centromeres through a bridging phospho-binding protein 14-3-3 (Goutte-Gattat et al. 2013). CENP-A is phosphorylated at Ser7 only during prophase to metaphase (Kunitoku et al., 2003). While a previous study by Zeitlin et al (2001) found that mutating CENP-A Ser7 does not interfere with kinetochore formation, spindle assembly, or cell cycle progression, but leads to delays in the completion of cytokinesis. A recent mass spectrometry-based study failed to identify CENP-A Ser7 phosphorylation (Bailey et al. 2013), but perhaps CENP-A Ser7 phosphorylation is highly labile or it represents a only a small proportion of total CENP-A. CENP-A Ser16/18 has been shown to be doubly phosphorylated and has been proposed to affect higher order folding of CENP-A-containing nucleosomal arrays (Bailey et al., 2013). In a more recent study, CENP-A Ser18 phosphorylation appears to negatively regulate centromeric localization of CENP-A (Takada et al., 2017). CENP-A Ser68 phosphorylation is proposed to impair CENP-A interaction with HJURP and prevent deposition of CENP-A (Yu et al., 2015). CENP-A Ser68 phosphorylation by kinase CDK1 occurs during early stages of mitosis and as the cell proceeds into G1 Ser68 is dephosphorylated by phosphatase PP1α, ensuring precise CENP-A deposition during the cell cycle (Yu et al., 2015). CENP-A

is ubiquitylated on Lys124 during mitosis and early G1 phases of the cell cycle by CUL4A E3 ligase and this facilitates the interaction of CENP-A with HJURP and its deposition at centromeres (Niikura et al., 2015). However, a recent study suggests that Ser68 phosphorylation and Lys124 ubiquitylation of CENP-A are in fact dispensable for centromeric chromatin assembly (Fachinetti et al., 2017). CENP-A Lys124 is also acetylated at G1/S but switches to monomethylation during early S and mid-S phases (Bui et al., 2017). CENP-A Lys124 acetylation is proposed to impede/reduce affinity for CENP-C (Bui et al., 2017). However, the precise role of acetylation and monomethylation of CENP-A on Lys124 is unclear.

In *Drosophila*, CENP-A^{CID} is acetylated on Lys105 only in cytosolic CENP-A^{CID} samples (Boltengagen et al. 2016). CENP-A^{CID} is phosphorylated on Ser20 and Ser75 in cytoplasmic and nucleoplasmic CENP-A^{CID} samples and is also phosphorylated on Ser77 only in the nucleoplasmic CENP-A^{CID} samples (Boltengagen et al. 2016). Based on their differential patterns in cytosolic and nucleosomal fractions, these modifications have been suggested to determine the localization of CENP-A^{CID} (Boltengagen et al. 2016). The closely spaced Ser75/77 in the long N-terminal tail of Drospohila CENP-A^{CID} has been suggested to be reminiscent of the Ser16/18 pattern in the shorter human CENP-A N-terminal tail (Boltengagen et al. 2016).

In *S. cerevisiae*, CENP-A^{Cse4} can be ubiquitylated at Lys4/131/155/163/172 by the E3 ubiquitin ligase Psh1 *in vitro* (Hewawasam et al., 2010). Mutating all 16 lysines in CENP-A^{Cse4} to alanines stabilizes CENP-A^{Cse4}, suggesting that lysine ubiquitylation is required to promote CENP-A^{Cse4} degradation (Hewawasam et al., 2010; Collins et al., 2004). Phosphorylation of CENP-A^{Cse4} on Ser22/33/40/105 destabilizes misaligned kinetochores to promote biorientation and normal chromosome segregation (Boeckmann et al., 2013). Methylation of CENPA^{Cse4} on Arg37 is required for the recruitment of key kinetochore components to centromeres to prevent aberrant chromosome segregation (Samel et al., 2012). CENP-A^{Cse4} Lys49 acetylation was detected in the study by Boeckmann et al. (2013), while its function is currently unknown. CENP-A^{Cse4} sumoylation at Ser65 by small ubiquitin-related modifier (SUMO) E3 ligases Siz1 and Siz2, which attract SUMO-targeted E3 ubiquitin ligase Slx5 to ubiquitylate CENP-A^{Cse4}, independent of Psh1, and promotes CENP-A^{Cse4} proteolysis (Ohkuni et al. 2016; Ohkuni et al. 2018).

CENP-A PTMs regulate CENP-A deposition at centromeres, CENP-A protein stability, and CCAN recruitment, and therefore, these PTMs play an important role during chromosome segregation. Despite the current knowledge of CENP-A PTMs in human, *Drosophila* and *S. cerevisiae*, no PTMs are known for *S. pombe* CENP-A^{Cnp1}.

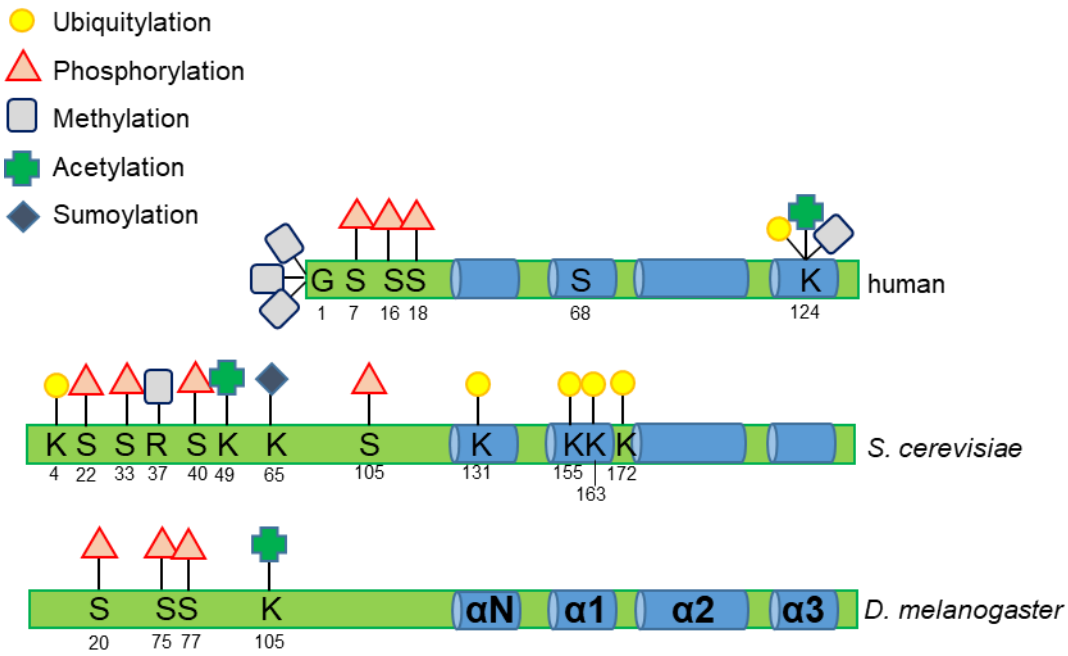

Figure 1.9: Posttranslational modifications of CENP-A

A schematic of CENP-A secondary structure showing the locations of posttranslational modifications. Note that human CENP-A Ser16, Ser18 and Gly1 are numbered based on the removal of the initiating methionine.

Table 1.1: Posttranslational modifications of CENP-A in humans, *Drosophila* and *S. cerevisiae*

Organism	CENP-A residue	Modification	Function/Remark	Reference
Human	Gly1	Trimethylation	Full recruitment of CENP-I and CENP-T and proper chromosome segregation	Bailey et al. 2013; Sathyan et al., 2017
	Ser7	Phosphorylation	May promote CENP-C localization through 14-3-3 during mitosis	Goutte-Gattat et al., 2013;
	Ser16/18	Phosphorylation	Proposed to facilitate higher order chromatin organization and required for proper chromosome segregation	Bailey et al., 2013
	Ser68	Phosphorylation	May prevent CENP-A and HJURP interaction and therefore prevent deposition of CENP-A	Yu et al., 2015
	Lys124	Ubiquitylation	Facilitates interaction of CENP-A to HJURP and deposition at centromeres	Niikura et al., 2015
	Lys124	Acetylation	Unknown function	Bui et al., 2017
	Lys124	Methylation	Unknown function	Bui et al., 2017
Drosophila	Lys105	Acetylation	Unknown function	Boltengagen et al., 2016
	Ser20/75/77	Phosphorylation	Unknown function	Boltengagen et al., 2016
S. cerevisiae	Lys4/131/155/163/172	Ubiquitylation	Required for CENP-A^{Cse4} proteolysis	Hewawasam et al., 2010
	Ser22/33/40/105	Phosphorylation	May serve to destabilize defective microtubule attachments	Boeckmann et al., 2013
	Arg37	Methylation	Recruitment of kinetochore component	Samel et al., 2012
	Lys49	Acetylation	Unknown function	Boeckmann et al., 2013
	Lys65	Sumoylation	Mediate proteolysis of CENP-A^{Cse4}	Ohkuni et al. 2018

1.11 The ubiquitin-proteasome pathway controls CENP-A levels

Ubiquitin is a small 76-residue protein that can be covalently linked to lysines in other proteins (Hershko, 1983). The ubiquitin-proteasome system comprises of two discrete steps: (a) covalent attachment of multiple ubiquitin molecules to the protein substrate and degradation of the polyubiquitylated protein by the 26S proteasome complex (Suh et al., 2013). Ubiquitin-dependent proteolysis has been show to mediate cell cycle control, differentiation, signal transduction, membrane trafficking and programmed cell death (Varshavsky, 2005; Nakayama and Nakayama, 2006; Suh et al., 2013). Ubiquitin is transferred to the target protein through E1, E2, and E3 enzymes (Figure 1.10 A). The ubiquitin-activating enzyme E1, uses ATP to form a high-energy thioester bond with the terminal glycine residue in ubiquitin (Varshavsky, 2005). Activated ubiquitin is then transferred to a cysteine residue in the E2 enzyme via transesterification (Varshavsky, 2005). The last step of the ubiquitin pathway is the transfer of the ubiquitin molecule to the substrate, which is catalyzed by the E3 ubiquitin ligases (Varshavsky, 2005). Proteins can either remain monoubiquitylated or undergo subsequent conjugation of additional ubiquitin residues, resulting in a polyubiquitin chain (Varshavsky, 2005). Ubiquitin ligases are responsible for substrate specificity, and multiple E3s can work with each E2 (Finley et al., 2012). The two main families of E3 ligases are HECT (Homologous to E6-AP Carboxy Terminus) and RING (Really Interesting New Gene) domain containing proteins. The HECT E3 ligases transfers ubiquitin from the E2 to the E3 enzyme, and then E3 directly ubiquitylates the substrate. RING E3 ligases serve as adapters to bring the E2 protein conjugated to ubiquitin in close proximity to the substrate, without an E3 conjugated step (Varshavsky, 2005). K48-linked polyubiquitin-dependent proteolysis is well studied, although other unconventional linkages have been suggested that can also lead to protein degradation (Akutsu et al., 2016). Ubiquitin is removed from proteins before proteolysis by de-ubiquitinases on the lid of the proteasome, so that ubiquitin can then be recycled in the cell (Finley et al., 2012).

When translation is inhibited, CENP-A is quickly degraded, in a proteasome dependent manner in *S. cerevisiae* (Collins et al., 2004; Hewawasam et al., 2010; Ranjitkar et al., 2010) and *Drosophila* (Moreno-Moreno et al., 2006; Moreno-Moreno et al., 2011). In *S. cerevisiae*, the first E3 ubiquitin ligase shown to affect CENP-A^{Cse4} turnover was a RING domain protein Psh1 (Hewawasam et al., 2010; Ranjitkar et al.,

2010). Psh1-dependent ubiquitylation and proteolysis requires the CATD (CENP-A centromere targeting domain) within the C-terminal histone fold domain of CENP-A^{Cse4} (Ranjitkar et al., 2010). Phosphorylation of Psh1 by Casein Kinase 2 (Cka2) is crucial in Psh1-assisted control of CENP-A^{Cse4} degradation (Hewawasam et al., 2014). However, deletion of Psh1 does not completely stabilize CENP-A^{Cse4}, suggesting that other mechanisms may be involved in regulation of CENP-A^{Cse4} stability (Hewawasam et al., 2010; Ranjitkar et al., 2010). In addition, mass spectrometry analysis of recombinant CENP-A^{Cse4} showed that the lysine residues K131, K155, K163 and K172 are the main targets of Psh1 mediated ubiquitylation *in vitro* (Hewawasam et al., 2010). The peptidyl prolyl cis-trans isomerase Fpr3 protein is required for the interaction between CENP-A^{Cse4} and Psh1, potentially through structural changes in between the *cis* and *trans* form of CENP-A^{Cse4} proline 134, and therefore promote Psh1-mediated CENP-A^{Cse4} ubiquitylation and degradation (Ohkuni et al., 2014).

In addition, Doa1 is required for ubiquitylation of the N-terminus of CENP-A^{Cse4} independent of Psh1 (Au et al., 2013). CENP-A^{Cse4} is also SUMOylated by the SUMO E3 ligases Siz1 and Siz2, and this targets it for Slx5-mediated ubiquitylation and proteolysis in a Psh1 independent fashion (Ohkuni et al., 2016). The F-box protein Rcy1 was recently implicated in CENP-A^{Cse4} turnover (Cheng et al., 2016; Cheng et al., 2017). Recently, E3 ligase protein Ubr1 is also shown to promote CENP-A^{Cse4} ubiquitylation and degradation (Cheng et al., 2017). The triple mutant *psh1Δ slx5Δ ubr1Δ* showed increased CENP-A^{Cse4} stability than the *psh1Δ slx5Δ* double mutant , suggesting that Ubr1 works in a pathway separate from Psh1 and Slx5. (Cheng et al., 2017). In the quadruple mutant *psh1Δ rcy1Δ slx5Δ ubr1Δ*, CENP-A^{Cse4} was significantly stabilized with only residual degradation, suggesting that additional ubiquitin ligases or a small pool of stable CENP-A^{Cse4} may exist (Cheng et al., 2017). The three E3 ubiquitin ligases, Ubr1, Slx5, Psh1 and a F-box protein, Rcy1, work in parallel to ubiquitylate CENP-A^{Cse4} and target CENP-A^{Cse4} for proteasomal degradation (Figure 1.10 B).

In *Drosophila*, F-box protein Partner of Paired (PPA) has been shown to mediate proteasomal degradation of CENP-A^{CID} (Moreno-Moreno et al., 2006; Moreno-Moreno et al., 2011). While CUL3/RDX also mediates monoubiquitylation on CENP-A^{CID}, which leads to a more stable centromeric nucleosome (Bade et al., 2014). Human CENP-A has been shown to be subject to proteasome-mediated degradation in

Herpes simplex virus type 1 infection (Lomonte et al., 2001; Gross et al., 2012). In *S. pombe*, the N-terminal domain of CENP-A^{Cnp1} prevents CENP-A^{Cnp1} assembly at ectopic loci and thus was proposed to be dependent on ubiquitin-dependent proteolysis (Gonzalez et al., 2014). Taken together, proteasomal degradation of CENP-A in many species represents a conserved mechanism in regulation of CENP-A.

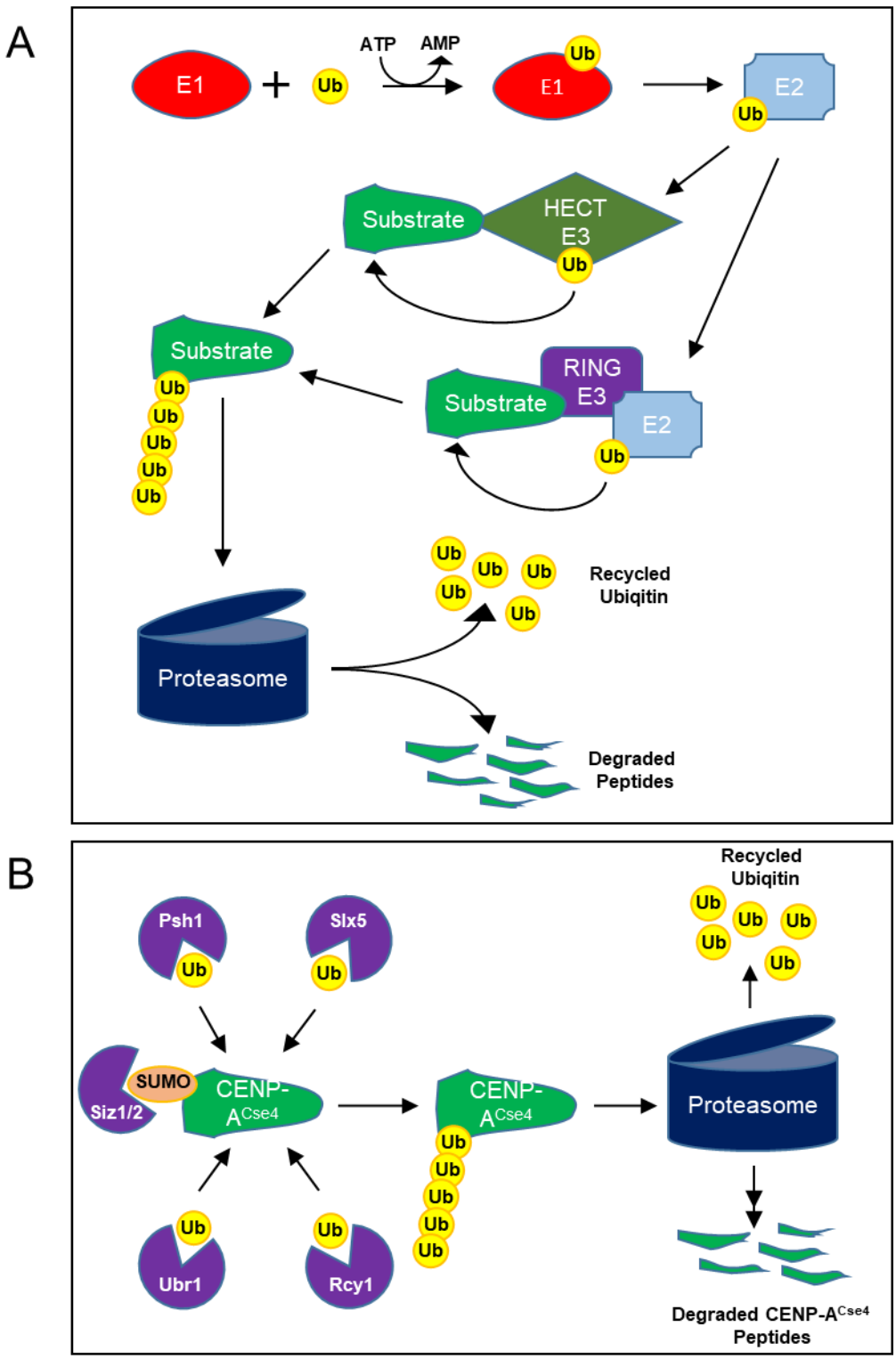

Figure 1.10: The ubiquitin-proteasome system and CENP-A^{Cse4} ubiquitylation and proteolysis

(A) Ubiquitin is conjugated to the E1 in an ATP dependent step. The E1 then transfers ubiquitin to an E2 enzyme, which either transfers the ubiquitin to an E3 (HECT) or binds to an E3 (RING) to transfer the ubiquitin to the substrate protein. Poly-ubiquitylated substrates are targeted to the proteasome for degradation and ubiquitin is recycled for subsequent use. (B) Four E3 ligases Psh1, Rcy1, Ubr1, and Slx5 independently regulate CENP-A^{Cse4} ubiquitin-dependent proteolysis. Siz1/2-directed sumoylation is required for Slx5-dependent ubiquitylation of CENP-A^{Cse4}

1.12 Aims of this thesis

In the centromere research field, *S. pombe* is a model system to investigate the establishment, maintenance, and function of centromeres. To date, no proteomic study of CENP-A^{Cnp1} chromatin composition in *S. pombe* has been performed. In this context the purpose of the analyses presented here was threefold: first, to expand the knowledge of fission yeast CENP-A^{Cnp1} chromatin by purifying CENP-A^{Cnp1} chromatin followed by state-of-the-art mass spectrometric analysis; second, to assess the role of proteins enriched in CENP-A^{Cnp1} chromatin in centromere function; third, to characterize the contribution of Hap2 and Dbl5 in the regulation of CENP-A^{Cnp1} in *S. pombe*.

Chapter 2

Materials and Methods

2.1 General media and solutions

Media and plates

Yes liquid (900ml): 5g Yeast extract (DIFCO)

30g D-glucose anhydrous

0.2g Arginine (Sigma)

0.2g Lysine (Sigma)

0.2g Histidine (Sigma)

0.2g Uracil (Sigma)

0.2g Leucine (Sigma)

4×YES liquid: As above all reagents ×4

YES agar (900ml): 5g Yeast extract (DIFCO)

30g D-glucose anhydrous

0.2g Arginine (Sigma)

0.2g Lysine (Sigma)

0.2g Histidine (Sigma)

0.2g Uracil (Sigma)

0.2g Leucine (Sigma)

20g Agar (OXOID)

PMG liquid (900ml): 3g Pthallic acid

2.2g di-sodium orthophosphate

	3.75g glutamic acid
	20g D-glucose anhydrous
	1ml vitamins 1000x
	0.1ml minerals 10,000x
	20ml salts 50x
PMG agar (900ml):	3g Pthallic acid
	2.2g di-sodium orthophosphate
	3.75g glutamic acid
	20g D-glucose anhydrous
	1ml vitamins 1000x
	0.1ml minerals 10,000x
	20ml salts 50x
	20g Agar (OXOID)
Malt Extracts (ME) plates:	27g Malt extract (OXOID)
(900ml)	0.2g Arginine (Sigma)
	0.2g Lysine (Sigma)
	0.2g Histidine (Sigma)
	0.2g Uracil (Sigma)
	0.2g Leucine (Sigma)
Vitamins 1000x (100ml):	0.5g Pantothenic acid
	1g Nicotinic acid
	1g Inositol
	1mg Biotin
	Filter sterilized

Minerals 1000x (100ml):	5g Boric acid
	4g MnSO4
	4g ZnSO4
	2g FeCl2.6H2O
	1.6g Molybdic acid
	0.4g CuSO4.5H2O
	10g Citric acid
	Filter sterilized
Salts 50x (1000ml):	53.5g Magnesium chloride
	1g Calcium chloride
	50g Potassium chloride
	2g di-sodium sulphate
Supplement stocks:	5g/L Adenine 50x (Sigma)
	10g/L Arginine 100x (Sigma)
	10g/L Lysine 100x (Sigma)
	10g/L Histidine 100x (Sigma)
	2g/L Uracil 20x (Sigma)
	10g/L Leucine100x (Sigma)

Additional supplements:

Thiamine (Sigma) – final concentration of 15µM

Fluoroorotic acid (FOA) (Melford Laboratories) – final concentration of 1g/L

Thiabendazole (TBZ) (Sigma) – final concentration of 10µg/ml

Nourseothricin (cloNAT) (Werner BioAgents) - final concentration of 2000x

Geneticin (G418) (Gibco) – final concentration of 0.1mg/ml

Hygromycin B (Hyg) (Duchefa Biochemie) – final concentration of 0.123mg/ml

General solutions

PBS:	137mM Nacl
	2.7mM KCl
	10mM Na2HPO4
	1.8mM KH2PO4 pH: 7.4
PBST:	PBS with 0.1% Tween20
TE:	Tris-HCl pH8
	EDTA
20x TBE:	Tris Base
	Boric Acid
	EDTA

2.2 Fission yeast protocol

Growth conditions

S. pombe cultures and colonies were incubated at temperatures between 18ºC and 36ºC for overnight and 7 days as indicated for each experiment. Haploid strains will grow with the following generation times:

Medium	**Temperature ºC**	**Generation times**
YES	25	3 hours
	32	2 hours 10 minutes
	36	2 hours

Medium	**Temperature ºC**	**Generation times**
PMG	25	4 hours

32	2 hours 30 minutes
36	2 hour 20 minutes

Cell counting

Cell number was estimated using a haemocytometer (microscope slide with a grid etched onto the glass). Once the coverslip has been applied to the slide, 10µl of culture is pipetted underneath. This creates a known volume of $0.1mm^3$. The number of cells/ml can be calculated by multiplying the number of cells in 25 large squares by $1x10^4$.

Cell culture

Cells were grown to a mid-log phase which is between $2x10^6$ and $1x10^7$ cells/ml in appropriate medium and temperature. Cells were grown to $2x10^7$ cells/ml in 4xYES. To generate culture, the 10ml culture was inoculated with S. pombe strain and grown overnight to until cells reach early stationary phase and then diluted in an appropriate volume for a suitable amount of time to reach the desired concentration.

Auxotrophy

The most commonly used auxotrophic marker in *S. pombe* are adenine, histidine, uracil, arginine and leucine. These amino acids are used at a final concentration of 100µg/ml in the culture. To test auxotrophy, cells are grown as single colonies on non-selective media and then replicated on PMG media lacking the appropriate supplements and incubated for 2-3 days and examined for growth.

Spotting assay (Serial dilution assay)

To assay the growth of different fission yeast strains on different non-selective and selective media, identical amounts of cells were resuspended in 200µl of water followed by 1:4 dilutions made in sterile microtitre plates in water and 5µl of each dilution was plated on the appropriate media. Cells were then incubated at the desired temperature (25^oC, 30^oC, 32^oC and/or 36^oC) until colonies were formed.

Mating and random spore analysis

Crosses were carried out on ME plates in order to starve the cells which causes the cells to undergo meiosis and subsequent sporulation. Two fission yeast strains from

opposite mating types (h+ and h-) were mixed together and grown on ME plates and incubated for 2 days at 32^{o}C (or 25^{o}C for temperature sensitive strains). The presence of asci containing four spores was assessed by light microscopy. To isolate the spores, cells were resuspended in 200µl of 1:100 diluted glusulase (NEN) and incubated overnight at 36oC (or 25oC for two days for temperature sensitive strains). Glusulase digests the vegetative cells and asci walls leaving the spores intact and viable. 5 ml of sterile water was then added and different volumes of the diluted spores were plated on selective media and grown at the appropriate temperature.

Establishment assay

S. pombe with a nonsense mutation on the *ade6* gene (*ade6-704*) forms red colonies while *ade6+* strains have white colonies on YES 1/10th adenine plates. *S. pombe* strains with *ura- ade6-704* were used for complementation *ura4+* and *sup3e* tRNA (nonsense suppressor of *ade6-704*) on pCC2K" minichromosome. Cells were transformed with pCC2K" minichromosome DNA (electroporation method) and plated on PMG ade- ura- plates to select for the minichromosome and incubated at 32^{o}C for 7 days. Colonies were replica plated on YES 1/10th adenine plate and PMG ade- ura- plate and grown for 2 days and incubated at 4^{o}C overnight. Colonies with established minichromosomes were white/pale pink on YES low ade (segregation ability was checked for these colonies), colonies which have lost the minichromosome were red on YES 1/10th adenine plate and minichromosome integrants were pure white and have lost their segregation ability. The frequency of establishment on pCC2K" minichromosome was calculated as the percentage of white/pale pink vs total colonies.

Minichromosome loss assay

Cells with established minichromosomes were taken from PMG ade- ura- plates and grown overnight at 32oC in PMG ade- ura- liquid media and then plated on YES 1/10th adenine plate to get single colonies. Loss of minichromosome leads to red sectors within a colony and a half red sectored colony represents the loss

Central core silencing assay

URA3 catalyzes 5-Fluoroorotic acid (FOA) into toxic 5-fluorouracil that causes cell death. Cells with *ura4+* gene inserted into central core grow on FOA plates under

restrictive adenine conditions due to transcriptional repression of the *ura4*+ gene. Mutants which alleviates silencing at the central core grows on ura- plate and dies on FOA plates. Spotting assay was performed to assess the central core silencing.

Heterochromatin silencing assay

Cells with *ade6*+ gene inserted into centromeric outer repeats are red when grown under restrictive adenine conditions due to transcriptional repression of *ade6*+ gene which causes the accumulation of amino-imidazole ribonucleotide (AIR). White colonies are formed for the mutants that alleviate silencing. Spotting assay was performed to assess the heterochromatin silencing.

2.3 Bacterial protocol

Bacterial media

LB medium (1000ml)	10g Sodium chloride
	10g Bacto tryptone
	5g Bacto yeast extract
LB agar (1000ml)	10g Sodium chloride
	10g Bacto tryptone
	5g Bacto yeast extract
Supplement	100µg/ml Ampicillin
	50µg/ml Carbenicillin

Transformation of competent cells

1 to 5 ng of plasmid DNA was transformed in 30µl of DH5α (Invitrogen). The DNA and cells were pipette mixed and incubated on ice for 20 minutes, heat shocked for 45 seconds at 42oC and incubated on ice for additional 2 minutes on ice before addition of 1 ml LB media. Cells were then grown for 1 hour at 37oC and plated on LB agar plates with appropriate selection.

Plasmid miniprep

Bacterial cells containing plasmid of interest was grown overnight in 5ml LB media with the selection at 37ºC. Plasmid extraction was performed using QIAGEN miniprep kit (according to manufacturer's protocol) and eluted in water.

2.4 Molecular genetics

Transformation of fission yeast (Electroporation)

50 ml culture of cells were grown to log phase (5×10^6 to 1×10^7 cells/ml) and harvested at 3500rpm for 2 minutes. The pellet was incubated in pre-transformation buffer (25mM DTT, 0.6M sorbitol and 20mM HEPES pH: 7.6) at 32ºC for 10 minutes, this incubation is performed only for the transformation of large minichromosome plasmids. The pellet was washed three times with 20ml of 1.2M ice-cold sorbitol and then resuspended in 600-1000µl of 1.2M ice-cold sorbitol. 200µl of cells were mixed with 100ng plasmid DNA or 10µg linear DNA fragments in an ice-cold electroporation cuvette. Cells were pulsed using a Bio-Rad Gene Pulser II at a setting of 2.25kV, 200Ω and 25µF. 500µl of 1.2M ice-cold sorbitol was immediately added after pulsing. Cells were either directly plated on selective media or grown overnight in 10ml of the non-selective medium before plating on selection and incubated at the appropriate temperature.

Transformation of fission yeast (Lithium acetate method)

50 ml culture of cells were grown to log phase (5×10^6 to 1×10^7 cells/ml) and harvested at 3500rpm for 2 minutes. The pellet was washed with 10ml 0.1M lithium acetate pH: 4.9 (adjusted with acetic acid) and resuspended in 0.1M lithium acetate at approximately 1×10^9 cells/ml and incubated at 32ºC for 30 minutes with shaking. 1-10µg of DNA was mixed by gentle vortexing (no more than 10µl) with 100µl of the resuspended cells and then 290µl of prewarmed 50% PEG 3350 was added and mixed by vortexing. Incubation was performed at 32oC for at least one hour. Cells were heat shocked at 42ºC for 20 minutes and spun at full speed for one minute to pellet the cells. Cells were either directly plated on selective media or grown overnight in 10ml of the non-selective medium before plating on selection and incubated at the appropriate temperature.

Gene disruption and gene tagging

Long primers were designed using BalherLab online tool with 80bp homology to *S. pombe* DNA sequence and a 20bp homology to the gene deletion/tagging pFA6 plasmids. Pfx pcr was performed to generate the deletion/tagging DNA fragment which was then transformed into cells using lithium acetate method and plated on selective media. Correct gene deletions and tags were selected by colony PCR.

2.5 DNA and RNA techniques

Genomic DNA isolation

Cells were harvested from the 10ml culture at 3500rpm for 2 minutes and resuspended in 300µl of DNA buffer (100mM Tris pH: 8, 100mM NaCl, 1mM EDTA and 1% SDS) and 300µl of phenol. Cells were then mechanically lysed using acid-washed glass beads (Sigma). The DNA was isolated by phenol/chloroform extraction and ethanol precipitation. The pellet was washed with 70% ethanol and resuspended in 100µl TE and stored at -20^{o}C.

Polymerase Chain Reaction (PCR)

PCR reactions were assembled on ice and carried out as follows in 0.2µl thin-walled PCR tubes: 2.5µl of 10X Taq buffer, 2µl of 2.5mM dNTPs, 2µl of 10µM forward and reverse primer each, 0.1µl of Taq polymerase, 1µl of template DNA and made up to 25µl with dH_20. For more accurate amplification, in case of cloning, Platinum Pfx Taq polymerase from Invitrogen was used as per manufactures instructions. The following programs were used for amplification:

Ura program: 94^{o}C for 5 minutes, (94^{o}C for 30 seconds, 55^{o}C for 30 seconds and 72^{o}C for 4 minutes) 34 cycles, 72^{o}C for 5 minutes and 4^{o}C for 5 minutes.

Pfx program: 94^{o}C for 5 minutes, (94^{o}C for 30 seconds, 55^{o}C for 45 seconds and 68^{o}C for 4 minutes) 34 cycles, 68^{o}C for 10 minutes and 4^{o}C for 5 minutes.

Colony-PCR

A small amount of a single colony was mixed with 10µl of SPZ buffer (1.2M sorbitol, 100mM sodium phosphate and 2.5mg/ml Zymolyase-100T (MP Biomedical)) in 0.2µl thin-walled PCR tube and incubated at 37^{o}C for 1 hour and then microwaved at high for 1 minute. 1µl of the genomic DNA was used as a template for the PCR reaction.

Agarose gel electrophoresis

Size of DNA fragments was analyzed by Agarose gel electrophoresis. Agarose was dissolved in the 1xTBE buffer by heating in a microwave to make an appropriate percentage of gel usually between 0.8 to 3% agarose. Once cooled, ethidium bromide (Sigma) was added to a final concentration of 0.3µg/ml. Orange G loading buffer (30% glycerol, 50mM EDTA and 0.15% orange G) was added to the DNA samples before loading the gel. After running the gel, the DNA was visualized by UV using a transilluminator.

Sequencing

ABI Prism Big Dye Terminator Cycle sequencing kit was used for the sequencing reaction. Reactions were set up as follows: 2µl of Big Dye, 3.2pmol/µl primer, template DNA (1-1000ng for PCR products and 200-500ng for dsDNA) and made up to 20µl with dH_2O in a 0.2µl thin-walled PCR tube.

Seq program: 95^oC for 5 minutes, (95^oC for 30 seconds, ramp 1^oC per second to 55^oC, 55^oC for 15 seconds, ramp 1^oC per second to 64^oC, 64^oC for 4 minutes) 25 cycles.

Total RNA isolation

RNA was isolated using a Qiagen RNeasy miniprep kit as per manufactures instruction. Alternatively, RNA was isolated by acid phenol extraction and ethanol precipitation. The pellet was washed with 70% ethanol and resuspended in 100µl TE and stored at -80^oC.

RT-PCR

The RNA prep was digested with Turbo DNAse at 37^oC (10µg RNA, 5µl Turbo DNAse buffer, 1µl Turbo DNAse and made up to 50µl with dH_2O) to digest the DNA. 1µg RNA was incubated with random hexamers at 65oC for minutes and then incubated on ice for 1 minute for annealing (1µg of RNA, 1µl of 50µM random hexamers, 1µl of 10mM dNTP mix and made up to 13µl with dH_2O). Subsequently, annealed RNA was reversed transcribed using Superscript II Reverse Transcriptase (Invitrogen) at 23^oC for 10 minutes followed by incubation at 55^oC for 10 minutes and inactivation at 80^oC for 10 minutes. A negative control was taken without the reverse transcriptase. 1µl of this cDNA was used as a template for qPCR reaction.

2.6 Protein techniques

Total protein extraction

Cells were grown to log phase and harvested at 3500rpm for 2 minutes at 4^{o}C. The pellet was transferred to a 2ml round-bottomed screw-cap tubes and washed once with 1ml water. The cell pellet was resuspended in 2x protein sample buffer (50mM Tris-HCl pH: 7, 2% SDS, 2mM EDTA, 0.03% bromophenol blue and 10% glycerol) supplemented with 5µM PMSF and 20µl/ml of β-mercaptoethanol at a concentration of 5×10^{7} cells per 100µl. The 1X volume of acid-washed glass beads (Sigma) was added to the sample and bead-beaten for two minutes and incubated at 95^{o}C for 5 minutes. The supernatant was clarified and stored at -20^{o}C.

SDS PAGE and Western blotting

NuPAGE Bis-Tris gels (Life technologies) were loaded with 10-20µl of protein prep. The gels were run at 200V in 1X NuPage MES or MOPS running buffer (Life technologies) depending on the size of the protein of interest. The proteins were then transferred to a nitrocellulose membrane in 1X NuPage Transfer buffer (Life Technologies) supplemented with 10% methanol (for membrane activation) in a semi-dry transfer in a mini-gel tank (Life Technologies) for 1 hour at 20V. The membrane was then stained with Ponceau S solution (Sigma) to confirm transfer and blocked with 5% milk in PBST for 2 hours at room temperature (RT). The membrane was incubated with the primary antibody in PBST overnight at 4^{o}C and washed three times with PBST for 10 minutes at RT with vigorous shaking followed by incubation with HRP-coupled/Fluorophore-coupled secondary antibody for 1 hour at RT with gentle shaking. Three washed with PBST were performed for 10 minutes at RT with vigorous shaking. The protein of interest was detected by luminescence using an enhanced Chemi-Luminescence kit (Amersham) or by fluorescence using LiCor Odyssey CLx.

Chromatin immunoprecipitation (ChIP)

Total of $2.5x10^{8}$ cells mid-log phase cells in a 50ml culture were grown and fixed with 1-3% paraformaldehyde (PFA) in a fume hood for 10-20 minutes. Fixation was stopped by adding 1/20th volume of 2.5M glycine. Cells were transferred to a 50ml falcon tube and washed twice with ice-cold PBS and stored in 2ml round-bottomed screw-cap tubes, flash frozen on dry-ice and stored at -80^{o}C. Cells were lysed by bead

beating (Biospec Products) in 350µl ChIP lysis buffer (50mM HEPES-KOH pH: 7.5, 140mM NaCl, 1% Triton-X-100, 0.1% Na-Deoxycholate and 1mM EDTA) supplemented with 1mM PMSF and 1/100 yeast protease inhibitor cocktail and lysed cell extract was collected in a 1.5ml eppendorf by puncturing holes at the bottom of the tube and centrifuging at 1000rpm for 1 minute. Crude whole cell extract was briefly vortexed and then sonicated using a Bioruptor (Diagenode) sonicator at 5oC on high for 20 minutes (30 seconds ON/OFF cycles). Solubilized chromatin was recovered by centrifugation at 13,000rpm for 15 minutes. 10µl of the whole cell extract was stored at -20^{o}C and remaining lysate was used for the immunoprecipitation using Protein G agarose beads or Protein G Dynabeads (Life Technologies). When using Protein G agarose beads, lysates were pre-cleared by incubating with 25µl of Protein G agarose beads for 1 hour at 4^{o}C. 300µl of the lysate was incubated with 25µl of Protein G agarose beads (only used for sheep α-Cnp1 serum) or 20µl Protein G Dynabeads and an appropriate amount of antibody overnight at 4^{o}C. IPs were washed with 1ml ChIP lysis buffer, followed by 1ml of high salt ChIP lysis buffer (50mM HEPES-KOH pH: 7.5, 500mM NaCl, 1% Triton-X-100, 0.1% Na-Deoxycholate and 1mM EDTA) for 10 minutes, 1ml of wash buffer (10 mM Tris-HCl pH: 8, 250mM LiCl, 0.5% NP40 (IGEPAL), 0.5% Na-Deoxycholate and 1 mM EDTA) for 10 minutes, and lastly with 1ml of TE for 1 minute. Beads following IP and 10µl whole cell extract samples were incubated with 100µl of 10% Chelex-100 resin (Bio-Rad) in dH_2O and boiled at 100^{o}C for 12 minutes. Samples were cooled at RT and treated with 2.5µl of 10mg/ml proteinase K for 30 minutes at 55^{o}C and then boiled again for 10 minutes to inactivate proteinase K. 60µl of the supernatant was carefully transferred into a new eppendorf tube and used for qPCR or stored at -20^{o}C.

Chip-exo (Nexus)

Chip-exo (Nexus) was performed as previously described in He at al., 2005.

Quantitative PCR (qPCR)

Quantitative analysis was performed by qPCR on diluted samples. The input DNA was diluted 1:100 in dH_2O and IP DNA samples were diluted 1:20 in dH_2O. qPCR was performed LightCycler 480 SYBR Green I Master Mix (Roche) in a LightCycler 480 Multiwell plate 96/384 (Roche). ChIP enrichments were calculated as the ratio of the

product of interest from IP sample normalized to the corresponding input sample and expressed as %IP.

DMP crosslinking of the antibody to dynabeads

To minimize the antibody contamination in the Co-IP samples, the antibody was covalently crosslinked to protein G Dynabeads by dimethyl pimelimidate (DMP). 200µg of the antibody and 500µl of washed protein G magnetic dynabeads were incubated in 10 ml of chip lysis buffer for 30 minutes at RT with rotation. Antibody-beads were washed twice with 10ml chip lysis buffer (LB) for 10 minutes and twice with 10ml of 100mM sodium borate (pH: 8.9). Antibody-beads were resuspended in 10ml of 100mM sodium borate and incubated with 20mM DMP at RT for 30 minutes with gentle rotation. The antibody crosslinked dynabeads were then incubated with 10ml of 200mM ethanolamine for 10 minutes with gentle rotation. Beads were washed twice with 10ml of LB buffer for 10 minutes at RT and transferred to an eppendorf tube. Beads were washed thrice with 1ml of PBS, incubated with 1ml of 1M glycine pH: 2 for 10 minutes and then washed again thrice with 1ml of PBS. Crosslinked antibody-dynabeads were resuspended in 500µl of PBS supplemented with 0.05% sodium azide and stored at 4^{o}C.

Native Co-immunoprecipitation (Co-IP)

S. pombe cells were grown in 4xYES at 32^{o}C to 2x10^{7} cells/ml. 2x10^{10} cells/IP were harvested, washed twice with ice-cold water, frozen in liquid nitrogen and stored at -80^{o}C. Cells were lysed by ball breaker twice for 2 minutes and stored again at -80^{o}C. For the IPs, cells were thawed at 4^{o}C for 1 hour and 10 ml MBuffer (10mM Tris-HCl pH: 7.5, 50mM NaCl, 5mM MgCl2, 5mM CaCl2 and 0.1% NP40) supplemented with 2mM PMSF and 1/50 yeast protease inhibitor cocktail was added. Chromatin was solubilized by digestion using 20µl or 100µl Micrococcal nuclease (SIGMA) and 20µl of 0.5M EGTA was added to stop the digestion. Chromatin extract was incubated at 4^{o}C for 1 hour with gentle rotations and then centrifuges at 20,000xg at 4oC to separate non-soluble pellet. Chromatin extracts were incubated with 50µl of the DMP crosslinked antibody-dynabeads for 1 hour at 4^{o}C with gentle rotations. Beads were separated using a magnet and transferred to a 1.5ml protein low-bind eppendorf tube and washed 5 times with 1ml MBuffer. Proteins were eluted twice with 50µl of 0.1% RapiGest SF Surfactant (Waters) in 50mM Tris-HCl pH: 8 at 50^{o}C, 1000rpm for 10

minutes. 1/10th of the sample was used for western blotting and silver staining (Invitrogen™ Novex™ SilverXpress™ Silver Staining Kit - according to the manufactures instructions) and the rest of the sample was stored at -80^{o}C.

2.7 Microscopy

Immunostaining:

The cells was grown to log phase and fixed by adding 3.7% formaldehyde and 0.0625% glutaraldehyde final concentration. Cells were fixed for 10 minutes at room temperature. Cells were pelleted by centrifugation at 3000rpm for 2 minutes and washed twice in 5ml PEM. Cells were resuspended in 1ml PEMS, transferred to 1.5ml eppendorf tubes and pelleted. Pellets were resuspended at 1x10^{8}/ml in PEMS containing 1mg/ml zymolyase and incubated for 1 hours at 37°C. After centrifugation, cells were washed in 0.5ml PEMS then incubated for 1 minute in 1ml PEMS containing 1% Triton-X100 (Sigma). Cells were again washed in 0.5ml PEMS and then incubated twice for 10 minutes in 2mg/ml sodium borohydride in PEM. After two further washes in PEM the cells were resuspended in PEMBAL and incubated at room temperature for 1 hour. Cells were then pelleted and resuspended in 100µl PEMBAL containing the appropriate dilution of primary antibody. Antibody incubations were carried out at 4°C overnight with rotation. Cells were washed three times in PEMBAL for 30 minutes at room temperature. Pellets were resuspended in Alexa green or Alexa red secondary conjugated antibody at 1:1000 in 100µl PEMBAL. Incubations were carried out at 4°C between 4 hours and overnight with rotation. Cells were washed once in 0.5ml PEMBAL for 3 hours three times then incubated in PEM + 0.1% sodium azide and 1:500 DAPI for 5 minutes. Cells were washed in PEM with 0.1% sodium azide for 3 hours three times and then resuspended in a small amount of PEM with sodium azide to make a cloudy suspension. 2tl of this suspension was applied to poly-L-lysine coated slides (Fisher) and spread with a pipette tip. Once cells were dry a small drop of Vectashield (Vector Laboratories Inc.) was added and a coverslip was sealed on top. Cells were visualised with a Carl Zeiss Microimaging, Inc Axioplan 2 IE fluorescence microscope with Chroma 83000 and 86000 filter sets, a Prior ProScan filter wheel (Prior Scientific), and Photometrics CoolSnapHQ CCD camera (Roper Scientific). Image capture was achieved using MetaMorph software (Universal Imaging Corp).

2.8 Mass spectrometry protocol and analysis

Filter Aided Sample Preparation (FASP) mediated trypsinization

Proteins were digested with trypsin into peptides and analyzed by mass spectrometry. Proteins were denatured by adding 25mM DTT to 50-80µl of the immunoprecipitated proteins and incubated at 95^{o}C for 5 minutes. Samples were cooled at RT and 200µl of 8M Urea in 100mM Tris-HCl pH: 8 was added and passed through Vivacon 500 column (30,000 MWCO, Sartorius) by centrifugation at 14,000xg for 30 minutes. Cysteine residues were alkylated to prevent free sulfhydryls from reforming disulfide bonds by incubation with 100µl of 0.05M Iodoacetamide (Sigma) in 8M urea for 20 minutes at 27^{o}C in the dark and centrifuged at 14,000xg to remove the supernatant. Columns were then washed once with 100µl of 8M urea and twice with 100µl of 0.05M ammonium bicarbonate (ABC). Proteins were digested by addition of 100µl of 0.05M ABC containing 0.3µg of trypsin at 37^{o}C for 16 hours. Columns were spun at 14,000xg to collect the digested peptides and washed again with 100µl of 0.05M ABC. Trypsinization was stopped by addition of 10µl of 10% trifluoroacetic acid (TFA) to bring the pH to ~2.0 and were stored at -80^{o}C.

Stage tip preparation for mass spectrometry

C18 reverse-phase resin was used to desalt peptide samples prior to LC-MS/MS. A stage tip was packed tightly with 2 layers of C18 resin. The resin was conditioned with 30µl of 100% methanol, washed with 30µl of 80% acetonitrile (ACN) to remove impurities, equilibrated by passing 30µl of 0.1% TFA. The trypsinized peptide solution was passed through the stage tip by centrifugation at 2600rpm for binding. Stage tips were washed with 200µl of 0.1% TFA and the stage tips were stored at -20^{o}C. For loading into the LC-MS/MS the peptides were eluted from the stage tip twice with 10µl of 80% ACN.

Mass Spectrometry and Data Analysis

Following stage tip desalting, samples were diluted with equal volume of 0.1% TFA and spun onto StageTips as described by Rappsilber et al, 2003. Peptides were eluted in 40 µL of 80% acetonitrile in 0.1% TFA and concentrated down to 2 µL by vacuum centrifugation (Concentrator 5301, Eppendorf, UK). The peptide sample was then prepared for LC-MS/MS analysis by diluting it to 5 µL by 0.1% TFA.

LC-MS-analyses were performed on an Orbitrap Fusion™ Lumos™ Tribrid™ Mass Spectrometer and on a Q Exactive (both from Thermo Fisher Scientific, UK) both coupled on-line, to an Ultimate 3000 RSLCnano Systems (Dionex, Thermo Fisher Scientific, UK). In both cases, peptides were separated on a 50 cm EASY-Spray column (Thermo Scientific, UK), which was assembled on an EASY-Spray source (Thermo Scientific, UK) and operated at 50^{o}C. Mobile phase A consisted of 0.1% formic acid in LC-MS grade water and mobile phase B consisted of 80% acetonitrile and 0.1% formic acid. Peptides were loaded onto the column at a flow rate of 0.3 µL min^{-1} and eluted at a flow rate of 0.2 µL min^{-1} according to the following gradient: 2 to 40% mobile phase B in 150 min and then to 95% in 11 min. Mobile phase B was retained at 95% for 5 min and returned back to 2% a minute after until the end of the run (190 min).

For Fusion Lumos, FTMS spectra were recorded at 120,000 resolution (scan range 350-1500 m/z) with an ion target of 7.0e5. MS2 was performed in the ion trap with ion target of 1.0E4 and HCD fragmentation (Olsen et al., 2007) with normalized collision energy of 27. The isolation window in the quadrupole was 1.4 Thomson. Only ions with charge between 2 and 7 were selected for MS2. For Q Exactive, FTMS spectra were recorded at 70,000 resolution (scan range 350-1400 m/z) and the ten most intense peaks with charge ≥ 2 of the MS scan were selected with an isolation window of 2.0 Thomson for MS2 (filling 1.0E6 ions for MS scan, 5.0E4 ions for MS2, maximum fill time 60 ms, dynamic exclusion for 50 s).

The MaxQuant software platform (Cox and Mann, 2008) version 1.5.2.8 was used to process the raw files and search was conducted against *Schizosaccaromyces pombe* complete/reference proteome set of PomBase database (released in July, 2015), using the Andromeda search engine (Cox et al., 2011). For the first search, peptide tolerance was set to 20 ppm while for the main search peptide tolerance was set to 4.5 pm. Isotope mass tolerance was 2 ppm and maximum charge to 7. Digestion mode was set to specific with trypsin allowing maximum of two missed cleavages. Carbamidomethylation of cysteine was set as fixed modification. Oxidation of methionine, phosphorylation of serine, threonine and tyrosine and ubiquitination of lysine were set as variable modifications. Label-free quantitation analysis was performed by employing the MaxLFQ algorithm as described by Cox et al, 2014. Absolute protein quantification was performed as described in Schwanhäusser et al, 2011. Peptide and protein identifications were filtered to 1% FDR.

The Perseus software platform (Tyanova et al., 2016) version 1.5.5.1 was used to process LFQ intensities of the proteins generated by MaxQuant. The LFQ intensities were were transformed to $\log_2$ scale and list was filtered for proteins with at least 3 valid values in an IP. Missing values were imputed from normal distribution for that IP.

2.9 Strains used in this thesis

Strain number	Relevant genotype
1645	h+ ade6-210 arg3-D4 his3-D1 leu1-32 ura4-D18
1646	h- ade6-210 arg3-D4 his3-D1 leu1-32 ura4-D18
1891	h- ade6-210 arg3-D4 his3-D1 leu1-32 ura4-D18 TM1::ura4
3918	h- orp4::3xHA-ura4+ ura4D18 leu1-32
6023	h- mis6-302 ade6-704 leu1-32 ura4DSE?
6443	h+ GFPhht2 leu1-32 ade6-210
6960	h- leu1-32 ura4- cnp1::ura4+ lys1+::cnp1-1
9316	h- otr1R(Sph1):ade6 lys1::NatR ade6::HygR leu1-32 ura4D18
A7373	h- ade6-704-HYGMX6 his3-D1 leu1-32 ura4-DSE/D18? arg3? cc2D6kb:cc1
A7408	h- cc2D6kb:cc1 ars1:nmt41-GFP-cnp1-NAT ade6-704-HYGMX6 his3-D1 leu1-32 ura4-DSE/D18 arg3?
A8240	h- kanMX6-Pcnp1-mEGFP-cnp1 ade6-M210 leu1-32 ura4-D18
A88	h- leu1 ura4 mis15-GFP[ura4+]
A92	h- leu1 mis17-GFP[LEU2+]
A9339	h+ kanMX-Pnmt41-slp1+ ade6-M210/M216
A9733	h+ leu1-32 ura4-D18 ade6-M210 his3-D1 arg3-D4 fta7:FLAG-natMX6
B1232	h- hpz1::kanMX4 ura4-d18
B1233	h- hpz1:GFP:clonnatMX6 cdc10-M17
B1234	cdc25-22 hpz1:HA:kanMX6
B1387	h+ KanMX6-Pcnp1-mEGFP-cnp1 his3-D1 ura4D-18 leu1-32 ade-
B1390	h+ KanMX6-Pcnp1-mEGFP-cnp1 cdc25-22 ura4D-18 leu1-32 ade6M210
B1685	h? dbl5::Kan ade::HYG otr1R(Sph1):ade6 lys1::NatR ade6-210/216 ura-D18 leu1-32
B1689	h? hap2::Kan ade::HYG otr1R(Sph1):ade6 lys1::NatR ade6-210/216 ura-D18 leu1-32
B1691	h? hap2::Kan ade::HYG otr1R(Sph1):ade6 lys1::NatR ade6-210/216 ura-D18 leu1-32
B1709	h? dbl5::Kan TM1::ura ade6-210/216 ura-D18 leu1-44
B1718	h? hap2::Kan TM1::ura ade6-210/216 ura-D18 leu1-53
B1719	h? hap2::Kan TM1::ura ade6-210/216 ura-D18 leu1-54
B1797	h+ ade6-M210/M216 ura4-D18 leu1-32 top1::KanMX6
B1799	h+ ade6-M210/M216 ura4-D18 leu1-32 msh6::KanMX6
B1805	h+ ade6-M210/M216 ura4-D18 leu1-32 dbl5::KanMX6
B1819	h+ ade6-M210/M216 ura4-D18 leu1-32 hap2::KanMX6
B1843	h? ura- leu1-32 cnp1::ura4+ lys1+::cnp1-1 dbl5::KanMX29
B1844	h? ura- leu1-32 cnp1::ura4+ lys1+::cnp1-1 dbl5::KanMX30
B1858	h? ura- leu1-32 cnp1::ura4+ lys1+::cnp1-1 hap2::KanMX44
B1878	h? cc2D6kb:cc1 ars1:nmt41-GFP-cnp1-NAT ade6-704-HYGMX6 leu1-32 ura4-DSE/D18 dbl5::KanMX6
B1890	h? cc2D6kb:cc1 ars1:nmt41-GFP-cnp1-NAT ade6-704-HYGMX6 leu1-32 ura4-DSE/D18 hap2::KanMX6

B1916	h? ade6-704-HYGMX6 leu1-32 ura4-DSE/D18? cc2D6kb:cc1 dbl5::KanMX6
B1929	h? ade6-704-HYGMX6 leu1-32 ura4-DSE/D18? cc2D6kb:cc1 hap2::KanMX6
B2845	h? GFP-cnp1-NAT dbl5Δ::Kan cdc25-22 ura4-D18 leu1-32
B2869	h? hpz1::Kan cc2Δ6Kb:cc1 Ura4-DSE-sup3e-cc2-ura4+ H3.2-lox-HA-HYG-loxT7 ars1:pRAD11-Cre-EDB-LEU2+ cdc25-22 ade6-704-NAT his3D? ard3D4? ura4D18/DSE leu1-32
B2871	h? hap2::Kan cc2Δ6Kb:cc1 Ura4-DSE-sup3e-cc2-ura4+ H3.2-lox-HA-HYG-loxT7 ars1:pRAD11-Cre-EDB-LEU2+ cdc25-22 ade6-704-NAT his3D? ard3D4? ura4D18/DSE leu1-32
B2872	h? dbl5:: KAN mis6-302
B3109	h- hap2-GFP-Kan ade6-210 arg3-D4 his3-D1 leu1-32 ura4-D18
B3179	h- dbl5-GFP-Kan ade6-210 arg3-D4 his3-D1 leu1-32 ura4-D18
B324	h? cc2Δ6Kb:cc1 Ura4-DSE-sup3e-cc2-ura4+ H3.2-lox-HA-HYG-loxT7 ars1:pRAD11-Cre-EDB-LEU2+ cdc25-22 ade6-704-NAT his3D? ard3D4? ura4D18/DSE leu1-32
2017	h+ (Xba1-Spe1)clr4::LEU2 ade6-210 leu1-32 ura4-D18
B1671-B1696	h? gene::KanMX6 ade::HYG otr1R(Sph1):ade6 lys1::NatR ade6-210/216 ura-D18 leu1-32 (strains used for outer repeat silencing assay)
B1697-B1719	h? gene::KanMX6 TM1::ura ade6-210/216 ura-D18 leu1-32 (strains used for central core silencing)
B1820-B1859	h? gene::KanMX6 ura- leu1-32 cnp1::ura4+ lys1+::cnp1-1 (strains used for *cnp1-1* interaction)
B1860-B1891	h? gene::KanMX6 cc2D6kb:cc1 ars1:nmt41-GFP-cnp1-NAT ade6-704-HYGMX6 leu1-32 ura4-DSE/D18 (strains used for CENP-A^{Cnp1} overexpression)
B1900-B1932	h? gene::KanMX6 ade6-704-HYGMX6 leu1-32 ura4-DSE/D18? cc2D6kb:cc1 (strains used for centromere establishment assay)

2.10 Primers used in this thesis

Primer name	Sequence	Locus
WB3	CAGACAATCGCATGGTACTATC	cc1-F
WB4	AGGTGAAGCGTAAGTGAGTG	cc1-R
WB11	CATTAAACAAACAACGGCACAC	cc2-F (cc2-a-F)
WB12	TAAGCCAGCAAATTCCTTGAG	cc2-R (cc2-a-R)
PP76	CGTGCACATTTGTGAAAAGG	cc2-b-F
PP77	TATGTGTTTCGTATACACCC	cc2-b-R
PP78	CTAGACTTTAAGTTCTACCC	cc2-c-F
PP79	GCACATATTAGTTTATTCAAGC	cc2-c-R
WB10	CCCAAATCCAACCGTGAGAAGATG	act1-F
WB11	CCAGAGTCCAAGACGATACCAGTG	act1-R
WB5	AATTGTGGTGGTGTGGTAATAC	dg-F
WR6	GGGTTCATCGTTTCCATTCAG	dg-R
PP359	GCTAACGAGGCTAACCCACT	imr1-F
PP360	GAGGTTTTTCGTTCTTAGGGCT	imr1-R
PP48	TACGCGACGAACCTTGCATA	non-ARS-F
PP49	TTATCAGACCATGGAGCCCATT	non-ARS-R
PP38	TTGCTTATCTTTTGGGTAGTTTTCG	ARS2004-F
PP39	CTTACATTTTCGGGAACTTATTAGTCAA	ARS2004-R
WB471	ATCATTCAGAAAATCACCGGAGCAAT	K”-mini-F
WB472	CACTTTGCAACGATTACCGGTTTA	K”-mini-R
WB473	AATACGACTCACTATAGGGCGAATTG	K”-imr-F
WB474	ATCGTCACAGTTTACAAATTCGGT	K”-imr-R
WB292	ACTCAAATCCTCCCACGAAC	octo-cc2-F
WB293	GCAGAATGCATGGTCTGAAA	octo-cc2-R
WB254	CCCAATTGTTGTGATTGCTG	octo-otr-F
WB255	GCGGATGCAGTATTTCGTTT	octo-otr-R

Chapter 3

Isolation and analysis of fission yeast CENP-A^{Cnp1} associated complex

3.1 Introduction

Centromeres are pivotal for accurate chromosome segregation during cell division that lead to aneuploidy which is linked to several cancers (Kops et al., 2005). They form the chromatin foundation for the assembly of the kinetochore which is required for the microtubule attachment during cell division (Fukagawa and Earnshaw, 2014). Centromeres are epigenetically defined by the presence of histone H3-variant centromere protein A (Allshire and Karpen, 2008; McKinley and Cheeseman, 2016).

Centromeres were identified as primary constriction of the chromosome observable during metaphase (Earnshaw and Tomkiel, 1992). Anti-centromere autoantibody (ACA) was shown to associate with these chromosome constrictions throughout cell cycle (Moroi el. al., 1980 and Moroi et al., 1981). Immunofluorescence and immunoblotting analysis of affinity-purified antibodies from this serum was shown to recognize three antigens which were designated as CENP (CENtromere Protein) A, CENP-B, and CENP-C (Earnshaw and Rothfield, 1985). The budding yeast homolog of CENP-A, Cse4, was identified in a genetic screen designed for mutants affecting mitotic chromosome segregation (Stoler et al., 1995) and budding yeast homolog of CENP-C, Mif2, was identified in a genetic screen designed for mutants with reduced mitotic fidelity of chromosome transmission (Meeks-Wagner et al., 1986). Similar genetic studies identified many kinetochore-associated proteins in budding yeast (Maine et al., 1984; Spencer et al., 1990). In fission yeast, CENP-I^{Mis6} and CENP-O^{Mal2} were identified in screens for mutants with high frequency of minichromosome loss (Takahashi et al., 1994; Fleig et al., 1996). CENP-K^{Sim4} was identified in a screen for mutants with defective central core silencing (Pidoux et al., 2003). CENP-N^{Mis15} and CENP-U^{Mis17} were identified in a screen for temperature-sensitive (ts) mutants exhibiting chromosome missegregation (Hayashi et al., 2004).

Although genetic screens were useful in identifying kinetochore proteins, advances in mass spectrometry (MS) played a significant role in determining the protein

composition of centromeres. The large number of centromeric proteins known in humans derives from three main affinity purification mass spectrometry (AP-MS) studies which identified all constitutive centromere-associated network (CCAN) protein (Obuse et al., 2004; Foltz et al., 2006 and Okada et al., 2006). Similar AP-MS studies in *S. cerevisiae* (Akiyoshi et al., 2009 and Akiyoshi et al., 2010), *S. pombe* (Liu et al., 2005; Shiroiwa et al., 2011) and *T. brucei* (Akiyoshi and Gull, 2014); made significant contributions in understanding kinetochore proteome in various organisms.

Previous analysis of the *S. pombe* kinetochore proteins were carried out using affinity purification of the kinetochore proteins (CENP-K^{Sim4}, CENP-O^{Mal2}, CENP-I^{Mis6}, CENP-U^{Mis17}, dad1, nuf2, mis12, spc7, ask1 and dam1) and these resulted in the isolation of proteins from sub-complexes of the kinetochore rather than the whole kinetochore complex. To date, no CENP-A^{Cnp1} proteome study has been performed. Analysis of the CENP-A^{Cnp1} proteome can potentially shed light on not just the kinetochore composition but also identify chromatin remodellers, CENP-A^{Cnp1} assembly factors, transcription factors and other redundant factors missed by previous genetic screens and MS analysis.

The goal of this work was to identify proteins enriched in CENP-A^{Cnp1} chromatin and determine if they indeed have a centromere function and potentially CENP-A^{Cnp1} deposition role. Therefore, an affinity purification mass spectrometry (AP-MS) strategy was optimized and applied to enrich for fission yeast centromeric chromatin. Centromere-associated factors were subselected and subjected to various functional assays to assess their role in centromere function (Chapter 4).

3.2 Results

3.2.1 Workflow for CENP-A^{Cnp1} associated-chromatin isolation and characterization by AP-MS

To date, all kinetochore protein studies resulted in little to no CENP-A^{Cnp1} after AP-MS in fission yeast, therefore it is possible that CENP-A^{Cnp1} chromatin-associated proteins might not be represented in such analysis. To overcome this issue, affinity purification of N terminally tagged GFP-CENP-A^{Cnp1} was performed followed by mass spectrometry. GFP-CENP-A^{Cnp1} starin was functional (described in Coffman et al., 2011 and Lando et al., 2012). Cells without a GFP tag were used in control affinity purification for non-specific binding and cells expressing histone H3.2-GFP tagged

were also used in control IP for chromatin binding proteins. Affinity purification of GFP-CENP-A^{Cnp1} was performed to analyze the proteome of centromeric chromatin compared with both these control affinity purifications.

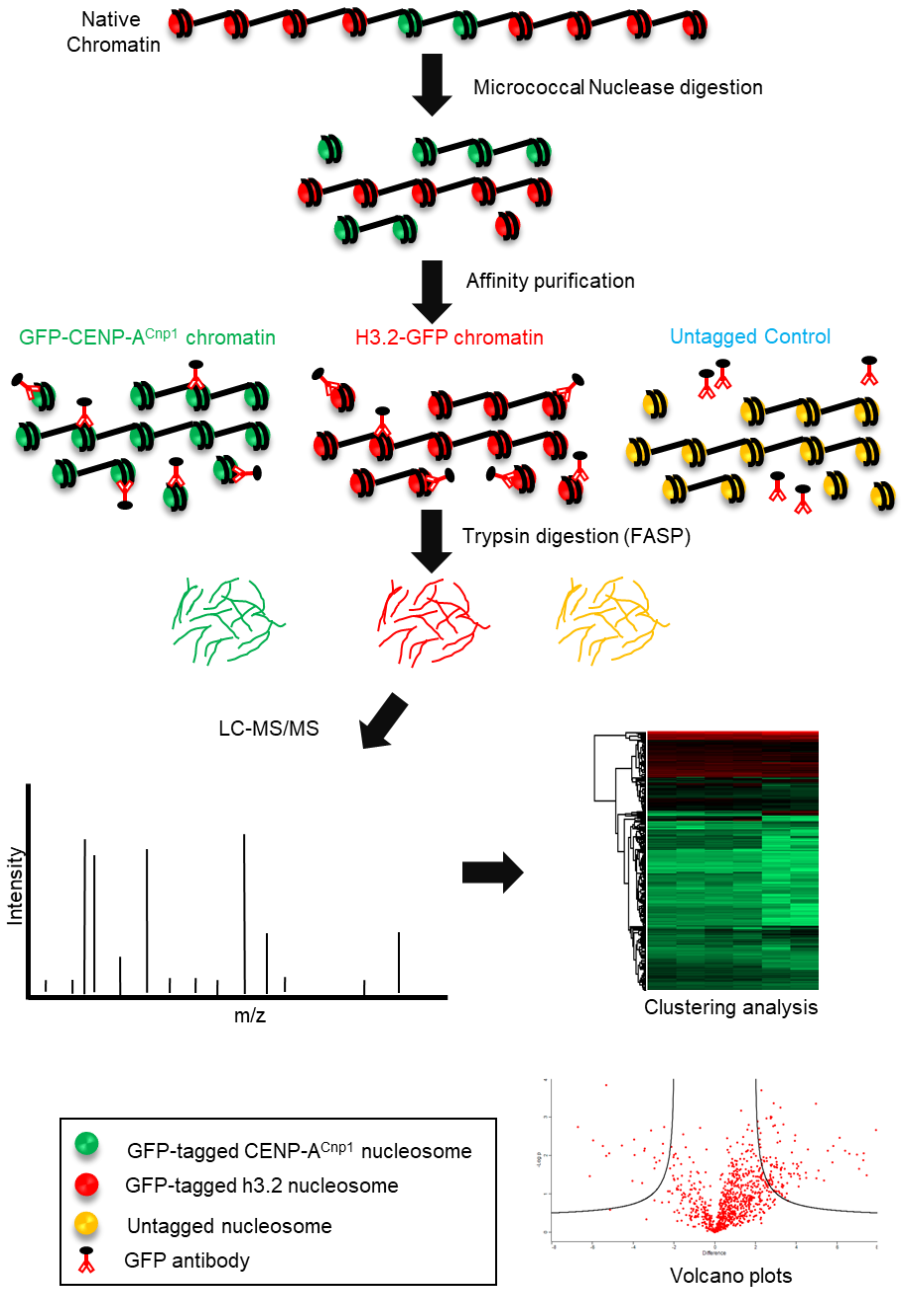

Figure 3.1: Scheme for affinity purification of CENP-A^{Cnp1} chromatin

GFP tagged-CENP-A^{Cnp1}, GFP tagged-histone H3.2, and untagged chromatin were lysed in liquid nitrogen by mechanical shearing. Micrococcal nuclease was used for chromatin digestion and immunoprecipitation was performed using α-GFP antibody crosslinked to protein G dynabeads. Eluted proteins were digested to smaller peptides using trypsin and LC-MS/MS was performed. Quantification of the data was performed using Maxquant and further analysis was carried out in Perseus. Enriched proteins were visualized by clustering analysis and volcano plots.

The schematic of the affinity purification workflow is shown in Figure 3.1. Unfixed cells were frozen in liquid nitrogen and lysed by mechanical shearing while cooling them occasionally in liquid nitrogen. Micrococcal nuclease (MNase) digestion was performed to solubilize chromatin. Solubilized chromatin was separated by centrifugation and the supernatant containing the solubilized chromatin was subjected to anti-GFP affinity purification using crosslinked GFP antibody-Protein G dynabeads. The eluate was digested with trypsin employing on-column proteolysis of proteins to generate peptides which were subjected to mass spectrometry (MS). Quantification of the MS data was performed using Maxquant and further analysis was carried out in Perseus to visualize enrichment of proteins by clustering analysis and volcano plots.

3.2.2 Optimization of CENP-A^{Cnp1} associated-chromatin immunoprecipitation

Small-scale experiments were performed to optimize cell lysis, CENP-A^{Cnp1} chromatin solubilization by MNase, fractionation and immunoprecipitation protocols. 2×10^{10} cells were frozen in liquid nitrogen, lysed and resuspended in MBuffer. Differential digestion of the chromatin was obtained with incubation of lysed cells with different amounts of MNase at 37^{o}C for 10 minutes. Two such digestion conditions high (20U of MNase) and low (4U of MNase) are shown in Figure 3.2 A. When extensive MNase digestion conditions were applied more mononucleosomal-sized 147bp DNA fragments were obtained. This predominant fragment represents the size of the DNA fragment protected by the nucleosome from MNase digestion. Lower digestion conditions resulted in a nucleosomal ladder representing a variety of mono and poly-nucleosomal sized DNA fragments. The solubilized chromatin was incubated with anti-GFP antibody cross-linked to protein G dynabeads for one hour. Quick washes were performed with ice-cold MBuffer to remove nonspecific-binding. Co-immunopurified proteins were eluted from the beads by incubating them in Rapigest. GFP-CENP-A^{Cnp1} was detected in the solubilized chromatin, non-soluble fraction and affinity-purified eluate (Figure 3.2 B). The abundance of GFP-CENP-A^{Cnp1} in the affinity-purified eluate is indicative of a successful affinity purification. To test the specificity of the affinity purification for centromeric chromatin, eluted DNA was assessed by qPCR for enrichment of centromeric DNA sequences. Centromeric central domain DNA (*cc2*) showed ~2000 fold enrichment relative to the actin gene (*act1*$^{+}$) in the GFP-CENP-A^{Cnp1} IP while no such enrichment was observed in untagged control IP (Figure 3.2 C). On the other hand, the centromeric outer repeat element (*dg*) showed only ~20

fold enrichment relative to actin gene (*act1*$^{+}$) in the GFP-CENP-A^{Cnp1} IP. High enrichment of the central domain region relative to the flanking outer repeat DNA suggests a highly efficient purification. To test the amount and the quality of the affinity purification, eluted proteins were separated on a denaturing polyacrylamide gel and stained with either coomassie blue or silver nitrate (Figure 3.2 D). Many unique protein bands were observed only in the GFP-CENP-A^{Cnp1} IP eluate. Furthermore, several bands in the CENP-A^{Cnp1} IP corresponding to the size of histone H2A, H2B, H3 and H4 proteins were also detected suggesting purification of intact GFP-CENP-A^{Cnp1} nucleosomes. Together, these observations suggest efficient purification of CENP-A^{Cnp1} chromatin.

With this optimized workflow, the CENP-A^{Cnp1}-associated complex could be reproducibly purified. LC-MS/MS analysis of CENP-A^{Cnp1} chromatin digested to mononucleosomal sized DNA yielded less efficient co-immunoprecipitation of other kinetochore proteins (data not shown). Therefore, for further experiments chromatin was digested to polynucleosomal sized DNA samples for immunoprecipitation. Four biological replicates of GFP-CENP-A^{Cnp1}, untagged and H3-GFP were purified. The amount of affinity purified sample subjected to MS detection was normalized to have similar amounts of tagged protein based on intensities of the tagged protein on silver stained gel. As GFP-CENP-A^{Cnp1} was enriched after affinity purification, MS analysis to identify enriched proteins carried out.

3.2.3 Characterization of CENP-A^{Cnp1} associated-chromatin by LC-MS/MS

Data processing of mass spectrometry data sets

Affinity purified CENP-A^{Cnp1}-associated proteins were digested to small peptides using trypsin by Filter-aided sample preparation (FASP) method (Wisniewski et al., 2009). Samples were desalted and concentrated. Analysis of these peptides was performed by an LC-MS/MS strategy. Identification and quantification was carried out using MaxQuant and further analysis and visualization was performed with Perseus 1.5.5.1 software (http://www.perseus-framework.org; Tyanova et al., 2016). MaxLFQ algorithm can be used for relative protein quantification (Cox et al., 2014). LFQ intensity is calculated for each protein using the maximum (pairwise) peptide ratio information from extracted peptide ion signal intensities. LFQ intensities of all the proteins in CENP-A^{Cnp1} chromatin IP and corresponding values in the untagged control

IP and histone H3.2 chromatin IP were transformed by applying the logarithm to the base of two. Only proteins having at least two valid values in at least one sample group were considered for further analysis. NaN values occurring if a protein is not identified in a given sample, were replaced by imputation with values taken from a normal distribution separately for each sample. An extended description of quantification and analysis can be found in (Section 2.8). Identified proteins in all data sets followed a Gaussian distribution and the imputed values were assigned low LFQ intensity (Figure 3.3 A). Different proteomes showed high correlation of all detected proteins which is a prerequisite for most statistical analysis (Figure 3.3 B).

Kinetochore proteins and potential CENP-A^{Cnp1}-associated proteins are clustered together

The above procedure was performed on four affinity purifications for GFP-CENP-A^{Cnp1}, untagged and H3-GFP samples. Hierarchical clustering provides an unbiased statistical approach to identify distinct protein complexes from affinity-purified samples analyzed by mass spectrometry. The clustering analysis arranged proteins according to similarities in patterns of enrichment within all proteomes and proteins in a group are more likely to be a part of a complex. Hierarchical clustering analysis was employed to identify groups of proteins in MS datasets that show a similar pattern of enrichments in CENP-A^{Cnp1} chromatin proteome. All 2387 detected proteins were computationally divided into 6 clusters with three clusters (171 proteins) showing greater enrichment in CENP-A^{Cnp1} chromatin: cluster 2, 3 and 5 (Figure 3.4A). Cluster 2 was found to be predominantly contain known kinetochore proteins (Figure 3.4B). Cluster 2 (19 proteins) showed the highest enrichment of proteins in the CENP-A^{Cnp1} affinity purified proteome compared to the untagged, cluster 3 (28 proteins) showed reasonable enrichments while cluster 5 (124 proteins) showed lower but reproducible enrichment (Figure 3.4C). Cluster 2, along with kinetotochore proteins, also contained non-kinetochore priteins: Topoisomerase Top1, transcription factor TFIIIB complex subunit Bdp1 and Brf1, bromodomain AAA-ATPase protein Abo1 which is proposed to have a chaperone function that maintains nucleosome architecture genome-wide (Gal et al., 2016). Hence, kinetochore proteins and potential CENP-A^{Cnp1}-associated proteins were clustered in groups that displayed similar patterns of enrichments in the four different GFP-CENP-A^{Cnp1} and control IPs.

Inner kinetochore and outer kinetochore complex proteins are enriched in CENP-A^{Cnp1}-associated chromatin proteome

A volcano plot provides a statistical approach to graphically visualize the nature of the relationship between the mean differences between groups and the statistical significance of those differences, for the dataset as a whole. Usually, -log (p-value) of the t-test is represented on the y-axis and the fold difference on the x-axis. Volcano plots are widely used in genomics, transcriptomics, proteomics and metabolomics to identify the most significant changes in long lists of thousands of replicate data points between two distinct conditions. Volcano plots were therefore used to graphically visualize the enrichment of proteins in GFP-CENP-A^{Cnp1} chromatin compared to untagged control and histone H3.2-GFP chromatin control and there t-test p-values.

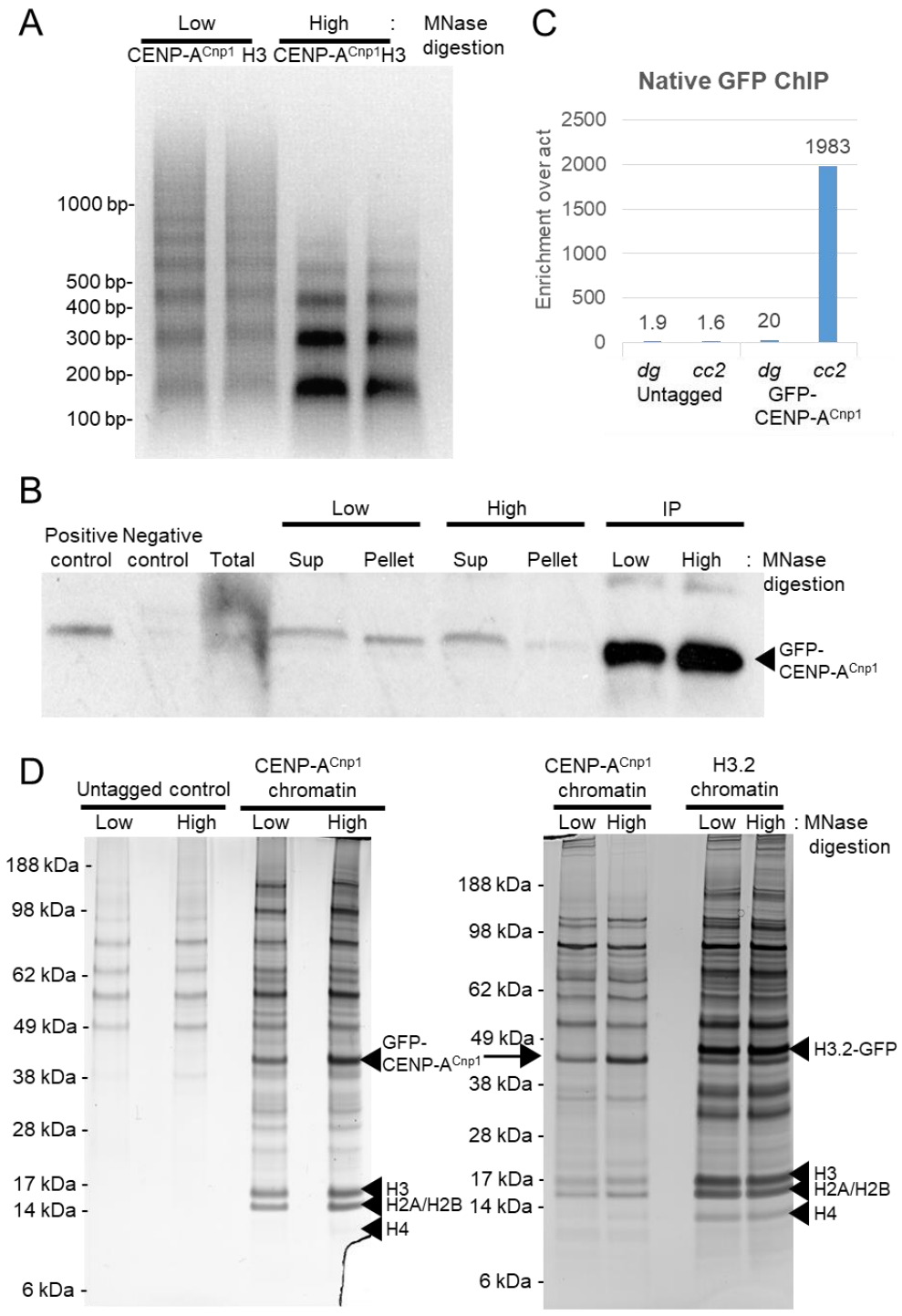

Figure 3.2: Standardization of affinity purification protocol for isolation of CENP-A^{Cnp1} chromatin
GFP-CENP-A^{Cnp1}, H3.2-GFP and untagged strains were used for the analysis. (A) Differential digestion of chromatin by Micrococcal Nuclease (MNase) was performed at 37^{o}C for 10 minutes. Low: 4U of MNase and High: 20U of MNase. (B) Western blot analysis of GFP-CENP-A^{Cnp1} following digestion by MNase in supernatant (sup), pellet and eluate obtained after immunoprecipitation (positive control: CENP-A^{Cnp1}-GFP and negative control: untagged strain). (C) qChIP of GFP-CENP-A^{Cnp1} at central core 2 (cc2) and at centromeric repeats (dg). (D) Silver staining of the affinity purified proteins after GFP immunoprecipitation from GFP-CENP-A^{Cnp1} strain, H3.2-GFP strain and untagged strain.

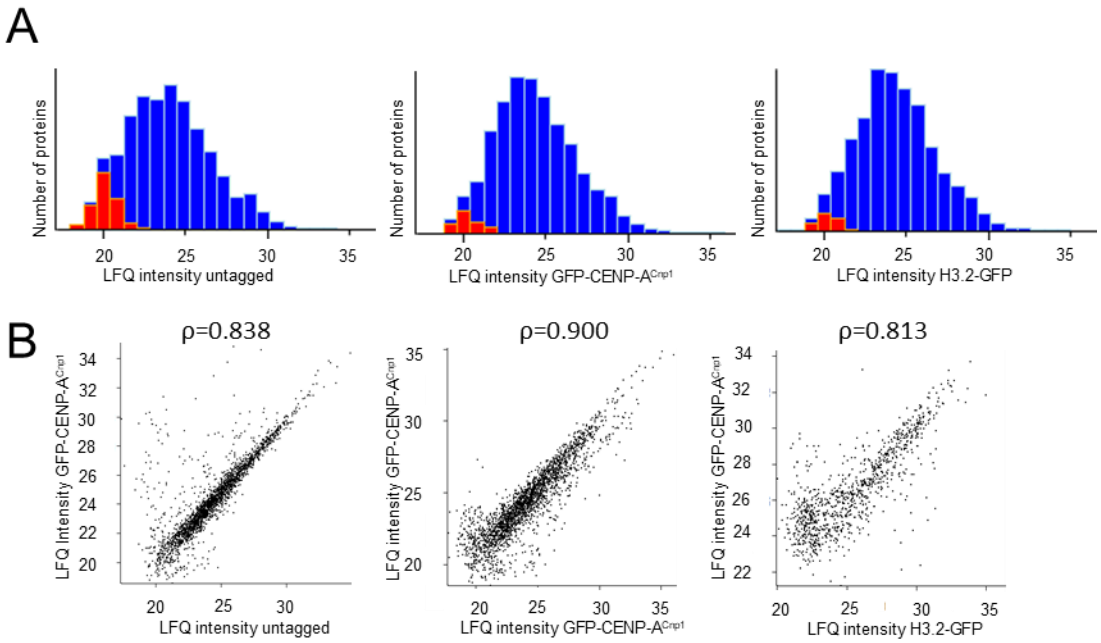

Figure 3.3: LFQ intensities of identified proteins showed a Gaussian distribution and high Pearson correlation in GFP-CENP-A^{Cnp1} compared to control IPs

(A) Distribution of all identified proteins grouped in 24 bins. X-axis: all LFQ intensities of one experiment. Y-axis: number of proteins in one group. Blue: proteins identified by MS and red: imputed values for NaN. The graph follows a Gaussian distribution which allows subsequent statistical analysis. (B) Both H3.2-GFP and untagged proteome show a high correlation with GFP-CENP-A^{Cnp1} proteome. Shown is the Pearson correlation between one of the four biological replicates of each proteome. Diagram created with Perseus.

First, CENP-A^{Cnp1} chromatin and untagged control datasets were analyzed (Figure 3.5 A). The previously identified 19 inner kinetochore CCAN proteins were significantly enriched along with 10 outer kinetochore NMS complex proteins (Liu et al., 2005; Shiroiwa et al., 2011). Dad1 was the only protein from the DASH complex that was enriched in GFP-CENP-A^{Cnp1} chromatin isolated from asynchronous fission yeast cells (Liu et al., 2005). Spindle assembly checkpoint proteins Bub1 and Bub3 (Rischitor et al., 2007) were also enriched in GFP-CENP-A^{Cnp1} chromatin. The CENP-A^{Cnp1} histone chaperone HJURP^{Scm3} (Pidoux et al., 2009), the NASP family chaperone Sim3 (Dunleavy et al., 2007) and Mis18 (Subramanian et al., 2014) were also enriched in centromere chromatin preparations.

The GFP-CENP-A^{Cnp1} chromatin dataset was compared with H3.2-GFP chromatin dataset (Figure 3.5 B). Consistent with the previous analysis, 19 inner kinetochore CCAN proteins and DASH complex protein Dad1 were significantly enriched in CENP-A^{Cnp1} chromatin. Although the inner kinetochore proteins (Ndc80, Nuf2, Spc7 and Mis13) and spindle assembly checkpoint proteins (Bub1 and Bub3) are detected, they did not show any significant enrichment. HJURP^{Scm3} and Mis18 were not detected in these preparations while Sim3 showed more enrichment in H3.2-GFP chromatin compared to CENP-A^{Cnp1} chromatin. In contrast, the histone H3-H4 chaperone Asf1, histone cell cycle regulator and histone chaperine (HIRA complex) proteins: Hip1, Hip3, Hip4 and Slm9, chromatin assembly factor-1 (CAF-1 complex) proteins: Pcf1, Pcf2 and Pcf3 and histone acetyltransferase mst2 complex proteins: Eaf1, Mst2, Nto1, Ptf1 and Ptf2; were enriched in the histone H3.2 chromatin proteome compared to CENP-A^{Cnp1} chromatin proteome. Together, these observations demonstrate that kinetochore proteins are enriched in these GFP-CENP-A^{Cnp1} chromatin preparations while general histone remodelers and chaperones were more prevalent in H3.2 chromatin.

Since the GFP-CENP-A^{Cnp1} chromatin samples showed significant enrichment of known kinetochore proteins compared to the untagged and histone H3.2 chromatin samples, these can be used to identify non-centromere specific proteins that may contribute to CENP-A^{Cnp1}/kinetochore assembly.

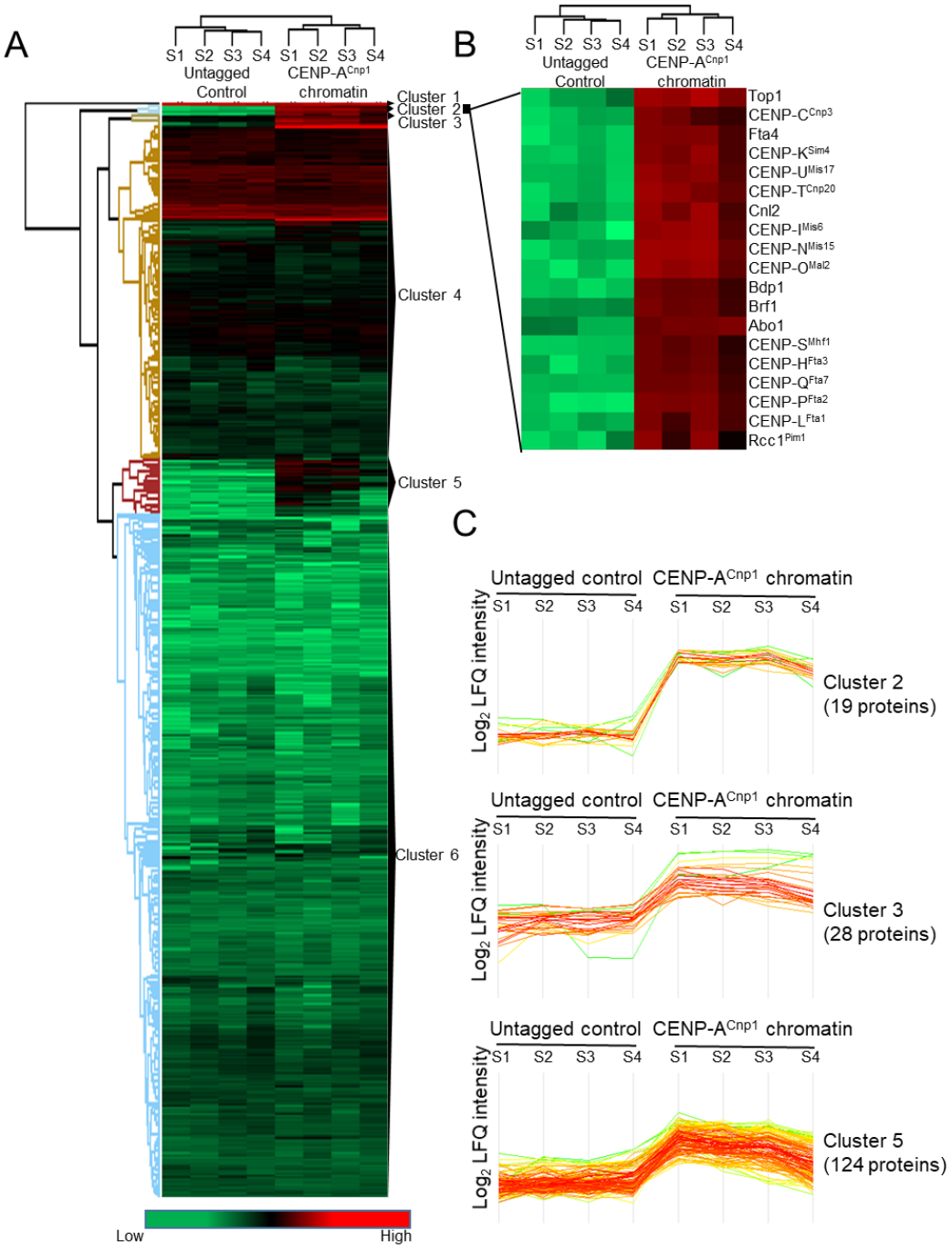

Figure 3.4: Hierarchical clustering grouped known kinetochore proteins and potential centromere-associated proteins in three clusters

(A) Quantitative heat map displaying LFQ intensities identified in each IP. Associated dendrograms display hierarchical clustering on the basis of euclidean distances. Six clusters were computationally generated based on their pattern of relative protein enrichment in CENP-A^{Cnp1} chromatin and untagged control and indicated by different colors. (B) An enlarged view of cluster 2 showing co-purification of many kinetochore proteins. (C) Log_2LFQ intensities of the proteins in Cluster 2 (19 proteins), cluster 3 (28 proteins) and cluster 5 (124 proteins) showing enrichment of these proteins in CENP-A^{Cnp1} chromatin compared to untagged control. Plot generated with Perseus. Four biological replicates were used for affinity purification and analysis: S1, S2, S3 and S4.

Inner and outer kinetochore are two distinct sub-complexes of the kinetochore

Outer kinetochore proteins are known to associate with CENP-A chromatin via long-range and indirect interactions compared to inner kinetochore proteins (Yamagishi et al., 2014). Such interactions might expected to be lost during immunoprecipitation as the employed protocol does not include a protein cross-linking step to preserve such long-range and indirect interactions. Therefore, it is expected that the outer kinetochore proteins will be less abundant compared to inner kinetochore proteins which reside in close proximity to CENP-A^{Cnp1} chromatin. The enrichment of inner and outer kinetochore proteins was therefore compared in CENP-A^{Cnp1} chromatin vs untagged control. All 19 inner kinetochore proteins showed significantly higher enrichments compared to the outer kinetochore NMS complex proteins (Figure 3.6 A, Table 3.1). This finding is consistent with finding in the other systems where it has been shown that the inner and outer kinetochore proteins represent two distinct sub-complexes of the kinetochore (Musacchio and Desai, 2017).

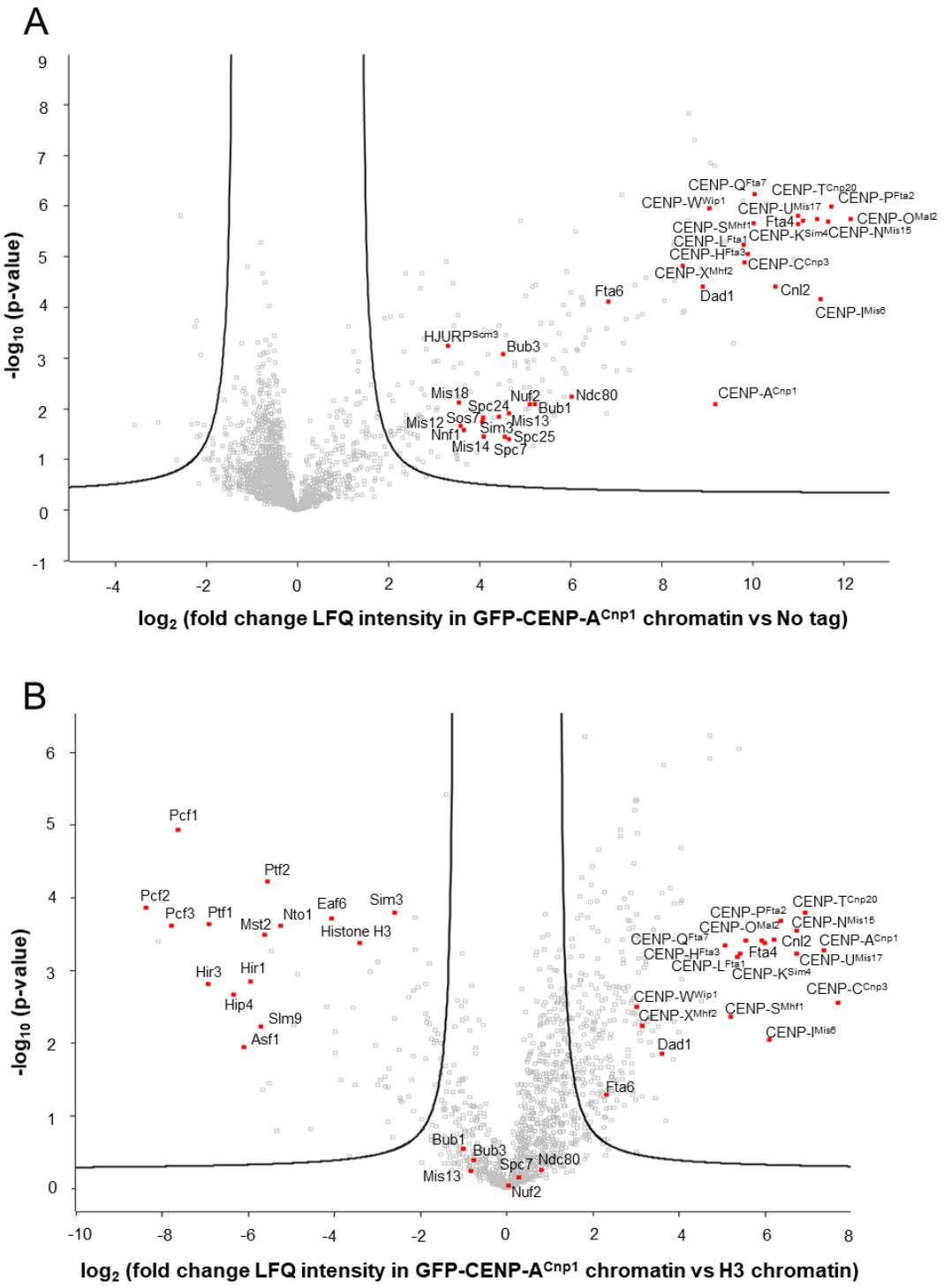

Figure 3.5: Volcano plot illustrating differential abundance of kinetochore proteins in CENP-A^{Cnp1} chromatin

(A) Volcano plot of proteins associated with CENP-A^{Cnp1} chromatin relative to untagged control (4 biological replicates). (B) Volcano plot of proteins associated with CENP-A^{Cnp1} chromatin relative to histone H3.2 control (4 biological replicates). X-axis: fold change and y-axis: -log$_{10}$(p-value). Each square represent identified proteins in the MS dataset (proteins represented by red filled squares are labelled). Plots generated with Perseus.

Relative amounts of inner kinetochore proteins at fission yeast centromeres

The human CENP-CHIKMLN complex can be reconstituted in an approximate ratio of 1:1:1:1:1:1:1 and a single CENP-A nucleosome core particle can bind two CENP-LN or CHIKMLN complexes (Weir et al., 2016). Whereas, CENP-O/P/Q/U/R are proposed to self-assemble on kinetochores with varying stoichiometry (Eskat et al., 2012). To gains insights into stoichiometries of kinetochore proteins, a label-free quantitative proteomic approach was used to calculate iBAQ scores for all detected proteins. iBAQ scores corresponds to the sum of all the peptides intensities divided by the number of observable peptides of a protein and it is used as an efficient label-free quantification method to determine the stoichiometries of individual protein subunits within complexes (Fabre et al., 2014). The LFQ protein intensity for CENP-A^{Cnp1} in affinity purified GFP-CENP-A^{Cnp1} chromatin was much higher than any of the other kinetochore proteins detected (Table 3.1). iBAQ analysis revealed ≥20 times more molecules of CENP-A^{Cnp1} compared to any other kinetochore protein (data not shown). To explain this discrepancy, immunoprecipitation of other kinetochore proteins was performed to find conditions that gave the most consistent LFQ intensities for kinetochore proteins. Therefore, affinity purification of CENP-Q^{Fta7}-FLAG, CENP-U^{Mis17}-GFP and CENP-N^{Mis15}-GFP was performed and LFQ intensities of one experiment are shown in Table 3.1 (Gabor Varga assisted with the affinity purification of CENP-Q^{Fta7}-FLAG and CENP-U^{Mis17}-GFP). CENP-Q^{Fta7} affinity purification only allowed enrichment of CENP-LN and CENP-OPQU complexes with Fta4/Fta6/Cnl2 while no CENP-A^{Cnp1} was co-immunopurified. A greater number of kinetochore proteins were enriched in affinity purifications of CENP-U^{Mis17}-GFP (Table 3.1). CENP-N^{Mis15}-GFP affinity purification gave the most consistent result with all inner kinetochore proteins apart from CENP-W^{Wip1} enriched along with a few proteins from outer kinetochore NMS complex. To calculate the relative stoichiometries of these kinetochore proteins, three independent CENP-N^{Mis15}-GFP affinity purifications were performed along with the untagged control. The iBAQ scores were normalized to iBAQ score of CENP-N^{Mis15} to calculate relative stoichiometries of kinetochore proteins. Consistent with the analysis of *S. cerevisiae* (Hinshaw and Harrison, 2013) and human (Weir et al., 2016) kinetochores, CENP-L^{Fta1} and CENP-N^{Mis15} were present in a 1:1 ratio (Figure 3.6B). This suggests a close and strong association between CENP-N^{Mis15} and CENP-L^{Fta1} in fission yeast. Relative to CENP-LN complex, CENP-A^{Cnp1}

was present in 1:2 ratio while CENP-C^{Cnp3} was the least abundant inner kinetochore protein in the preparation. CENP-K^{Sim4} and CENP-H^{Fta3} amounts were close to CENP-LN complex while CENP-I^{Mis6} was relatively less abundant. CENP-S^{Mhf1}, CENP-T^{Cnp20} and CENP-X^{Mhf2} were present in a 1:1:1 ratio, while CENP-W^{Wip1} was the only inner kinetochore protein absent in this purified kinetochore complex. Interestingly, CENP-OPQU was enriched several fold more relative to the CENP-LN complex, however all of CENP-OPQU subunits were present in varying amounts. The Mis6-Sim4 complex subunits Fta4 and Cnl2 have been shown to interact in yeast two-hybrid (Y2H) assays suggesting direct association (Vo et al., 2016). Fta4 showed ~10 fold enrichment and Cnl2 showed ~7 fold enrichment compared to CENP-LN. The Fta6 subunit was relatively less abundant than CENP-LN complex suggesting weaker association with the Mis6-Sim4 complex. Outer kinetochore NMS complex proteins were either absent or present in only trace amounts. These results indicate that CENP-N^{Mis15} is closely associated with CENP-L^{Fta1} and present at same stoichiometric ratios in affinity selected kinetochores. Lower relative enrichments could be explained by less stable interactions while the higher relative enrichment of CENP-OPQU, Fta4 and Cnl2 needs further investigation. Protein cross-linking coupled with mass spectrometry (XL-MS) could be performed to accurately determine stoichiometries of kinetochore proteins in these kinetochore preparations and to map their interactions.

Post-translational modifications of kinetochore proteins

Post-translational modifications (PTM) of proteins play an important role in cellular functions by affecting protein folding, stability, conformation, etc. The proteome-wide analysis of PTMs, including serine (Ser), threonine (Thr), and tyrosine (Tyr) phosphorylation and lysine (Lys) ubiquitylation was performed for GFP-CENP-A^{Cnp1} and CENP-N^{Mis15}-GFP purified samples. 12 new phosphorylation sites were found in CENP-A^{Cnp1}, CENP-I^{Mis6}, CENP-P^{Fta2}, CENP-O^{Mal2}, CENP-C^{Cnp3}, CENP-N^{Mis15} and CENP-Q^{Fta7} (Table 3.4). Four phosphorylation sites in CENP-N^{Mis15} were previously detected (Kettenbach et al., 2015). Only one new acetylation site was detected in CENP-A^{Cnp1} (Table 3.5). 22 new ubiquitylation sites were detected in CENP-P^{Fta2}, CENP-O^{Mal2}, CENP-A^{Cnp1}, CENP-C^{Cnp3} and CENP-Q^{Fta7} (Table 3.6). 9 new methylation sites including mono/di/tri-methylation were detected in CENP-I^{Mis6}, CENP-U^{Mal2}, Mis13 and Ndc80 (Table 3.7). 4 new sumoylation sites were detected in CENP-C^{Cnp3}, CENP-T^{Cnp20} and Mis14 (Table 3.7). The functional relevance of these

post-translational modifications requires further analysis. Ubiquitylation of CENP-A^{Cnp1} is discussed in chapter 6.

Table 3.1: LFQ intensities of kinetochore proteins in affinity purified CENP-A^{Cnp1}, CENP-Q^{Fta7}, CENP-U^{Mis17} and CENP-N^{Mis15} complex.

Sub complex	Protein	GFP-CENP-A^{Cnp1}	CENP-Q^{Fta7} -FLAG	CENP-U^{Mis17} -GFP	CENP-N^{Mis15} -GFP
		LFQ protein intensity			
Inner Kinetochore Complex	CENP-A^{Cnp1}	3E+10	-	2E+07	4E+07
	CENP-C^{Cnp3}	2E+09	-	1E+06	2E+06
	CENP-L^{Fta1}	3E+09	2E+06	9E+07	2E+08
	CENP-N^{Mis15}	8E+09	5E+06	4E+08	4E+08
	CENP-O^{Mal2}	8E+09	5E+08	7E+08	2E+09
	CENP-P^{Fta2}	4E+09	3E+08	7E+08	1E+09
	CENP-Q^{Fta7}	3E+09	3E+08	2E+08	6E+08
	CENP-U^{Mis17}	6E+09	2E+08	1E+09	8E+08
	CENP-H^{Fta3}	3E+09	-	3E+07	1E+08
	CENP-I^{Mis6}	8E+09	-	1E+08	2E+08
	CENP-K^{Sim4}	4E+09	-	1E+08	2E+08
	CENP-S^{Mhf1}	3E+09	-	-	2E+07
	CENP-T^{Cnp20}	7E+09	-	2E+07	8E+07
	CENP-X^{Mhf2}	1E+09	-	-	8E+06
	CENP-W^{Wip1}	8E+08	-	-	-
	Fta4	4E+09	2E+08	4E+08	2E+09
	Fta6	6E+08	2E+08	-	1E+07
	Cnl2	7E+09	8E+06	9E+08	2E+09
Outer Kinetochore NMS Complex	Ndc80	4E+08	-	-	3E+06
	Nuf2	2E+08	-	-	2E+06
	Spc24	2E+08	-	-	-
	Spc25	2E+08	-	-	8E+05
	Mis12	7E+07	-	-	-
	Mis13	2E+08	-	-	-
	Mis14	1E+08	-	-	-
	Nnf1	8E+07	-	-	-
	Spc7	4E+08	-	-	-
	Sos7	2E+08	-	-	-

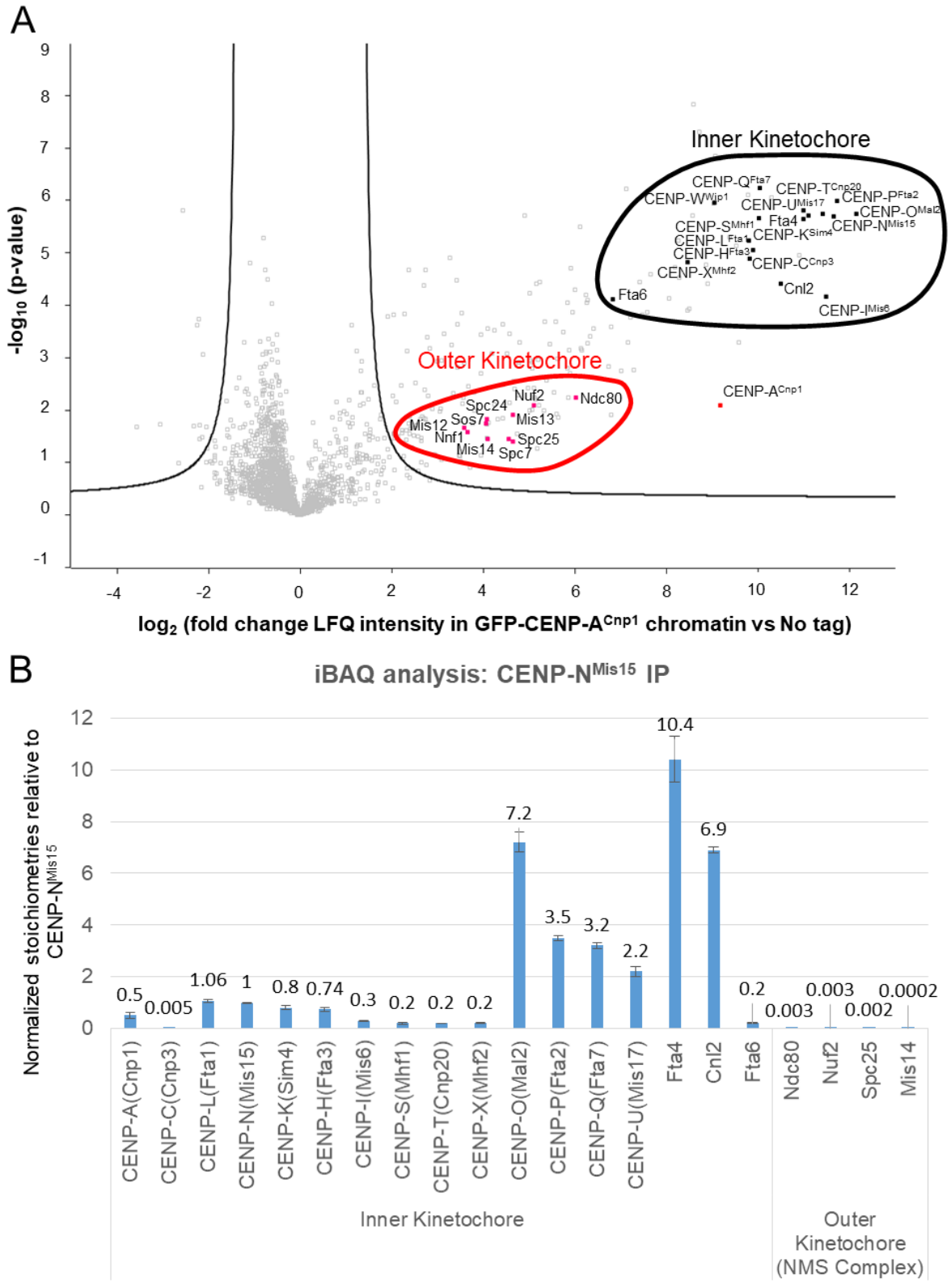

Figure 3.6: Inner and outer kinetochore proteins are two sub-complexes of the kinetochore
(A) Volcano plot of CENP-A^{Cnp1}-associated proteins relative to untagged control. Inner kinetochore proteins have similar but higher enrichments while outer kinetochore proteins have similar but lower enrichment, suggesting two different subcomplexes of the kinetochore. (B) Stoichiometries of kinetochore proteins relative to CENP-N^{Mis15} as indicated by the iBAQ analysis.

3.2.4 Characterization of CENP-A^{Cnp1}-associated chromatin during metaphase by LC-MS/MS

The 16-subunit Constitutive Centromere-Associated Network (CCAN) complex is known to localize at centromeres and provide the foundation for outer kinetochore assembly on the underlying CENP-A chromatin (Cheeseman and Desai, 2008). Similarly in fission yeast, CCAN proteins are also localized at the centromere throughout the cell cycle. Outer kinetochore proteins of the DASH complex (Ask1, Dam1, Dad2 and Spc34) only localize at kinetochores during mitosis (Liu et al., 2005). Although kinetochore proteins are well studied and they can be divided into several subcomplexes, it remains unclear how kinetochore protein complex composition and organization varies as the cell cycle progresses. To address this, the CENP-A^{Cnp1} proteome was analyzed from asynchronous cells and mitotically arrested cells. Cells with *slp1*$^{+}$ gene (required for the metaphase to anaphase transition) under a thiamine repressible promoter were blocked in metaphase by addition of thiamine. After three hour incubation in presence of thiamine, 100% of the cells (n=500) were blocked in metaphase (Figure 3.7 A and B). GFP-CENP-A^{Cnp1} chromatin was immunopurified and LC-MS/MS analysis was performed. All kinetochore proteins from the inner kinetochore and outer kinetochore NMS complex were isolated from both asynchronous and mitotic cells (Table 3.2). The DASH complex proteins, Duo1, Ask1, Dam1, Spc19 and Spc34 were only enriched in GFP-CENP-A^{Cnp1} chromatin isolated from mitotic cells. Dad2-5 were absent in both purifications while Dad1 was absent in mitotic kinetochore purification. The presence of DASH complex proteins validate purification of mitotic CENP-A^{Cnp1} chromatin-associated proteins as it appears to be distinct from CENP-A^{Cnp1} chromatin isolated from asynchronous cell cultures. More detailed analysis of the mitotic CENP-A^{Cnp1} chromatin preparations is required to assess differences in the stoichiometries of kinetochore proteins and centromere-associated proteins compared to preparations from interphase cells.

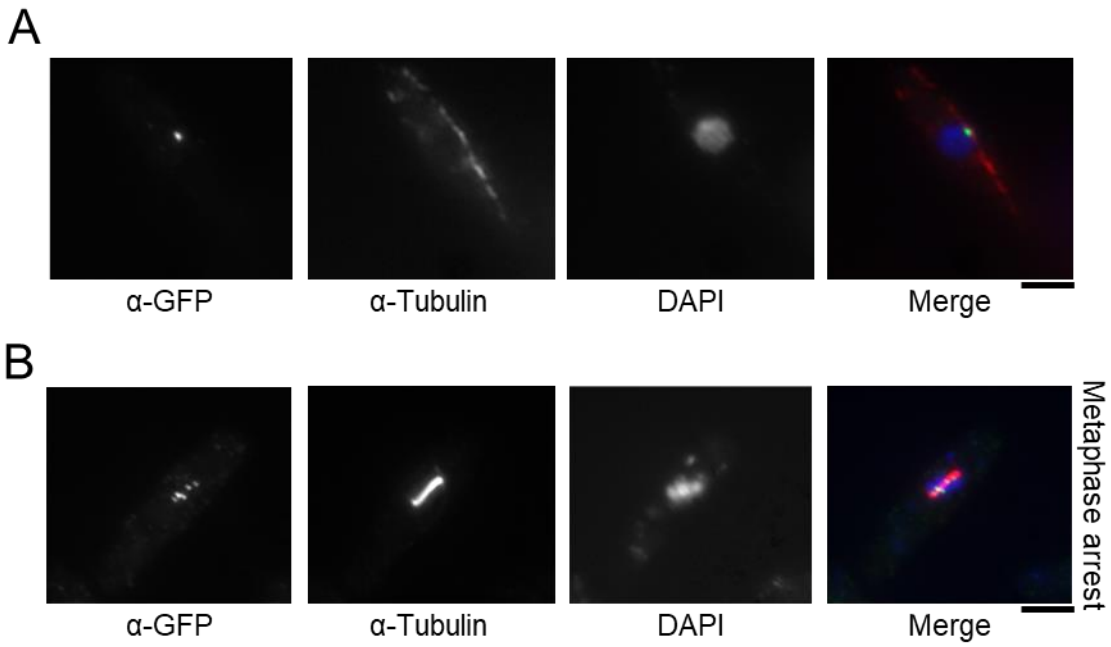

Figure 3.7: Metaphase arrested cells for isolation of mitotic-kinetochore complex. (A) Interphase fission yeast cell. Bar: 5 µm. (B) Cells with Pnmt41-Slp1 were blocked in metaphase after three hour incubation in thiamine-containing medium. Green: GFP-CENP-A^{Cnp1}, red: Tubulin and blue: DAPI. Bar: 5 µm.

Table 3.2: DASH complex proteins are enriched in GFP-CENP-A^{Cnp1} chromatin affinity purification from mitotic cells.

Sub complex	Protein	Asynchronous cells	Mitotic cells (Metaphase arrest)
Inner Kinetochore Complex	CENP-A^{Cnp1}	Present	Present
	CENP-C^{Cnp3}	Present	Present
	CENP-L^{Fta1}	Present	Present
	CENP-N^{Mis15}	Present	Present
	CENP-O^{Mal2}	Present	Present
	CENP-P^{Fta2}	Present	Present
	CENP-Q^{Fta7}	Present	Present
	CENP-U^{Mis17}	Present	Present
	CENP-H^{Fta3}	Present	Present
	CENP-I^{Mis6}	Present	Present
	CENP-K^{Sim4}	Present	Present
	CENP-S^{Mhf1}	Present	Present
	CENP-T^{Cnp20}	Present	Present
	CENP-X^{Mhf2}	Present	Present
	CENP-W^{Wip1}	Present	Present
	Fta4	Present	Present
	Fta6	Present	Present
	Cnl2	Present	Present
Outer Kinetochore (NMS) Complex	Ndc80	Present	Present
	Nuf2	Present	Present
	Spc24	Present	Present
	Spc25	Present	Present
	Mis12	Present	Present
	Mis13	Present	Present
	Mis14	Present	Present
	Nnf1	Present	Present
	Spc7	Present	Present
	Sos7	Present	Present
DASH complex (Dad2-5 are absent in both)	Duo1	Absent	Present
	Dam1	Absent	Present
	Ask1	Absent	Present
	Spc19	Absent	Present
	Spc34	Absent	Present
	Dad1	Present	Absent

3.2.5 Origin replication complex proteins are enriched at the centromere

The Origin Recognition Complex (ORC) is a six-subunit complex which recognizes and binds to replication origin sites in an ATP-dependent manner and serves as a scaffold for the assembly of other key replication initiation factors (Bell, 2002). It was identified as a factor that specifically binds to the yeast replication origions (Bell and Stillman, 1992). Since then ORC subunits have been implicated in diverse non-replication roles (Sasaki and Gilbert, 2007). Orc2 has been detected at centromeres on human and mouse metaphase chromosomes (Prasanth et al., 2004). In human and *Drosophila* cells, Orc2 was found to localize to heterochromatin (Prasanth et al., 2010; Pak et al., 1997). Thus ORC may play a conserved role with respect to heterochromatin. Interestingly, depletion of Orc2 was found to disrupt heterochromatin organization, spindle integrity, chromosome segregation and condensation (Prasanth et al., 2004; Auth et al., 2006). In fission yeast, despite the passive replication of central domain DNA from replication forks originating from within the flanking outer repeats, ORC subunits have been shown to be enriched at central domains DNA (Kim et al., 2003; Hayashi et al., 2007).

LC-MS/MS analysis CENP-A^{Cnp1}-associated chromatin compared to the untagged control showed >5 fold enrichment of Orc1, Orc2, Orc3, Orc4, Orc5 and Orc6 (Figure 3.8 A). Interestingly, CENP-A^{Cnp1}-associated chromatin compared to the histone H3.2-associated chromatin control showed no such enrichment and most ORC subunits (Orc2, Orc3, Orc4, Orc5 and Orc6) were enriched in histone H3.2-associated chromatin (Figure 3.8 B). This is presumably because of the binding of ORC to DNA replication origins distributed throughout the genome (Hayashi et al., 2007). Due to their known association with centromeric chromatin, ORC subunits were used to validate enrichment of centromeric chromatin-binding protein in GFP-CENP-A^{Cnp1} IPs.

The association of ORC with the central domain of fission yeast centromeres was determined using a strain containing HA tagged Orc4 (a DNA binding subunit of ORC containing nine repeats of AT-hook motifs). ChIP-qPCR showed that Orc4-HA was ~10 fold enriched within cc2 relative to a non-origin locus (*nonARS*) (Figure 3.8 C). Orc4 enrichment in the central domain were significantly enriched compared to a known replication origin ARS2004. To gain further insight into centromere-wide localization of Orc4, high resolution mapping of Orc4 and GFP-CENP-A^{Cnp1} was

performed using ChIP-Exo (Nexus). ChIP-Exo (Nexus) has been shown to provide better resolution and specificity compared to existing ChIP protocols (He et al., 2015). Orc4 binding sites were found to be distributed throughout the entire central domain (Figure 3.8 D; these analysis performed in collaboration with Manu Shukla and Nick Toda). Consistent with Orc4-HA qChIP, high levels of enrichment of Orc4 was observed in all centromeres compared to an adjacent replication origin ARSII-1589. Together, these observations confirm that Orc4 is highly enriched with CENP-A^{Cnp1} chromatin at fission yeast centromeres. Thus ORC proteins are an excellent control for the non-kinetochore GFP-CENP-A^{Cnp1} chromatin-associated proteins.

Analysis of ORC proteins in fission yeast confirmed its localization at the central domain by ChIP- qPCR and ChIP-Exo (Nexus). Despite the high enrichment of central domain centromere DNA in Orc4-HA ChIP and the abundance of ORC proteins associated with affinity selected CENP-A^{Cnp1} chromatin, ORC proteins display greater relative enrichment in histone H3.2-associated chromatin which is possibily due ORC binding to replication origins throughout the genome. Enrichment of ORC subunits in CENP-A^{Cnp1} chromatin preparations validates the comparison of proteins enriched in GFP-CENP-A^{Cnp1} AP-MS with the untagged control rather than H3.2-GFP to identify general chromatin factors that are also enriched in CENP-A^{Cnp1} chromatin.

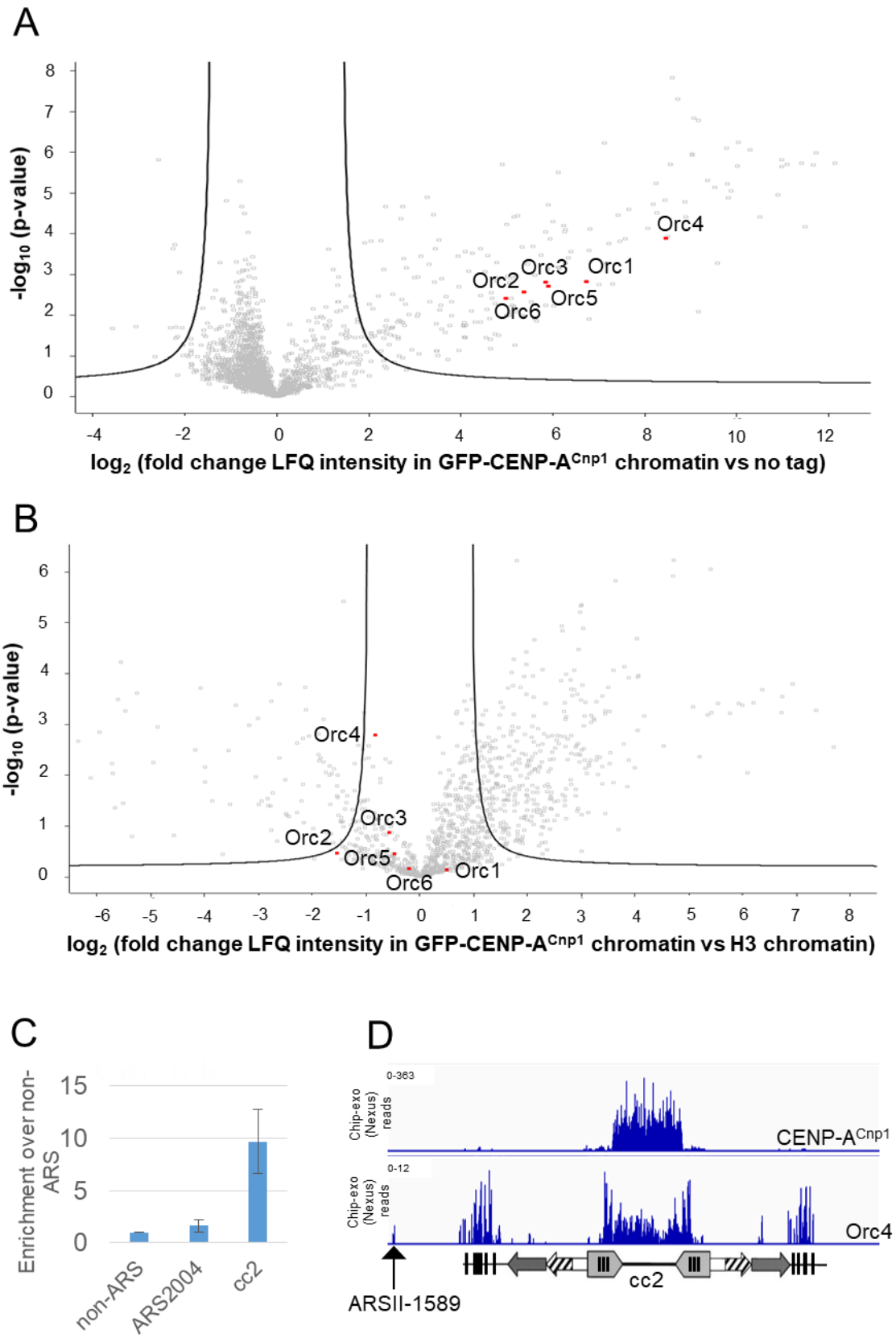
A
-log10 (p-value)
Orc4
Orc3
Orc1
Orc2
Orc5
Orc6
log2 (fold change LFQ intensity in GFP-CENP-ACnp1 chromatin vs no tag)
B
-log10 (p-value)
Orc4
Orc3
Orc2
Orc5
Orc6
Orc1
log2 (fold change LFQ intensity in GFP-CENP-ACnp1 chromatin vs H3 chromatin)
C
Enrichment over non-ARS
non-ARS
ARS2004
cc2
D
Chip-exo (Nexus) reads
CENP-ACnp1
Orc4
cc2
ARSII-1589

Figure 3.8: Origin replication proteins are enriched at centromeres

(A) Volcano plot of proteins associated with CENP-A^{Cnp1} chromatin relative to untagged control. Orc1, Orc2, Orc3, Orc4, Orc5 and Or6 are labelled. They showed enrichment in CENP-A^{Cnp1} chromatin compared to untagged control. (B) Volcano plot of proteins associated with CENP-A^{Cnp1} chromatin relative to histone H3.2 chromatin control. Orc1, Orc2, Orc3, Orc4, Orc5 and Or6 are labelled. They showed no significant relative enrichment in CENP-A^{Cnp1} chromatin and histone H3.2 chromatin control. (C) Orc4 is associated with origin ARS2004 and highly enriched at the central domain (*cc2*) relative to non-origin locus (non-ARS) (D) Chip-exo (Nexus) read cound form GFP-CENP-A^{Cnp1} and Orc4-HA affinity purification. Orc4 associate with the whole central domain sequence and more enriched compared to a likely origin ARSII-1589.

3.2.6 Ino80 complex subunits are enriched in CENP-A^{Cnp1} chromatin

The Ino80 (inositol-requiring mutant 80) ATP-dependent chromatin-remodeling complex functions in transcriptional regulation, DNA damage response, and replication (Hogan et al., 2010). In budding yeast, the Ino80 complex is involved in maintaining chromatin structure at pericentric chromatin but not the CENP-A^{Cse4} nucleosome (Chambers et al., 2012). In fission yeast, the Ino80 complex subunits have a genome-wide distribution and they also localize to the central domain of centromeres. The Ino80 complex has been proposed to evict histone H3 from chromatin thereby promoting CENP-A^{Cnp1} chromatin assembly (Hogan et al., 2010; Choi et al., 2017).

All 15 subunits of the Ino80 complex were found to be enriched in GFP-CENP-A^{Cnp1} chromatin (Figure 3.9 A). Comparison of GFP-CENP-A^{Cnp1} affinity selected chromatin with the untagged control showed that the Ino80 complex subunits were >4 fold enriched. Arp42 was only 2 fold enriched but it is known to be a component of other complexes (Monahan et al., 2008). Analysis of Ino80 complex subunits in CENP-A^{Cnp1} chromatin compared to the histone H3.2 chromatin control showed no such enrichment (Figure 3.9 B). All Ino80 subunits were enriched in histone H3.2 chromatin. Ino80 and its subunits are distributed at genes and other locus throughout the genome (Hogan et al., 2010; Choi et al., 2017). Due to their known association and function at centromeres, Ino80 complex was used to validate enrichment of centromeric chromatin binding protein in GFP-CENP-A^{Cnp1} IPs. Similar to the enrichment of ORC

subunits, comparison with H3.2-GFP suppresses enrichment of Ino80 proteins at centromeres.

These analysis demonstrate that the comparison of CENP-A^{Cnp1} chromatin vs histone H3.2 chromatin control certainly identify enrichment of kinetochore proteins but the enrichment of more general chromatin factors like ORC subunits and Ino80 subunits cannot be detected. Therefore comparison of CENP-A^{Cnp1} chromatin with untagged control which is likely to identify additional general chromatin factors in CENP-A^{Cnp1} purifications was preferred for candidate selection of potential centromere-associated proteins.

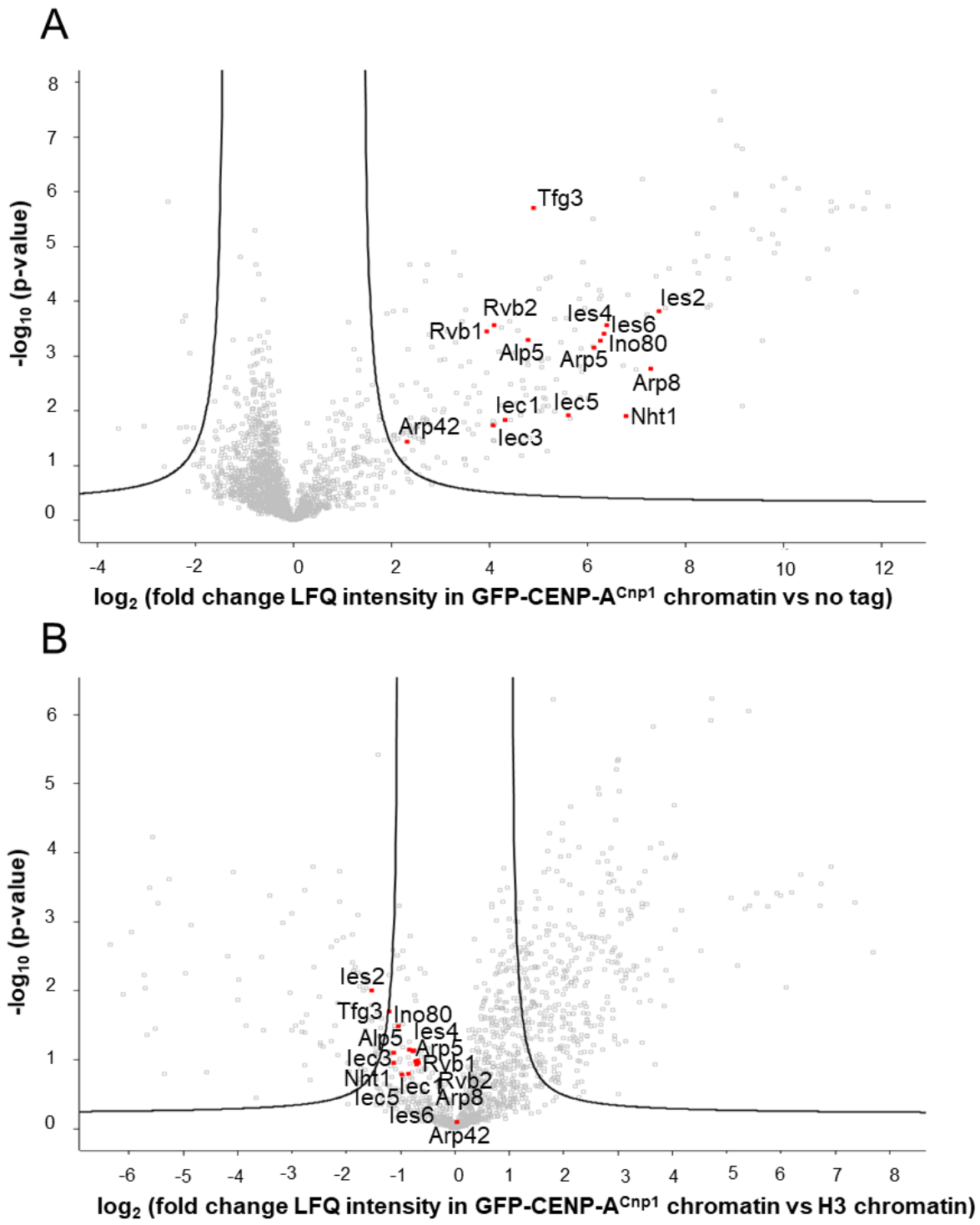

Figure 3.9: Ino80 complex subunits are enriched with CENP-A^{Cnp1} chromatin

(A) Volcano plot of proteins associated with CENP-A^{Cnp1} chromatin relative to untagged control (4 biological replicates). All Ino80 complex subunits are labelled and showed enrichment over untagged control. (B) Volcano plot of proteins associated with CENP-A^{Cnp1} chromatin relative to histone H3.2 chromatin control (4 biological replicates). All Ino80 complex subunits are labelled and showed enrichment in histone H3.2 chromatin-associated complex.

3.2.7 Identification of potential centromere-associated proteins by label-free quantification

Other potential CENP-A^{Cnp1} chromatin enriched proteins were identified by comparison with untagged control. A student t-test was performed to determine the significance of change in LFQ intensities of all proteins detected in CENP-A^{Cnp1} chromatin samples vs control samples. Based on this relative-enrichments and student t-test p values, 199 proteins were identified that showed at least two-fold enrichment in CENP-A^{Cnp1} chromatin over the untagged control. The available literature was integrated for any prior knowledge concerning these proteins in order to categorize these proteins with respect to future analysis. GO term analysis was performed to categorize these proteins base on their previous known function (Table 3.3). A high proportion of these candidates were assigned a role in chromatin organization and transcriptional regulation. To further investigate the intricate network of interactions between these proteins STRING analysis was performed. The STRING database was used to collect and integrate functional interactions between all 199 proteins by combining all information concerning these proteins from different experimental and curated databases (BIND, DIP, GRID, HPRD, IntAct, MINT, PID, Biocarta, BioCyc, GO, KEGG, and Reactome; Szklarczyk et al., 2017). A minimum required interaction score of 0.400 (medium confidence) was used for these analysis. STRING database analysis recognized different clusters indicating copurification of protein complex assemblies (Figure 3.10); kinetochore, origin recognition complex (ORC), Ino80 complex, facilitates chromatin transcription (FACT) complex, remodelling the structure of chromatin (RSC) complex, histone deacetylase Rpd3S complex, DNA-directed RNA pol I, II and III complex and TFIIIB/TFIIIC complex. Many proteins were not connected to any kinetochore protein which may be due to a lack of fission yeast CENP-A^{Cnp1} proteome studies prior to this work.

Non-essential genes were selected for further investigation and gene knockouts were obtained from the bioneer deletion library version 2 (http://pombe.bioneer.co.kr/). Out of 199 CENP-A^{Cnp1} chromatin enriched proteins, 78 proteins were non-essential for cell viability and 55 corresponding gene knockouts were viable in bioneer deletion library version 2. To determine whether the correct genes had been deleted in these bioneer strains, colony PCR was performed. Surprisingly, only 23 strains of these 55 strains showed bands that confirmed the gene knockout (data not shown). These 23

mutants were selected for further investigation while other 55 non-essential genes (not included in this investigation) should be knocked out and investigated for their role in centromere function. All 23 proteins showed at least 2 fold enrichment in CENP-A^{Cnp1} chromatin compared to the untagged control (Figure 3.11 A). When compared to histone H3.2 chromatin control only 20 out of 23 proteins passed the threshold and only eight proteins were relatively enriched in CENP-A^{Cnp1} chromatin (Figure 3.9 B). Heterochromatin protein Swi6 was the most abundant candidate protein followed by ubiquitin-like protein modifier Pmt3, repair protein Msh6, kinetochore protein Fta6 and Ino80 complex-associated protein Hap2. E3 ubiquitin-protein ligase Dbl5, zf-PARP type zinc finger protein Hpz1 and DNA topoisomerase Top1 showed lower enrichments in CENP-A^{Cnp1} chromatin. While the other 12 proteins showed similar enrichments in both samples or greater enrichment in H3.2 chromatin. All 23 non-essential proteins were chosen for further analysis (Chapter 4).

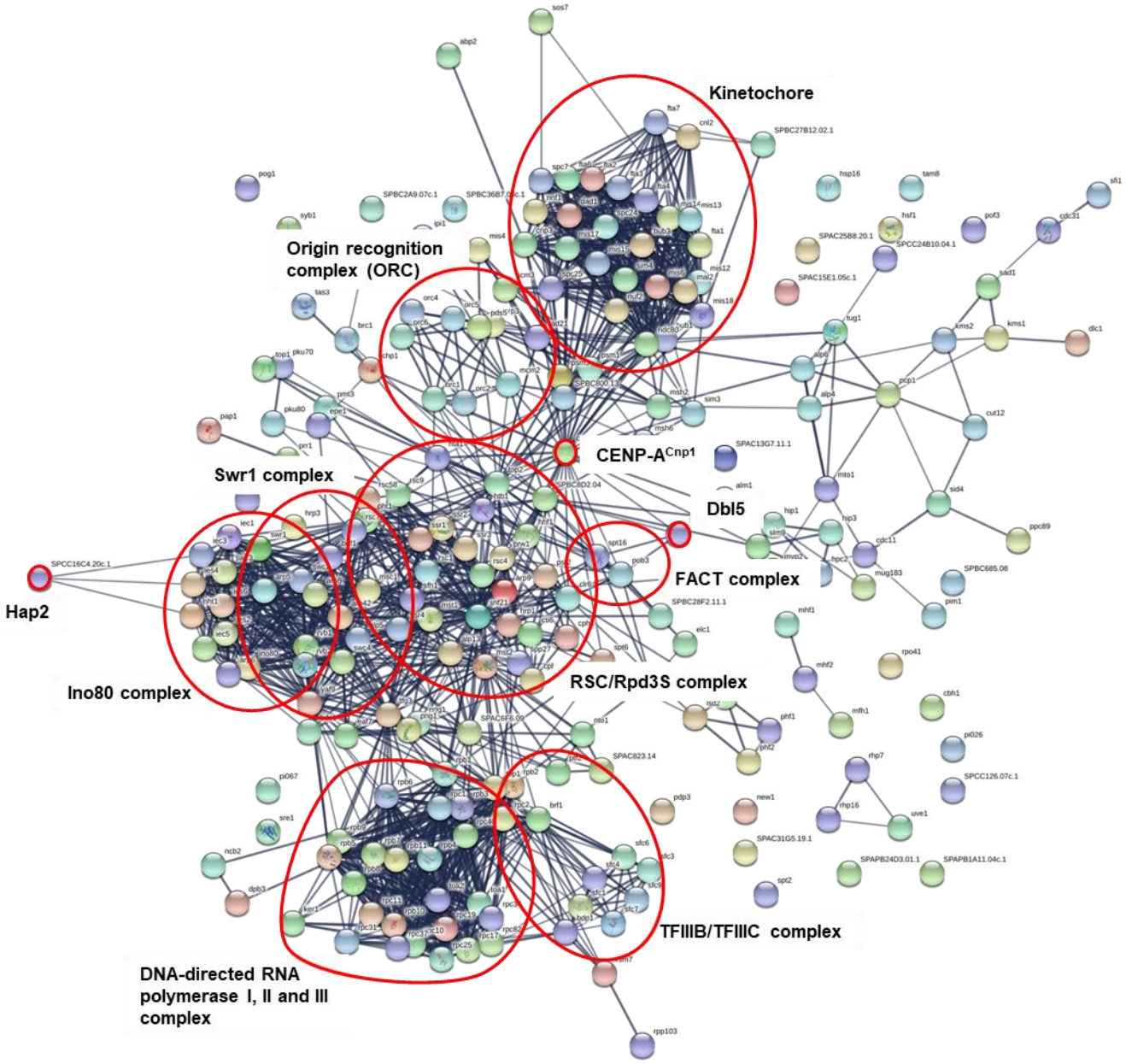

Figure 3.10: String database network indicates known relationships of proteins enriched with CENP-A^{Cnp1}

All proteins (199) having more than two-fold enrichment with CENP-A^{Cnp1} chromatin relative to untagged control are taken for string analysis. Thickness of blue line indicates confidence score of the data support for the interaction. Minimum required interaction score of medium confidence 0.400 was chosen for the analysis. Many complex assemblies are co-purified with CENP-A^{Cnp1} chromatin.

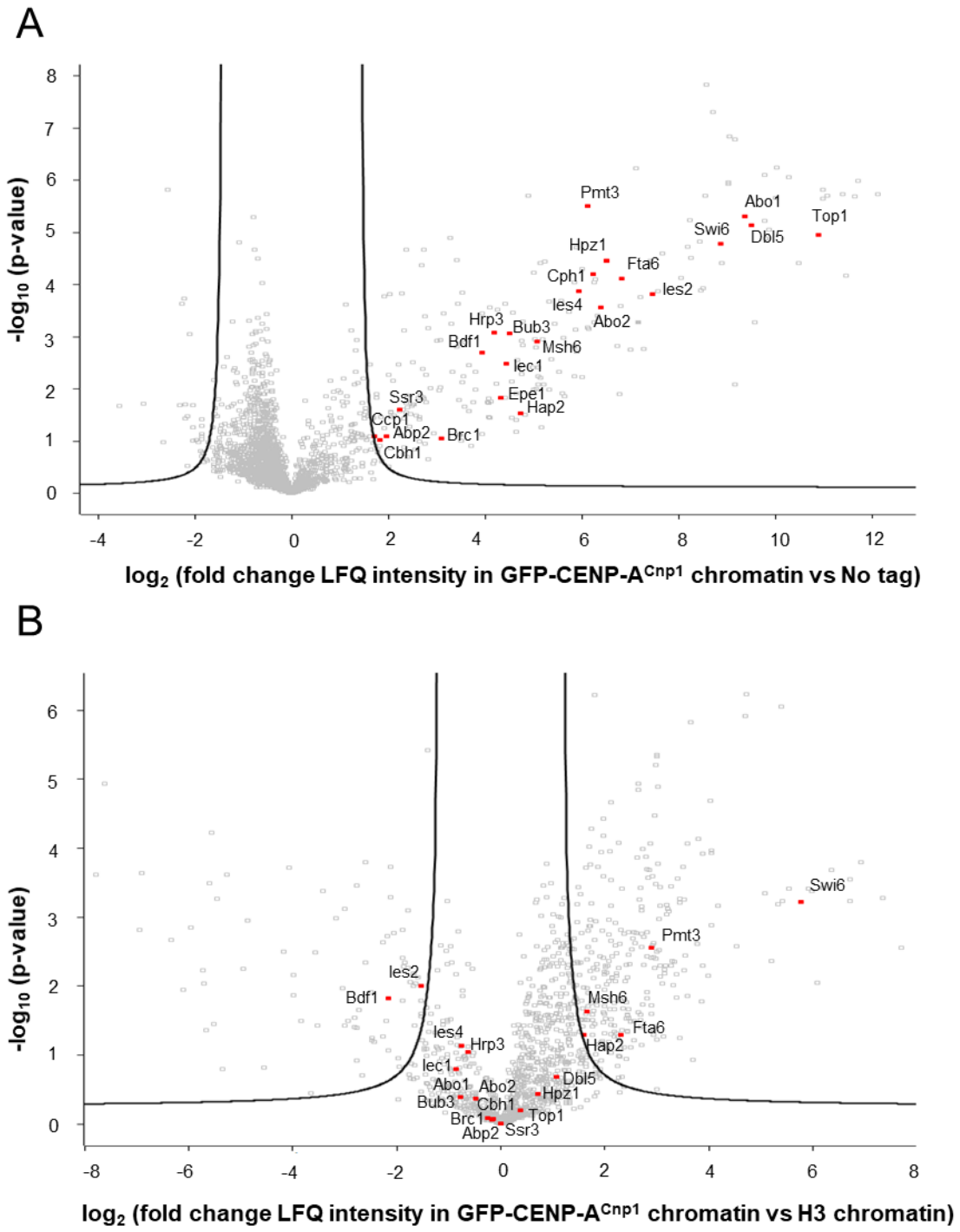

Figure 3.11: Relative enrichment of selected candidate proteins in CENP-A^{Cnp1} chromatin

(A) Volcano plot of proteins associated with CENP-A^{Cnp1} chromatin relative to histone H3.2 chromatin control (4 biological replicates). Selected candidate proteins are labelled and show enrichment over untagged control. (B) Volcano plot of proteins associated with CENP-A^{Cnp1} chromatin relative to histone H3.2 chromatin control (4 biological replicates). 23 selected candidate proteins are labelled.

3.3 Discussion

The aim of this work is to better understand the centromere proteome and characterize non-kinetochore CENP-A^{Cnp1} chromatin-associated proteins in fission yeast. This study comprises the first proteomic screen to identify CENP-A^{Cnp1} chromatin-associated proteins in fission yeast. A protocol was developed that uses GFP-CENP-A^{Cnp1} as bait to affinity select interactors. In order to isolate GFP-CENP-A^{Cnp1} chromatin and kinetochore proteins in its native state, chromatin was solubilized and GFP-CENP-A^{Cnp1} chromatin was affinity purified. A common issue of affinity purification is the co-enrichment of proteins that non-specifically binds to the affinity matrix. Untagged chromatin was included as a control to filter out generic immunoprecipitation background in this proteomic screen. Apart from unspecific binding to the affinity matrix, CENP-A^{Cnp1} chromatin affinity selection was also expected to include general chromatin proteins. Therefore, GFP tagged-histone H3.2 chromatin was included to discriminate centromere enriched factors from general chromatin components.

The affinity selection protocol described in Figure 3.1 was standardized for low abundance complexes. Because high salt conditions (~300mM NaCl) previously used to purify human and *Drosophila* CENP-A^{Cnp1}-associated proteins (Foltz et al., 2006; Barth et al., 2014) may disrupt unstable and dynamic protein-protein interactions, a low salt concentration of 50mM NaCl was used during digestion, affinity purification and washes. The affinity selection of CENP-A^{Cnp1} chromatin complex was efficient and allowed enrichment of subunits of inner and outer kinetochore complex thus validating the purification of CENP-A/kinetochore complex (Figure 3.5; Table 3.1). CCAN proteins were found to have higher enrichments than the outer NMS kinetochore proteins suggesting that CCAN proteins make more stable interactions with CENP-A^{Cnp1} than NMS proteins (Figure 3.6 A).

Label-free quantitative proteomic approaches have been developed to study the composition of protein complexes (Fabre et al., 2014). In humans, CENP-CHIKMLN have predicted stoichiometry of 1:1:1:1:1:1:1 (Weir et al., 2016). In affinity purified CENP-N^{Mis15} samples, CENP-N^{Mis15} and CENP-L^{Fta1} were present in a 1:1 ratio which is consistent with human kinetochore (Figure 3.6B). Compared to CENP-N^{Mis15}, slightly lower stoichiometries were detected for CENP-K^{Sim4} and CENP-H^{Fta3}. CENP-A^{Cnp1}

was present in 1:2 ratio relative to CENP-N^{Mis15}. Interestingly, CENP-OPQU complex, Fta4 and Cnl2 were present in much higher amounts than CENP-N^{Mis15}. Less stable dynamic interactions might explain lower relative stoichiometries for CENP-CHIKM. Protein cross-linking is commonly used to form bridges between lysine residues that are in close proximity to each other (Young et al., 2000). This can provide site-specific structural restraints that can then be used for fold identification, identification of protein–protein interactions and characterization of the subunit architecture of protein complexes (Merkley et al., 2014). For more accurate stoichiometric analysis of the kinetochore proteins with affinity selected CENP-A^{Cnp1} chromatin, a crosslinking step could be included in the protocol to stabilize more dynamic protein-protein interactions.

Mass spectrometric studies provide advantage over genetic screens as they detect interacting proteins and provide information about post-translational modifications of these proteins. Such PTMs may confer an important role in regulating protein folding, stability and interactions (Hennrich and Gavin, 2015). The analysis performed identified 12 phosphorylation, 1 acetylation, 22 ubiquitination, 9 methylation and 4 sumoylation sites on kinetochore proteins that were previously unknown. Ubiquitylation and acetylation of CENP-A^{Cnp1} on lys4 and phosphorylation of CENP-A^{Cnp1} on Ser5 was also identified. Point mutations of these residues should be performed to evaluate their influence on kinetochore structure and function.

In asynchronous fission yeast cultures, only 5-10% of the cells are undergoing mitosis. Therefore, affinity selection of CENP-A^{Cnp1} chromatin/kinetochores from asynchronous cultures primarily isolate non-mitotic kinetochore complexes. CENP-A^{Cnp1} chromatin affinity selected from mitotic cells allowed determination of a higher number of outer kinetochore proteins including proteins from DASH complex that is known to associate with kinetochore only during mitosis (Liu et al., 2005). This observation suggests that the CENP-A^{Cnp1}-kinetochore complex isolated from the mitotic cells is distinct from the CENP-A^{Cnp1}-kinetochore complex isolated form asynchronous cells (Table 3.2). Comprehensive LC-MS/MS analysis of affinity selected mitotic CENP-A^{Cnp1}-kinetochores is required to fully determine its distinct composition compared to non-mitotic CENP-A^{Cnp1}-kinetochore complex. Similar mass spectrometric analysis could be performed on late S/ early G2 cells to study whether any proteins are recruited specifically during this stage when CENP-A^{Cnp1} is deposited at centromeres in fission yeast.

Stoichiometric analysis of the inner kinetochore proteins showed strong association of CENP-N^{Mis15} and CENP-L^{Fta1} with equal amounts present in the affinity selected CENP-N^{Mis15} (Figure 3.6). While amount of CENP-A^{Cnp1} was exactly half compared to CENP-LN complex. This is consistent with *in vitro* assemblies in human kinetochore proteins (Weir et al., 2016). Interestingly, relatively higher amounts of CENP-OPQU, Fta4 and Cnl2 were purified with CENP-N^{Mis15}, suggesting a complex organization of fission yeast kinetochore proteins. The XL-MS analysis could shed light on this complexity and also provide information about interactions of kinetochore protein in fission yeast.

Histone H3 affinity selection has been used previously as a control for CENP-A purifications (Foltz et al., 2006; Barth et al., 2014). ORC and Ino80 subunits, despite their enrichment in CENP-A^{Cnp1} chromatin compared to untagged control, they are relatively more enriched in H3 chromatin (Figure 3.8 and Figure 3.9), suggesting that analysis of CENP-A^{Cnp1} chromatin vs untagged control is more likely to identify CENP-A^{Cnp1} enriched proteins compared to H3.2-GFP control. Detailed analysis of multiple CENP-A^{Cnp1} chromatin isolates compared to untagged control allowed identification of 199 proteins with ≥2 fold enrichment in CENP-A^{Cnp1} chromatin. String analysis revealed co-purification of proteins that clusters into functional groups (Figure 3.10). Potential candidate proteins were selected based on their enrichment in CENP-A^{Cnp1} chromatin and presence of correct gene knockout strains in fission yeast gene deletion library. 23 non-essential candidate proteins were considered for assessing their role in centromere function.

In summary, the first proteomic study of fission yeast CENP-A^{Cnp1} chromatin proteome was performed. Together the analysis that CENP-A^{Cnp1}-kinetochore composition in fission yeast is more complex than anticipated.

Table 3.3: GO term analysis of CENP-A^{Cnp1} proteome

GO Term (GO ID)	GO Term Usage in Gene List
chromatin organization (GO:0006325)	84 of 199 genes, 42.21%
regulation of transcription, DNA-templated (GO:0006355)	67 of 199 genes, 33.67%
transcription, DNA-templated (GO:0006351)	49 of 199 genes, 24.62%
mitotic sister chromatid segregation (GO:0000070)	47 of 199 genes, 23.62%
protein-containing complex assembly (GO:0065003)	39 of 199 genes, 19.60%
DNA repair (GO:0006281)	22 of 199 genes, 11.06%
meiotic nuclear division (GO:0140013)	19 of 199 genes, 9.55%
DNA replication (GO:0006260)	16 of 199 genes, 8.04%
microtubule cytoskeleton organization (GO:0000226)	12 of 199 genes, 6.03%
DNA recombination (GO:0006310)	11 of 199 genes, 5.53%
regulation of mitotic cell cycle phase transition (GO:1901990)	9 of 199 genes, 4.52%
protein modification by small protein conjugation or removal (GO:0070647)	8 of 199 genes, 4.02%
mRNA metabolic process (GO:0016071)	7 of 199 genes, 3.52%
signaling (GO:0023052)	6 of 199 genes, 3.02%
mitotic cytokinesis (GO:0000281)	4 of 199 genes, 2.01%
nucleocytoplasmic transport (GO:0006913)	4 of 199 genes, 2.01%
telomere organization (GO:0032200)	4 of 199 genes, 2.01%
conjugation with cellular fusion (GO:0000747)	3 of 199 genes, 1.51%
actin cytoskeleton organization (GO:0030036)	3 of 199 genes, 1.51%
protein catabolic process (GO:0030163)	3 of 199 genes, 1.51%
mitochondrion organization (GO:0007005)	2 of 199 genes, 1.01%
establishment or maintenance of cell polarity (GO:0007163)	2 of 199 genes, 1.01%
protein folding (GO:0006457)	1 of 199 genes, 0.50%
apoptotic process (GO:0006915)	1 of 199 genes, 0.50%
lipid metabolic process (GO:0006629)	1 of 199 genes, 0.50%
ribosome biogenesis (GO:0042254)	1 of 199 genes, 0.50%
carbohydrate metabolic process (GO:0005975)	1 of 199 genes, 0.50%
tRNA metabolic process (GO:0006399)	1 of 199 genes, 0.50%
membrane organization (GO:0061024)	1 of 199 genes, 0.50%
mitochondrial gene expression (GO:0140053)	1 of 199 genes, 0.50%

Table 3.4: Phosphorylation sites identified on the CCAN proteins

Proteins	Positions within protein	Number of Phospho (STY)	Phospho (STY) Probabilities	
CENP-A^{Cnp1}	5	1	S(1)LMAEPGDPIPR	This study
CENP-I^{Mis6}	27, 28	2	NSENLS(0.982)S(0.577)S(0.441)KK	This study
CENP-P^{Fta2}	36	1	T(0.004)VAHRS(0.996)PNTTLNGMP	This study
CENP-O^{Mal2}	9	1	MDDEEGNAT(1)LIDEISVLEAR	This study
CENP-C^{Cnp3}	463	1	VDDPS(0.495)PS(0.505)IR	This study
CENP-U^{Mis17}	166	1	DNIETSDAYSSSILENS(1)PPNK	Kettenbach et al., 2015
CENP-U^{Mis17}	102	1	ENS(0.886)VS(0.047)S(0.067)IENV	Kettenbach et al., 2015
CENP-U^{Mis17}	104	1	ENS(0.028)VS(0.586)S(0.386)IENVSS	Kettenbach et al., 2015
CENP-U^{Mis17}	105	1	ENS(0.01)VS(0.115)S(0.875)IENVSSS	Kettenbach et al., 2015
CENP-N^{Mis15}	277	1	SPLDT(0.009)RPILS(0.937)DDNS(0.027)S(0.027)LIADSTQNCEK	This study
CENP-Q^{Fta7}	198, 200	2	PFT(0.961)KT(0.961)MQIHANKT(0.074)VQLS(0.002)QT(0.002)IQK	This study
CENP-Q^{Fta7}	36, 49	2	T(0.815)CS(0.184)RLVLNT(0.068)IKS(0.294)ET(0.638)R	This study
CENP-Q^{Fta7}	150	1	LHPY(1)LKKGLK	This study

Table 3.5: Acetylation sites identified on the CCAN proteins

Proteins	Positions within protein	Number of Acetyl (K)	Acetyl (K) Probabilities	
CENP-A^{Cnp1}	4	1	K(1)SLMAEPGDPIPRPR	This study

Table 3.6: Ubiquitylation sites identified on the CCAN proteins

Proteins	Positions within proteins	Number of GlyGly (K)	GlyGly (K) Probabilities	
CENP-P^{Fta2}	214	1	K(1)ELSSFSDSAIQCLDIVALLR	This study
CENP-O^{Mal2}	96	1	K(1)TGAIETAPSIPLLGVR	This study
CENP-O^{Mal2}	57	1	NLSVNNEFLK(1)ETPLNQPALHYDR	This study
CENP-O^{Mal2}	42	1	SLDNATLSDLVQK(0.996)PELSK(0.004)	This study
CENP-O^{Mal2}	47	1	SLDNATLSDLVQK(0.103)PELSK(0.856)NLSVNNEFLK(0.041)	This study
CENP-A^{Cnp1}	4	1	K(1)SLMAEPGDPIPRPR	This Study
CENP-C^{Cnp3}	217	1	DDNVQESPAFPDENITALQK(0.948)NVANFTSIK(0.052)	This Study
CENP-C^{Cnp3}	226	1	NVANFTSIK(1)DSGGR	This Study
CENP-C^{Cnp3}	452	1	IPALPEVK(1)QIIR	This Study
CENP-C^{Cnp3}	241	1	DNLYIQTISK(1)PR	This Study
CENP-C^{Cnp3}	564	1	EEPSFAAGVVEMPAGAEK(0.503)PVK(0.44)PSK(0.057)	This Study
CENP-C^{Cnp3}	333	1	EGESNPVVK(1)R	This Study
CENP-C^{Cnp3}	197	1	IPSSTPK(1)DDNVQESPAFPDENITALQK	This Study
CENP-C^{Cnp3}	359	1	LEIGNSVQTSEATQVK(0.974)GAK(0.026)	This Study
CENP-C^{Cnp3}	481	1	RSGVEIK(1)SNLEAK	This Study
CENP-C^{Cnp3}	313	1	TPNK(1)PLQESSINSVK	This Study
CENP-Q^{Fta7}	173	1	K(1)LNTEDSNTSK	This study
CENP-Q^{Fta7}	152, 153, 156	3	LHPYLK(1)K(1)GLK(1)	This study
CENP-Q^{Fta7}	199	1	PFTK(0.826)TMQIHANK(0.174)TVQLSQTIQK(0.001)	This study
CENP-Q^{Fta7}	217	1	TVQLSQTIQK(1)ATLLLQR	This study

Table 3.7: Methylation sites identified on the CCAN proteins

Proteins	Positions within proteins	Type	Methyl (K) Probabilities	
CENP-I^{Mis6}	529	mono-	LMDSR(1)IDAISK(1)	This study
CENP-I^{Mis6}	535	mono-	LMDSR(1)IDAISK(1)	This study
CENP-U^{Mis17}	11	mono-	MENNSHNVDER(0.999)R(0.949)	This study
CENP-U^{Mis17}	12	mono-	MENNSHNVDER(0.999)R(0.949)	This study
Mis13	203	di-	LTQLHNEEAAWR(1)	This study
CENP-I^{Mis6}	306	di-	NK(1)NVYYSR(1)	This study
CENP-I^{Mis6}	312	di-	NK(1)NVYYSR(1)	This study
CENP-U^{Mis17}	15	di-	MENNSHNVDER(0.001)R(0.051)AAR(0.947)	This study
Ndc80	314	tri-	TMQRDEVK(1)	This study

Table 3.8: Sumoylation sites identified on the CCAN proteins

Proteins	Positions within proteins	SUMO - QQTGG (K) Probabilities	
CENP-C^{Cnp3}	263	QNK(1)QK(1)EEK	This study
CENP-C^{Cnp3}	265	QNK(1)QK(1)EEK	This study
CENP-T^{Cnp20}	111	SQK(1)TPRLSSNK	This study
Mis14	154	NVK(1)DDYVSLQDK	This study

Chapter 4

Investigating CENP-A^{Cnp1} associated proteins for their role in centromere function

4.1 Introduction

CENP-A is the most consistent feature of the centromere and it is an epigenetic mark for determining centromere identity (Allshire and Karpen, 2008; Mendiburo et al., 2011). Centromeric sequence in general is neither necessary nor sufficient for centromere identity; also neocentromeres can be formed on noncentromeric DNA (Scott and Sullivan, 2014). Despite centromeric DNA sequence is not the sole determinant of centromere identity yet it provides a favorable environment for CENP-A^{Cnp1} deposition (Catania et al., 2015; Tong et al., 2018). This suggests that centromeric sequences might possess properties that promote CENP-A nucleosome incorporation, and whether or not these are involved in *de novo* CENP-A establishment remain to be experimentally addressed.

CENP-A chromatin might be regulated by transcription, nucleosome assembly/exchange and remodeling (Allshire and Karpen, 2008). In fission yeast, many factors are known to regulate CENP-A^{Cnp1} chromatin. Kinetochore proteins: CENP-C^{Cnp3},CENP-I^{Mis6}, CENP-K^{sim4}, CENP-N, CENP-U; CENP-A^{Cnp1} chaperone: HJURP^{Scm3}, NASP family chaperone: Sim3, Mis18 complex: Mis18, Mis16 and Mis19^{Eic1} are required for efficient deposition and maintenance of CENP-A^{Cnp1} at the centromere (Takahashi et al., 2000; Pidoux et al., 2003; Hayashi et al., 2004; Dunleavy et al., 2007; Fujita et al., 2007; Pidoux et al., 2009; Williams et al., 2009; Tanaka et al., 2009; Carroll et al., 2009; Moree et al., 2011; Hayashi et al., 2014; Subramanian et al., 2014). RNAPII transcription has been proposed to aid deposition of CENP-A^{Cnp1} by regulating nucleosome dynamics through FACT (facilitates chromatin transcription) and Clr6-CII complex (histone deacetylase) (Choi et al., 2012). Several ATP-dependent chromatin remodeling complexes like Ino80 complex and CHD family member Hrp1, have been proposed to regulate histone H3 dynamics thereby regulating centromere assembly and centromere function (Walfridsson et al., 2005; Choi et al., 2011; Choi et al., 2017).

Active centromeres can be established by introducing naked centromeric DNA sequences into cells (Hahnenberger et al., 1989; Harrington et al., 1997; Folco et al., 2008). In fission yeast, centromere domain sequence adjacent to H3K9me2-assembled chromatin is sufficient to promote de novo CENP-A^{Cnp1} establishment (Folco et al., 2008, Kagansky et al., 2009). The mechanism linking CENP-A^{Cnp1} establishment and heterochromatin requirement remains elusive.

Despite the knowledge of many factors required for the maintenance of CENP-A^{Cnp1} chromatin, not much is known about their contribution in the de novo establishment of CENP-A^{Cnp1} chromatin and other factors which might be responsible for de novo CENP-A^{Cnp1} establishment. Most research have been focused on factors required for the maintenance of CENP-A chromatin while studies on CENP-A establishment is underwhelming. Therefore, it is interesting to address if proteins enriched at the centromere might be involved in CENP-A^{Cnp1} establishment on naïve centromeric sequences.

In this chapter, I investigate the contribution of CENP-A^{Cnp1} chromatin-associated proteins obtained in my CENP-A^{Cnp1} AP-MS analysis (chapter 3) to the establishment of CENP-A^{Cnp1} chromatin on a naïve minichromosome containing a centromere sequence. For CENP-A^{Cnp1} chromatin-associated proteins I can envisage several scenarios: (a) they might be involved in centromere maintenance only, (b) they might be involved in centromere establishment and (c) they might be involved in both establishment and maintenance of centromeres. Therefore, along with *de novo* centromere establishment assay other functional assays were performed to have a better insight into centromere related function of CENP-A^{Cnp1}-associated proteins.

4.2 Results

4.2.1 Analysis of candidate gene deletion mutants to evaluate their role in centromere function

A. Centromere establishment assay

De novo centromere establishment was assessed for pcc2K" minichromosome. pcc2K" minichromosome has a fission yeast centromere *cc2* sequence along with part of *imr* sequence adjacent to a K" repeat. K" repeat is required for efficient segregation of the minichromosome as it is capable of heterochromatinization (Folco et al., 2008).

Endogenous *cc2* sequence was replaced with *cc1* sequence were transformed with pcc2K" minichromsome, therefore, *cc2* sequence of pcc2K" minichromosome provides an ectopic naïve template for chromatinization and segregation through generations.

After transformation of pcc2K" minichromosome into the fission yeast cells (*cc2Δ::cc1*), transformants were grown and selected for the presence of the minichromosome. Colonies were replica plated on low-ade YES plates without selection. Transformant with no centromere establishment on the minichromosomes will lose the minichromosome during subsequent generations and form red colonies. Transformants which have integrated the minichromosome into their genome form pure white colonies. Transformants with established centromeres on the minichromosomes form pinkish/white colonies. To test centromere function, cells from pinkish/white colonies with putative centromeres were picked from ade-ura- PMG plates and streaked to single colonies on low ade YES plates. Sectored red/white colonies indicates centromere function, while minichromosome integrants produce pure white colonies. Establishment frequency is the number of centromere established pinkish/white colonies divided by the number of red colonies with no centromere establishment.

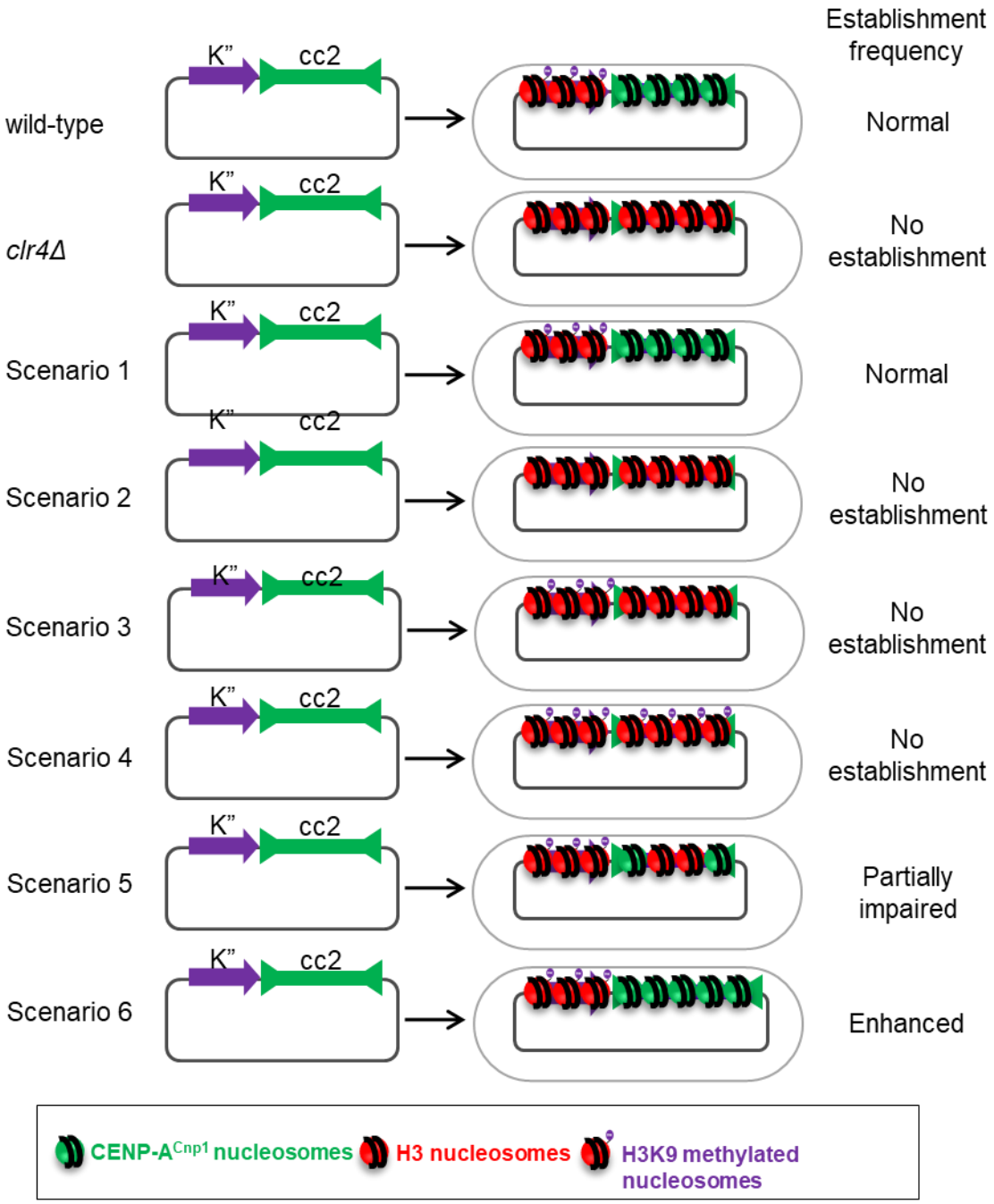

Figure 4.1: Establishment assay: de novo establishment of CENP-A^{Cnp1} chromatin on circular minichromosomes

Fission yeast cells were transformed with pcc2K” circular minichromosomes having K” repeat capable of assembling heterochromatin and centromere 2 central domain DNA (cc2) capable of assembling CENP-A^{Cnp1} chromatin. In a wild type cell, functional centromeres can be established on the minichromosomes while cells without H3K9me2 (eg. *clr4*Δ) have no colonies with established functional centromeres. Six possible scenarios of establishment frequencies with varying establishment of either heterochromatin or CENP-A^{Cnp1} chromatin are depicted.

In wild type cells, the K" repeat establishes heterochromatin and centromere 2 central domain DNA (*cc2*) is assembled into CENP-A^{Cnp1} chromatin on the minichromosomes, thereby minichromosomes will be segregated and inherited through generations. Wild type strains show an initial establishment frequency of ~ 10-12% (Table 4.1). Adjacent H3K9me2 chromatin is required for the establishment of the CENP-A^{Cnp1} chromatin and cells with inefficient heterochromatin establishment function show lower establishment frequencies. For example, histone H3 lysine methyltransferase Clr4 is required for H3K9 methylation and cells without *clr4* gene are deficient in H3K9me2 and impaired in establishment of CENP-A^{Cnp1} within the central domain on the minichromosome (Folco et al., 2008; described in Figure 4.1). Similarly, loss of HP1 family chromodomain protein Swi6 (positive control for decreased establishment frequency), heterochromatin integrity is compromised, although K" sequence on the minichromosomes does assemble H3K9me but cc2 DNA on the minichromosome fails to assemble into CENP-A^{Cnp1} chromatin and established frequency is abolished (Table 4.1). Swi6 protein was enriched with CENP-A^{Cnp1} chromatin compared to mock and H3.2 affinity-purifications (Figure 3.11) and used as a positive control for the centromere establishment assay.

Six possible scenarios of centromere establishment on the minichromosome are described in Figure 4.1. Scenario 1 – gene is not required for any aspect of centromere establishment then the observed establishment frequency will be similar to the wild type cells. Scenario 2 – gene required for heterochromatin establishment / maintenance then both K" repeat and *cc2* sequence on the minichromosome will assemble in H3 chromatin and the establishment frequency will be abolished. Scenario 3 – gene required for CENP-A^{Cnp1} establishment but not heterochromatin establishment/maintenance then *cc2* sequence will be assembled in H3 chromatin despite the adjacent H3K9me chromatin. Scenario 4 – gene required to prevent heterochromatin spreading than both K" repeat and cc2 sequence will be assembled in H3K9me chromatin and establishment frequency will be alleviated. Scenario 5 – gene required for centromere establishment than the establishment frequency will either be lower compared to wild type. Scenario 6 – gene required to limit *de novo* establishment of CENP-A^{Cnp1} or H3K9me chromatin than the observed establishment frequency will be higher in these mutants compared to the wild type cells.

B. Central core silencing assay

Reporter gene placed within fission yeast centromeres are transcriptionally silenced and exhibit positional effect variegation (Allshire et al., 1994; Allshire et al., 1995). Transcriptional silencing at the central core reflect maintenance of CENP-A^{Cnp1} and assembly of a fully functional kinetochore complex. Several temperature sensitive mutants have been identified that alleviate transcriptional silencing at centromere central domain; CENP-I^{Mis6} (Partridge et al., 2000), CENP-O^{Mal2} (Jin et al., 2002), HJURP^{Scm3}, CENP-A^{Cnp1}, Sim3 (NASP chaperone) and CENP-K^{Sim4} (Pidoux et al., 2003). A strain containing the *ura4*$^{+}$ gene inserted at central domain 1 (*TM1::ura4*$^{+}$) was used as a reporter for mutations affecting silencing at the central domain. Cells repressing *ura4*$^{+}$ gene expression fails to grow on plates lacking uracil but grow strongly on plates containing the counter-selective 5-fluoro-orotic acid (FOA). Mutants alleviating *ura4*$^{+}$ repression will grow better on media lacking uracil but fail to grow well on FOA plates (Boeke et al., 1984).

C. Heterochromatin silencing assay

H3K9me is characteristic of silent heterochromatin (Allshire and Madhani, 2018). A strain containing the *ade6*$^{+}$ gene inserted within *SphI* site on *otr1R* (*otr1R(SphI):ade6*$^{+}$) was used as a reporter for mutations affecting silencing at pericentric outer repeats. Cells repressing *ade6*$^{+}$ gene expression form red colonies on plates containing limiting adenine. Defects in the *ade6*$^{+}$ gene causes accumulation of phosphoribosylaminoimidazole (AIR) (Fisher, 1969). The AIR intermediate is uncolored however subsequent events are required for the red color to appear. Mutations which cause the alleviation of *ade6*$^{+}$ expression result in white colonies.

D. Genetic interaction with CENP-A^{Cnp1}

To identify factors that interact with CENP-A^{Cnp1}, a temperature-sensitive (ts) allele *cnp1-1* (L87Q mutation) which exhibits decreased viability after unequal mitotic segregation at the restrictive temperature (36°C) was used for the assay (Takahashi et al., 2000). Positive and negative interactions of CENP-A^{Cnp1} mutation with candidate gene mutations were recorded at different temperatures.

E. Viability upon CENP-A^{Cnp1} overexpression

Fission yeast can tolerate overexpression of CENP-A^{Cnp1} (Castillo et al., 2007). FACT mutants are sensitive to CENP-A^{Cnp1} overexpression (Choi et al., 2012). CENP-A^{Cnp1} was overexpressed from a thiamine-inducible *nmt41* promoter in the candidate gene mutants to assess effect of overexpression on cell viability.

Knockout strains of 23 non-essential CENP-A^{Cnp1} chromatin-associated proteins from my CENP-A^{Cnp1} AP-MS analysis were obtained from the Bioneer deletion library version 2 (http://pombe.bioneer.co.kr/) and checked by colony PCR to confirm that correct gene was indeed knocked out (data not shown). Five different functional assays were performed to gain initial insight into their potential role in centromere function. A list of candidate genes and effect of gene deletion on de novo centromere establishment frequency, central core silencing, heterochromatin silencing, genetic interaction with CENP-A^{Cnp1} and cell viability upon CENP-A^{Cnp1} overexpression is summarized in Table 4.1 with ascending establishment frequency.

Table 4.1: Result of functional assays performed on candidate gene mutants.

Genotype	Establishment frequency [number of colonies]	Central core silencing	Hetero-chromatin silencing	Genetic interaction with cnp1-1	Viability upon CENP-A^{Cnp1} over-expression
wild type	**10-12% [175-886]**	**No effect**	**No effect**	**No effect**	**No effect**
***swi6*Δ**	**0% [340]**	**Mild alleviation**	**Mild alleviation**	**No effect**	**No effect**
***hap2*Δ**	**0% [897]**	**Alleviation**	**No effect**	**No effect**	**No effect**
***bdf2*Δ**	**0% [146]**	**N.D.**	**N.D.**	**No effect**	**No effect**
***iec1*Δ**	**0% [34]**	**Mild alleviation**	**Mild alleviation**	**No effect**	**No effect**
***ccp1*Δ**	**0.8% [115]**	**No effect**	**No effect**	**No effect**	**No effect**
***cph1*Δ**	**1% [94]**	**N.D.**	**N.D.**	**Enhancer (Weak)**	**No effect**
***hrp3*Δ**	**1.6% [543]**	**No effect**	**No effect**	**No effect**	**No effect**
***msh6*Δ**	**1.8% [661]**	**No effect**	**No effect**	**Enhancer (Weak)**	**No effect**
***dbl5*Δ**	**1.8% [688]**	**No effect**	**No effect**	**Suppressor (Weak)**	**Hypersensitive**
***top1*Δ**	**2.3% [642]**	**No effect**	**No effect**	**No effect**	**No effect**
***hpz1*Δ**	**2.9% [342]**	**No effect**	**No effect**	**No effect**	**No effect**
***brc1*Δ**	**3.6% [1025]**	**No effect**	**No effect**	**No effect**	**No effect**
***pmt3*Δ**	**3.6% [515]**	**No effect**	**No effect**	**Suppressor (Weak)**	**No effect**
***epe1*Δ**	**4.6% [495]**	**N.D.**	**N.D.**	**No effect**	**No effect**
***cbh1*Δ**	**5.2% [288]**	**No effect**	**N.D.**	**Enhancer (Weak)**	**No effect**
***fta6*Δ**	**5.3% [245]**	**No effect**	**No effect**	**Enhancer (Weak)**	**No effect**
***abo1*Δ**	**7% [412]**	**N.D.**	**N.D.**	**Suppressor (Weak)**	**No effect**
***bub3*Δ**	**11.6% [266]**	**N.D.**	**N.D.**	**No effect**	**No effect**
***abo2*Δ**	**12.9% [139]**	**N.D.**	**N.D.**	**Enhancer (Weak)**	**No effect**
***abp2*Δ**	**14.1% [156]**	**N.D.**	**N.D.**	**No effect**	**No effect**
***ies4*Δ**	**18.9% [79]**	**No effect**	**Mild alleviation**	**Enhancer (Weak)**	**No effect**
***ssr3*Δ**	**20% [176]**	**N.D.**	**N.D.**	**No effect**	**No effect**
***ies2*Δ**	**37.5% [373]**	**Mild alleviation**	**Mild alleviation**	**No effect**	**No effect**

N.D. – Not determined

Heterochromatin protein: Swi6

Swi6 is an orthologue of the chromodomain-containing heterochromatin protein 1 (HP1) which is known to bind methylated H3K9 and contribute to the formation of silent chromatin formation (Allshire and Ekwall, 2015). Swi6 is required to maintain transcriptional repression at mating type locus and centromeres (Allshire et al., 1995). In absence of Swi6, no significant reduction of H3K9me levels is observed but these cells show spreading of H3K9me beyond normal boundaries of heterochromatin especially at the inverted repeat element IRC1R (Stunnenberg et al., 2015). In swi6Δ, mild alleviation of transcriptional silencing of *ura4*$^{+}$ gene at the central domain and partial silencing of *ade6*$^{+}$ gene at the pericentric outer repeats was observed (Table 4.1). Centromere establishment is completely abolished for pcc2K" minichromosome in *swi6Δ,* which is consistent with the absence of CENP-A^{Cnp1} chromatin on cc2 sequence of the minichromosome (Folco et al., 2008). Therefore, I used *swi6Δ* as a positive control for defective centromere assembly in the centromere establishment assay.

Ino80 complex: Iec1, Ies4, Ies2 and Hap2

Ino80 is an ATP-dependent nucleosome remodeling enzyme involved in transcription, replication, and DNA damage repair. Ino80 is a member of SWI2/SNF2 superfamily (Clapier et al., 2017). In budding yeast, Ino80 activity is required for proper centromere function by maintaining a normal pericentric heterochromatin structure possibly by regulating H2A.Z eviction (Papamichos-Chronakis et al., 2011; Chambers et al., 2012). In fission yeast, Ino80 complex might promote CENP-A^{Cnp1} chromatin integrity by regulating histone H3 eviction (Choi et al., 2017). Iec1, Ies2 and Ies4 are associated with Ino80 complex (Table 5.1). Iec1 has no apparent orthologue in budding yeast but it is similar to human Yin-Yang-1 (YY1) transcription factor at the level of their C2H2 zinc finger motifs that associates with the Ino80 complex in humans (Cai et al., 2007). Iec1-Ino80 complex might be involved in nucleosome eviction in fission yeast, as absence of Iec1 leads to increased H3 occupancy over promoters and gene bodies of *apt1*, *ade1*, *aah1*, *pho1*, and *pho4* upon phosphate starvation, also Ino80 recruitment at these regions is Iec1 dependent. Interestingly, loss of either Iec1 or Ies2 affects phosphate and adenine metabolism, while the double mutant *Δiec1Δies2* suppress these defects and is similar to the wild type, suggesting that the different Ino80-

interacting proteins may program the complex differently in possibly opposing ways (Hogan et al., 2009). Consistent with this, *iec1*Δ cannot establish de novo centromere on pcc2K" minichromosome while *ies2*Δ and *ies4*Δ have higher establishment frequency compared to the wild type (Table 4.1), suggesting variable functions of Ino80-interacting proteins.

Hap2 was first identified as a potential Ino80 complex associated protein and no further characterization was performed (Hogan et al., 2009). The Hap2 protein confers resistance against DNA intercalator doxorubicin (which inhibit re-ligation of double strand breaks) and shown to have a role in DNA damage response in fission yeast (Tang et al., 2015). De novo centromere establishment on the minichromosome is abolished in hap2Δ strains (Table 4.1). This implicate Hap2 in de novo centromere establishment.

Loss of Iec1, Ies2 and Hap2 alleviates central core silencing; and loss of Iec1, Ies2 and Ies4 alleviates heterochromatin silencing, suggesting a role of Ino80 complex at centromeres. Hap2 is an uncharacterized Ino80 complex associated protein which affect centromere establishment frequency and silencing at centromeric central domain, therefore, it was chosen for further investigated for its role at the centromere and the work is described in detail in Chapter 5.

<u>E3 ubiquitin ligase: Dbl5</u>

Dbl5 was first identified in a proteome-wide visual screen to localize to DNA double-strand breaks and named as DNA-break-localizing proteins 5 (Dbl5) (Yu et al., 2013). Fission yeast Dbl5 is an orthologue of budding yeast Psh1. To investigate whether Dbl5 has a role in establishment and maintenance of CENP-A^{Cnp1} chromatin, the dbl5Δ mutant was analyzed by assays designed to test its centromere function. Compared to wild-type cells, *dbl5*Δ showed a decreased frequency of centromere establishment when transformed with pcc2K" minichromosome (Table 4.1). To test the integrity of CENP-A^{Cnp1} chromatin and heterochromatin at endogenous centromeres silencing assays were performed. The *dbl5*Δ cells showed no alleviation of transcriptional silencing at central core chromatin and pericentric heterochromatin (Table 4.1). To gain further insight into its interaction with CENP-A^{Cnp1}, *dbl5*Δ mutants were combined with *cnp1-1* ts mutant. Loss of Dbl5 partially suppressed *cnp1-1* lethality at non permissive temperature (Table 4.1). In budding yeast, expressing excess CENP-A^{Cse4}

is lethal in *psh1*∆ cells (Ranjitkar et al., 2010; Hewawasam et al., 2010). Consistent with this, in *S. pombe* overexpression of CENP-A^{Cnp1} is lethal in the *dbl5Δ* cells (Table 4.1). Role of Dbl5 is further investigated and discussed in detail in Chapter 6.

DNA repair protein: Msh6

The MutSα heterodimer (Msh2-Msh6) can recognize structural alterations in the DNA and initiates the repair of single-base mismatch, single-base insertion/deletion (IDLs) and small loops (Tornie et al., 2001; Marti et al., 2003; Villahermosa et al., 2017). Once DNA damage is recognized by MutS, MutL homologs Mlh1 and Pms1 are recruited along with the exonuclease Exo1. Inactivation of MutSα can causes instability of tetra-nucleotide repeats (Villahermosa et al., 2017). Centromeric bacterial artificial chromosome (B18) associates with Msh2-Msh6 but not with single-strand binding protein (RPA) in *Xenopus* egg extract, also loss of Msh6 impair B18 replication, indicating that Msh6 is required for efficient centromeric DNA replication (Aze et al., 2016). Electron microscopy revealed dsDNA loops in the centromeric DNA that resemble previously proposed centromeric loop organization (Bloom, 2014). Like other eukaryotes, repetitive DNA elements are enriched at the centromeres in fission yeast and even the non-repetitive unique central core sequence might adopt non-B-form conformations such as stem-loops or cruciform similar to higher order structure observed in vitro and/or in vivo in many organisms including humans (Garavis et al., 2015; Aze et al., 2016; Kasinathan and Henikoff, 2018). Therefore, it is possible that the MutSα is required to suppress repair response by binding to putative non-B DNA structures at centromeres in fission yeast.

To investigate whether Msh6 has a role at *S. pombe* centromeres, the *msh6*∆ cells was analyzed by assays designed to test centromere function and the integrity of centromeric chromatin. *msh6*∆ showed a five-fold reduction in the frequency of centromere establishment on pcc2K" minichromosome compared to wild-type cells (Table 4.1). As the pcc2K" minichromosome did establish centromere function in *msh6*∆, the stability of the minichromosome was tested in minichromosome loss assay. *msh6*∆ showed an increased rate of minichromosome loss (Figure 4.2 A). This suggests a defect in centromere function – in either CENP-A^{Cnp1}/kinetochore or heterochromatin/cohesion.

To test the integrity of heterochromatin at endogenous centromeric outer repeats a heterochromatin silencing assay was performed. *msh6*Δ showed no defect in outer repeat silencing (Table 4.1). Consistent with this observation, *msh6*Δ showed wild-type levels of outer repeat transcripts (*dg*), whereas a mutant defective in the H3K9-histone methyltransferase *clr4*Δ showed high levels of *dg* transcripts (Figure 4.2 B). Therefore, *msh6*Δ shows no evidence of a defect in maintenance of endogenous outer repeat heterochromatin. The integrity of central domain CENP-A^{Cnp1} chromatin at endogenous centromeres was tested in various assays. Mutants defective in assembly of CENP-A^{Cnp1} chromatin, such as *scm3,* show alleviation of marker gene inserted at the central domain (Pidoux et al., 2003). However, *msh6*Δ mutant showed no defect in transcriptional silencing at central core sequence (Table 4.1). *msh6*Δ displayed wild-type levels of CENP-A^{Cnp1} and histone H3 at endogenous centromeres (Figure 4.2C and D). However, in common with *sim* mutants that affects CENP-A^{Cnp1} chromatin (Pidoux et al., 2003), *msh6*Δ *cnp1-1* double mutant showed increased lethality compared to the *cnp1-1* single mutant (Table 4.1). Unlike some *sim* mutants, *msh6*Δ was not suppressed by overexpression of CENP-A^{Cnp1} (Table 4.1). To gain further insight into the possible defects in establishment of centromeric chromatin, a plasmid bearing only central core sequence (without adjacent heterochromatin) was introduced into *msh6*Δ cells overexpressing CENP-A^{Cnp1}. In wild-type cells overexpression of CENP-A^{Cnp1} bypasses the requirement for heterochromatin and central core sequence on the pcc2 plasmid is assembled in CENP-A^{Cnp1} (Catania et al., 2015). *msh6*Δ was competent to assemble CENP-A^{Cnp1} on pcc2 in this assay but at a reduced level (Figure 4.2E). This suggests that the *msh6*Δ cells have a partial defect in the ability to establish *de novo* CENP-A^{Cnp1} chromatin. Together, these observations suggest that *msh6* mutant has a mild defect in the ability to establish CENP-A^{Cnp1} chromatin, but this needs to be explored further. For instance, CENP-A^{Cnp1} and H3K9me2/3 ChIP should be performed on pcc2K" minichromosome in *msh6*Δ strains.

HJURP (CENP-A chaperone) can specifically bind to synthetic cruciform/holliday junction DNA structure (Kato et al., 2007) raising the possibity that the proposed non-B DNA structures at the central domain might recruit HJURP^{Scm3} thereby facilitating deposition of CENP-A^{Cnp1} over these sequences. The putative higher order DNA structures at central core DNA (Kasinathan and Henikoff, 2018) may associate with

Msh6 which might stabilize these structure and suppress induction of repair response. Therefore Msh6 activity might provide a substrate for HJURP^{Scm3} recruitment which in turn facilitate CENP-A^{Cnp1} deposition.

A

Minichromosome loss (pcc2K") Half sectoring assay	
Strain	Loss frequency
wild type	4.65 %
wild type	4.53 %
msh6Δ	12.5 %
msh6Δ	12.33 %

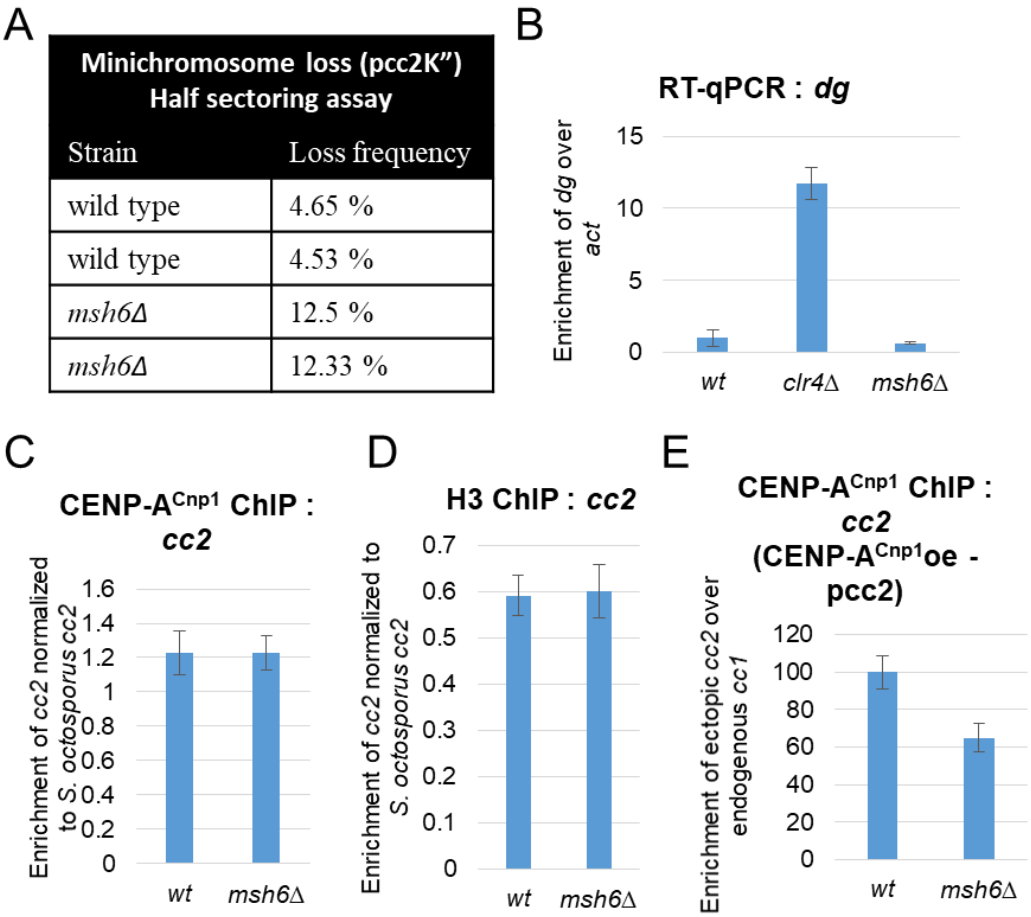

Figure 4.2: Msh6 does not affect nucleosome occupancy and heterochromatin at the centromere but loss of *msh6* have high minichromosome loss and inefficient *de novo* CENP-A^{Cnp1} deposition

(A) Minichromosome loss frequency of pcc2K" with established centromere in one cell division was assessed by half-sectoring assay. Cells were transformed with pcc2K" minichromosome and two colonies with established centromeres on the minichromosome for wild-type and *msh6*Δ were plated on low adenine plates to obtain single cell colonies (n>1000). Single cell colonies that have lost the minichromosome in the first cell division have a ≥ half continuous red sector. Percentage of half-sectored colonies was calculated relative to colonies that retained the minichromosome during their first cell division. (B) RT-qPCR of *dg* transcripts in wild-type, *clr4*Δ and *msh6*Δ cells normalized to *actin* transcripts. Mean ± S.D. of n=3 biological replicates is shown. (C and D) qChIP of CENP-A^{Cnp1} and histone H3 levels at *cc2* in wild-type and *msh6*Δ cells normalized to spiked in *S. octosporus cc2*. Mean ± S.D. of n=3 biological replicates is shown. (E) qChIP of CENP-A^{Cnp1} levels at *cc2* on pcc2 minichromosome in wild-type and *msh6*Δ cells with CENP-A^{Cnp1} overexpression (oe) normalized to endogenous *cc1* levels. Cells were transformed with pcc2 minichromosome and grown on ade- ura-

medium plates. Three random colonies were picked and grown under selection for ChIP. Mean ± S.D. of n=3 biological replicates is shown.

Topoisomerase Top1

DNA topoisomerases are required to control double-helix DNA supercoiling and entanglements arising during replication, transcription, repair, recombination and chromatin remodeling (Pommier et al., 2016). Two classes of topoisomerases can relieve DNA helical tension: type I – induces single strand breaks and type II – induces double-strand breaks. Further sub-classification are based on linkage to 3' (IA) or 5' (IB) phosphate or based on the structure (IIA or IIB). Fission yeast have three topoisomerases, Top1 and Top3 are type I topoisomerase and Top2 is a type II topoisomerase. Site-specific cleavage by Top2 within active centromeres is conserved widely across eukaryotes and detectable in humans, chicken DT-40 cells, fission yeast and *Drosophila*, suggesting Top2 might recognize a fundamental aspect of the centromere, such as structure of DNA/chromatin (Spence et al., 2005; Mills et al., 2018). Top3 and CENP-A^{Cnp1} occupancies shows a positive correlation at the central domain and regulate levels of CENP-A^{Cnp1} at the centromere (Norman-Axelsson et al., 2013). Top1 is a non-essential topoisomerase while Top2 and Top3 are essential. Top1 associates with actively transcribed promoters and is required to maintain nucleosome occupancy and levels of H3K9Ac at target gene promoters (Durand-Dubief et al., 2010). Top1 functional studies in fission yeast were done in *top1*Δ*top2-191* (Durand-Dubief et al., 2010), which makes it hard to uncouple the contribution of Top1 in these studies.

To determine the role of Top1 in establishment and maintenance of CENP-A^{Cnp1} chromatin, functional assays were performed. Compared to wild-type cells, *top1*Δ showed ~4 fold reduction in the frequency of centromere establishment on pcc2K" (Table 4.1). This deficiency could be due to defects in the ability to establish heterochromatin or CENP-A^{Cnp1} chromatin, or both. As the pcc2K" minichromosome did establish centromere function in *top1*Δ, the stability of the minichromosome was tested in minichromosome loss assay. *top1*Δ showed an increased rate of minichromosome loss (Figure 4.3 A). This suggesting a defect in centromere function – in either heterochromatin/cohesion or CENP-A^{Cnp1}/kinetochore.

To test the integrity of heterochromatin at endogenous centromeric outer repeats, heterochromatin silencing assay was performed. *top1*Δ showed no defect in outer repeat silencing (Table 4.1). Consistent with this observation, *top1*Δ showed wild-type levels of outer repeat transcripts (*dg*), whereas a mutant defective in the H3K9-histone methyltransferase *clr4*Δ showed high levels of *dg* transcripts (Figure 4.3B). H3K9me levels at the pericentric outer repeats (*dg*) in *top1*Δ were comparable to wild-type cells (Figure 4.3C). Therefore, *top1*Δ showed no evidence of a defect in the maintenance of endogenous outer repeat heterochromatin. The integrity of central domain CENP-A^{Cnp1} chromatin at endogenous centromeres was tested. *top1*Δ showed no defect in central core silencing (Table 4.1). It also displayed wild-type levels of CENP-A^{Cnp1} at endogenous centromeres (Figure 4.3 D). However, *top1*Δ did not show any defects with *cnp1-1* and cells overexpressing CENP-A^{Cnp1} (Table 4.1). To gain further insight into the possible defects in establishment of centromeric chromatin, *top1*Δ cell were transformed with pcc2K" minichromosome and *top1*Δ overexpressing CENP-A^{Cnp1} cells were transformed with pcc2 minichromosome. In both cases, *top1*Δ showed similar levels of CENP-A^{Cnp1} at *cc2* compared to wild type cells (Figure 4.3 E and F).

This indicates that Top1 is not required for *de novo* CENP-A^{Cnp1} establishment. Top2 might substitute for the activity of Top1 (Uemura and Yanagida, 1984). It is still surprising to see a significant effect on centromere establishment frequency and minichromosome loss in single mutation of Top1. It is possible that the minichromosome is lost from the cells even with CENP-A^{Cnp1} deposition on the *cc2* sequence due to the increased minichromosome loss in cells lacking Top1.

A

Minichromosome loss (pcc2K")	
Strain	Loss frequency
wild type	4.65 %
wild type	4.53 %
top1Δ	9.74 %
top1Δ	10.01%

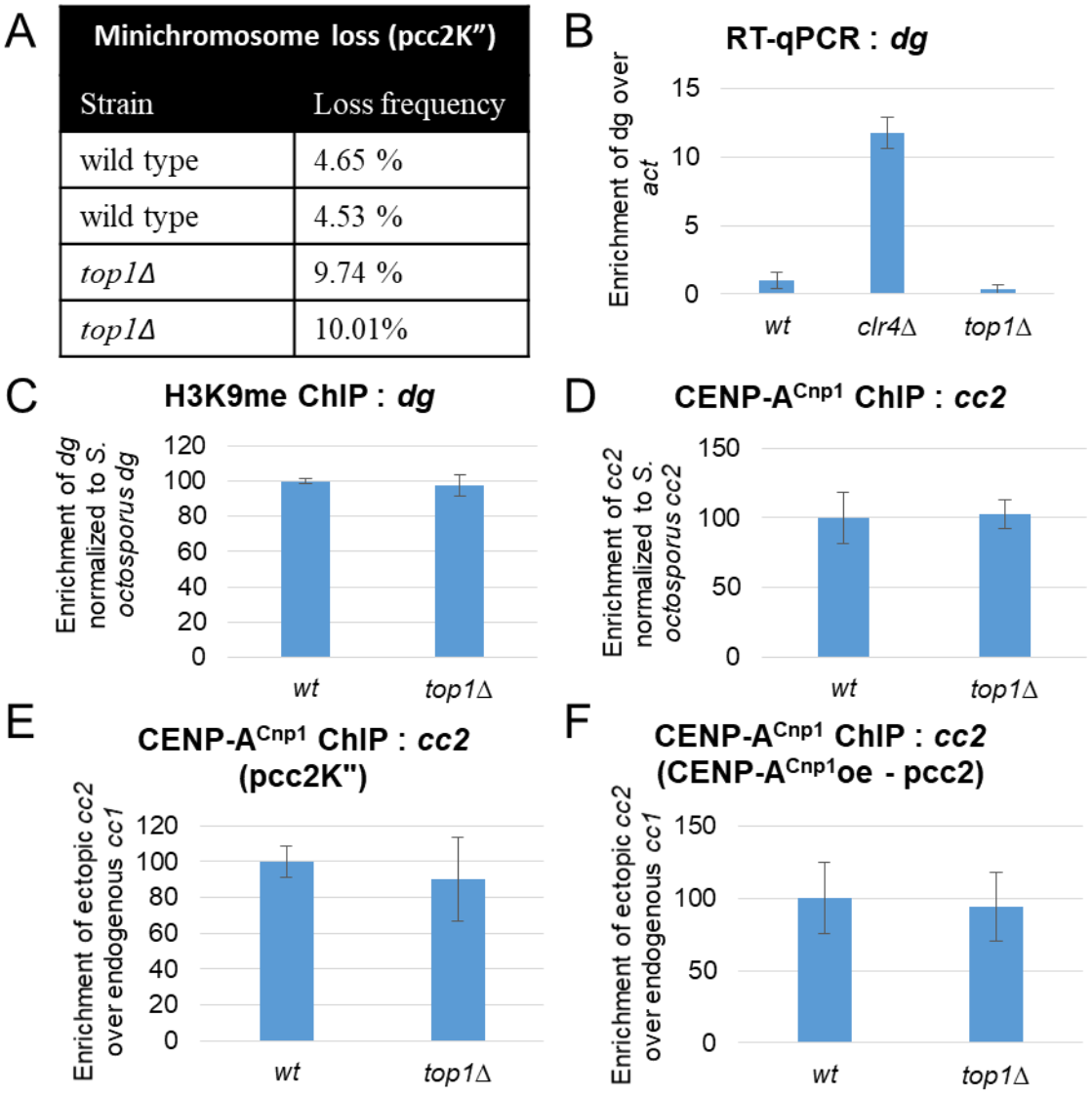

Figure 4.3: Top1 is not required for centromere establishment/maintenance

(A) Minichromosome loss frequency of pcc2K" with established centromere in one cell division as assessed by half-sectoring assay. Single cell colonies that have lost the minichromosome in the first cell division form a ≥ half continuous red sector. (B) RT-qPCR of *dg* transcripts in wild-type, *clr4*Δ and *top1*Δ cells normalized to *actin* transcripts. Mean ± S.D. of n=3 biological replicates is shown. (C) qChIP of H3K9me levels at *cc2* in wild-type and *top1*Δ cells normalized to spiked in *S. octosporus dg*. Mean ± S.D. of n=3 biological replicates is shown. (D) qChIP of CENP-A^{Cnp1} levels at *cc2* in wild-type and *top1*Δ cells normalized to spiked in *S. octosporus cc2*. Mean ± S.D. of n=3 biological replicates is shown. (E and F) qChIP of CENP-A^{Cnp1} levels at *cc2* on pcc2K" and pcc2 minichromosome in wild-type and *top1*Δ cells with normal CENP-A^{Cnp1} levels and CENP-A^{Cnp1}-overexpression (oe), respectively, normalized to endogenous *cc1* levels. Cells were transformed with either pcc2K" or pcc2 minichromosome and selected on ade- ura- medium plates. Three random colonies were picked and grown under selection for ChIP. Mean ± S.D. of n=3 biological replicates is shown.

Hpz1

Hpz1 is a Homologue of PARP-type Zinc-finger. The PARP-type Zn-finger motif have conserved residues in fission yeast Hpz1 compared to human PARP1 protein (Bøe et al., 2012). The active site of PARPs contain a highly conserved 50 amino acid sequence, PARP signature (Bøe et al., 2012). No obvious PARP signature was found in the Hpz1 sequence, and moreover, to this date no poly(ADP-ribosyl)ated proteins have been detected in cell extracts from fission yeast (Bøe et al., 2012). To investigate whether Hpz1 has a role at *S. pombe* centromeres, a centromere establishment assay was performed. Compared to wild-type cells, *hpz1*Δ showed a ~ 3 fold reduction in the frequency of centromere establishment on pcc2K" minichromosome (Table 4.1). As the pcc2K" minichromosome did establish centromere function in *hpz1*Δ, the stability of the minichromosome was tested in minichromosome loss assay. *hpz1*Δ showed no increase in the rate of loss of the minichromosome (Figure 4.4 A). This suggests that once a centromere is established on the minichromosome Hpz1 does not affect its centromere function.

To test the integrity of endogenous centromeres, transcriptional silencing was assessed at the central domain and outer repeat sequence. *hpz1*Δ showed no defect in outer repeat silencing (Table 4.1). Consistent with this observation, *hpz1*Δ showed similar levels of outer repeat transcripts (*dg*) comared to wild type, whereas *clr4*Δ showed high levels of *dg* transcripts (Figure 4.4 B). Therefore *hpz1*Δ shows no evidence of a defect in maintenance of endogenous outer repeat heterochromatin. The integrity of central domain CENP-A^{Cnp1} chromatin at endogenous centromeres was assessed. The *hpz1*Δ mutant showed no defect in transcriptional silencing at central core sequence (Table 4.1). Effect of loss of *hpz1* on nucleosome occupancy at the centromere was evaluated by GFP-CENP-A^{Cnp1} and H3 ChIP. Surprisingly, Chip analysis showed that the *hpz1*Δ mutant have reduced occupancy of CENP-A^{Cnp1} and a reciprocal increase in histone H3 levels (Figure 4.4 C and D). Taken together, the data indicate *hpz1*Δ may have a subtle effect on maintenance of CENP-A^{Cnp1} chromatin at endogenous centromeres. Hpz1 localize to the nucleus and present during G1-S-early G2 phase of the cell cycle (Bøe et al., 2012). As Hpz1 is required to maintain nucleosome occupancy at centromeres, it is possible that Hpz1 might associate with centromeres. To investigate this possibility, Hpz1 was tagged with GFP and anti-GFP ChIP was performed. Hpz1-GFP was found to associate with central

core region (*cc2*), outer repeat region (*dg*) and actin locus (*act1*) (Figure 4.4 E). These observations suggest that Hpz1-GFP is localized at centromeres and also at other chromatin regions. Hpz1 expression is regulated during the cell cycle (Bøe et al., 2012). It is possible that centromeric association of Hpz1 might be regulated by cell cycle. To investigate this possibility, cell cycle synchronized Hpz1-HA cells were used for anti-HA ChIP. Hpz1-HA was found to associate with central core region (*cc2*) during S-phase of the cell cycle (Figure 4.4 F). The cell cycle profile for the association of Hpz1 at central core sequence is similar to histone H3 deposition/eviction profile (Shukla et al., 2017). Histone H3 competes with CENP-A^{Cnp1} for incorporation into centromeres and eviction of histone H3 is postulated to provide an opportunity for CENP-A^{Cnp1} nucleosome deposition (Castillo et al., 2007; Allshire and Karpen, 2008). As Hpz1 is required to maintain CENP-A^{Cnp1} levels at centromeres and follows a similar profile as histone H3 eviction, it is possible that Hpz1 might promote histone H3 eviction and consequently facilitate CENP-A^{Cnp1} deposition. To test this possibility, replication-independent H3 turnover was measured by Recombination Induced Tag Exchange (RITE) system (described in Chapter 5; Figure 5.6). Similar histone H3 turnover was observed at ectopically inserted *cc2* sequence and endogenous central domain sequence in *hpz1*∆ compared to wild type cells (Figure 4.4 G and H).This suggests that Hpz1 does not influence histone H3 turnover at least in G2 phase. As Hpz1 is predominantly associated with the central domain during S phase, histone H3 turnover during S phase should be assessed. It has been proposed that the dyad symmetries found in the central domain sequence can adopt non-B-form DNA structures which might favor the deposition of CENP-A^{Cnp1} at these sequences (Kasinathan and Henikoff, 2017). Similarity of zf-PARP domain in Hpz1 and human PARP1, raises another possibility as PARP1 can bind in vitro to non-B-form DNA structures (Lonskaya et al., 2005), fission yeast Hpz1 might also bind to the proposed DNA structures and promote deposition of CENP-A^{Cnp1}. Future work is need to understand role of Hpz1 at the centromere.

A

Minichromosome loss (pcc2K")	
Strain	Loss frequency
wild type	4.65 %
wild type	4.53 %
hpz1Δ	4.53 %
hpz1Δ	4.28 %

B

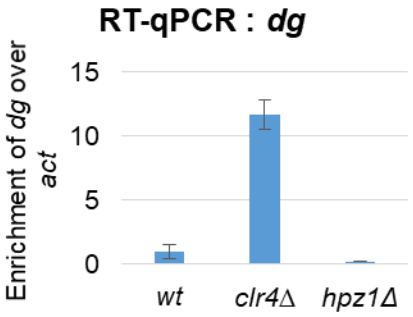

C

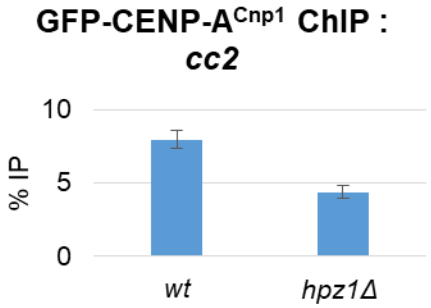

D

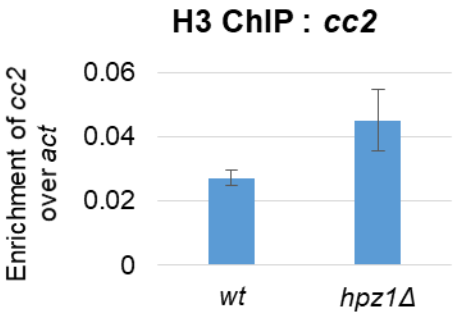

E

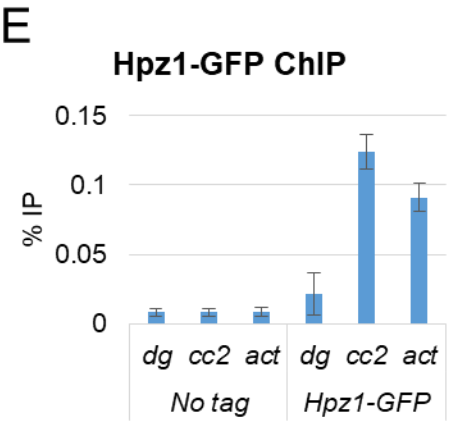

F

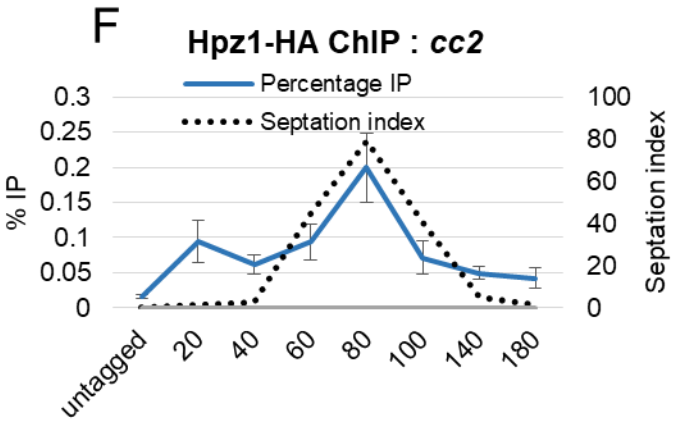

G

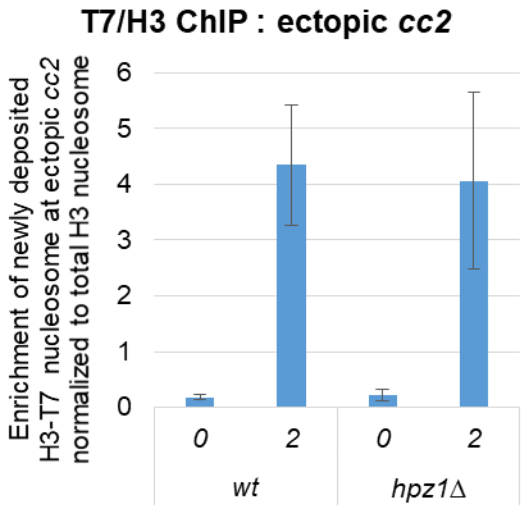

H

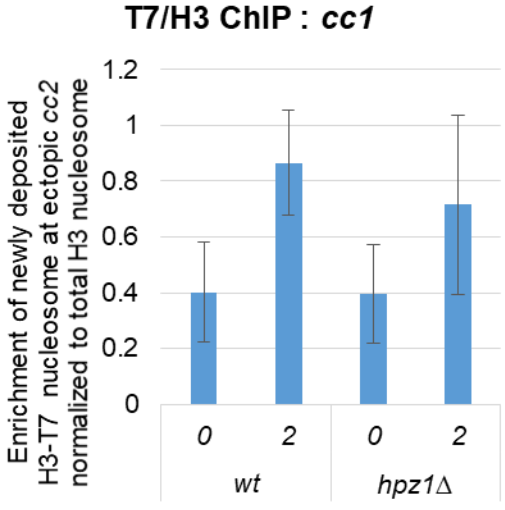

Figure 4.4: Hpz1 is required for efficient centromere function

(A) Minichromosome loss frequency of pcc2K" with established centromere in one cell division as assessed by half-sectoring assay. Cells were transformed with pcc2K" minichromosome and two colonies with established centromeres on the minichromosome for wild-type and hpz1Δ were plated on adenine- plates to obtain single cell colonies (n>1000). Single cell colonies that have lost the minichromosome in the first cell division have a ≥ half continuous red sector. (B) RT-qPCR of *dg* transcripts in wild-type, *clr4*Δ and *hpz1*Δ cells normalized to actin transcripts. Mean ± S.D. of n=3 biological replicates is shown. (C and D) qChIP of CENP-A^{Cnp1} and H3 levels at *cc2* in wild-type and *hpz1*Δ cells as percentage IP and enrichment over act^{+}, respectively. Mean ± S.D. of n=3 biological replicates is shown. (E) qChIP of Hpz1-HA levels at centromere central domain *cc2*, outer repeats sequence *dg* and *act* in wild-type and *dbl5*Δ cells. Mean ± S.D. of n=3 biological replicates is shown. (F) qChIP of Hpz1-HA levels at *cc2* in *cdc25-22* cells with synchronized cell cycle. S-phase cells with septum were counted using a light microscope. About 80% synchronized S-phase cells were present in the culture after 80 minutes of release. Mean ± S.D. of n=3 biological replicates is shown. (G and H) Replication-independent H3 turnover was measured by Recombination Induced Tag Exchange (RITE) system for H3-HA/T7. *cdc25-22* mutant cells were blocked in G2 by incubation at 36°C for two hours (time point 0). HA-to-T7 tag swap on H3 was induced by addition of β-estradiol in G2 blocked cells at 37°C and samples then collected after 2 additional hours at 37°C (time point 2) and analyzed by ChIP. Mean ± S.D. of n=3 biological replicates is shown.

4.3 Discussion

In this chapter, following AP-MS analysis of the CENP-A^{Cnp1}-associated chromatin, 23 candidate proteins were analysed by five functional assays to investigate their role in centromere establishment and maintenance and possible interaction with CENP-A^{Cnp1}.

Gene knockouts were obtained from the Bioneer deletion library and checked by colony PCR. The finding of functional assays are summarized in Table 4.1. Based on establishment frequency on pcc2K" minichromosome, proteins were grouped into three catagories: (a) first group consists of 16 proteins and deletion of the corresponding gene led to a reduction in establishment, suggesting a possible role in establishment of functional centromeres on the minichromosome. (b) second group consists of four proteins and deletion of corresponding gene did not have a considerable variation in establishment frequency compared to wild-type. (c) third group consists of three proteins and deletion of theses genes lead to an increase in establishment frequency on pcc2K".

In the first group, 11 proteins have been previously known to influence either CENP-A^{Cnp1} chromatin or centromeric heterochromatin: Swi6, Bdf1, Epe1, Cbh1, Brc1, Pmt3, Hrp3, Cph1, Ccp1, Iec1 and Fta6. Swi6, an orthologue of heterochromatin protein 1 (HP1), is known to bind methylated H3K9 and contribute to the formation of silent chromatin formation (Allshire and Ekwall, 2015). The Swr1 complex subunit, Bdf1, interacts with a JmjC domain containing protein, Epe1, which is required for the boundary function, also Bdf1 recruitment at the heterochromatin boundary is dependent on Epe1 (Ayoub et al., 2003; Trewick et al., 2007). Bdf1 is enriched at the heterochromatin boundaries similar to H4K16Ac at CENP-A^{Cnp1} chromatin boundaries and Bdf1 is also required to prevent Sir2-mediated heterochromatin spreading near telomeres (Wang et al., 2013). Cbh1 has been shown to be required for transcriptional silencing at centromeric heterochromatin (Nakagawa et al., 2002). Brc1 has been shown to promote silencing at *imr1R* and *otr1R* at centromeres and regulation of H3K9me levels at outer repeats (Lee et al., 2013). Pmt3, ubiquitin-like SUMO protein modifier, has been shown to be required for controlling telomere length, chromosome segregation, silencing at *mat3* locus and outer repeats (Tanaka et al., 1999; Shin et al., 2005). Loss of Hrp3 represses transcriptional silencing of the *ura4*$^{+}$ gene inserted at the mating-type locus and has a subtle effect at centromere, telomere and rDNA locus (Yoo et al., 2002). Cph1 is a component of histone deacetylase Clr6-CII complex. Loss of Clr6 affects silencing at mating-type loci and pericentromeric regions and reduces fidelity of chromosome segregation (Grewal et al., 1998). Ccp1 has been shown to antagonize CENP-A^{Cnp1} loading and regulate epigenetic stability at centromeres (Dong et al., 2016; Lu and He, 2018). Additionally loss of Ccp1 leads to mislocalization of CENP-A^{Cnp1} (Dong et al., 2016). Ino80 complex has been proposed to mediate removal of histone H3 (Choi et al., 2017). Loss of Iec1 impairs assembly of centromeric CENP-A^{Cnp1} chromatin (Choi et al., 2017). Fta6 is a non-essentail inner kinetochore protein (Liu et al., 2005; Shiroiwa et al., 2011). Fta6 has no apparent orthologues in other species. As these proteins have been demonstrated to affect either outer repeat heterochromatin or centromeric CENP-A^{Cnp1} chromain, these proteins were not considered for further analysis.

Five proteins (Hap2, Dbl5, Msh6, Top1 and Hpz1) in the first group had no previously known role in assembly or function of centromeric chromatin. Loss of Hap2 results in alleviation of *de novo* centromere establishment on pcc2K" and transciptional silencing

within central domain at centromeres (Table 4.1). Role of Hap2 was further investigated and discussed in Chapter 5. Dbl5 is required for *de novo* establishment of functional centromeres on pcc2K" minichromosome (Table 4.1). Dbl5 is an orthologue of Psh1 in *S. cerevisiae*, which has been known to target CENP-A^{Cnp1} degradation function (Ranjitkar et al., 2010; Hewawasam et al., 2010). Therefore, Dbl5 was chosen for further study and the work is described in Chapter 6.

Msh6 is required for *de novo* centromere establishment on pcc2K" minichromosome and CENP-A^{Cnp1} *de novo* deposition on cc2 sequence lacking adjacent heterochromatin (Table4.1 and Figure 4.2). These observations suggest Msh6 may be required for *de novo* CENP-A^{Cnp1} establishment. The CENP-A^{Cnp1} levels on cc2 sequence of the minichromosome in top1Δ cells were similar to wild-type cells (Figure 4.3). Therefore Top1 was not considered for further analysis. Hpz1 is required for efficient *de novo* centromere establishment on pcc2K" minichromosome, nucleosome occupancy at the centromere and its deposition/eviction at the central domain is similar to histone H3 deposition/eviction (Figure 4.4). Although the loss of *hpz1* does not affect replication-independent H3 turnover (Figure 4.4). Histone H3 turnover should be looked during S phase in *hpz1*Δ cells.

Deletion of proteins from the second group, Abo1, Abo2, Bub3 and Abp2, did not show significant variation in establishment frequency on pcc2K" minichromosome. Abo1 has been shown to be required for efficient heterochromatin silencing while the affect of loss of Abo2 on heterochromatin is minimal (Gal et al., 2016). Bub3 has been shown to be required for spindle dynamics but has only a small influence on chromosome stability (Tange and Niwa, 2008). Abp2 is an ARS (autonomously replicating sequence) binding protein required for initiation of DNA replication (Sanchez et al., 1998). As in these mutants the establishment frequency were not significantly affected, they were not considered for further analysis.

The third group of proteins; Ies2, Ies4 and Ssr3, showed higher establishment frequency. Ies2 and Ies4 are subunits of Ino80 complex (Hogan et al., 2010). Interestingly, Iec1 and Hap2, *S. pombe* –specific Ino80 subunits (Table 5.1), fails to establish functional centromeres on cc2 sequence on the minichromosome. It is possible that these species-specific Ino80 subunits might program complex differently for different tasks, possibly in opposing ways.

In summary, two proteins with previously unknown function in *S. pombe*, Hap2 and Dbl5, were chosen for further analysis and described in Chapter 5 and Chapter 6, repectively.

Chapter 5

Hap2 facilitates *de novo* CENP-A^{Cnp1} establishment and maintenance through replication-independent histone H3 turnover

5.1 Introduction

Chromatin dynamics are important for regulation of gene expression and chromosome function (Hübner and Spector, 2010). Chromatin dynamics involves the action of histone chaperones, histone modifications and ATP-dependent chromatin-remodeling complexes (Clapier and Cairns, 2009). The assembly of chromatin was long thought to be an S phase specific event but the last couple of decades have shed light on the influence of replication-independent chromatin assembly (Ahmad and Henikoff, 2002; Ray-Gallet et al., 2011)

Centromere function is influenced by the activity of chromatin remodelers. In budding yeast, ATP-dependent SWI/SNF and RSC chromatin remodeling complexs are required to allow proper chromosome transmission (Hsu et al., 2003; Gkikopoulos et al., 2011). The Ino80 complex has been shown to maintain the integrity of pericentric chromatin in budding yeast (Chambers et al., 2012). In DT40 cells, CENP-H is required for centromeric association of FACT (facilitates chromatin transcription) which interacts with the chromatin remodeling factor CHD1, and knockdown of either FACT or CHD1 attenuates the incorporation of newly synthesized CENP-A into centromeric chromatin (Okada et al., 2009). In human cells, ATP-dependent remodeling and spacing factor (RSF) associates with centromere region in mid-G1 phase of the cell cycle and stabilizes centromeric CENP-A, while RNAi of RSC delays cell cycle progression and causes kinetochore misalignment (Perpelescu et al., 2009). A recent study suggests that tethering RSF1 may promote CENP-A and histone H3.3 assembly into chromatin (Ohzeki et al., 2016).

Schizosaccharomyces pombe centromeres provide an excellent model for dissecting the mechanism of CENP-A chromatin assembly due to its epigenetically regulated centromeres share features with those of metazoa. Many chromatin remodeling complexes have been described that contribute to CENP-A^{Cnp1} localization. FACT and the Clr6-CII HDAC complex regulate CENP-A^{Cnp1} incorporation by influencing

transcription-coupled nucleosome dynamics (Choi et al., 2012). ATP-dependent chromatin remodeling complexes Ino80 complex and the CHD family member Hrp1, regulate histone dynamics, consequently affecting CENP-A^{Cnp1} dynamics (Walfridsson et al., 2005; Choi et al., 2011; Choi et al., 2017).

During replication, parental CENP-A nucleosomes are distributed equally to daughter chromatids at vertebrate and Drosophila centromeres, suggesting CENP-A levels are replenished outside of S-phase. (Shelby et al., 2000; Mellone et al., 2011). The timing of CENP-A incorporation varies between organisms, cell types and developmental stages (Jensen et al., 2007; Dunleavy et al., 2012; Lando et al., 2012; Lidsky et al., 2013). Replicated centromeric DNA, depending on CENP-A availability might become associated with a placeholder histone H3 variant or generate gaps that are completely devoid of nucleosomes (Sullivan, 2001; Allshire and Karpen, 2008; Probst et al., 2009; Shukla et al., 2017). In humans, analysis of centromere chromatin fibers suggests that H3.3 is deposited as a placeholder in S-phase that is later replaced by new CENP-A (Dunleavy et al., 2011). Interestingly, histone H3.3 exchange has been shown to be coupled to transcription (Schwartz and Ahmad, 2005). Transcription has been detected at centromeres in many organisms (Topp et al., 2004; Ohkuni and Kitagawa, 2011; Choi et al., 2011; Chan et al., 2012; Chen et al., 2015; Grenfell et al., 2016; McNulty et al., 2017). Histone H3 competes with CENP-A^{Cnp1} for incorporation into centromeres and eviction of histone H3 is postulated to provide an opportunity for CENP-A^{Cnp1} nucleosome deposition (Castillo et al., 2007; Allshire and Karpen, 2008).

Recently, Ino80 complex has been proposed to be required for proper assembly of centromeric chromatin and for removal of histone H3-containing nucleosomes as a prerequisite for CENP-A^{Cnp1} deposition (Choi et al., 2017). CENP-A^{Cnp1} nucleosome assembly at the centromere occurs via replication-independent incorporation of CENP-A^{Cnp1} during mid G2 phase of the cell cycle (Lando et al., 2012; Shukla et al., 2017). CENP-A^{Cnp1} chromatin assembly in fission yeast is sensitive to the levels of CENP-A^{Cnp1} and other core histones (Castillo et al., 2007). Therefore by altering histone dynamics, chromatin remodeling complexes could contribute to the regulation of centromere assembly and centromere function.

As described in chapter 4, Hap2 was identified as being enriched in CENP-A^{Cnp1} chromatin and found to be required for the establishment of functional centromeres on

naïve centromeric DNA. In addition, deletion of the *hap2* gene attenuated transcriptional silencing within the central CENP-A^{Cnp1} domain of fission yeast centromeres. Hap2 is a potential non-conserved auxiliary component of the chromatin remodeling Ino80 complex in fission yeast (Hogan et al., 2010). In this chapter, I further investigate the involvement of Hap2 in the assembly of CENP-A^{Cnp1} chromatin in fission yeast.

5.2 Results

5.2.1 The *hap2*Δ mutant fails to establish de novo CENP-A^{Cnp1} chromatin on naïve centromeric DNA

Centromere establishment assays measure the frequency of *de novo* establishment of functional centromeres. Intact heterochromatin is required to promote the *de novo* establishment of CENP-A^{Cnp1} chromatin on naïve centromeric sequences and also ensures sister-centromere cohesion to promote segregation (Folco et al., 2008, Kagansky et al., 2009; Bernard et al., 2001; Nonaka et al., 2002). Therefore, centromere establishment on the minichromosome requires both formation of heterochromatin on K" repeat sequence and establishment of CENP-A^{Cnp1} chromatin on adjacent cc2 DNA. As described in Chapter 4, *hap2*Δ mutants fail to establish a centromere on naïve centromeric DNA borne by the pcc2K" minichromosome (Table 4.1). The lack of establishment could result from a defect in the establishment of either heterochromatin or CENP-A^{Cnp1} chromatin, or both on the minichromosome. To test if CENP-A^{Cnp1} chromatin is established, the association of CENP-A^{Cnp1} and histone H3 with central core domain 2 (*cc2*) sequence on the minichromosome was assessed in *hap2*Δ. The *cc2* sequence on the pcc2K" minichromosome is normally assembled in CENP-A^{Cnp1} nucleosomes with very low levels of detectable histone H3 nucleosomes (Folco et al., 2008). As expected in wild type cells, the *cc2* DNA on pcc2K" minichromosome displayed strong enrichment of CENP-A^{Cnp1} but very low levels of histone H3 (Figure 5.1 B and C). In *hap2*Δ, very low levels of CENP-A^{Cnp1} were associated with *cc2* sequence of the pcc2K" minichromosome while a high level of histone H3 association was observed (Figure 5.1 B and C). The presence of histone H3 instead of CENP-A^{Cnp1} could explain the lack of establishment of functional centromeres in *hap2*Δ. To test for the heterochromatin formation on the minichromosome, H3K9me2 ChIP was performed. H3K9me2 levels on the K" repeat

region of the pcc2K” minichromosome in *hap2*Δ were similar to that of wild-type cells (Figure 5.1D; primer: *K”-mini* and *K”-imr*). This suggests that normal assembly of heterochromatin had occurred on the K” repeat of the minichromosome. However, high H3K9me2 levels were also observed within the *cc2* region of pcc2K” in *hap2*Δ cells (Figure 5.1D; primer: *cc2*). This suggests that the inability of *hap2*Δ to establish centromere function is perhaps primarly due to inefficient CENP-A^{Cnp1} chromatin establishment and spreading of heterochromatin over the *cc2* region of pcc2K” minichromosome. To explore this possibility, CENP-A^{Cnp1} ChIP qPCR was performed to assess the *de novo* incorporation of CENP-A^{Cnp1} on a cc2 sequence without the adjacent K” repeat in cells over expressing CENP-A^{Cnp1}, which has been shown to bypass the requirement of heterochromatin (Catania et al., 2015). *hap2*Δ showed no association of CENP-A^{Cnp1} at plasmed-bourne cc2 DNA (Figure 5.1 G; Primer cc2-a, cc2-b and cc2-c). Together, these observations clearly shows that Hap2 is required for *de novo* deposition of CENP-A^{Cnp1} on naïve centromeric sequences which is independent of adjacent heterochromatin requirement.

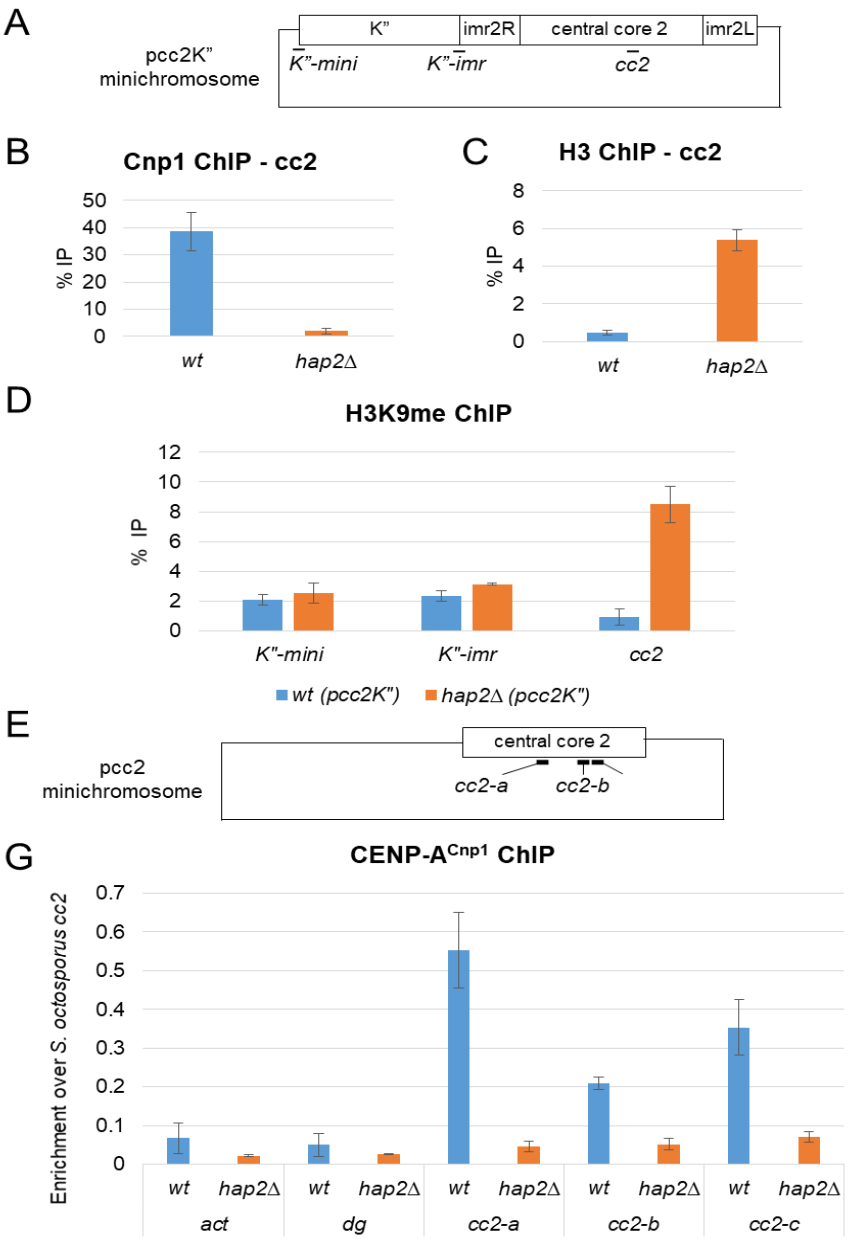

Figure 5.1: Hap2 is required for *de novo* CENP-A^{Cnp1} assembly on minichromosomes

(A) Schematic of pcc2K" minichromosome and primer positions (B and C) qChIP of CENP-A^{Cnp1} and H3 levels at *cc2* on pcc2K" and pcc2 minichromosome in wild-type and *hap2*Δ cells. Three random colonies with transformed minichromosome were picked from -ade-ura medium plate and grown under selection for ChIP. Mean ± S.D. of n=3 biological replicates is shown. (D) qChIP of H3K9me on the pcc2K" minichromosome at *K"-mini*, *K"-imr* and *cc2* locus on the minichromosome. Three random colonies with transformed minichromosome were picked from -ade-ura medium plate and grown under selection for ChIP. (E) Schematic of pcc2 minichromosme and primer positions on *cc2* DNA. (F) qChIP of CENP-A^{Cnp1} levels at *act1*$^{+}$, outer repeat region *dg* and plasmid bourne *cc2* sequence cc2-a, cc2-b and cc2-c in wild-type and *hap2*Δ cells overexpressing CENP-A^{Cnp1}. Cells were transformed with pcc2 minichromosome and grown on ade- ura- medium plates. Three random colonies were picked and grown under selection for ChIP Mean ± S.D. of n=3 biological replicates is shown.

5.2.2 Hap2 is not required to maintain pericentric heterochromatin

To determine if Hap2 contributes to endogenous outer repeat heterochromatin integrity, various assays were performed. Mutants with defective heterochromatin, such as *clr4*, *rik1* and *swi6*, show alleviation of marker genes inserted at various positions within centromeric outer repeats (Allshire et al., 1995). To investigate whether Hap2 affects transcriptional silencing within centromeric outer repeats, thus *hap2*Δ cells with the *ade6*$^+$ gene inserted at *SphI* site in otr1 were used (Figure 5.2 A). Wild type cells with *otr1R(SphI):ade6*$^+$ insertion form red colonies on limiting adening (low ade) plates due to the repression of *ade6*$^+$ gene. The *hap2*Δ form pale colour on indicator plates suggesting alleviates *ade6*$^+$ gene repression (Figure 5.2 B). Deletion of genes encoding non-essential subunits of the Ino80 complex (*iec1*Δ, *arp8*Δ, *ies6*Δ and *ies2*Δ) affects phosphate and adenine metabolism and consequently these colonies fail to turn red on low-adenine plates (Hogan et al., 2010). Hap2 is an Ino80 complex-associated protein, and consequently it might also affect adenine metabolism and represent a false positive with respect to heterochromatin silencing assay. Therefore, transcriptional silencing at the centromeric outer repeats should be re-tested using a *ura4*$^+$ reporter gene instead of *otr1R(SphI):ade6*$^+$.

Mutants with defective heterochromatin, such as *clr4*, show alleviation of marker gene inserted at centromeric outer repeats along with accumulation of non-coding centromeric outer repeat transcripts (Allshire et al., 1995; Bayne et al., 2014). Therefore the levels of non-coding centromeric outer repeat transcripts were analyzed by RT-qPCR. The *hap2*Δ mutant exhibited no detectable accumulation of centromeric outer repeat (*dg*) transcripts (Figure 5.2 C). It is possible that in this mutant centromeric silencing is disrupted without any observable increase in centromeric transcript accumulation if, for example, transcription is impaired or the transcripts are rapidly degraded. To further investigate transcription of centromeric outer repeats, RNAPII ChIP could be performed in *hap2*Δ cells. A defining feature of centromeric heterochromatin is methylation of lysine 9 of histone H3 (H3K9me; Grewal and Jia, 2007). ChIP revealed that H3K9 methylation levels on the endogenous centromeric repeats (*dg*) were unaffected in the absence of Hap2 (Figure 5.3 D). Together these data suggests that Hap2 might not play a significant role in promoting heterochromatin integrity over the centromeric outer repeats.

At endogenous centromeres tRNA genes are known to act as boundary elements and prevent spreading of H3K9me2 into the central CENP-A^{Cnp1} domain (Scott et al., 2006). The pcc2K" minichromosome lacks a tRNA gene between the K" repeat and adjacent *cc2* DNA. Indeed ChIP analysis showed that deletion of *hap2* leads to spreading of H3K9me over the nearby *cc2* sequence on the minichromosome (Figure 5.1). To investigate heterochromatin spreading at endogenous centromeres, the levels of H3K9me2 at *imr1* were assessed. Cells lacking the *hap2* gene showed no observable increase in the levels of H3K9me at *imr1* (Figure 5.2 E), indicating that Hap2 is not required to prevent heterochromatin from spreading in the central domain at endogenous centromeres. It is possible that the increased levels of H3K9me on cc2 of the pcc2K" minichromosome results from the lack of a tRNA gene boundary element.

5.2.3 Hap2 is required to maintain normal CENP-A^{Cnp1} levels and transcriptional silencing in the central domain of centromeres

Deletion of subunits of Ino80 complex have varying degree of alleviation of transcriptional silencing in the centromeric central domain of fission yeast centromeres (Choi et al., 2017). The integrity of the CENP-A^{Cnp1} chromatin domain at endogenous centromeres was tested in *hap2*Δ cells using a central core silencing assay. A strain containing the *ura4*$^{+}$ gene inserted in the central domain of cen1 (*TM1::ura4*$^{+}$) was used as a reporter for transcriptional silencing (Figure 5.3 A). Wild type cells containing *TM1::ura4*$^{+}$ grow slower on FOA containing plates compared to cells completely lacking the *ura4*$^{+}$ gene. The *hap2*Δ mutation alleviates *TM1::ura4*$^{+}$ repression, as shown by impaired growth on FOA plate (Figure 5.3 B). The effect of *hap2*Δ on CENP-A^{Cnp1} and H3 incorporation at centromeres was evaluated by GFP-CENP-A^{Cnp1} and H3 ChIP. Consistent with defective central domain silencing, ChIP analyses showed that *hap2*Δ cells exhibit reduced CENP-A^{Cnp1} and a reciprocal increase in histone H3 levels within the central domain of cen2 (Figure 5.3 C and D). These observations directly implicate Hap2 in the maintenance of CENP-A^{Cnp1} chromatin at fission yeast centromeres.

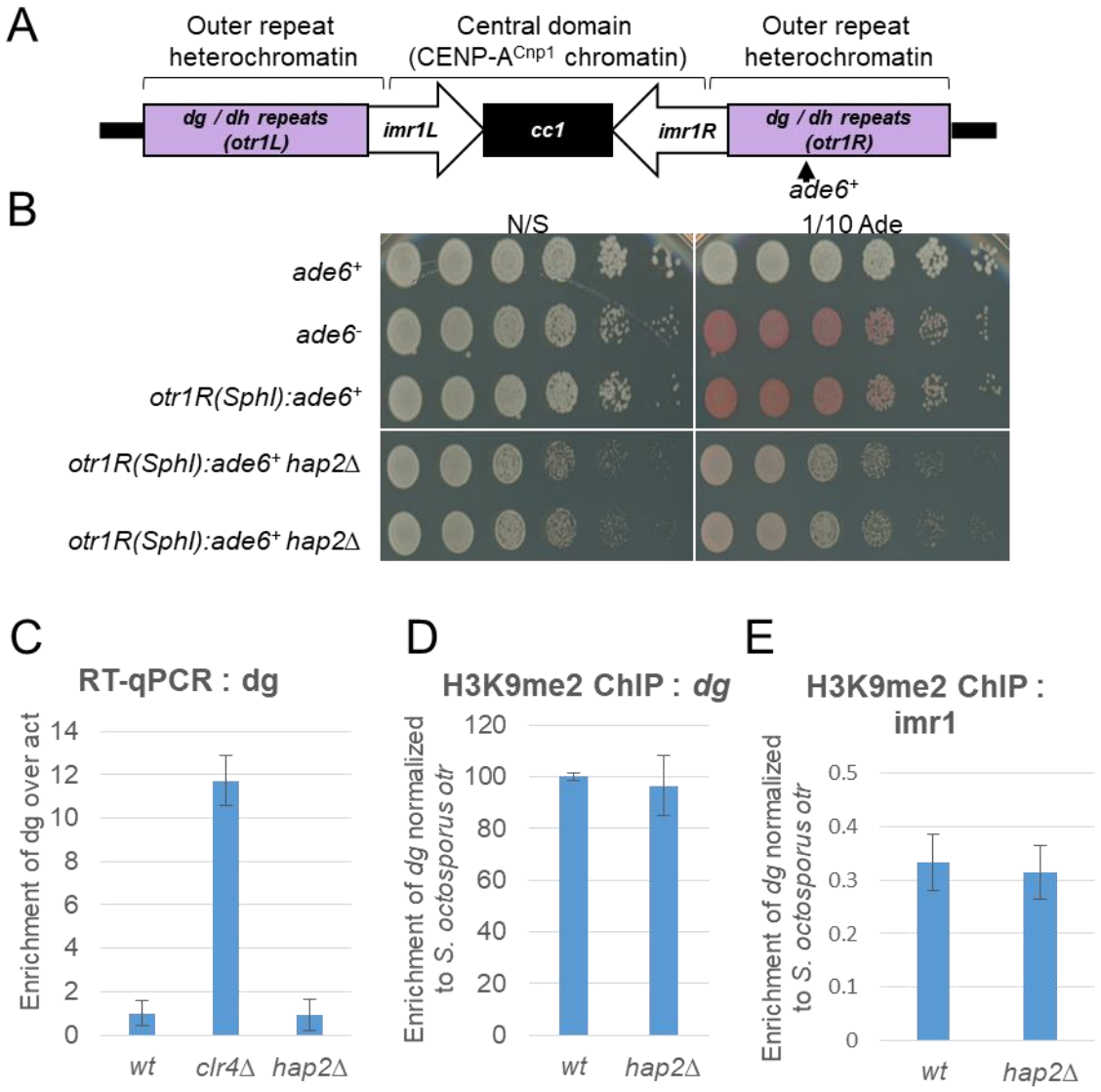

Figure 5.2: Hap2 is not required to maintain pericentric heterochromatin at centromeres

(A) Schematic representation of the *ade6*+ gene integration site at centromere 1 used for pericentric heterochromatin silencing assay. (B) Serial dilution spotting assay of wild type and *hap2* mutants. Cells are plated on rich medium (YES) and with limiting amount of adenine (1/10th ade). Progeny from a *hap2*Δ *otr1R(SphI)* were analysed. (C) RT-qPCR of *dg* transcripts in wild-type, *clr4*Δ and *hap2*Δ cells normalized to *actin* transcripts. Mean ± S.D. of n=3 biological replicates is shown. (D) qChIP of H3K9me2 levels at *dg* in wild-type and *hap2*Δ cells normalized to spiked in *S. octosporus otr*. Mean ± S.D. of n=3 biological replicates is shown. (E) qChIP of H3K9me at *imr1* in wild-type and *hap2*Δ cells. Mean ± S.D. of n=3 biological replicates is shown.

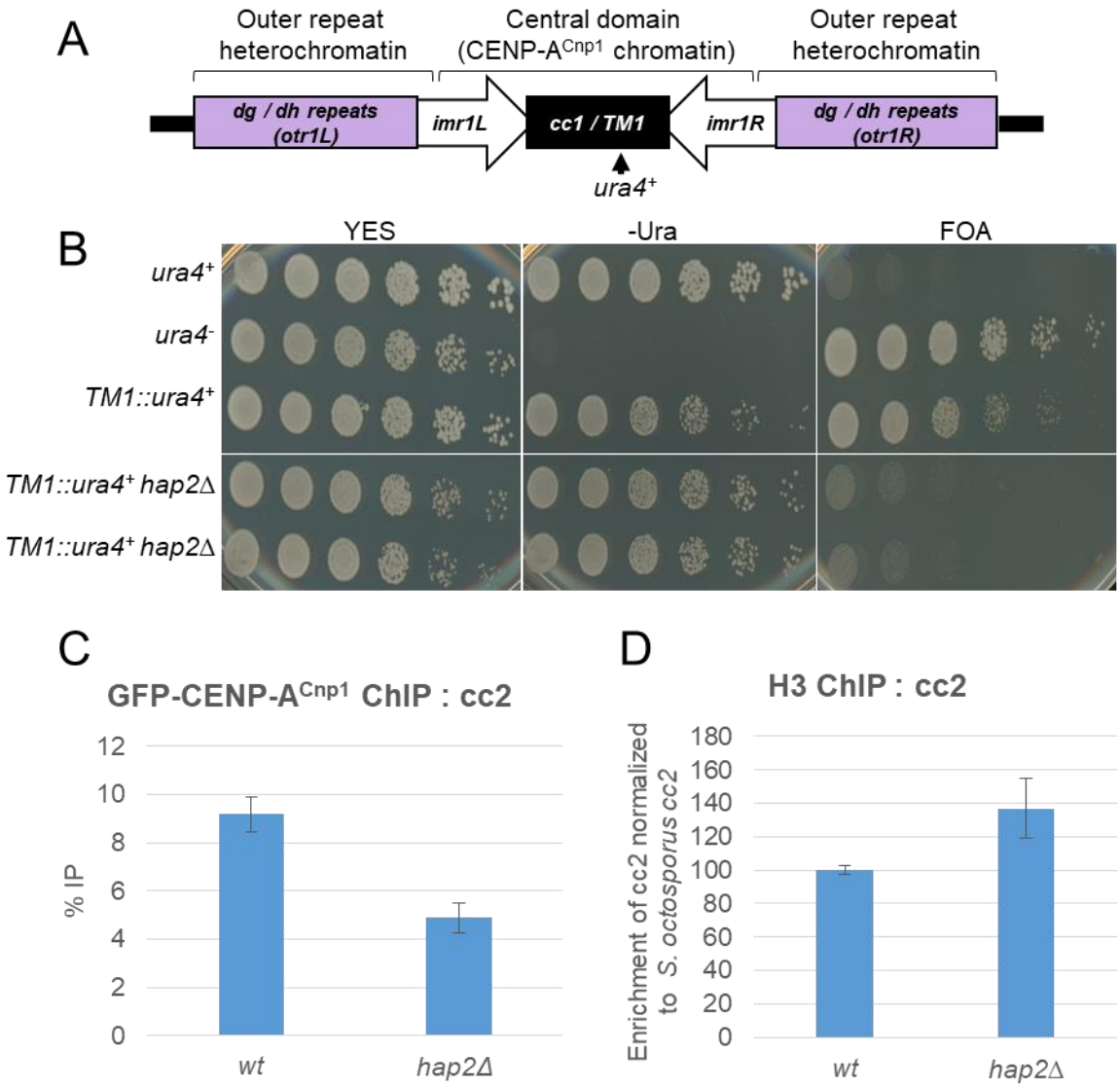

Figure 5.3: Hap2 is required to maintain transcriptional silencing and CENP-A^{Cnp1} occupancy at centromeres

(A) Schematic representation of the *ura4*$^+$ gene integration site at centromere 1 used in the central domain silencing assay. (B) Spotting assay of wild type and mutants with *ura*+ inserted within the central domain. Cells are plated on rich medium (YES), uracil deficient plates (ura-) and FOA containing plates (FOA). In wild type cells (*TM1::ura4*$^+$) silencing of the central domain is maintained and cells are able to grow in medium containing the counter selective drug FOA and grow poorly on medium lacking uracil. Progeny from a *hap2*Δ*TM1::ura4*$^+$ were analysed. (C and D) qChIP of CENP-A^{Cnp1} and histone H3 levels at endogenous *cc2* Mean ± S.D. of n=3 biological replicates is shown.

5.2.4 Tagged Hap2-GFP localizes to the nucleus and it is associated with centromeres

Hap2 is a non-essential putative auxiliary component of the Ino80 remodeling complex (Hogan et al., 2010). Most Ino80 complex subunits have a nuclear localization (Matsuyama et al., 2006). To investigate the localization of Hap2, strains expressing tagged Hap2-GFP were analysed. Hap2-GFP was found to be nucleus (Figure 5.4 A). This is consistent with the nuclear localization of Ino80 subunits (Matsuyama et al., 2006). The functionality of Hap2-GFP should be tested and the establishment frequency for tagged strain should be similar to that for the wild type strain.

Kinetochore proteins such as CENP-I^{Mis6} and CENP-O^{Mal2} mutants alleviate central core silencing and are specifically enriched across the central domain (Partridge et al., 2000; Jin et al., 2002; Subramanian et al., 2014). *sim* mutants also alleviate central core silencing and show centromere specific localization, except NASP related chaperone Sim3 (Pidoux et al., 2003; Dunleavy et al., 2007). Recently, deletion of Ino80 subunits Iec1 and Ies6 were shown to weakly alleviate transcriptional silencing within the central domain and Iec1 and Ies6 widely associated across the central domain as well as with specific regions of the flanking outer repeats (Choi et al., 2017). Since *hap2*Δ also alleviates central domain silencing and associates with Ino80 complex, it is possible that Hap2 also associates with centromeres. To investigate this possibility, Hap2 was tagged with GFP and anti-GFP ChIP was performed. Hap2-GFP was found to be enriched within central core (*cc1* and *cc2*) and outer repeat (*dg*) regions (Figure 5.4 B). Analysis of immunoprecipitated DNA indicated that Hap2-GFP was in fact more enriched at a euchromatic *act1*$^{+}$ locus (Figure 5.4 B). This result is not surprising considering the nuclear localization of Hap2-GFP. Together, these observations suggest that Hap2-GFP associates with centromeric chromatin in addition to other chromatin regions.

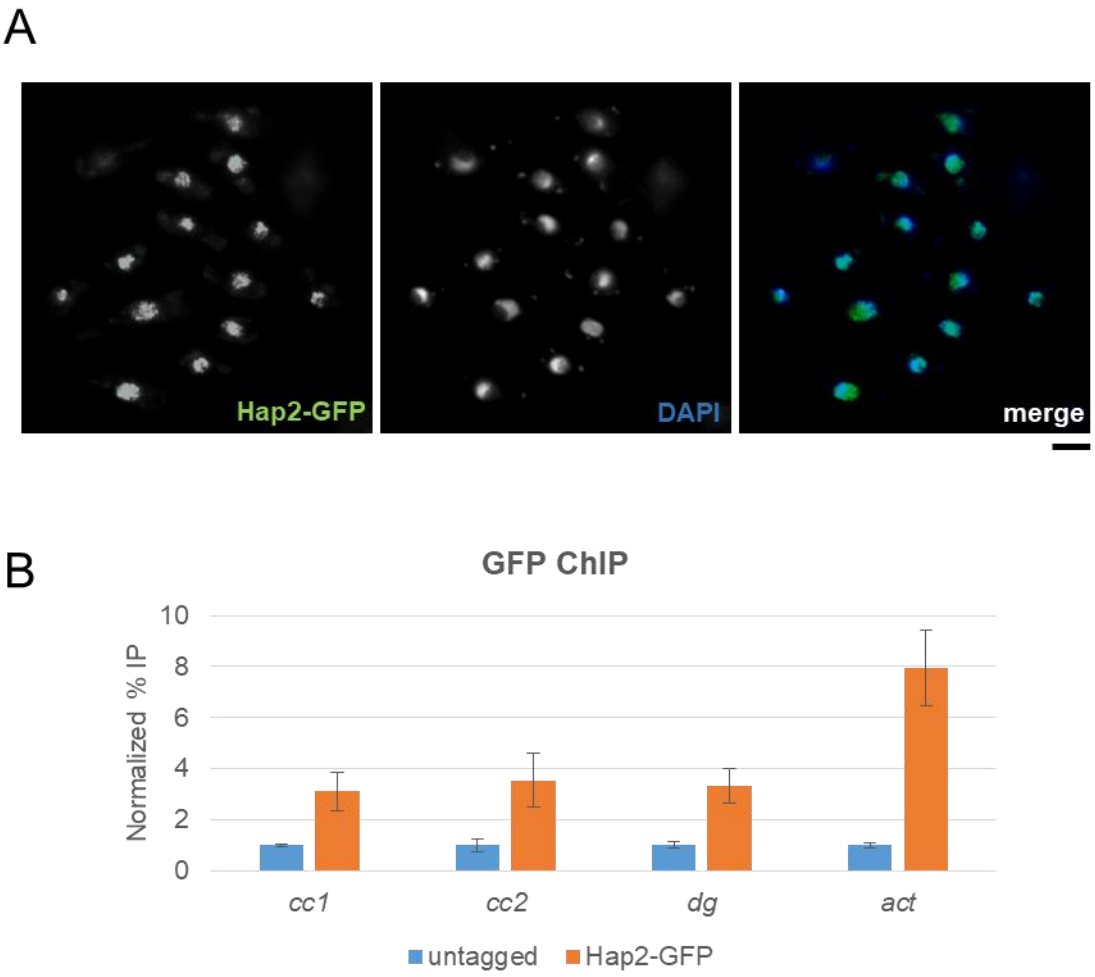

Figure 5.4: Hap2-GFP protein is localized to the nucleus and it is associated with centromeres. (A) Localization of Hap2-GFP shows nuclear localization. Blue: DAPI and green: GFP. Bar: 5 µm. (B) qChIP of Hap2-GFP levels at central domain 1 (*cc1*), central domain 2 (*cc2*), pericentric outer repeat region (*dg*) and *act1*+ gene. Mean ± S.D. of n=3 biological replicates is shown.

5.2.5 Hap2-GFP affinity selection confirms that Hap2 is an Ino80 complex subunit

The ATP-dependent chromatin remodeling Ino80 complex has been shown to be involved in transcription regulation as well as DNA repair (Clapier and Cairns, 2009). The Ino80 complex comprises of a core with nine proteins: Ino80, Rvb1, Rvb2, Arp4, Arp5, Arp8, Ies2 and Ies6. These core proteins are conserved from yeast to human, along with several species-specific proteins that associate with the core (Table 5.1; Chen et al., 2011; Tosi et al., 2013). Nuclear actin associates with the Ino80 complex and contributes to the interaction of Ino80 with chromatin (Kapoor et al., 2013). The

other core subunits bind to Ino80 via either the helicase SANT-associated (HSA) domain or the SNF2 ATPase domain (Figure 5.5 A and B). These subunits form different modules of the Ino80 complex that are required for the function of the Ino80 complex (Figure 5.5 C; Gerhold and Gasser, 2014).

The N terminus of Ino80 binds to species-specific subunits (Table 5.1; Figure 5.5). In *S. cerevisiae*, the NHP10 module consists of NHP10, IES1, IES3 and IES5 which associates with Ino80 and has been shown to form a stable complex *in vitro* (Tosi et al., 2013). The N terminus of human Ino80 recruits a distinct set of human-specific NTD binding proteins (Chen et al., 2011). These observations suggest both a conserved and divergent functional architecture of the Ino80 complex. *S. pombe* has the conserved Ino80 core subunits along with subunits that have orthologues only in either *S. cerevisiae* (Nhp1, Ies4 and Tfg3) or humans (Iec1). It also contains three species-specific subunits: Iec3, Iec5 and Hap2 (Table 5.1)

Hap2 was first identified as an Ino80 interacting protein in a study by using Ino80-FLAG pulldowns (Hogan et al., 2010). However, Hap2 was not found to coprecipitate with Iec1-HA (Hogan et al., 2010). A previous study by Shevchenko et al. (2008) did not identify Hap2 and Iec5 in affinity selected TAP-tagged Ies6 preperations. These differences may relate to the distinct purification protocols used or detection sensitivities in the two studies. Alternatively, Hap2 might have a distinct or dynamic interaction with the core Ino80 complex. It is also possible that the detection of Hap2 just represented a false positive in Ino80-FLAG pulldowns. To further investigate these possibilities, affinity purification of Hap2-GFP along with untagged control was performed. Western analysis revealed high enrichment of Hap2-GFP after immunoprecipitation (Figure 5.6 A). To test the amount and the quality of the affinity purification, eluted proteins were separated on a denaturing polyacrylamide gel and stained with silver nitrate. Many unique protein bands were observed only in the Hap2-GFP IP but not in the control IP (Figure 5.6 B). Furthermore, several bands detected in the Hap2-GFP IP corresponding to the size of histone H2A, H2B, H3 and H4 proteins suggesting that Hap2-GFP affinity selection resulted in the enrichment of a chromatin-associated complex. Samples were next subjected to LC-MS/MS analysis to identify Hap2 associated proteins.

Quantitative proteomic analysis of Hap2-GFP associated proteins was performed to determine what proteins associate with Hap2. Volcano plots were used to graphically visualize the enrichment of proteins with Hap2-GFP compared to untagged control (Figure 5.6 C). All Ino80 subunits were identified and all except Act1 showed ≥ 8 fold enrichment with Hap2-GFP (Figure 5.6 C). H2A.Z^{Pht1} showed > 6 fold enrichment with Hap2-GFP (Figure 5.6 C), suggesting association of H2A.Z^{Pht1} with Hap2-Ino80 complex. Ino80 regulates the genome-wide distribution of the histone variant H2A.Z possibly by replacing H2A.Z/H2B dimers with H2A/H2B dimers in nucleosomes as determined in vitro in budding yeast (Papamichos-Chronakis et al., 2011; Papamichos-Chronakis and Peterson, 2013).

iBAQ analysis allows the relative stoichiometry of the identified proteins within complexes to be assessed (Chapter 3; Fabre et al., 2014). To calculate the relative stoichiometries of the identified Ino80 complex subunits, the iBAQ scores for each protein were normalized to the iBAQ score for Hap2. All 15 Ino80 complex proteins showed significantly higher relative stoichiometries compared to Hap2 including Act1 (Figure 5.6 D). This suggest that Hap2 might be associated with the Ino80 complex. Rvb1 and Rvb2 showed the highest relative stoichiometries which can be explained by the heterohexameric ring structure formed by these proteins (Gribun et al., 2008). The budding yeast INO80 complex contains equivalent stoichiometric levels of INO80, Arp4, Arp5, Arp8, and actin (Shen et al., 2000). In the fission yeast Hap2-GFP pulldown, Ino80 and these actin-related proteins also showed relatively similar enrichments (Figure 5.6 D). The stoichiometries of Iec1/3/5, Ies2/4/6, Nht1 and Tfg3 were also higher than Hap2 although lower than other core Ino80 subunits (Figure 5.5 D). A lower stoichiometry of H2A.Z^{Pht1} was observed (Figure 5.6 D). This is consistent with H2A.Z^{Pht1} being a substrate of Ino80 complex rather than a component of Ino80 complex (Papamichos-Chronakis et al., 2011). iBAQ analysis demonstrated higher stoichiometries for Ino80 subunit compared to Hap2, suggesting that Hap2 has a complicated relationship with the Ino80 complex. As proteins are lost during the immunoprecipitation protocol, iBAQ analysis is not completely reliable for determining the stoichiometry of subunits within complexes. Further investigation is needed, for example, size exclusion chromatography and XL-MS analysis of Hap2 complex.

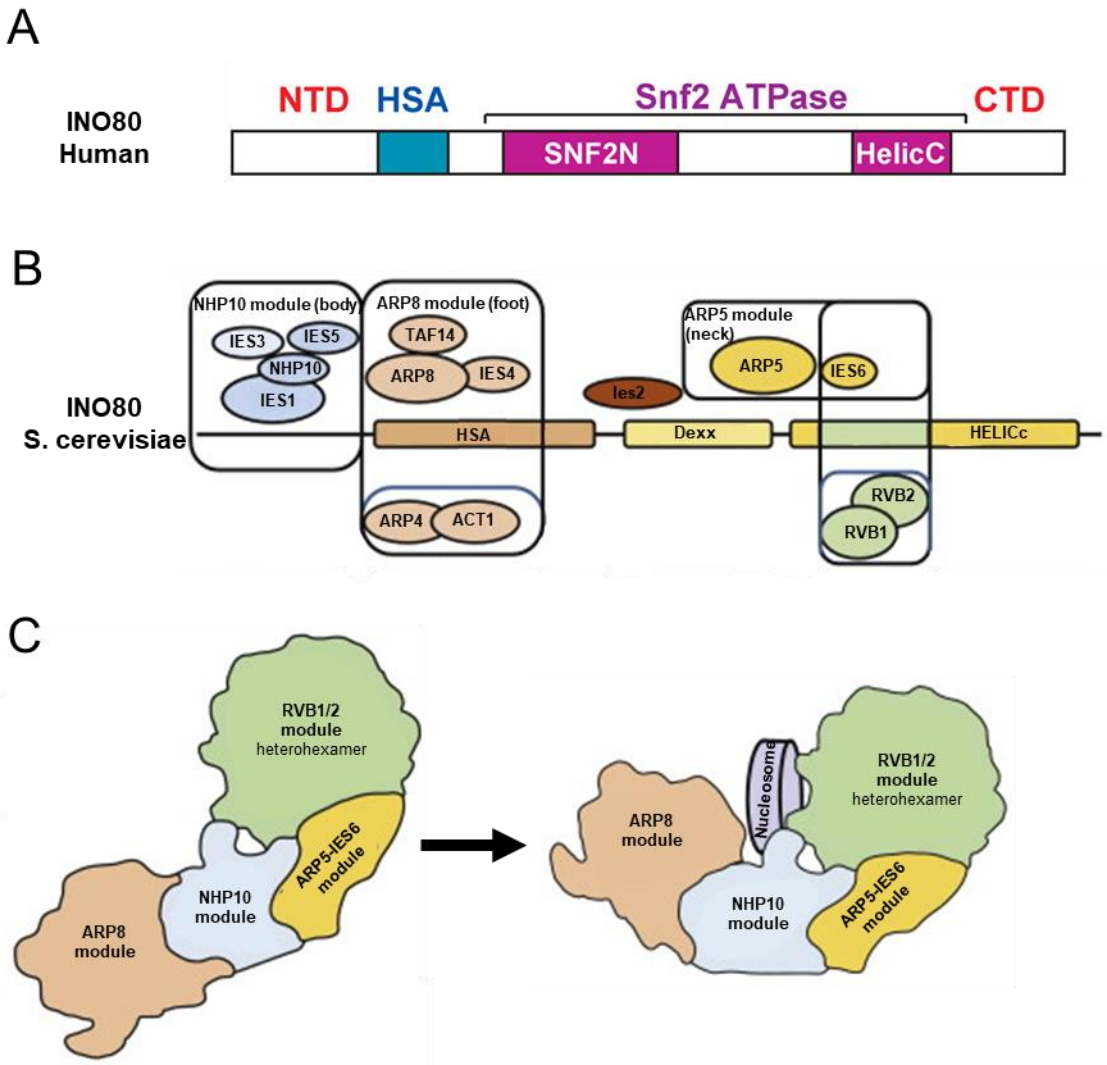

Figure 5.5: Human and *S. cerevisiae* INO80 complex. (A) Domain organization of human INO80 protein. Adapted from Chen et al. (2011). (B) Domain architecture of INO80 adapted from Gerhold and Gasser (2014). (C) Structural model of *S. cerevisiae* nucleosome-bound INO80 complex adapted from Gerhold and Gasser (2014). ARP8 module undergoes a major structural rearrangement to bind to one side of the nucleosome while the other side faces RVB1/2 module. The NHP10 module holds the nucleosome in place.

Table 5.1: Comparison of the subunit compositions of *S. pombe*, *S. cerevisiae* and Human INO80-related chromatin remodeling complexes

S. pombe	S. cerevisiae	Human	Comment
Ino80	INO80	hINO80	SNF2-like helicase
Rvb1	RVB1	RVBL1	DNA helicases (also a subunit of Nu4A complex, Swr1 complex and ASTRA complex)
Rvb2	RVB1	RVBL2	
Ies2	IES2	INO80B	Ino80 complex subunit
Arp5	ARP5	ACTR5	Actin-related protein
Ies6	IES6	INO80C	Ino80 complex subunit
Nhp1	NHP10	-	HMG-type domain; DNA binding
-	IES1	-	Ino80 complex subunit
-	IES3	-	Ino80 complex subunit
-	IES5	-	Ino80 complex subunit
Arp8	ARP8	ACTR8	Actin-related protein
Ies4	IES4	-	Ino80 complex subunit
Tfg3	TAF14	-	TATA binding protein-Associated Factor (also a subunit of SWI/SNF complex, TFIID and TFIIF complex)
Alp5	ARP4	ACTL6A	Actin-related protein (Alp5 is also a subunit of NuA4 complex and Swr1 complex)
Act1	ACT1	Actin family	Actin (also part of NuA4 complex and Swr1 complex)
-	-	INO80D	FLJ20309
-	-	INO80E	FLJ90652
-	-	TFPT	TCF3 fusion partner
-	-	NFRKB	nuclear factor related to kappaB binding protein
-	-	MCRS1	FHA domain in the C terminus
-	-	UCHL5	ubiquitin C-terminal hydrolase L5
Iec1	-	YY1	YY1 transcription factor
Iec3	-	-	Ino80 complex subunit
Iec5	-	-	Ino80 complex subunit
Hap2	-	-	HMG box protein (predicted)
Ino80	Conserved core Ino80 complex (conserved from yeast to humans)		
Head	RVB1/2 module		Structural information based on *S. cerevisiae* INO80 EM and XL-MS data (Tosi et al., 2013)
Neck	ARP5-IES6 module		
Body	NHP10 module		
Foot	ARP8 module		
	NTD binding module		Subunit organization of human INO80 complex (Chen et al., 2011)
	HSA binding module		
	Snf2 ATPase module		

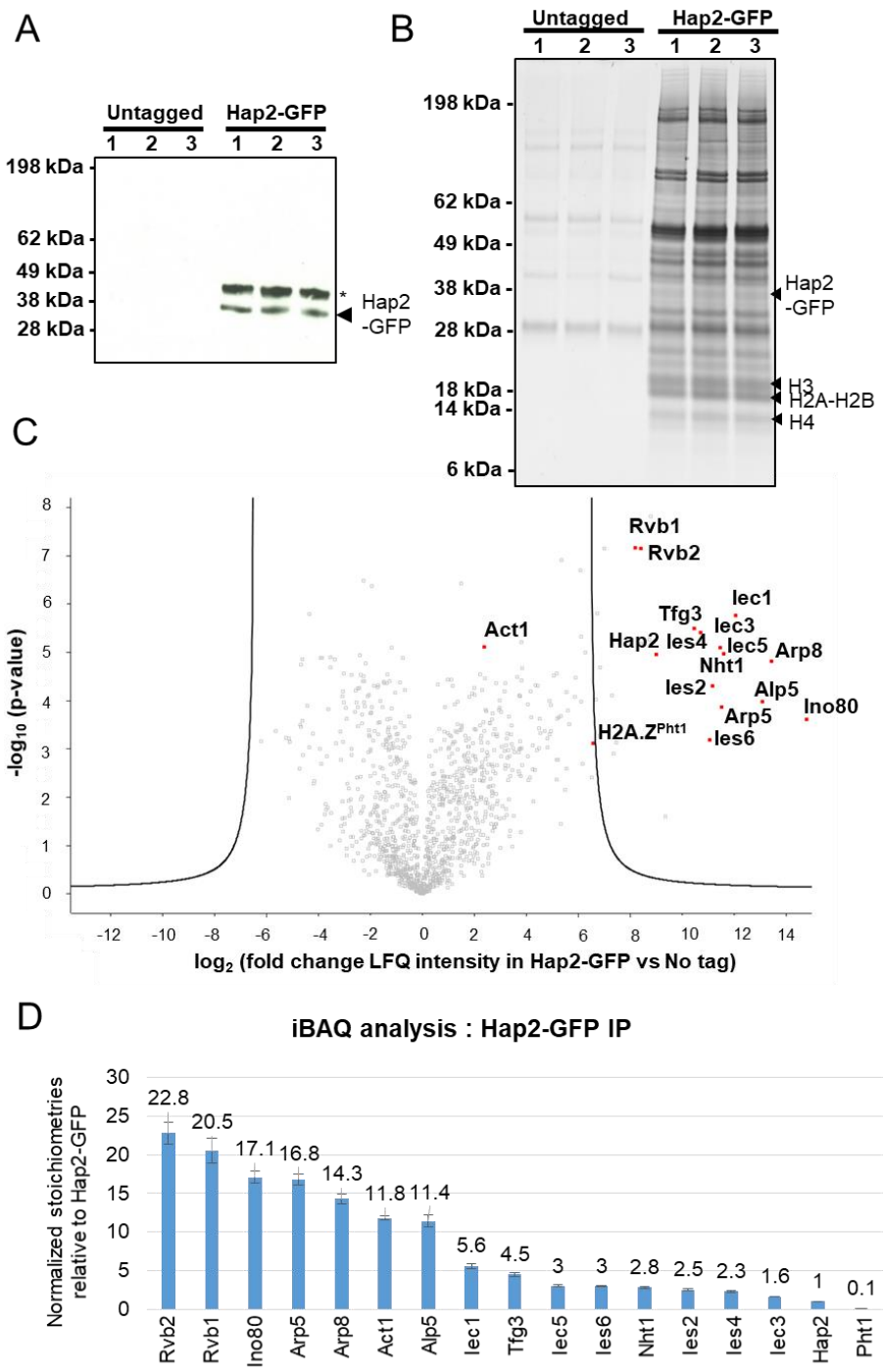

Figure 5.6: Hap2 is an Ino80 complex subunit. (A) A western blot analysis of Hap2-GFP after native affinity purification. Untagged and Hap2-GFP cells were frozen using liquid N2 and lysed by bead beating. Solubilized chromatin extract was used for affinity purification of Hap2-GFP complex under mild conditions along with untagged as control. Three biological replicates were used for the experiment. (B) Eluates from native affinity purifications of Hap2-GFP were separated by SDS–PAGE and visualized by silver staining. Labelled proteins based on predicted molecular weights. (C) Volcano plot representation of protein abundances in Hap2-GFP proteome compared to untagged control. Hap2 and subunits of Ino80 complex were significantly enriched in Hap2-GFP proteome. (D) Relative stoichiometries of Ino80 complex subunits in Hap2-GFP pulldown as indicated by the iBAQ values.

5.2.6 Hap2 facilitates replication-independent histone H3 turnover at centromeres

ATP-dependent chromatin remodeling factors can disassemble nucleosomes or exchange histone subunits within nucleosomes (Clapier and Cairns, 2009; Papamichos-Chronakis et al., 2011). ATP-dependent chromatin remodeling complexes such as the Ino80 complex and CHD family member Hrp1, regulate histone dynamics (Walfridsson et al., 2005; Choi et al., 2011; Choi et al., 2017). Histone H3 competes with CENP-A^{Cnp1} for incorporation into centromeres and eviction of histone H3 is postulated to provide an opportunity for CENP-A^{Cnp1} nucleosome deposition (Castillo et al., 2007; Allshire and Karpen, 2008; Choi et al., 2012; Shukla et al., 2017). In *S. cerevisiae*, the Ino80 complex has been shown to maintain chromatin structure at pericentric chromatin but not the CENP-A^{Cse4} nucleosome (Chambers et al., 2012). A recent study by Choi et al. (2017) showed that the Ino80 complex is required for CENP-A^{Cnp1} chromatin assembly at centromeres. They found a correlation between Ino80 complex localization of and removal of histone H3 from these regions in *ies6*Δ cells and proposed a model that Ino80 complex acts at centromeres to remove histone H3-containing nucleosomes and consequently results in CENP-A^{Cnp1} deposition (Choi et al., 2017). Eviction of histone H3 can assessed at cc2 sequence assembled in H3 nucleosome using a histone H3 turnover assay (Shukla et al., 2017). If Hap2 and Ino80 are involved in removing H3 from centromeres then the rate of histone H3 turnover should be altered in the absence of Hap2/Ino80.

To measure replication-independent H3 turnover, the recombination induced tag exchange (RITE) system (Verzijlbergen et al., 2010; Svensson et al., 2015; Shukla et al., 2017) was employed to assess the rate of incorporation of newly synthesized T7-tagged histone H3 in wild-type and *hap2*Δ cells. Cells containing *cdc25-22* were blocked in G2/M by incubation at restrictive temperature for 150 minutes followed by addition of β-estradiol to induce nuclear import of Cre-EBD in arrested cells to mediate recombination between LoxP sites therefore newly synthesized H3 was tagged with T7 epitope (Figure 5.7). ChIP analysis was performed to measure the levels of total H3 (using anti-H3 antibody) and newly synthesized H3-T7 (using anti-T7 antibody). Histone turnover at a locus was represented as enrichment of newly synthesized H3-T7 normalized to the total histone H3 level.

The lack of centromere establishment in *hap2*Δ cells might be due to altered histone H3 dynamics on naïve central domain centromeric sequences in pcc2K". To test this possibility, histone H3 turnover was measured on *cc2* DNA ectopically inserted at a chromosomal locus to assess the affect of Hap2 on cc2 sequence assembeled in H3 nucleosomes. Changes in turnover of H3 nucleosomes at these sequences might explain the loss of de novo CENP-A^{Cnp1} establishment. All strains used have 6 kb of *cen2* central domain DNA replaced with 5.5 kb of cen1 central domain DNA (*cc2Δ::cc1*) and 8.5 kb of ectopic *cc2* DNA inserted at non-centromeric *ura4* locus (*ura4:cc2*). This ectopic *cc2* DNA is assembled in H3 nucleosomes and completely devoid of CENP-A^{Cnp1} nucleosomes (Shukla et al., 2017). Lower histone H3 turnover was observed on this ectopic *cc2* DNA in *hap2*Δ cells compared to wild-type (Figure 5.8; primers: *cc2-a*, *cc2-b* and *cc2-c*). This reduced H3 turnover could explain the failure of *hap2*Δ cells to establish CENP-A^{Cnp1} chromatin on the pcc2K" minichromosome (Figure 5.1). Lower histone H3 turnover was also observed within the endogenous central domain of cen1 (Figure 5.8; primer: *cc1*). Therefore, the reduced CENP-A^{Cnp1} levels detected at endogenous centromeres (Figure 5.3 C) could result from inefficient replication-independent histone H3 turnover at centromeres. Consistent with no obvious decrease in the levels of H3K9me2 was detected (Figure 5.2 D), histone H3 turnover in *hap2*Δ at the outer repeats regions *dg* was similar to the wild type (Figure 5.8; primer: *dg*). Histone H3 turnover was also measured at other non-centromeric loci like *act1*$^{+}$ along highly expressed *pyk1*$^{+}$ gene and lowly expressing *spd1*$^{+}$, all displayed reduced histone H3 turnover in *hap2*Δ cells relative to wild-type (Figure 5.8; primer: *act1* and data not shown). Together, these observations indicate that Hap2 is required for histone H3 turnover at central domain sequences and other genomic loci. Genome-wide histone H3 turnover should be performed to see if some regions are more sensitive to loss of Hap2 than others.

As turnover of histone H3 nucleosome might provide the opportunity for the assembly of CENP-A^{Cnp1} in their place (Allshire and Karpen, 2008), diminished turnover of histone H3 would be expected to curtail the deposition of CENP-A^{Cnp1}. Taken together, these observations indicate a role of Hap2 in regulating replication-independent turnover of histone H3 within centromeres thereby influencing CENP-A^{Cnp1} establishment and maintenance.

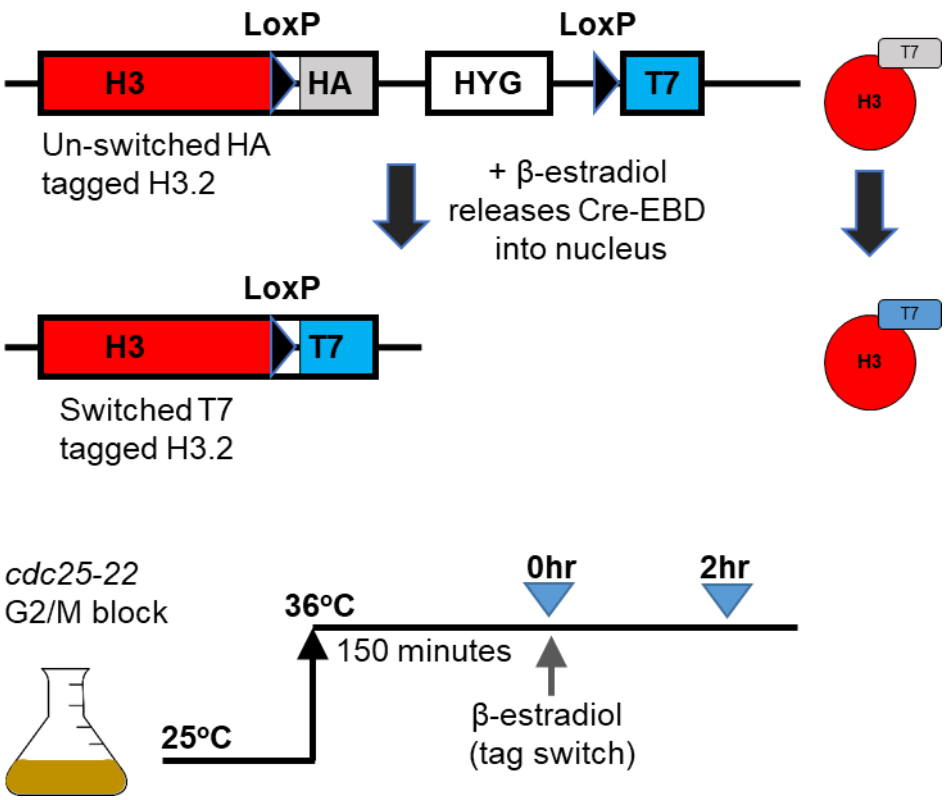

Figure 5.7: Diagram of recombination induced tag exchange (RITE) system

cdc25-22 mutant cells were blocked in G2/M by incubation at 36°C for 150 minutes. Samples with un-switched HA tagged H3 were collected (0hr). Tag swap was induced by β-estradiol addition. Samples were collected to measure incorporation of newly synthesized T7-tagged H3 after two hours (2hr).

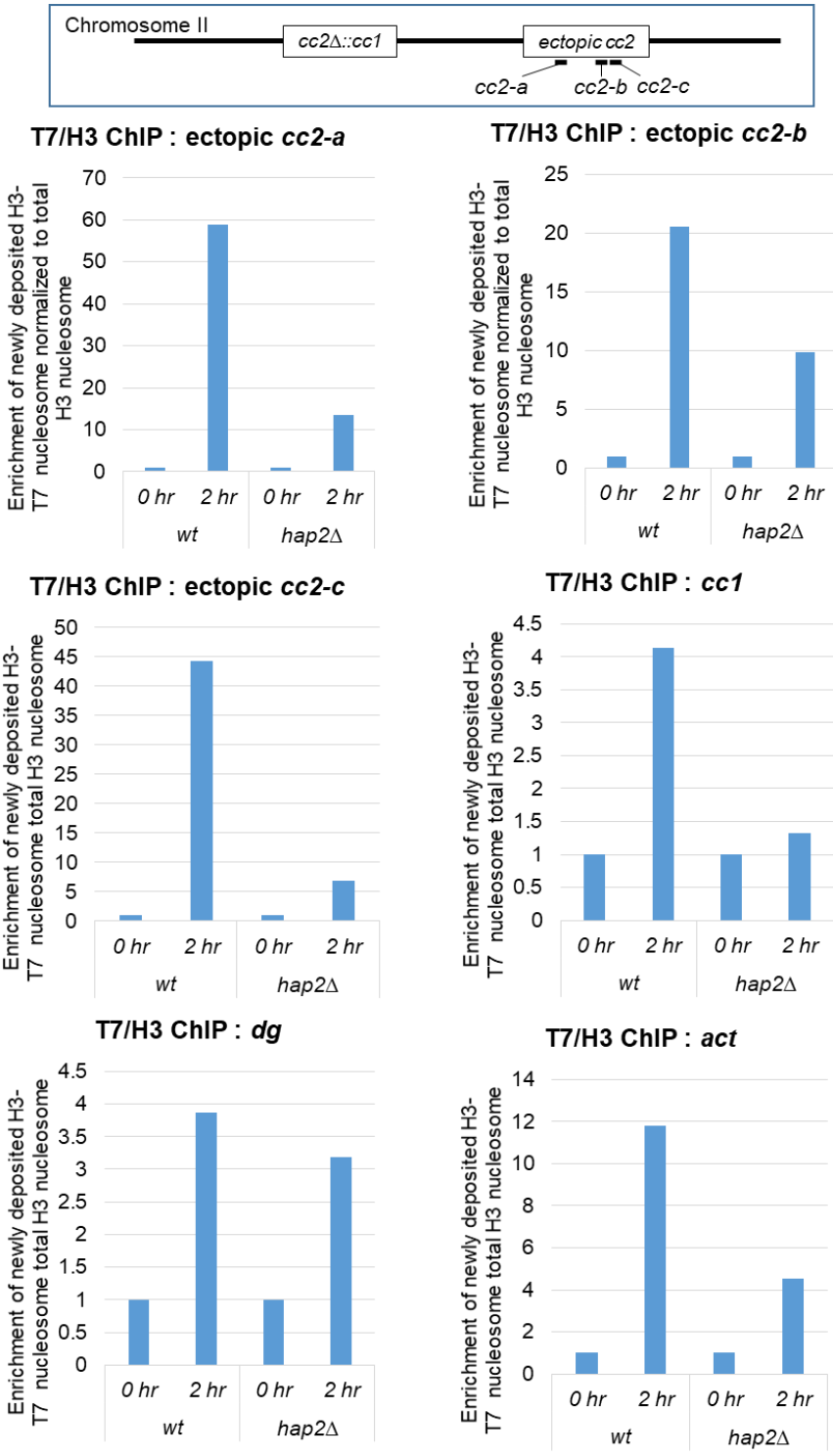

Figure 5.8: Hap2 is required for efficient replication-independent histone H3 turnover

Schematic of ectopically inserted *cc2* DNA on chromosome II and primer positions. qChIP of T7 tagged histone H3 and total histone H3 levels in wild-type and *hap2*Δ cells. Replication-independent H3 turnover was measured by Recombination Induced Tag Exchange (RITE) system. Replication-independent histone H3 turnover rate at ectopic central core sequence without CENP-A^{Cnp1} nucleosomes (*cc2-a*, *cc2-b* and *cc2-c*), endogenous centromere with CENP-A^{Cnp1} nucleosomes (*cc1*), pericentric outer repeats (*dg*) and actin locus (*act*) were measured.

5.3 Discussion

In this chapter, the role of Hap2 in CENP-A^{Cnp1} establishment and maintenance was investigated. *De novo* centromere establishment on the pcc2K" minichromosome requires heterochromatin formation on the K" outer repeat which in turn promotes the assembly of CENP-A^{Cnp1} chromatin over adjacent *cc2* DNA (Folco et al., 2008; Kagansky et al., 2009; Catania et al., 2015). ChIP analysis revealed that *hap2*Δ cells fail to deposit any CENP-A^{Cnp1} on minichromosome-borne *cc2* DNA (Figure 5.1 B and C). Normal levels of H3K9 methylation were observed on the K" repeat sequence of the minichromosome in *hap2*Δ cells, however H3K9 methylation spread over the adjacent cc2 sequence on the minichromosome (Figure 5.1 D). At endogenous centromeres spreading of H3K9 methylation into central domains was not observed (Figure 5.2 E). tRNA genes are known to form boundaries at endogenous centromere and prevent the spread of H3K9me (Scott et al., 2006). It is possible that the observed spreading of H3K9 methylation on the pcc2K" minichromosome could be due to lack of a tRNA gene between *cc2* and K" repeat sequence, and this could be explored further using different minichromosome. For instance, a tRNA gene should be inserted between *cc2* and K" sequence on the minichromosome to investigate whether the presence of such a boundary element prevents H3K9me from spreading. In addition the genome-wide distribution of H3K9me could be compared in wild-type and *hap2*Δ cells to detect differences by ChIP-seq. Consistent with complete loss of functional centromere establishment in *hap2*Δ cells, no CENP-A^{Cnp1} deposition was detected over the central domain (Figure 5.1 B).

Reporter genes inserted within fission yeast centromeres are transcriptionally silenced and efficient silencing reflects the maintenance of endogenous centromeric chromatin (Allshire et al., 1994; Allshire et al., 1995; Partridge et al., 2000; Jin et al., 2002; Pidoux et al., 2003). Transcriptional silencing assays within outer repeat regions should be performed with *ura4*$^{+}$ reporter gene insertions instead of an *ade6*$^{+}$ reporter gene as it is now known that the Ino80 complex can affect adenine metabolism (Hogan et al., 2010). Related to this, *hap2*Δ cells showed no defect in H3K9 methylation and no accumulation of transcripts from outer repeat regions (Figure 5.2). However, central domain silencing was alleviated in *hap2*Δ cells consistent with a decrease of CENP-A^{Cnp1} levels at endogenous centromeres (Figure 5.3). Therefore, Hap2 is required for

the maintenance of normal levels of CENP-A^{Cnp1} chromatin, but not heterochromatin, at endogenous centromeres.

The Hap2 protein was found to localize to the nucleus in all cells suggesting that Hap2 is present in all stages of the cell cycle (Figure 5.4 A). Other Ino80 subunits are also known to have a nuclear localization in fission yeast (Matsuyama et al., 2006). ChIP analysis showed association of Hap2 with centromeres and non-centromeric loci (Figure 5.4 B). Genome-wide Hap2 localization would reveal if Hap2 is concentrated in certain chromosomal regions and if its distribution is correlated with that of other Ino80 subunits.

Choi et al. (2017) showed that the Ino80 subunits, Iec1 and Ies6, associate with centromeres and in cells with defective CENP-A^{Cnp1} (*cnp1-1*), the levels of Iec1 and Ies6 bound to the central domain were diminished whereas their association with the outer repeats was completely abolished. Choi et al. (2017) proposed that CENP-A^{Cnp1} is required for recruitment Ino80 complex to centromeres. It remains to be tested whether Hap2 association with central domain chromatin is CENP-A^{Cnp1} dependent or a property of central domain DNA itself.

Histone H3 nucleosomes have been detected in the central domain but they are underrepresented in this region relative to the rest of the genome (Choi et al., 2011; Shukla et al., 2017). Decreased CENP-A^{Cnp1} levels within central domains leads to a reciprocal increase in histone H3 levels (Pidoux et al., 2003; Walfridsson et al., 2005; Dunleavy et al., 2007; Choi et al., 2011; Choi et al., 2017). The Chd1^{Hrp1} chromatin remodeling factor was previously implicated in CENP-A^{Cnp1} chromatin assembly (Walfridsson et al., 2005; Choi et al., 2011). Recently, Choi et al. (2017) found a correlation between the localization of Ino80 subunits and removal of histone H3 in *ies6* mutants, implicating Ino80 complex in removing histone H3 nucleosomes and thereby promoting CENP-A^{Cnp1} deposition (Choi et al., 2017). It has been proposed that transcription of centromeric DNA might facilitate the replacement of histone H3 with CENP-A or facilitate localization of factors required for CENP-A deposition (Allshire and Karpen, 2008). The association of CENP-A^{Cnp1} with endogenous centromeres is reduced and *de novo* CENP-A^{Cnp1} assembly on minichromosome is completely abolished in cells lacking Hap2. Reciprocally, the amount of histone H3 is increased in both assays (Figure 5.1 and 5.3). Hap2 appears to function by facilitating

the exchange of histone H3 for CENP-A^{Cnp1} since decreased replication-independent histone H3 turnover was observed at centromeres and on ectopically inserted central domain DNA (Figure 5.8). This observation could explain the loss of CENP-A^{Cnp1} establishment and the CENP-A^{Cnp1} maintenance defects observed on centromere DNA in *hap2*Δ cells.

All subunits of the Ino80 complex were significantly enriched with affinity selected Hap2-GFP, suggesting that Hap2 is a component of Ino80 complex (Figure 5.6). H2A.Z^{Pht1} was also enriched in Hap2 purifications but showed significantly lower stoichiometry, consistent with H2A.Z^{Pht1} being a substrate for the Ino80 remodeling complex rather than a core subunit of the Ino80 complex itself (Papamichos-Chronakis et al., 2011). Interestingly, all subunits of Ino80 complex showed higher stoichiometry than Hap2, suggesting that the Hap2 directly associates with the Ino80 complex. Budding yeast Ino80 complex is known to contain stoichiometric levels of Ino80, Arp4, Arp5, Arp8, and actin (Shen et al., 2000). Consistent with this, in the fission yeast Hap2 complex, comparable amounts of Ino80, Arp5, Arp8, Alp5 and Act1 were recovered. The organization of Hap2 within Ino80 complex require further investigation to find which module of Ino80 does Hap2 interacts with.

In the study by Hogan et al. (2010), deletions of genes encoding the Ino80 complex subunits *iec1* or *ies2* from fission yeast resulted in loss of viability in low-phosphate medium and loss of pink color on low adenine medium while the normal growth and color was restored in double mutants lacking both *iec1* and *ies2*. They proposed that Iec1 might be in a distinct complex (or function in isolation) whose function is antagonized by an Ies2-containing complex. The authors proposed that different Ino80 subunits may program the complex differently and possibly in opposing ways. Consistent with this idea, in both *hap2*Δ and *iec1*Δ cells, *de novo* centromere establishment was found to be abolished, while in *ies2*Δ and *ies4*Δ cells frequency of establishment was higher compared to wild type cells (Table 4.1). Ies2 is a subunit of the conserved ARP5-IES6 module and Ies4 is a subunit of the conserved ARP8 module, while Iec1 and Hap2 are species-specific subunits of fission yeast Ino80 complex. (Table 5.1). Fission yeast Iec1 and the mammalian YY1 protein have a conserved HTGEKPF motif, although human YY1 cannot substitute for Iec1 in fission yeast (Hogan et al., 2010). Fission yeast, budding yeast and humans have various species-specific Ino80 subunits (Table 5.1). It is possible that these species-specific

Ino80 subunits might program complex differently for different tasks, possibly in opposing ways. Further investigation is needed to assess the combinatorial effect of different Ino80 subunits on CENP-A^{Cnp1} establishment and maintenance in fission yeast.

In summary, the analyses presented here, implicate Hap2-Ino80 complex in the establishment and maintenance of CENP-A^{Cnp1} chromatin possibly through replication-independent histone H3 turnover that promotes replacement of histone H3 with CENP-A^{Cnp1} nucleosome in centromere DNA.

Chapter 6

Dbl5 regulates CENP-A^{Cnp1} stability in fission yeast

6.1 Introduction

Centromere are chromosomal loci that coordinate chromosome movement during cell division (Westhorpe and Straight, 2014). Evidence from many eukaryotes indicates that centromere DNA sequences is neither necessary nor sufficient for the identity and function of centromeres (Allshire and Karpen, 2008). Centromere location in most organisms is determined epigenetically by the centromere-specific histone H3 variant CENP-A (Henikoff and Dalal, 2005; Karpen and Allshire, 1997; Black and Cleveland, 2011; Perpelescu and Fukagawa, 2011). CENP-A is required for the recruitment of the constitutive centromere-associated network (CCAN) and thus outer kinetochore proteins which bind microtubule to mediate chromosome segregation (Mellone and Allshire, 2003; Foltz et al., 2006; Black et al., 2010). Artificial tethering of CENP-A, CENP-C, CENP-T, CENP-I or the CENP-A-specific chaperone, HJURP, at non-centromeric loci is sufficient to assemble a functional kinetochore capable of microtubule attachments and chromosome segregation (Barnhart et al., 2011; Mendiburo et al., 2011; Hori et al., 2013). How CENP-A is specifically localized and restricted only to centromeres is an interesting question.

CENP-A has a highly divergent N terminal tail and a C terminal region that is similar to that of canonical histone H3 (Sullivan et al., 1994). Post translational modifications (PTMs) of histones are well known to regulate many biological processes, such as chromatin condensation, gene expression, cell differentiation and apoptosis (Xu et al., 2014; Srivastava and Foltz, 2018). At least 17 different types of PTMs on more than 30 amino acid residues of human histone H3 variants have been reported (Xu et al., 2014). Thus PTMs may contribute to the regulation and function of CENP-A. Recent reports have identified many PTMs on CENP-A (Table 1.1). In humans, tri-methylation of Gly1 on CENP-A is required for CCAN formation and normal chromosome segregation (Sathyan et al., 2017). Phosphorylated CENP-A Ser7 is proposed to form a bridge with CENP-C via the phosphobinding protein 14-3-3 during mitosis (Goutte-Gattat et al., 2013). CENP-A Ser16/18 phosphorylation is required for normal

chromosome segregation during mitosis (Bailey et al., 2013). CENP-A Ser68 phosphorylation is proposed to impair CENP-A interaction with HJURP and prevent deposition of new CENP-A (Yu et al., 2015). CENP-A is also ubiquitylated on Lys124 by CUL4A E3 ligase and this facilitates the interaction of CENP-A with HJURP and its deposition at centromeres (Niikura et al., 2015). However, a recent study suggests that Lys124 ubiquitylation and Ser68 phosphorylation of CENP-A are infact dispensable for centromeric chromatin assembly (Fachinetti et al., 2017). In *S. cerevisiae*, phosphorylation of CENP-A^{Cse4} on Ser22/33/40/105 destabilizes misaligned kinetochores to promote biorientation and normal chromosome segregation (Boeckmann et al., 2013). CENP-A^{Cse4} Arg-37 methylation is required for the recruitment of key kinetochore components to centromeres to prevent aberrant chromosome segregation defects (Samel et al., 2012). CENP-A^{Cse4} sumoylation at Ser-65 directs CENP-A^{Cse4} for Slx5-mediated proteolysis (Ohkuni et al. 2018). Recombinant CENP-A^{Cse4} can be ubiquitylated at K4/131/155/163/172 by the E3 ubiquitin ligase Psh1 *in vitro* (Hewawasam et al., 2010). Mutating all 16 lysines to alanines in CENP-A^{Cse4} stabilizes CENP-A suggesting that lysine ubiquitylation is required to promote CENP-A^{Cse4} degradation (Hewawasam et al., 2010; Collins et al., 2004). Thus PTMs appear to play diverse roles in CENP-A function but much remains to be investigated.

Overexpression of CENP-A leads to mislocalization of CENP-A into non-centromeric regions in *S. pombe*, *S. cerevisiae*, humans, *Drosophila*, (Castillo et al., 2013; Hildebrand and Biggins, 2016; Van Hooser et al., 2001; Huen et al., 2006). In *Drosophila*, the F-box protein partner of paired (Ppa) is a variable component of the E3-ubiquitin ligase SCF, it is proposed that SCF^{Ppa} regulates CENP-A^{CID} proteolysis (Moreno-Moreno et al., 2011). Human CENP-A has been shown to be subject to proteasome-mediated degradation in Herpes simplex virus type 1 infection (Lomonte et al., 2001; Gross et al., 2012). In *S. cerevisiae*, multiple E3 ubiquitin ligases (Psh1, Rcy1, Slx5 and Ubr1) have been shown to ubiquitylate CENP-A^{Cse4} and target CENP-A^{Cse4} for proteasomal degradation (Cheng et al., 2017; Ohkuni et al., 2018). In *S. pombe*, the N-terminal domain of CENP-A^{Cnp1} prevents CENP-A^{Cnp1} assembly at ectopic loci and thus was proposed to be dependent on ubiquitin-dependent proteolysis (Gonzalez et al., 2014). Proteasomal degradation is therefore implicated in the regulation of CENP-A levels and thus may represent a conserved mechanism

for preventing ectopic accumulation of CENP-A and consequently chromosome missegregation.

Dbl5, an E3 ubiquitin ligase, is the fission yeast orthologue of *S. cerevisiae* Psh1. As discussed in chapter 4, Dbl5 was found to be required for establishment of functional centromeres on minichromosomes. In this chapter, the role of Dbl5 in centromeric chromatin assembly and in regulation of CENP-A^{Cnp1} stability in fission yeast is further investigated.

6.2 Results

6.2.1 Dbl5 is not required for *de novo* CENP-A^{Cnp1} establishment

The *dbl5*Δ mutant display ~5 fold reduction in centromere establishment frequency compared to wild type (Table 4.1). The *de novo* assembly of functional centromeres on minichromosomes requires both the establishment of heterochromatin on K" repeat sequence and CENP-A^{Cnp1} chromatin on the adjacent region *cc2* (Folco et al., 2008, Kagansky et al., 2009). Heterochromatin establishment was tested by H3K9me ChIP, H3K9me levels on the K" repeat sequence of the minichromosome in the *dbl5*Δ mutant was similar to that of wild type cells (Figure 6.1B; primer: K"-mini and K"-imr). Thus *de novo* heterochromatin formation on the minichromosome is unaffected in the cells lacking Dbl5. Heterochromatin can spread into the adjacent ectopic cc2 sequence as shown in *hap2*Δ cells (Figure 5.1 D). To determine whether reduced establishment in in *dbl5*Δ cells is due to heterochromatin spreading, H3K9me levels were analysed on the pcc2K" minichromosome. H3K9me levels on the cc2 region of the pcc2K" minichromosome remained very low in *dbl5*Δ cells as in wild type cells (Figure 6.1 B; primer: cc2). Together, these observations indicate that H3K9me establishment on the K" repeat of the pcc2K" minichromosome is unaffected and no obvious spreading of heterochromatin into cc2 occurs. Surprisingly, CENP-A^{Cnp1} ChIP on pcc2K" revealed no reduction in the levels of CENP-A^{Cnp1} within the cc2 region on the minichromosome in *dbl5*Δ cells (Figure 6.1 C). These observations suggest that the loss of centromere establishment is not due to inefficient establishment of heterochromatin or CENP-A^{Cnp1} chromatin on the minichromosome.

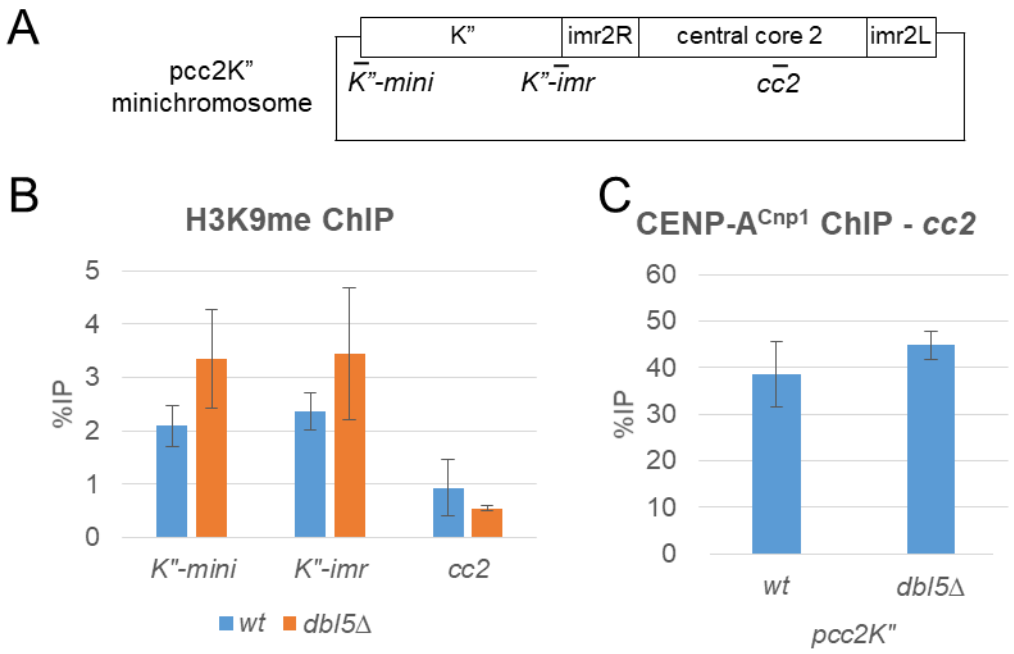

Figure 6.1: Dbl5 is not required for de novo H3K9me or CENP-A^{Cnp1} establishment on minichromosomes

(A) Schematic of pcc2K" and pcc2 minichromosome and primer positions. (B) qChIP of H3K9me on pcc2K" minichromosome at *K"-mini*, *K"-imr* and ectopic *cc2* loci on the minichromosome.Three random colonies with transformed minichromosome were picked from ade-ura- medium plate and grown under selection for ChIP. Mean ± S.D. of n=3 biological replicates is shown. (C) qChIP of CENP-A^{Cnp1} levels at ectopic *cc2* on pcc2K" minichromosome in wild-type and *dbl5*Δ cells. Three random colonies with transformed minichromosome were picked from ade-ura- medium plate and grown under selection for ChIP. Mean ± S.D. of n=3 biological replicates is shown.

6.2.2 Dbl5 is not required for the maintenance of centromeric chromatin

Reporter genes placed within fission yeast centromeres are transcriptionally silenced (Allshire et al., 1994; Allshire et al., 1995). Transcriptional silencing in the central domain reflects maintenance of CENP-A^{Cnp1} and the assembly of a fully functional kinetochore (Partridge et al., 2000; Jin et al., 2002; Pidoux et al., 2003). The integrity of central CENP-A^{Cnp1} domain chromatin at endogenous centromeres was tested in *dbl5*Δ cells using a central core silencing assay. A strain containing the *ura4*$^{+}$ gene inserted in central domain1 (*TM1::ura4*$^{+}$) was used as a reporter for transcriptional silencing (Figure 6.2 A). *dbl5*Δ cells showed no defect in transcriptional silencing of *TM1::ura4*$^{+}$ (Figure 6.2 B and C). Consistent with normal silencing, *dbl5*Δ cells

displayed wild-type levels of CENP-A^{Cnp1} at endogenous central domain and no increase in CENP-A^{Cnp1} levels on the flanking outer repeats (Figure 6.2 D and E).

Marker genes inserted within the outer repeats show alleviation of transcriptional silencing (Allshire et al., 1995). Outer repeat silencing was assessed in cells lacking Dbl5 with *ade6*$^{+}$ gene inserted at the *SphI* site in *otr1* (Figure 6.3 A). *dbl5*Δ cells showed no defect in outer repeat silencing (Figure 6.3 B). Consistent with this observation, no change in outer repeat transcript levels or associated H3K9 methylation was detected in *dbl5*Δ cells (Figure 6.3 C and D), whereas *clr4*Δ cells exhibited high levels of *dg* transcripts.

Together, these observations suggest that Dbl5 is not required for the maintenance of CENP-A^{Cnp1} chromatin or centromeric heterochromatin.

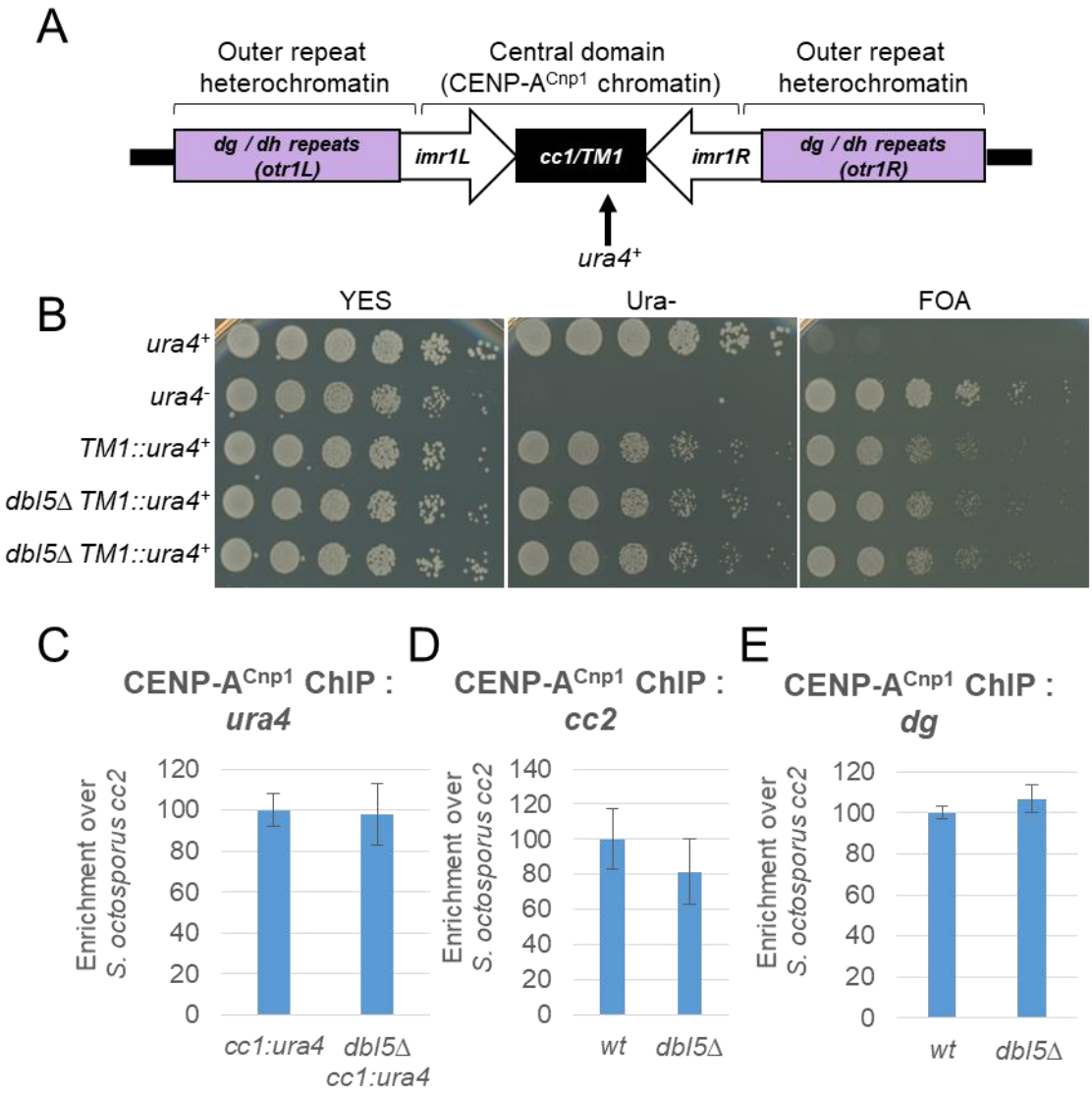

Figure 6.2: Dbl5 is not required for the maintenance of CENP-A^{Cnp1} chromatin

(A) Schematic representation of the *ura4*+ gene integration site at centromere 1 used in the central domain silencing assay. (B) Spotting assay of wild type and mutants with *ura4*+ inserted within the central domain. Cells are plated on rich medium (YES), uracil deficient plates (*ura4*$^-$) and FOA containing plates (FOA). In wild type cells (*ura4-D18 TM1::ura4*$^+$) silencing of the central domain is maintained and cells are able to grow in medium containing the counter selective drug FOA and grow poorly on medium lacking uracil. *Progeny from a dbl5ΔTM1::ura4+ were analysed.* (C) qChIP of CENP-A^{Cnp1} levels at *ura*+ gene inserted at the central domain 1 in wild-type and *dbl5*Δ cells. Mean ± S.D. of n=3 biological replicates is shown. (D and E) qChIP of CENP-A^{Cnp1} levels at central domain (*cc2*) and pericentric repeats (*dg*) in wild-type and *dbl5*Δ cells. Mean ± S.D. of n=3 biological replicates is shown.

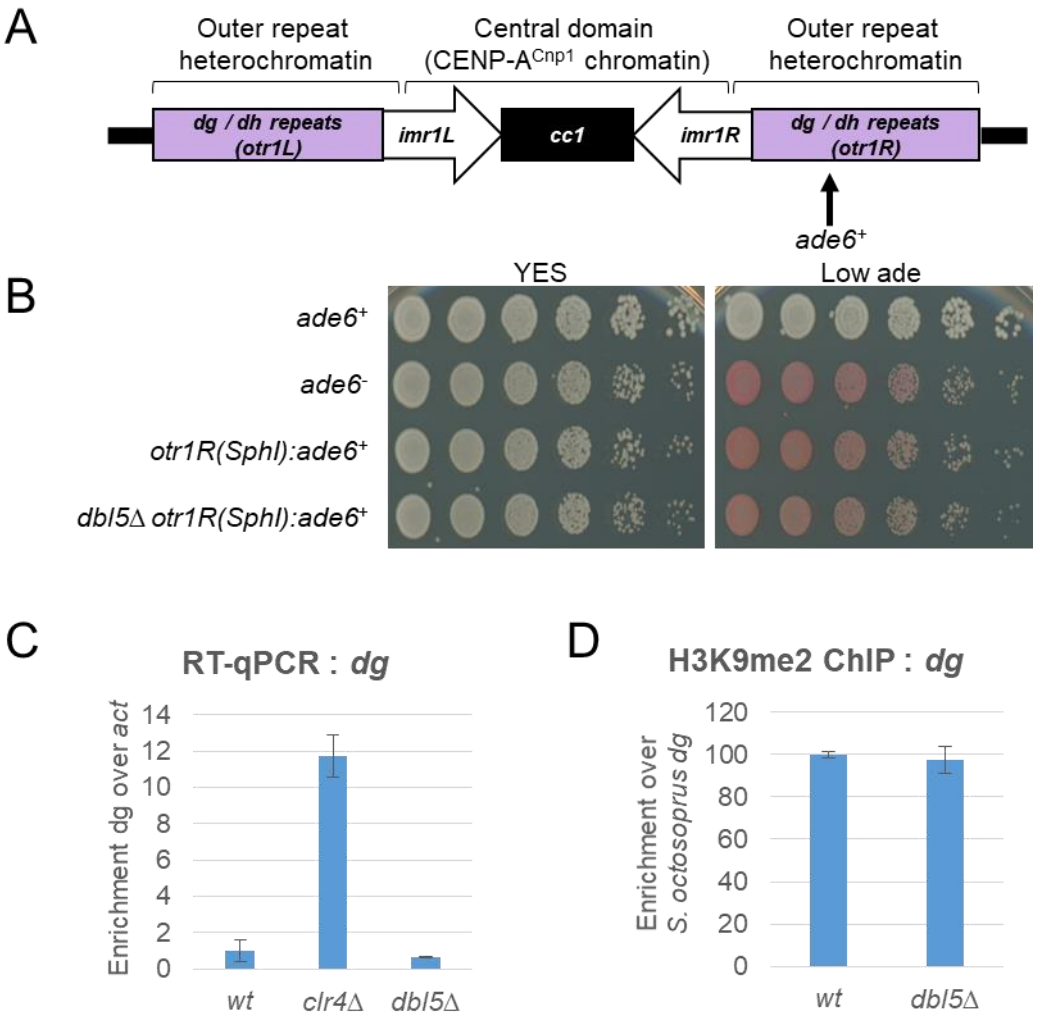

Figure 6.3: Dbl5 is not required to maintain pericentric heterochromatin silencing

(A) Schematic representation of the *ade6+* gene integration site at centromere 1 used in the pericentric heterochromatin silencing assay. (B) Serial dilution spotting assay of wild type and *dbl5*Δ mutants. Cells are plated on rich medium (YES) and with limiting amount of adenine (1/10th ade). Progeny from a *dbl5*Δ *otr1R(SphI)* were analysed. (C) RT-qPCR of *dg* transcripts in wild-type, *clr4*Δ and *dbl52*Δ cells normalized to *actin* transcripts. Mean ± S.D. of n=3 biological replicates is shown. (D) qChIP of H3K9me2 levels at *dg* in wild-type and *dbl5*Δ cells normalized to spiked in *S. octosporus otr*. Mean ± S.D. of n=3 biological replicates is shown.

6.2.3 Loss of *dbl5* partially rescues defective CENP-A^{Cnp1}

Factors involved in CENP-A^{Cnp1} regulation often display genetic interactions when combined with in CENP-A^{Cnp1} mutants (Pidoux et al., 2003). To investigate genetic interaction between Dbl5 and CENP-A^{Cnp1}, a temperature-sensitive (ts) CENP-A^{Cnp1} allele *cnp1-1* (L87Q mutation; Takahashi et al., 2000) which exhibits decreased viability at the restrictive temperature (36°C), was combined with *dbl5*Δ. Growth of single and double mutants was assayed at various temperatures for 5 days. The *dbl5Δ cnp1-1* double mutant exhibited more growth at 30°C and 32°C compared with the *cnp1-1* single mutant, while its growth was impaired similarly to *cnp1-1* alone at 36°C (Figure 6.4 A). These observations indicate that the temperature sensitivity of *cnp1-1* can be partially rescued by loss of Dbl5. To further analyze whether Dbl5 interact with other kinetochore components, the *dbl5Δ* mutant combined with *mis6-302*: the Mis6 protein is known to be required for the incorporation of CENP-A^{Cnp1} at centromeres (Saitoh et al., 1997; Takahashi et al., 2000). As with *cnp1-1*, the *dbl5Δ mis6-302* double mutant also showed suppression of temperature sensitivity compared to the *mis6-302* alone (Figure 6.4 B).

Ams2, a GATA-type zinc finger motif-containing factor, was isolated as a multicopy suppressor of *cnp1-1* (Chen et al., 2003). Ams2 governs the cellular levels of histones via transcriptional regulation of the core histone genes (Takayama et al., 2016). The relative levels of histone H3 and histone H4 are known to affect CENP-A^{Cnp1} deposition at centromeres (Castillo et al., 2007). To determine whether the partial suppression of *cnp1-1* is due to altered histone levels, western analysis was performed. No change in the levels of GFP-CENP-A^{Cnp1}, histone H3, or histone H4 was detected in *dbl5Δ* cells compared to wild-type (Figure 6.4 C). This suggests that the partial suppression of *cnp1-1* in *dbl5Δ* is not explained by alterations in the H3:H4 ratios.

Centromeric sequences cannot establish CENP-A^{Cnp1} chromatin without the adjacent K" repeat sequence (Folco et al., 2008). Elevated CENP-A^{Cnp1} levels can bypass the requirement of adjacent heterochromatin in the establishment of CENP-A^{Cnp1} chromatin (Catania et al., 2015). If cellular CENP-A^{Cnp1} levels are elevated in *dbl5*Δ cells then more CENP-A^{Cnp1} will be available for de novo CENP-A^{Cnp1} chromatin assembly, which may allow *dbl5*Δ cells to establish CENP-A^{Cnp1} chromatin on cc2 DNA on a minichromosome lacking heterochromatin (pcc2). To test this possibility, *dbl5*Δ

cells were transformed with *pcc2* and the levels of CENP-A^{Cnp1} on pcc2 were assessed. Essentially no CENP-A^{Cnp1} was detected on minichromosome cc2 in both *dbl5*Δ and wild-type cells (Figure 6.4 D). This assay suggests that cellular CENP-A^{Cnp1} levels are not altered in *dbl5*Δ cells and consistent with the finding that CENP-A^{Cnp1} levels are similar by western analysis.

Together, these observations indicate that loss of *dbl5* partially rescues *cnp1-1* lethality and completely rescues *mis6-302* lethality. Although CENP-A^{Cnp1} levels in *dbl5*Δ cells are similar to wild-type, it is possible that *dbl5*Δ increases the amount of CENP-A^{Cnp1} at centromeres but not total cellular levels. This might explain the partial rescue of the *cnp1-1* mutant. CENP-A^{Cnp1} levels at endogenous centromeres should be compared at semi-permissive temperatures in single and double mutants.

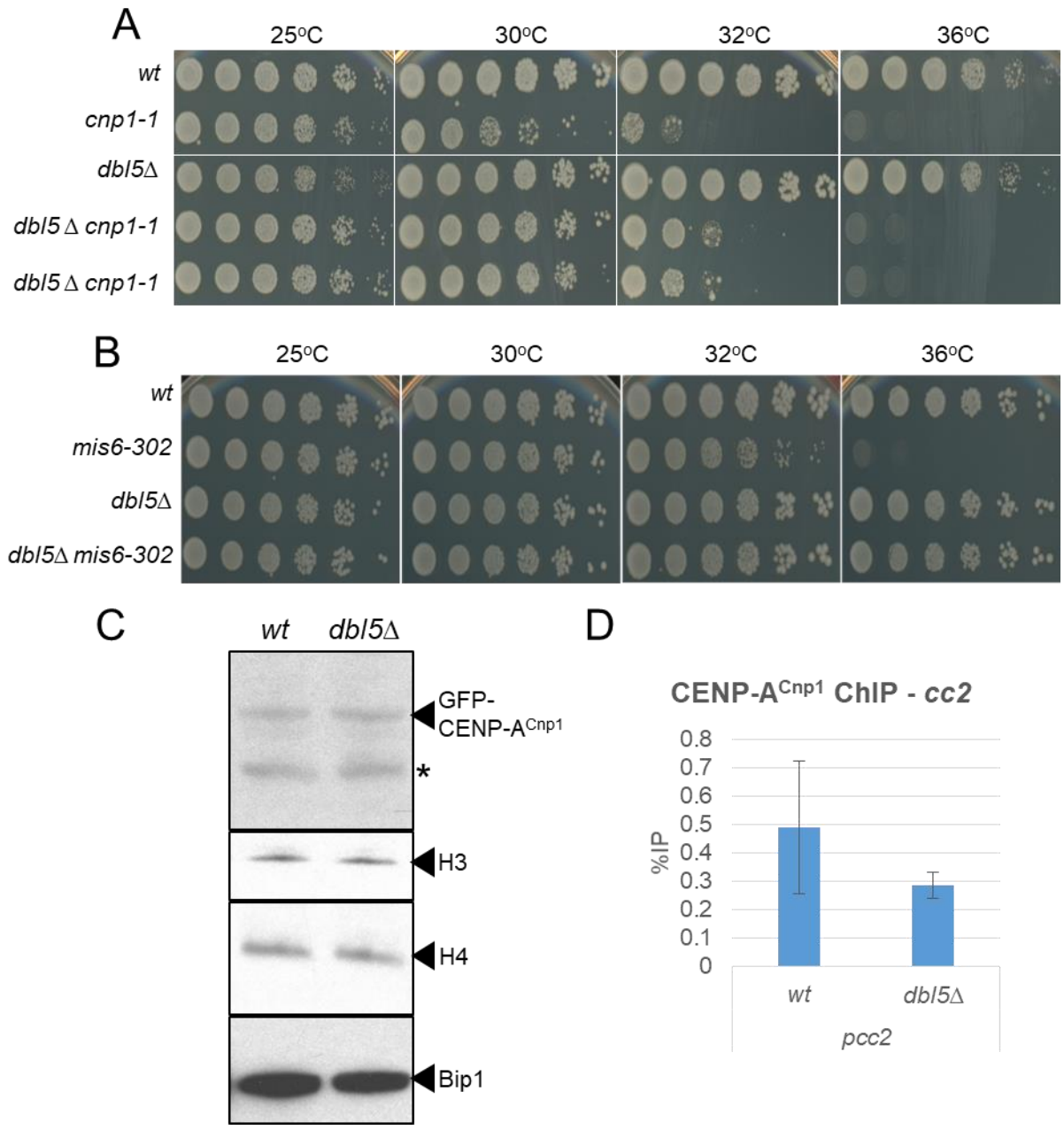

Figure 6.4: Deletion of *dbl5* rescues temperature sensitivity of *cnp1-1* and *mis6-302*.

(A) Spotting assay of wild type, temperature sensitive CENP-A (*cnp1-1)*, *dbl5*Δ and *cnp1-1 dbl5*Δ double mutant. Fivefold serial dilution were made for all the strains were plated on YES plate at various temperatures (25ºC, 30ºC, 32ºC and 36ºC). (B) Spotting assay of wild type, temperature sensitive CENP-I (*mis6-302)*, *dbl5*Δ and *mis6-302 dbl5*Δ double mutant. Fivefold serial dilution were made for all the strains were plated on YES plate at various temperatures (25ºC, 30ºC, 32ºC and 36ºC). (C) A western blot analysis of GFP-CENP-A^{Cnp1}, histone H3, histone H4 and α-Bip1 as loading control was performed in wild-type and *dbl5*Δ cells. The * indicates non-specific band. (D) qChIP of CENP-A^{Cnp1} levels at cc2 on pcc2 minichromosome in wild-type and *dbl5*Δ cells. Three random colonies with transformed minichromosome were picked from ade-ura- medium plate and grown under selection for ChIP. Mean ± S.D. of n=3 biological replicates is shown.

6.2.4 Dbl5 does not associate with the central domain of centromeres

ChIP and microarray analysis have shown that *S. cerevisiae* Psh1 associates with centromeres (Hewawasam et al., 2010). As Dbl5 was reproducibly detected with affinity selected CENP-A^{Cnp1}, it seems likely that Dbl5 might associate with centromeres. To investigate this possibility, ChIP was performed with GFP-tagged Dbl5. No enrichment of Dbl5-GFP was detected with the centromeric central domain (Figure 6.5 A). Perhaps Dbl5 only associates with soluble or misincorporated CENP-A^{Cnp1}. The functionality of Dbl5-GFP should be tested and the establishment frequency for tagged strain should be similar to that for the wild type strain.

The molecular function of Dbl5 is unknown, although like S. cerevisiae Psh1 E3 ligase, it contains a RING finger motif (Hewawasam et al., 2010; Ranjitkar et al., 2010). CENP-A^{Cse4} and Psh1 had been shown to reciprocally immunoprecipitate and kinetochore proteins also coIP with Psh1 (Ranjitkar et al., 2010; Hewawasam et al., 2010). Psh1 directly interacts with CENP-A^{Cse4}, but not histone H3 (Hewawasam et al., 2010). To determine if CENP-A^{Cnp1} is associated with Dbl5, Dbl5-GFP was affinity selected followed by LC-MS/MS analysis (Figure 6.5 B). Unlike *S. cerevisiae* Psh1, CENP-A^{Cnp1} and other kinetochore proteins do not co-purify with Dbl5-GFP (Figure 6.5 C). A transient interaction between Dbl5 and CENP-A^{Cnp1} might explain the lack of CENP-A^{Cnp1} in Dbl5 immunoprecipitates. As Dbl5-GFP does not associate with fission yeast centromeres the lack of associated kinetochore proteins is not surprising. It remains to be tested whether overexpression of CENP-A^{Cnp1} can favour interaction of Dbl5 and CENP-A^{Cnp1}.

S. cerevisiae Psh1 is so called because it is a Pob3/Spt16 and histone associated protein that is non-essential (Krogan et al., 2002). Psh1 interacts with FACT (facilitates chromatin transcription) complex (Spt16 and Pob3) and association of Psh1 with Spt16 promotes ubiquitylation and degradation of CENP-A^{Cse4} (Deyter and Biggins, 2014). However, FACT does not interact with CENP-A^{Cse4} in the absence of Psh1 (Ranjitkar et al., 2010). The FACT complex is known to promote histone H3 incorporation and prevent deposition of CENP-A^{Cnp1} on non-centromeric sequences in fission yeast (Choi et al., 2012). LC-MS/MS analysis of affinity selected Dbl5-GFP enriched both FACT subunits by 2 fold relative to untagged control (Figure 6.5 C). It is possible that the FACT complex only associates with subset of the Dbl5 pool.

In *S. cerevisiae*, phosphorylation of Psh1 by asein kinase 2 facilitates CENP-A^{Cse4} ubiquitylation and degradation (Hewawasam et al., 2014). In *S. pombe*, mass spectrometric analysis revealed 15 phosphorylation sites on Dbl5 (Table 6.1). Casein kinase 2 complex subunits, Cka1, Ckb1 and Ckb2, were enriched with Dbl5 IP (Figure 6.5 C). It remains to be tested how Dbl5 phosphorylation regulates its activity and whether Dbl5 phosphorylation is casein kinase 2 complex in *S. pombe*. Affinity selection of Dbl5 also enriched Hhp1, Hhp2 and Ppk6 kinases which could possibly phosphorylate Dbl5 (Figure 6.5 C). Affinity selection of Dbl5-GFP also enrichment most subunits of SAGA complex, NuA4 complex and elongator complex (Figure 6.5 C). It is possible that Dbl5 associates with these proteins and scans the chromosome for misincorporated CENP-A^{Cnp1}. The role of these complexes in Dbl5-dependent CENP-A^{Cnp1} degradation requires further investigation.

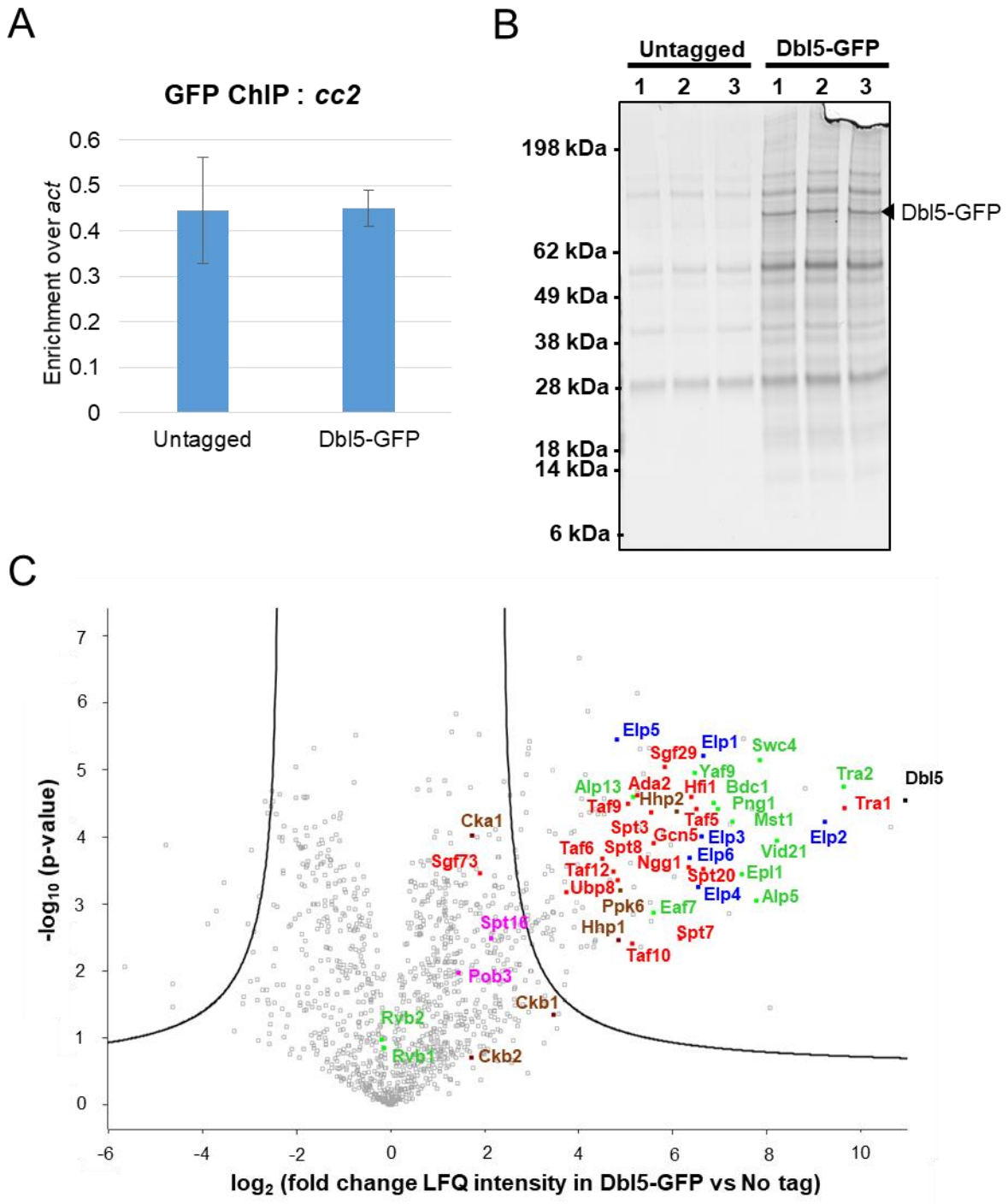

Figure 6.5: Dbl5 does not associate with the central domain of centromeres

(A) qChIP of Dbl5-GFP levels at centromere central domain cc2 in wild-type and dbl5Δ cells. Mean ± S.D. of n=3 biological replicates is shown. (B) Eluates from native affinity purifications of Dbl5-GFP were separated by SDS–PAGE and visualized by silver staining for three biological replicates (1, 2 and 3). Labelled proteins based on predicted molecular weights. (C) Volcano plot representation of protein abundances in Dbl5-GFP proteome compared to untagged control.

6.2.5 Cells lacking Dbl5 are sensitive to CENP-A^{Cnp1} overexpression

Dbl5 is the fission yeast orthologue of *S. cerevisiae* Psh1. Psh1 is known to facilitate CENP-A^{Cse4} degradation preventing it from accumulating at non-centromeric loci (Ranjitkar et al., 2010; Hewawasam et al., 2010). Overexpression of CENP-A^{Cse4} in *S. cerevisiae psh1*Δ cells leads to slower cell growth (Hewawasam et al., 2010). Fission yeast has been shown to tolerate CENP-A^{Cnp1} overexpression (Castillo et al., 2007). To determine whether loss of Dbl5 affects viability of cells upon CENP-A^{Cnp1} overexpression, CENP-A^{Cnp1} was overexpressed from the moderate strength *nmt41* promoter (Castillo et al., 2013). *dbl5*Δ cells lost viability when CENP-A^{Cnp1} was expressed whereas wild-type cells overexpressing CENP-A^{Cnp1} grew normally (Figure 6.6 A). Thus as in *S. cerevisiae*, high levels of expression of CENP-A^{Cnp1} appear to be necessary to reveal a function for Dbl5 with respect to centromeres.

In *S. pombe*, although CENP-A^{Cnp1} is normally restricted to the centromeric central domain and upon overexpression CENP-A^{Cnp1} can also assemble on non-centromeric DNA (Castillo et al., 2007; Castillo et al., 2013). In *S. cerevisiae*, transient CENP-A^{Cse4} overexpression in *psh1Δ* cells results in widespread euchromatic CENP-A^{Cse4} localization (Ranjitkar et al., 2010). To determine whether the loss of viability in *S. pombe dbl5*Δ cells overexpressing CENP-A^{Cnp1} was accompanied by ectopic CENP-A^{Cnp1} incorporation at non-centromeric loci, CENP-A^{Cnp1} localization was performed. Anti-GFP antibodies were used to stain GFP-CENP-A^{Cnp1} along with anti-α-tubulin as a marker to distinguish interphase and mitotic stages of the cell cycle. During interphase, the three centromeres are known to cluster together and appear as a single focus (Funabiki et al., 1993). As expected, wild-type cells transiently overexpressing CENP-A^{Cnp1}, a single focus was observed in interphase and two foci were visible during mitosis (Figure 6.5 B and C). Loss of Dbl5 resulted in a general increase in CENP-A^{Cnp1} overall chromatin and increase in the number of GFP-CENP-A^{Cnp1} foci (Figure 6.6 B and C). Moreover, transient CENP-A^{Cnp1} overexpression in *dbl5*Δ cells resulted in appearance of multiple CENP-A^{Cnp1} foci in 36% of interphase cells while 96% of late mitotic cells exhibited segregation defects (Figure 6.6 D). Depending on the level of CENP-A^{Cnp1} overexpression, higher levels of CENP-A^{Cnp1} can be deposited in chromosomal regions distinct from centromeres (Castillo et al., 2013). It therefore seems that ectopic CENP-A^{Cnp1} incorporation and defective chromosomal segregation results from increased levels of CENP-A^{Cnp1} in *dbl5*Δ cells.

6.2.6 Dbl5 regulates the stability of CENP-A^{Cnp1}

Previous studies have shown that ubiquitin-mediated proteolytic degradation of CENP-A is important for preventing its euchromatin localization in *S. cerevisiae* and *Drosophila* (Collins et al., 2004; Ranjitkar et al., 2010; Hewawasam et al., 2010, Moreno-Moreno et al., 2006; Moreno-Moreno et al., 2011; Cheng et al., 2017). It is likely, like *S. cerevisiae* Psh1 orthologue (Ranjitkar et al., 2010; Hewawasam et al., 2010), Dbl5 also acts as an E3 ligase to ubiquitylate CENP-A^{Cnp1} and targets it for proteolysis. If this is the case then loss of Dbl5 would be expected to stabilize CENP-A^{Cnp1}. To test this hypothesis the stability of overexpressed GFP-CENP-A^{Cnp1} was assessed in wild-type and *dbl5Δ* cells. Cycloheximide (CHX) was added to repress protein translation and GFP-CENP-A^{Cnp1} levels were determined by western analysis at increasing time points. Interestingly, GFP-CENP-A^{Cnp1} levels were four times higher in *dbl5Δ* compared to wild-type cells (Figure 6.7 A and B). This increase in CENP-A^{Cnp1} levels may explain the ectopic incorporation of CENP-A^{Cnp1} and loss of viability in *dbl5Δ* cells. Overexpressed GFP-CENP-A^{Cnp1} has a short half-life of about 20 minutes in wild-type cells (Figure 6.7 A and C). In *S. pombe*, CENP-A^{cnp1}-GFP has been shown to be degraded within 2 hours of treatment with CHX (Gonzalez et al., 2014). Loss of Dbl5 significantly increased the stability of CENP-A^{Cnp1} (Figure 6.7 A and D). These results are consistent with the hypothesis that Dbl5 targets CENP-A^{Cnp1} for ubiquitin-mediated proteolysis, and therefore, CENP-A^{Cnp1} is more stable in a *dbl5* mutants. Together, these observations show that in *S. pombe* Dbl5 is required to control the cellular levels of CENP-A^{Cnp1}.

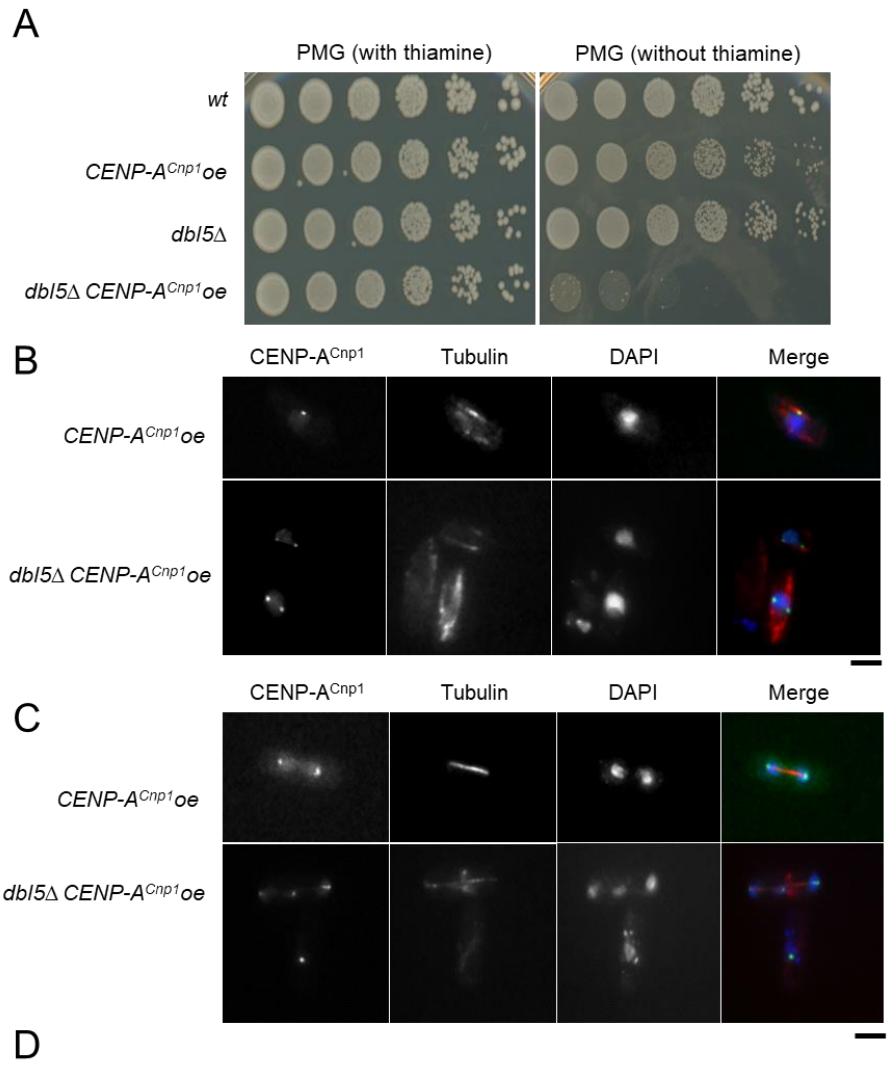

Strain	Interphase cells		Mitotic cells				
	Single foci	Multiple foci	Lagging chromosome	Lagging chromosomes with multiple foci	Unequal segregation	Normal segregation	Abnormal segregation
CENP-A^{Cnp1}oe	100%	0%	0%	0%	0%	100%	0%
dbl5Δ CENP-A^{Cnp1}oe	64%	36%	26%	18%	46%	4%	6%

Figure 6.6: Overexpression of CENP-A^{Cnp1} causes segregation defects in *dbl5*Δ

(A) Spotting assay of wild type, CENP-A^{Cnp1}-overexpression (oe), *dbl5*Δ and CENP-A^{Cnp1} (oe) *dbl5*Δ strains. GFP-CENP-A^{Cnp1} was expressed under a thiamine repressible promoter (nmt41). Viability of cells was assessed on PMG plates with and without thiamine. (B and C) Localization of GFP-CENP-A^{Cnp1} in cells overexpressing CENP-A^{Cnp1} with and without Dbl5. Cells were grown in YES medium at 32oC overnight and inoculated into PMG full medium (without thiamine) to transiently express GFP-CENP-A^{Cnp1} for 16 hours. Green: GFP, Tubulin: and blue: DAPI. Bar: 5 µm. (D) Quantification of B and C. n= 500 interphase cells and 100 mitotic cells.

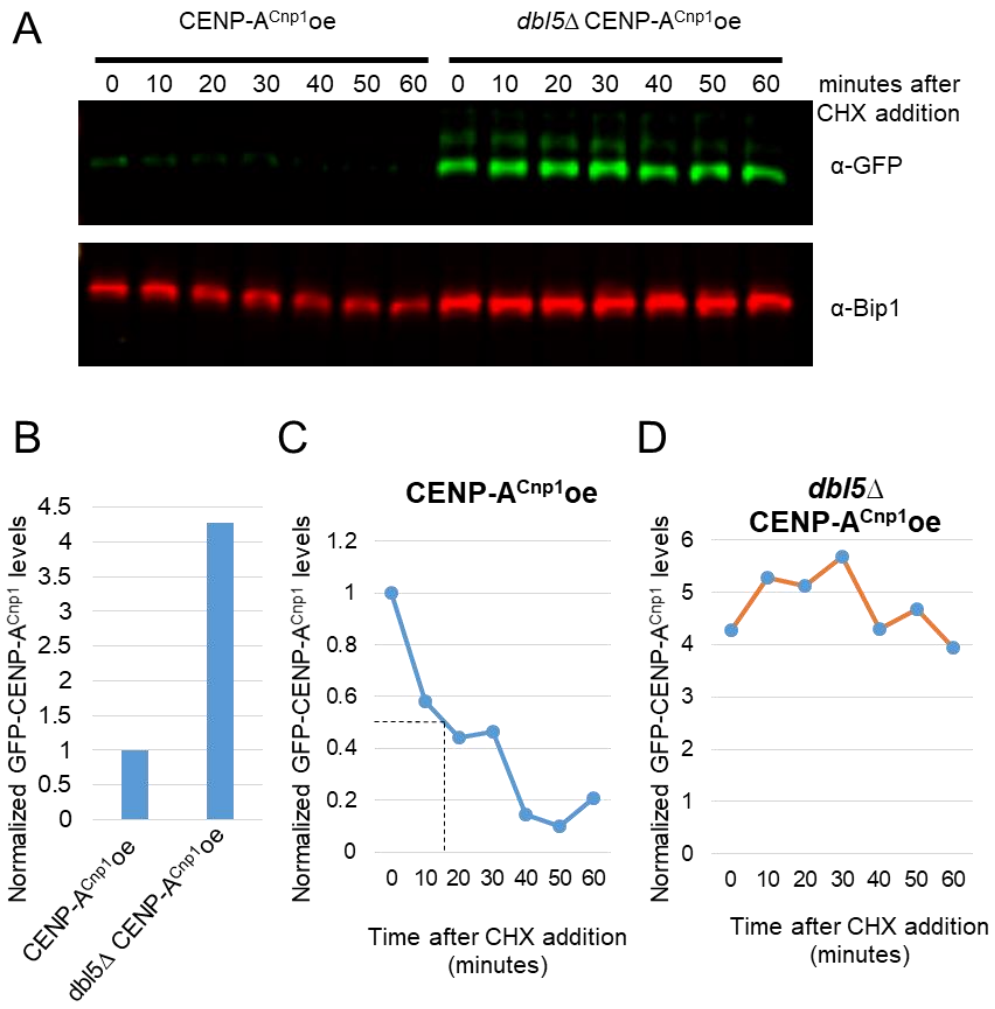

Figure 6.7: Deletion of *dbl5* stabilizes CENP-A^{Cnp1} protein level

(A) GFP-CENP-A^{Cnp1} was expressed from nmt41 promoter for 16 hours in thiamine deficient medium. Cells were incubated in 5mg/ml cycloheximide (CHX) for indicated time. A western blot analysis of GFP-CENP-A^{Cnp1} and α-Bip1 as loading control was performed. (B) Quantification of levels of GFP-CENP-A^{Cnp1} before the addition of CHX (C and D) Quantification of GFP-CENP-A^{Cnp1} levels in cells expressing GFP-CENP-A^{Cnp1} and with or without Dbl5, respectively.

6.2.7 Excess CENP-A^{Cnp1} accumulates at outer repeats at centromeres in cells lacking Dbl5

In *S. cerevisiae*, CENP-A^{Cse4} overexpression has no obvious growth defects but CENP-A^{Cse4} accumulates at non-centromeric sites (Hildebrand and Biggins, 2016). In *S. pombe*, excess CENP-A^{Cnp1} leads to its accumulation on centromeric outer repeats, telomere repeats and rDNA (Castillo et al., 2013). In *Drosophila*, overexpression of

CENP-A^{CID} results in its preferential accumulation at heterochromatin boundaries (Olszak et al. 2011). To determine whether *S. pombe* CENP-A^{Cnp1} spreads from the central domain into adjacent outer repeat region in *dbl5*Δ cells, CENP-A^{Cnp1} ChIP was performed following transient moderate CENP-A^{Cnp1} overexpression. Moderate overexpression of GFP-CENP-A^{Cnp1} resulted in its accumulation within the central domain and spreading over outer repeats in *dbl5*Δ relative to wild-type cells (Figure 6.8 A and B). *dbl5*Δ cells expressing CENP-A^{Cnp1} at normal levels displayed no change in the levels of CENP-A^{Cnp1} at centromeres (Figure 6.2). Thus, transient CENP-A^{Cnp1} overexpression allows CENP-A^{Cnp1} to accumulate over outer repeat regions at centromeres. The severe growth defect associated with CENP-A^{Cnp1}oe in *dbl5*Δ cells presumably results from elevated chromosome missegregation caused by widespread ectopic CENP-A^{Cnp1} and perhaps kinetochore assembly (Figure 6.6).

The phenotype of *dbl5*Δ cells with CENP-A^{Cnp1} overexpressed from the medium strength *nmt41* promoter is similar to that of wild-type cells overexpressing CENP-A^{Cnp1} from the strong nmt1 promoter (Castillo et al., 2013). Therefore, it is likely that its associated phenotypes result from excess undegraded CENP-A^{Cnp1} that persists in *dbl5*Δ cells.

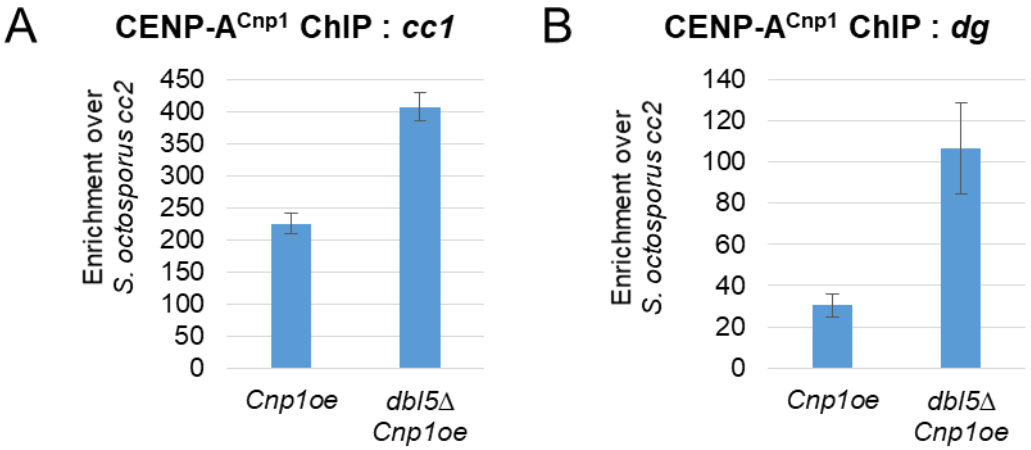

Figure 6.8: Overexpression of CENP-A^{Cnp1} without *dbl5* leads to spreading of CENP-A^{Cnp1} into pericentric outer repeats (A and B) qChIP of CENP-A^{Cnp1} levels at *cc1* and *dg* in cells overexpressing GFP-CENP-A^{Cnp1} (*Cnp1oe*) with or without *dbl5*. Cells were grown in YES medium at 32^{o}C overnight and inoculated into PMG full medium (without thiamine) to overexpress CENP-A^{Cnp1} for 16 hours. Mean ± S.D. of n=3 biological replicates is shown.

6.2.8 CENP-A^{Cnp1} is ubiquitylated at lysine 4 *in vivo*

Ubiquitylation primarily occurs on lysine (K) residues (Hochstrasser, 2009). In *S. cerevisiae*, ubiquitin-mediated proteolysis has been shown to regulate levels of CENP-A^{Cse4} and recombinant CENP-A^{Cse4} can be ubiquitylated at K4, K131, K155, K163 and K172 *in vitro* (Hewawasam et al. 2010). Dbl5 is a presumed E3 ubiquitin ligase that clearly regulates CENP-A^{Cnp1} levels in fission yeast (Figure 6.7). CENP-A^{Cnp1} is ubiquitylated and targeted for proteasomal degradation (Gonzalez et al., 2014). Deletion of first 20 amino acid residues from the N terminus of CENP-A^{Cnp1} has been shown to increase the stability and may lead to reduced CENP-A^{Cnp1} ubiquitylation and incorporation at ectopic loci (Gonzalez et al., 2014). It is therefore possible that lysines in the N-terminal tail of CENP-A^{Cnp1} are required to mediate ubiquitin-dependent degradation of CENP-A^{Cnp1}. To identify ubiquitylated lysine residues on CENP-A^{Cnp1}, affinity purification of GFP-CENP-A^{Cnp1} was performed. Subsequent mass spectrometric analysis reproducibly detected ubiquitylation on lysine 4 of CENP-A^{Cnp1} (Figure 6.9; Table 3.6). Peptide fragmentation in MS/MS mode allowed unequivocal confirmation of the CENP-A^{Cnp1} peptide as "4-K(GlyGly)SLMAEPGDPIPRPR-18" (Figure 6.9). Therefore, CENP-A^{Cnp1} is ubiquitylated *in vivo* in fission yeast.

6.2.9 CENP-A^{Cnp1} is ubiquitylated in Dbl5-dependent manner

To determine if ubiquitylation of CENP-A^{Cnp1} is Dbl5 dependent, western analysis was performed in GFP-CENP-A^{Cnp1} tagged and untagged strains transformed with the pREP41-6xHis-2xMyc-Ub plasmid which allows induced expression of Myc-tagged ubiquitin in the absence of thiamine. GFP-CENP-A^{Cnp1} was affinity selected with anti-GFP antibodies from solubilized chromatin extracts. Higher molecular weight Myc-tagged ubiquitylated CENP-A^{Cnp1} was enriched in the eluate obtained from cell expressing GFP-CENP-A^{Cnp1} and Dbl5 (Figure 6.10). Loss of Dbl5 leads to reduced isolation of ubiquitylated CENP-A^{Cnp1} (Figure 6.10). The intensity of signal from the ubiquitylated CENP-A^{Cnp1} was very low and required a long exposure. The low intensity signal suggests that only a small fraction of affinity purified GFP-CENP-A^{Cnp1} were ubiquitylated. Similar observations were reported with respect to CENP-A^{Cse4} in *S. cerevisiae* (Cheng et al., 2014).

CENP-A^{Cnp1} Lys4 could be mutated to arginine to determine if the resultant Cnp1-K4R mutant phenocopies *dbl5*Δ. Together, these observations confirm that CENP-A^{Cnp1} is ubiquitylated *in vivo*, specifically at lysine 4 and Dbl5 is required for ubiquitylation of CENP-A^{Cnp1}.

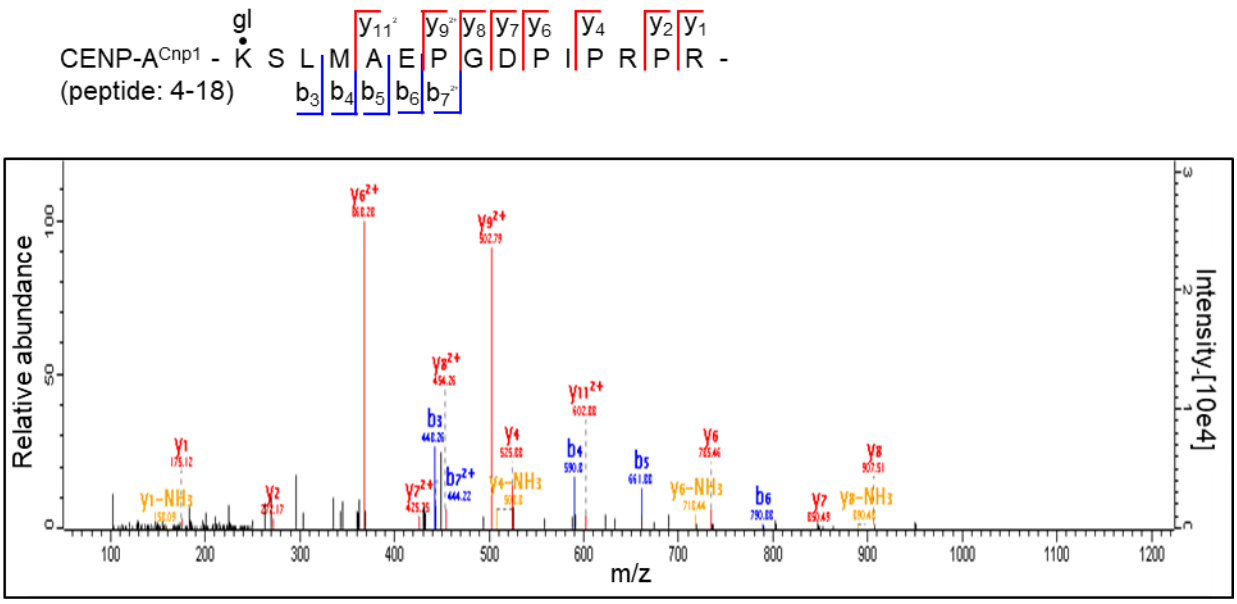

Figure 6.9: CENP-A^{Cnp1} is ubiquitylated at lysine 4 *in vivo*

The HCD MS2 spectrum of the N terminal CENP-A^{Cnp1} peptide showing ubiquitylation on lysine 4 and sequence coverage of the MS2 spectrum of the trypsin-generated CENP-A^{Cnp1} peptide. X-axis represents mass to charge ratio for each peptide detected in MS2, y-axis (right) represents the intensity of each peptide and y-axis (left) represents relative abundance of each peptide relative to the intensity of y_6^{2+} peptide.

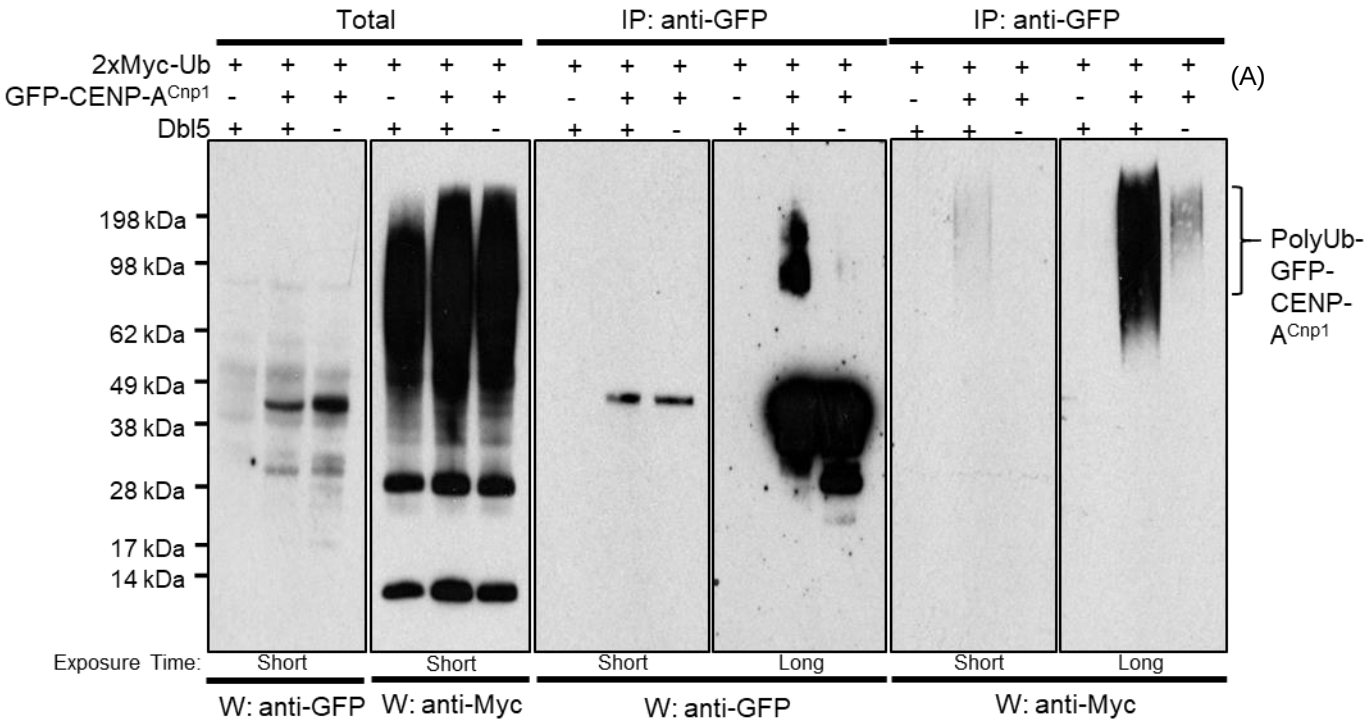

Figure 6.10: CENP-A^{Cnp1} is ubiquitylated in Dbl5-dependent manner

Solubilized chromatin extracts were prepared from cells containing Myc-tagged ubiquitin and subjected to GFP-CENP-A^{Cnp1} affinity purification. Soubilized chromatin extracts (Total) and affinity purified extracts (IP) were analyzed by western blotting using anti-Myc and anti-GFP antibodies in the absence (-) and presence (+) of Dbl5.

6.3 Discussion

In this chapter, the relationship of the E3 ligase Dbl5 with CENP-A^{Cnp1} and its regulation was investigated. The *dbl5*Δ mutant exhibits a reduced frequency of centromere establishment (described in chapter 4). *De novo* centromere establishment requires both the assembly of CENP-A^{Cnp1} chromatin on a naïve sequence and formation of heterochromatin nearby (Folco et al., 2008; Kagansky et al., 2009). ChIP analysis revealed that CENP-A^{Cnp1} and H3K9me chromatin establishment were normal in *dbl5*Δ cells (Figure 6.1).This suggests that the reduced centromere establishment frequency observed was not caused by defective heterochromatin or CENP-A^{Cnp1} chromatin establishment on the minichromosome. Possible explanations are that defective minichromosome missegregation due the loss of cohesion or that minichromosome replication is impaired due to mislocalized

heterochromatin of CENP-A^{Cnp1} on the plasmid backbone or improper minichromosome segregation (Metzger et al., 2017). Further analysis are required to assess these possibilities.

In *S. cerevisiae*, Psh1 facilitates CENP-A^{Cse4} degradation, thereby controlling CENP-A^{Cse4} levels (Ranjitkar et al., 2010; Hewawasam et al., 2010). An obvious explanation for the genetic interaction of Dbl5 with CENP-A^{Cnp1} and Mis6 is that loss of Dbl5 affects the relative levels of CENP-A^{Cnp1} and canonical histones. However, no difference in the levels of CENP-A^{Cnp1}, histone H3 or histone H4 was detected in *dbl5*Δ cells compared to wild-type cells (Figure 6.4 C). CENP-A^{Cnp1} can be deposited on cc2 DNA of a minichromosome that lacks adjacent heterochromatin but only in cells expressing elevated CENP-A^{Cnp1} levels (Catania et al., 2015). If Dbl5 is involved in limiting CENP-A^{Cnp1} levels then in the absence of Dbl5 CENP-A^{Cnp1} might also be deposited on cc2 DNA in absence of adjacent heterochromatin. However, deletion of Dbl5 was insufficient to bypass the requirement for adjacent heterochromatin in depositing CENP-A^{Cnp1} on cc2 DNA (Figure 6.4 D). Together, these observations suggest that in *dbl5*Δ cells the levels of CENP-A^{Cnp1} are not dramatically affected.

In *S. cerevisiae*, Psh1 has been shown to physically interacts with CENP-A^{Cse4} and localize at centromeres (Hewawasam et al., 2010). However, in fission yeast, Dbl5 does not associate with centromeres (Figure 6.5). One possibility is that Dbl5 and CENP-A^{Cnp1} do associate but that interaction is unstable or more transient and is lost in cell extracts. It is also possible that GFP tagged Dbl5 is not fully functional and consequently such interactions are compromised. In *S. cerevisiae*, FACT complex interacts with Psh1 and regulates CENP-A^{Cse4} ubiquitylation and degradation (Deyter and Biggins, 2014). Both subunits of FACT were found in association with Dbl5, however further analysis are required to determine its functional significance (Figure 6.5 C).

In *S. cerevisiae*, the role of Psh1 is only apparent in cells expressing additional CENP-A^{Cse4} (Hewawasam et al., 2010; Ranjitkar et al., 2010). Similarly, Dbl5 the orthologue of Psh1, it is possible that the role of Dbl5 could also be visible in cells expressing extra CENP-A^{Cnp1}. Indeed a moderate increase in the expression of CENP-A^{Cnp1} was lethal in *dbl5*Δ cells which also exhibited aberrant GFP-CENP-A^{Cnp1} localization and chromosome segregation defects (Figure 6.6). Since similar defects have been

previously observed in cells expressing additional CENP-A^{Cnp1} (Castillo et al., 2013), it seems reasonable to conclude that Dbl5 affects CENP-A^{Cnp1} levels and consequently the viability of cells with extra CENP-A^{Cnp1}. Fission yeast centromeres and telomeres are known to cluster at the nuclear periphery (Funabiki et al., 1993). Fluorescence in situ hybridization (FISH) to detect centromere and telomere could be performed to determine whether the additional CENP-A^{Cnp1} foci observed in *dbl5Δ* cells is due to CENP-A^{Cnp1} incorporation near telomeric regions or if it results from the declustering of centromeres.

In cells expressing extra GFP-CENP-A^{Cnp1} four times higher levels were detected in *dbl5*Δ compared to wild type cells (Figure 6.7). Thus, the loss of Dbl5 make this additional GFP-CENP-A^{Cnp1} resistant to degradation. This result is consistent with the finding that loss of *S. cerevisiae* Psh1 also increases the stability of CENP-A^{Cse4} (Hewawasam et al., 2010; Ranjitkar et al., 2010). However, unlike in *S. cerevisiae*, GFP-CENP-A^{Cnp1} levels were very stable when translation was inhibited, suggesting Dbl5-dependent CENP-A^{Cnp1} degradation is a major pathway for regulating CENP-A^{Cnp1} levels in *S. pombe*. CENP-A^{Cnp1} has been shown to accumulate on the central domain, outer repeats and in sub-telomeric regions when CENP-A^{Cnp1} is overexpressed (Castillo et al., 2013). The fact that *dbl5*Δ cells also exhibit increased CENP-A^{Cnp1} on the central domain and outer repeats is consistent with Dbl5 being required to degrade excess CENP-A^{Cnp1} (Figure 6.8). CENP-A^{Cnp1} ChIP-seq analysis would allow differences in the genome-wide distribution of CENP-A^{Cnp1} to be determined in *dbl5*Δ cells.

CENP-A has been shown to be ubiquitylated in *S. cerevisiae* and humans, although CENP-A ubiquitylation in *S. cerevisiae* facilitates deposition while in humans CENP-A ubiquitylation is shown to promote CENP-A and HJURP interaction and thus facilitates CENP-A incorporation (Hewawasam et al. 2010; Niikura et al., 2015). In *Drosophila*, CENP-A^{CID} localization is impaired in the presence of the proteasome inhibitor MG132 (Moreno-Moreno et al., 2006). The proteasomal degradation of ubiquitylated CENP-A^{Cnp1} may also be conserved in *S. pombe*. High-molecular weight ubiquitylated species associated with GFP-CENP-A^{Cnp1} and mass spectrometry analysis detected that CENP-A^{Cnp1} is ubiquitylated on lysine 4 (Figure 6.9 and 6.10). However, the deletion of the first 11 residues of CENP-A^{Cnp1} has been shown to not significantly affect centromere function (Folco et al., 2015). In *S. cerevisiae*, multiple ubiquitylated

lysines occur on CENP-A^{Cse4} and no single lysine residue was found to be responsible for CENP-A^{Cse4} degradation (Collins et al., 2004; Hewawasam et al. 2010). Therefore, it is possible that multiple lysines on *S. pombe* CENP-A^{Cnp1} are also ubiquitylated to regulate its stability. In my mass spec analysis CENP-A^{Cnp1} protein had low sequence coverage (62.5 %) and Lys-4 was the only lysine included (data not shown). Thus it is entirely possible that other lysines on CENP-A^{Cnp1} are ubiquitylated. The low coverage of CENP-A^{Cnp1} protein is a consequence of the high number of lysine and arginine residues in CENP-A^{Cnp1} that are cleaved by trypsin. Thus the resulting peptides are too small for the analysis by mass spectrometry. Alternative endoproteinases like LysC, ArgC, AspN, and GluC need to be used to improve coverage and mapping of PTMs on CENP-A^{Cnp1} (Swaney et al., 2010).

PTMs are known to control the activity of and interactions with proteins (Hennrich and Gavin, 2015). In *S. cerevisiae*, phosphorylation of Psh1 promotes degradation of CENP-A^{Cse4} and auto-ubiquitylation of Psh1 is proposed to control Psh1 levels through proteolysis (Hewawasam et al., 2014). Here I detected, 15 phosphorylation and 1 ubiquitylation site on *S. pombe* Dbl5 (Table 6.1 and 6.2). Functional assays will be required to determine the significance of these modifications with respect to Dbl5 regulation of CENP-A^{Cnp1}.

In summary, Dbl5 is an E3 ligase that regulates the stability of CENP-A^{Cnp1} and prevents mislocalization of CENP-A^{Cnp1} to non-centromeric loci. This is consistent with finding in other systems showing that the ubiquitin-dependent proteolytic machinery targets CENP-A^{Cnp1} for degradation (Collins et al., 2004; Moreno-Moreno et al., 2006; Ranjitkar et al., 2010; Hewawasam et al., 2010; Gonzalez et al., 2014). It will be interesting to investigate if Dbl5 mediates ubiquitylation of CENP-A^{Cnp1} Lys4 and other lysine residues.

Table 6.1: Phosphorylation sites identified on the Dbl5 protein

Protein name	Position within protein	Phospho (STY) Probabilities	
Dbl5	384	ELADIQNES(0.98)LDS(0.02)LNS(0.09)S(0.698)S(0.205)NNS(0.005)PS(0.001)HNNIHSR	This study
	387	ELADIQNES(0.236)LDS(0.733)LNS(0.02)S(0.006)S(0.003)NNS(0.001)PSHNNIHSR	Kettenbach et al., 2015
	390	ELADIQNES(0.003)LDS(0.029)LNS(0.706)S(0.19)S(0.054)NNS(0.014)PS(0.002)HNNIHS(0.003)R	Kettenbach et al., 2015
	391	ELADIQNES(0.98)LDS(0.02)LNS(0.09)S(0.698)S(0.205)NNS(0.005)PS(0.001)HNNIHSR	This study
	392	ELADIQNES(0.039)LDS(0.198)LNS(0.53)S(0.53)S(0.53)NNS(0.146)PS(0.027)HNNIHSR	This study
	233*	EWFWDGENAES(0.635)DS(0.182)S(0.182)LNGDNT(0.001)R	This study
	235*	EWFWDGENAES(0.059)DS(0.483)S(0.454)LNGDNT(0.004)R	This study
	236	EWFWDGENAES(0.014)DS(0.206)S(0.779)LNGDNTR	This study
	409*	QHPFS(1)S(1)DEDEGNIVTNGTGLR	Kettenbach et al., 2015
	410*	QHPFS(1)S(1)DEDEGNIVTNGTGLR	Kettenbach et al., 2015
	182	S(1)ILVDS(1)EDGVLR	Kettenbach et al., 2015
	187	S(1)ILVDS(1)EDGVLR	Kettenbach et al., 2015
	280*	FDEGEEFVGS(0.649)DLES(0.649)DFS(0.649)GPGEY(0.054)DVDDGFIDNR	This study
	284*	FDEGEEFVGS(0.649)DLES(0.649)DFS(0.649)GPGEY(0.054)DVDDGFIDNR	This study
	287	FDEGEEFVGS(0.649)DLES(0.649)DFS(0.649)GPGEY(0.054)DVDDGFIDNR	This study
* Predicted phosphorylation sites for casein kinase 2 by NetPhosK (Blom et al., 1999)			

Table 6.2: Ubiquitylation sites identified on the Dbl5 protein

Protein name	Position within protein	GlyGly (K) Probabilities	
Dbl5	164	QK(1)EVLFDGMFK	This study

Chapter 7

Discussion and Future Directions

Faithful segregation of the genome during cell division is essential for cell viability and prevention of aneuploidy, a hallmark of cancer (Kops et al., 2005). In eukaryotes, this process requires the attachment of each replicated sister chromatid to opposing poles of the mitotic spindle so that the genetic material is accurately partitioned into the two daughter cells (Cleveland et al., 2003). A region of each chromosome, the centromere, mediates the attachment of the chromosome to the spindle microtubules (Pidoux and Allshire, 2000; Fukagawa and Earnshaw, 2014). Centromeric chromatin contains conserved histone H3 variant, CENP-A, which is a constitutive chromatin component that provides the foundation for the assembly of the kinetochore (Allshire and Karpen, 2008; McKinley and Cheeseman, 2016).

Over last three decades, both genetic and biochemical approaches have been used to identify components of CENP-A^{Cnp1} chromatin and kinetochore in yeast (Stoler et al., 1995; Meeks-Wagner et al., 1986; Maine et al., 1984; Spencer et al., 1990; Takahashi et al., 1994; Fleig et al., 1996; Pidoux et al., 2003; Hayashi et al., 2004). Advancements in mass spectrometry led to the discovery of large number of centromere-associated proteins (Obuse et al., 2004; Foltz et al., 2006; Okada et al., 2006; Liu et al., 2005; Shiroiwa et al., 2011; Akiyoshi et al., 2009; Akiyoshi et al.,2010; Barth et al., 2015). Previous analysis of *S. pombe* kinetochore proteins were carried out using affinity purification of inner and outer kinetochore protein (Liu et al., 2005; Shiroiwa et al., 2011) and these resulted in the isolation of sub-complexes of the kinetochore rather than the kinetochore-chromatin complex. To date, no CENP-A^{Cnp1} proteomic study of *S. pombe* had been performed. This study described in this thesis set out to explore the protein composition of CENP-A^{Cnp1} chromatin in fission yeast.

7.1 The fission yeast kinetochore

In order to isolate CENP-A^{Cnp1} chromatin and the kinetochore in its native state, GFP-tagged CENP-A^{Cnp1} was affinity purified (Figure 3.1 and 3.2). The affinity selection of CENP-A^{Cnp1} chromatin complex efficiently enriched all known subunits of inner and outer kinetochore complex (Figure 3.5), thus validating the purification of the CENP-

A^{Cnp1}-kinetochore complex. In the CENP-N^{Mis15} pulldown that I also performed, CENP-N^{Mis15} and CENP-L^{Fta1} were present in roughly equal amounts and twice as much compared to CENP-A^{Cnp1} (Figure 3.6 B). This is consistent with *in vitro* studies on recombinant human kinetochores (Weir et al., 2016). Interestingly, CENP-OPQU, Fta4 and Cnl2 showed higher relative enrichment (Figure 3.6 B). Consistent with the proposed idea that human CENP-OPQUR have varying stoichiometries at the kinetochore (Eskat et al., 2012). As the CENP-OPQUR subunits are not essential for kinetochore function, their contribution at the kinetochore has not been intensively studied.

Protein cross-linking is commonly used to form bridges between lysine residues that are in close proximity to each other to stabilize dynamics protein-protein interactions (Young et al., 2000). Introduction of cross-links at specific residues provides spatial information about the protein assemblies (Holding, 2015; Liu and Hech, 2015; Chu et al., 2018). Cross-linking mass spectrometry (XL-MS) could provide information about transient or dynamic protein–protein interactions, which form and break easily (Sinz et al., 2015). Such analysis of kinetochore complex could reveal interactions of kinetochore proteins to generate a linkage map of the fission yeast kinetochore and determine the stoichiometries of all kinetochore proteins *in vivo*. A schematic of the XL-MS workflow is shown in Figure 7.1 A. The procedure uses a BS3 cross-linker (bis(sulphosuccinimidyl)suberate), which reacts with primary amines in lysine side chains and protein N-termini (Chen et al., 2016). A preliminary cross-linking experiment was performed, following affinity selection of GFP-CENP-A^{Cnp1}, eluate was incubated in BS3 cross-linker. Western blot analysis of GFP-CENP-A^{Cnp1} indicates efficient cross-linking of GFP-CENP-A^{Cnp1} (Figure 7.1). MS analysis detected inner kinetochore proteins in the cross-linked samples (data not shown). Preliminary observations were promising and require further optimization and large scale isolation of crosslinked kinetochore complex. Defining the stoichiometric composition of the kinetochore subunits remains an important outstanding goal and will be followed in the future.

Post translational modifications (PTMs) on kinetochore proteins could affect its function and at centromere. The analysis of PTMs identified previously unknown modifications on kinetochore proteins: 12 phosphorylations, 1 acetylation, 22 ubiquitylations, 9 methylations (inclusive mono/di/tri) and 4 sumoylation residues

(Table 3.4-8). I identified acetylation of Lys-4, ubiquitylation of Lys-4 and phosphorylation of Ser-5 on CENP-A^{Cnp1}. Functional analysis of these modifications is required to evaluate their influence on kinetochore structure/function. *S. pombe* CENP-A^{Cnp1} Lys-4 ubiquitylation is conserved in *S. cerevisiae* CENP-A^{Cse4}, which is shown to regulate CENP-A^{Cse4} degradation along with ubiquitylation on other lysines (Hewawasam et al. 2010). In humans, CENP-A Lys-124 has different modifications in different stages of the cell cycle (Table1.1; Srivastava and Foltz, 2018) and CENP-A Ser-68 phosphorylation is proposed to impair CENP-A interaction with HJURP and prevent deposition of CENP-A outside of G1 (Yu et al., 2015). It is possible that the PTMs on *S. pombe* kinetochore proteins might be constitutive or regulated during cell cycle. To gain insight into the dependence of these modifications on cell cycle, CENP-A^{Cnp1} pulldown should be performed in cells blocked at different stages of the cell cycle or through cell cycles in synchronized populations. This analysis will also provide a wealth of information about the variation in composition of CENP-A^{Cnp1} chromatin during the cell cycle.

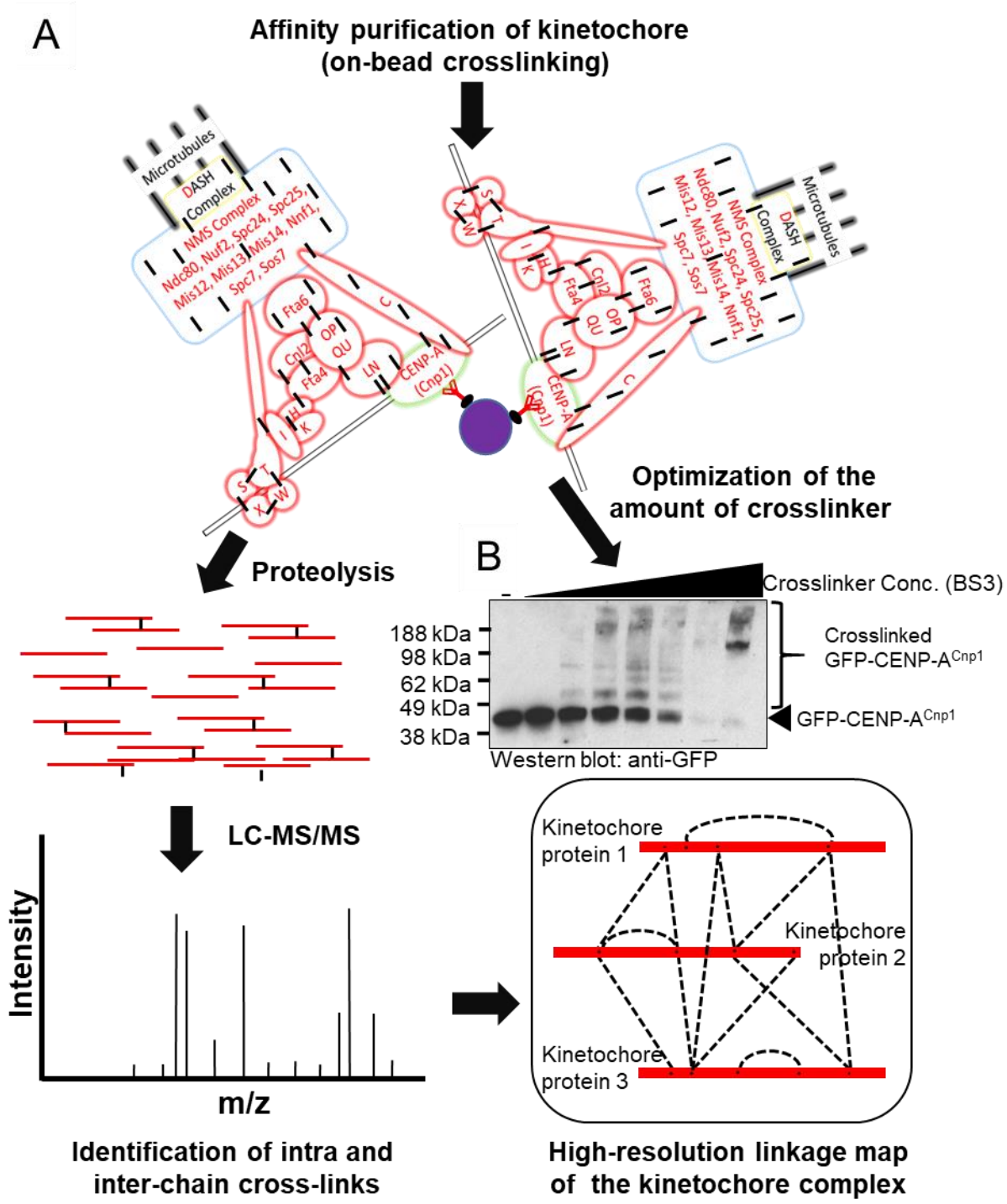

Figure 7.1: Scheme for affinity purification of the kinetochore and identification of inter/intra-chain cross-links. (A)Affinity purification of the kinetochore complex with anti-GFP followed by on-bead crosslinking. Eluted cross-linked proteins were digested to smaller peptides using trypsin followed by LC-MS/MS to detect intra and inter-chain cross-links of kinetochore proteins to generate a high resolution linkage map of fission yeast kinetochore. (B) On-bead crosslinking of proteins was performed on GFP-CENP-A^{Cnp1} pulldown with different concentrations of BS3 (bis(sulfosuccinimidyl)suberate), an amine-to-amine crosslinker. Western blot analysis of GFP-CENP-A^{Cnp1} on eluate obtained after crosslinking.

7.2 The role of Hap2 in the establishment and maintenance of CENP-A^{Cnp1} chromatin

Hap2 was enriched in the affinity selected GFP-CENP-A^{Cnp1} chromatin. Hap2 was previously identified as a potential Ino80 complex associated protein (Hogan et al., 2009). Hap2-GFP purification resulted in isolation of all subunits of the Ino80 complex (Figure 5.5). The Ino80 complex contains stoichiometric amounts of Ino80, Arp4, Arp5, Arp8, and actin in *S. cerevisiae* and *S. pombe* (Shen et al., 2000; Hogan et al., 2010). Consistent with this, in the purified Hap2-GFP complex, relatively equal amounts of Ino80, Arp4, Arp5, Arp8 and actin were pulled down (Figure 5.6 D). This suggests that Ino80 complex integrity is maintained and all subunits are purified with Hap2-GFP. Of all the Ino80 subunits, Hap2 was the least abundant in purified Hap2-GFP (Figure 5.6 D). A possible explanation for lower Hap2 compared to other Ino80 subunits is that Hap2 might mediate the interaction between multiple Ino80 complexes. Further investigation is needed to explore this possibility, for example, size exclusion chromatography and XL-MS analysis of affinity selected Hap2-GFP complex.

All subunits that are specific to Ino80 complex are non-essential, except Ino80 itself. In *S. cerevisiae*, an INO80 complex which lacks the core subunit Arp8 is defective in DNA binding and nucleosome remodeling activity (Shen et al., 2003). The Ino80 complex in *S. cerevisiae* is proposed to catalyze the removal of H2A.Z from chromatin (Papamichos-Chronakis et al., 2011) and required to maintain a normal pericentric heterochromatin structure (Chambers et al., 2012). In *S. pombe*, the Ino80 complex plays a prominent role in removing histone H2A.Z^{Pht1} from chromatin (Choi et al., 2017). However, deletion of Ies6 does not exhibit significant enrichment of H2A.Z^{Pht1} at centromeres (Choi et al., 2017). Absence of Iec1 or Ies6 results in increased histone H3 occupancy at centromeres (Hogan et al., 2010; Choi et al., 2017). In this study I have shown that Hap2 is required for establishment of CENP-A^{Cnp1} chromatin on plasmid-borne central core sequence (Figure 5.1). However, loss of Hap2 exhibits heterochromatin spreading into plasmid-borne-central core sequence from adjacent heterochromatin repeat sequence (Figure 5.1). Spreading of H3K9me was not observed at endogenous centromeres. Hap2 is also required for the maintenance of CENP-A^{Cnp1} chromatin at endogenous centromeres (Figure 5.3). It has been proposed that eviction of histone H3 through turnover mechanism provides an opportunity for CENP-A^{Cnp1} nucleosome deposition (Sullivan, 2001; Allshire and Karpen, 2008;

Probst et al., 2009; Shukla et al., 2017). Therefore, it is possible that altered histone H3 turnover may be responsible for reduction in CENP-A^{Cnp1} deposition in the *hap2*Δ mutant. Deletion of Hap2 resulted in decreased replication-independent histone H3 turnover at centromeres, ectopically inserted central core sequences and non centromeric sequences (Figure 5.8). The Ino60 subunit, Ies6, can be co-immunoprecipitated with CENP-A^{Cnp1} from cells overexpressing CENP-A^{Cnp1} (Choi et al., 2017). Another possibility is that Hap-Ino80 may be able to interact directly with CENP-A^{Cnp1} and facilitates its deposition. Increased RNAPII stalling facilitates establishment of CENP-A^{Cnp1} (Catania et al., 2015). I propose a model where RNAPII stalling might recruit Hap2-Ino80 complex at centromeric sequences or vice-versa and facilitates transcription-coupled remodeling leading to higher histone H3 turnover providing opportunity for CENP-A^{Cnp1} deposition (Figure 7.2). If this model is correct, increased amounts of RNAPII S2P at ectopic centromere should be observed in *hap2*Δ. Further investigation is needed to explore whether Hap2 association at central domain is dependent on CENP-A^{Cnp1} or CENP-A^{Cnp1}-chaperone HJURP^{Scm3}. In summary, the analyses presented in Chapter 5, implicate Hap2-Ino80 complex in the establishment and maintenance of CENP-A^{Cnp1} chromatin.

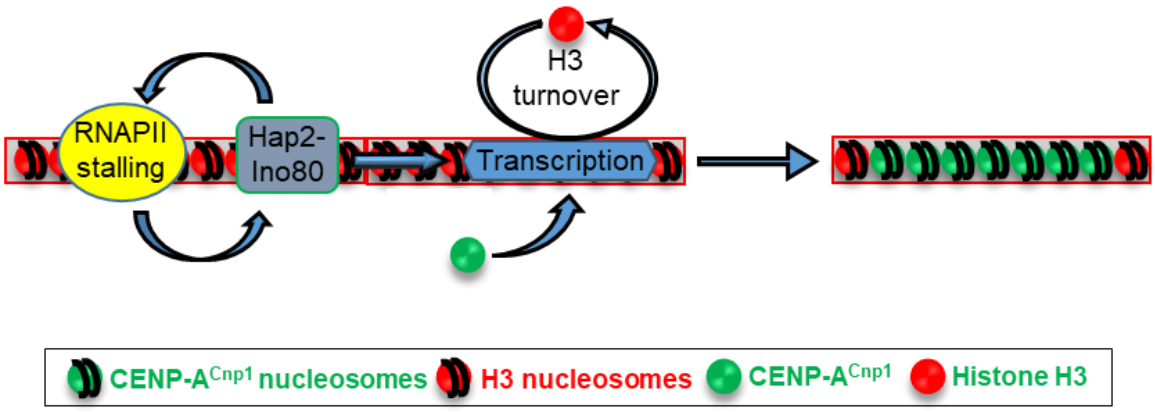

Figure 7.2: Models to explain why Hap2 is required for the establishment and maintenance of CENP-A^{Cnp1} chromatin. (A) The Hap2-Ino80 complex is required for efficient histone H3 turnover. (B) Removal of histone H3 by Hap2-Ino80 might provide opportunity for CENP-A^{Cnp1} deposition. (C) Hap2-Ino80 complex might associate with CENP-A^{Cnp1} and facilitate its deposition.

7.3 The role of Dbl5 in the regulation of CENP-A^{Cnp1}

Dbl5 was enriched in the affinity selected GFP-CENP-A^{Cnp1} chromatin. Dbl5 is a fission yeast orthologue of *S. cerevisiae* Psh1, which regulates CENP-A^{Cse4} degradation and prevent its euchromatic accumulation (Ranjitkar et al., 2010; Hewawasam et al., 2010). Similar to Psh1, Dbl5 promotes CENP-A^{Cnp1} degradation in fission yeast (Figure 6.7). Based on my findings, I propose a model for how Dbl5 controls CENP-A^{Cnp1} degradation (Figure 7.3). Dbl5-GFP ChIP from cell expressing normal levels of CENP-A^{Cnp1} suggests that Dbl5 does not associate with centromeric central domain (Figure 6.5 A). Dbl5 is detected in purification of CENP-A^{Cnp1} but not kinetochore protein CENP-N^{Mis15} (data not shown). These observations suggests that Dbl5 is not associated with fission yeast centromeres/kinetochores and possibly explain why centromeric CENP-A^{Cnp1} is not targeted for degradation (Figure 7.3 A). It has been proposed that HJURP^{Scm3} might protect CENP-A^{Cse4} from proteolysis by Psh1 in budding yeast (Hewawasam et al., 2010). The FACT subunit Spt16 interacts with Psh1 and promotes ubiquitylation and degradation of CENP-A^{Cse4} (Deyter and Biggins, 2014). The role of CENP-A^{Cnp1}-HJURP^{Scm3} interaction and FACT-Dbl5 association will be tested for Dbl5-dependent CENP-A^{Cnp1} degradation. MS analysis of Dbl5-GFP showed enrichment of SAGA complex, NuA4 complex and elongator complex (Figure 6.5 C). It is possible that Dbl5 associates with these proteins and scans the chromosome for misincorporated CENP-A^{Cnp1}. The role of these complexes in Dbl5-dependent CENP-A^{Cnp1} degradation requires further investigation.

To date there are four E3 ubiquitin ligases described in *S. cerevisiae* that facilitates CENP-A^{Cse4} degradation - Psh1 (Ranjitkar et al., 2010; Hewawasam et al., 2010; Hewawasam et al., 2014), Rcy1 (Cheng et al., 2016; Cheng et al., 2017), Ubr1 (Cheng et al., 2017) and Slx5 (Okhuni et al., 2016; Cheng et al., 2017). Treatment of *psh1*∆ cells with CHX for 1 hour leads to reduction of CENP-A^{Cse4} levels by more than 60% (Hewawasam et al., 2014), suggesting a role for other E3 ligases in CENP-A^{Cse4} degradation. Since then, four E3 ligases, Psh1, Rcy1, Ubr1 and Slx5, have been implicated in CENP-A^{Cse4} degradation (Ohkuni et al. 2016; Cheng et al., 2016; Cheng et al., 2017; Cheng et al., 2017; Ohkuni et al. 2018). However, in a quadruple mutant of all four E3 ligases, CENP-A^{Cse4} degradation is severely impaired but not eliminated (Cheng et al., 2017). In contrast, in *S. pombe*, deletion of Dbl5 E3 ligase results in very stable CENP-A^{Cnp1} levels (>95% after 1 hour of CHX incubation) (Figure 6.6). Dbl5 is

the only E3 ubiquitin ligase enriched with GFP-CENP-A^{Cnp1} chromatin. This suggests that Dbl5 may be the major E3 ligase involved in CENP-A^{Cnp1} degradation in *S. pombe*. Deletion of Dbl5 results in partial suppression of *cnp1-1* lethality (Figure 6.4 A). A possible explanation for this may be that loss of Dbl5 leads to accumulation of CENP-A^{Cnp1} in the cells. No obvious defect in total histone levels were observed in *dbl5*Δ cells. Another possibility if that at semi-permissive temperatures there is higher amounts of *cnp1-1* at centromeres in *dbl5*Δ cells and this could explain the partial suppression of *cnp1-1* lethality. To test this possibility CENP-A^{Cnp1} ChIP-qPCR could be performed in *dbl5*Δ*cnp1-1* double mutant grown at semi-permissive temperature.

CENP-A mislocalization to euchromatin can lead to ectopic kinetochore formation, CENP-A mislocalization and genome instability (Heun et al. 2006; Castillo et al., 2013; Hildebrand and Biggins 2016). It is therefore essential that CENP-A exclusively localizes to centromeres and does not stably incorporate into euchromatin. Moderate overexpression of CENP-A^{Cnp1} in the *dbl5*Δ mutants results in CENP-A^{Cnp1} accumulation in cells with additional foci of CENP-A^{Cnp1}, mitotic segregation defects and cell death (Figure 6.6-8). This suggests that Dbl5 is required to control amount of CENP-A^{Cnp1} in cells and its chromatin localization in fission yeast (Figure 7.3 B-D). In *S. cerevisiae* HJURP^{Scm3} has been shown to protect CENP-A^{Cse4} from degradation (Hewawasam et al., 2010). Role of HJURP^{Scm3} in Dbl5 dependent ubiquitylation of CENP-A^{Cnp1} and proteolytic degradation should be tested in fission yeast.

Mass spectrometry analysis of purified CENP-A^{Cnp1} reproducibly identified ubiquitylation of CENP-A^{Cnp1} at lys4 (Figure 6.9). Purification of CENP-A^{Cnp1} also resulted in detection of high molecular weight ubiquitylated CENP-A^{Cnp1} species only in the presence of Dbl5 (Figure 6.10). Multiple lysine residues on CENP-A^{Cse4} can be ubiquitylated by Psh1 in *S. cerevisiae* (Hewawasam et al., 2010) while no single substitution of lysine to arginine in CENP-A^{Cse4} leads to increase CENP-A^{Cse4} stability (Collins et al., 2004). Although Lys-4 is the only lysine of CENP-A^{Cnp1} detected in the MS analysis, it is possible that multiple lysines are ubiquitylated to facilitate CENP-A^{Cnp1} degradation. Further investigation is needed to determine whether ubiquitylation of CENP-A^{Cnp1} on lys4 is Dbl5 dependent.

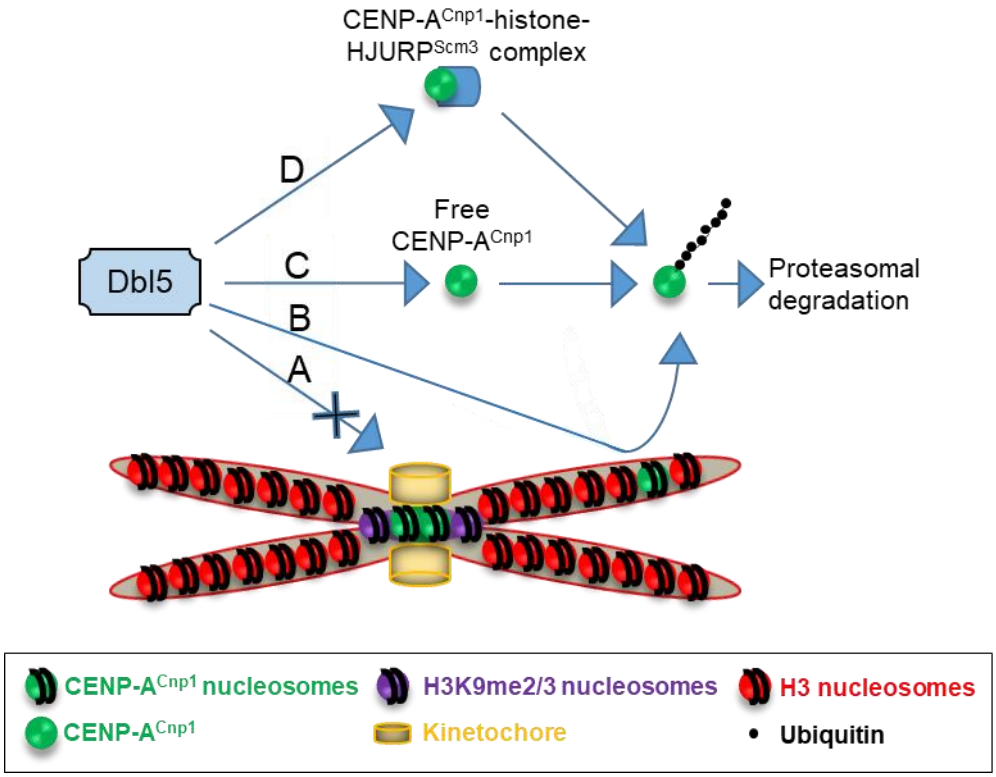

Figure 7.3: Dbl5-dependent CENP-A^{Cnp1} degradation. Dbl5 is an E3 ubiquitin-ligase that facilitates CENP-A^{Cnp1} ubiquitylayion and degradation. (A) Centromeric CENP-A^{Cnp1}-nucleosomes are protected from Dbl5. (B-D) Dbl5 may facilitate degradation of mislocalized CENP-A^{Cnp1} and soluble pool of CENP-A^{Cnp1}.

7.4 Conclusions

This study comprises the first proteomic screen to identify CENP-A^{Cnp1} chromatin-associated proteins in fission yeast. Affinity purification and mass spectrometry analysis of GFP-CENP-A^{Cnp1} was used to identify centromeric chromatin-enriched proteins. Purification of CENP-A/kinetochore complex was validated by the enrichment of all known inner/outer kinetochore proteins. I identified 48 PTMs on kinetochore proteins which were previously unknown. Analysis of these PTMs will be performed in the future to evaluate their influence on kinetochore structure and function. This protocol could be used to isolate and study variations in kinetochore complexes from different cell-cycle stages.

Potential candidate proteins were selected based on their enrichment in CENP-A^{Cnp1} chromatin. Functional assays were performed to investigate their role at centromeres. I identified an Ino80 subunit, Hap2, which is required for the establishment and

maintenance of CENP-A^{Cnp1} chromatin via replication-independent histone H3 turnover. Deletion of different Ino80 subunits showed opposite affect on the *de novo* establishment of functional centromeres. Further investigation is needed to assess the combinatorial effect of different Ino80 subunits on CENP-A^{Cnp1} establishment and maintenance in fission yeast.

I also identified Dbl5, an E3 ubiquitin ligase, which regulates the stability of CENP-A^{Cnp1} and prevents mislocalization of CENP-A^{Cnp1} to non-centromeric loci. Dbl5 is required for the ubiquitylation of CENP-A^{Cnp1} in fission yeast. The requirement of Dbl5 in ubiquitylation of CENP-A^{Cnp1} on lys4 remains to be investigated.

References

Agudo M, Abad JP, Molina I, Losada A, Ripoll P, Villasante A. A dicentric chromosome of Drosophila melanogaster showing alternate centromere inactivation. Chromosoma. 2000 Jun;109(3):190-6.

Ahmad K, Henikoff S. The histone variant H3.3 marks active chromatin by replication-independent nucleosome assembly. Mol Cell. 2002 Jun;9(6):1191-200.

Akiyoshi B, Nelson CR, Ranish JA, Biggins S. Quantitative proteomic analysis of purified yeast kinetochores identifies a PP1 regulatory subunit.Genes Dev. 2009 Dec 15;23(24):2887-99. doi: 10.1101/gad.1865909.

Akiyoshi B, Gull K. Evolutionary cell biology of chromosome segregation: insights from trypanosomes. Open Biol. 2013 May 1;3(5):130023. doi: 10.1098/rsob.130023.

Akiyoshi B, Gull K. Discovery of unconventional kinetochores in kinetoplastids. Cell. 2014 Mar 13;156(6):1247-1258. doi: 10.1016/j.cell.2014.01.049. Epub 2014 Feb 27.

Akiyoshi B, Sarangapani KK, Powers AF, Nelson CR, Reichow SL, Arellano-Santoyo H, Gonen T, Ranish JA, Asbury CL, Biggins S. Tension directly stabilizes reconstituted kinetochore-microtubule attachments. Nature. 2010 Nov 25;468(7323):576-9. doi: 10.1038/nature09594.

Akutsu M, Dikic I, Bremm A. Ubiquitin chain diversity at a glance. J Cell Sci. 2016 Mar 1;129(5):875-80. doi: 10.1242/jcs.183954. Epub 2016 Feb 15.

Allshire RC, Javerzat JP, Redhead NJ, Cranston G. Position effect variegation at fission yeast centromeres. Cell. 1994 Jan 14;76(1):157-69.

Allshire RC, Nimmo ER, Ekwall K, Javerzat JP, Cranston G. Mutations derepressing silent centromeric domains in fission yeast disrupt chromosome segregation. Genes Dev. 1995 Jan 15;9(2):218-33.

Allshire RC, Karpen GH. Epigenetic regulation of centromeric chromatin: old dogs, new tricks? Nat Rev Genet. 2008 Dec;9(12):923-37. doi: 10.1038/nrg2466.

Allshire RC, Ekwall K. Epigenetic Regulation of Chromatin States in Schizosaccharomyces pombe. Cold Spring Harb Perspect Biol. 2015 Jul 1;7(7):a018770. doi: 10.1101/cshperspect.a018770.

Allshire RC, Madhani HD. Ten principles of heterochromatin formation and function. Nat Rev Mol Cell Biol. 2018 Apr;19(4):229-244. doi: 10.1038/nrm.2017.119. Epub 2017 Dec 13.

Arents G, Burlingame RW, Wang BC, Love WE, Moudrianakis EN. The nucleosomal core histone octamer at 3.1 A resolution: a tripartite protein assembly and a left-handed superhelix. Proc Natl Acad Sci U S A. 1991 Nov 15;88(22):10148-52.

Au WC, Dawson AR, Rawson DW, Taylor SB, Baker RE, Basrai MA. A novel role of the N terminus of budding yeast histone H3 variant Cse4 in ubiquitin-mediated proteolysis. Genetics. 2013 Jun;194(2):513-8. doi: 10.1534/genetics.113.149898. Epub 2013 Mar 22.

Auth T, Kunkel E, Grummt F. Interaction between HP1alpha and replication proteins in mammalian cells. Exp Cell Res. 2006 Oct 15;312(17):3349-59. Epub 2006 Jul 28.

Ayoub N, Noma K, Isaac S, Kahan T, Grewal SI, Cohen A. A novel jmjC domain protein modulates heterochromatization in fission yeast. Mol Cell Biol. 2003 Jun;23(12):4356-70.

Aze A, Sannino V, Soffientini P, Bachi A, Costanzo V. Centromeric DNA replication reconstitution reveals DNA loops and ATR checkpoint suppression. Nat Cell Biol. 2016 Jun;18(6):684-91. doi: 10.1038/ncb3344. Epub 2016 Apr 25.

Babu A, Verma RS. Chromosome structure: euchromatin and heterochromatin. Int Rev Cytol. 1987;108:1-60.

Bade D, Pauleau AL, Wendler A, Erhardt S The E3 ligase CUL3/RDX controls centromere maintenance by ubiquitylating and stabilizing CENP-A in a CAL1-dependent manner. Dev Cell. 2014 Mar 10;28(5):508-19. doi: 10.1016/j.devcel.2014.01.031.

Bailey AO, Panchenko T, Sathyan KM, Petkowski JJ, Pai PJ, Bai DL, Russell DH, Macara IG, Shabanowitz J, Hunt DF, Black BE, Foltz DR. Posttranslational modification of CENP-A influences the conformation of centromeric chromatin. Proc Natl Acad Sci U S A. 2013 Jul 16;110(29):11827-32. doi: 10.1073/pnas.1300325110. Epub 2013 Jul 1.

Barnhart MC, Kuich PH, Stellfox ME, Ward JA, Bassett EA, Black BE, Foltz DR. HJURP is a CENP-A chromatin assembly factor sufficient to form a functional de novo kinetochore. J Cell Biol. 2011 Jul 25;194(2):229-43. doi: 10.1083/jcb.201012017. Epub 2011 Jul 18.

Barrey EJ, Heun P. Artificial Chromosomes and Strategies to Initiate Epigenetic Centromere Establishment. Prog Mol Subcell Biol. 2017;56:193-212. doi: 10.1007/978-3-319-58592-5_8.

Barth TK, Schade GO, Schmidt A, Vetter I, Wirth M, Heun P, Thomae AW, Imhof A. Identification of novel Drosophila centromere-associated proteins. Proteomics. 2014 Oct;14(19):2167-78. doi: 10.1002/pmic.201400052. Epub 2014 Jul 14.

Basilico F, Maffini S, Weir JR, Prumbaum D, Rojas AM, Zimniak T, De Antoni A, Jeganathan S, Voss B, van Gerwen S, Krenn V, Massimiliano L, Valencia A, Vetter IR, Herzog F, Raunser S, Pasqualato S, Musacchio A. The pseudo GTPase CENP-M drives human kinetochore assembly. Elife. 2014 Jul 8;3:e02978. doi: 10.7554/eLife.02978.

Bauer F, Matsuyama A, Candiracci J, Dieu M, Scheliga J, Wolf DA, Yoshida M, Hermand D. Translational control of cell division by Elongator. Cell Rep. 2012 May 31;1(5):424-33.

Baum M, Ngan VK, Clarke L. The centromeric K-type repeat and the central core are together sufficient to establish a functional Schizosaccharomyces pombe centromere. Mol Biol Cell. 1994 Jul;5(7):747-61.

Bayne EH, Bijos DA, White SA, de Lima Alves F, Rappsilber J, Allshire RC. A systematic genetic screen identifies new factors influencing centromeric heterochromatin integrity in fission yeast. Genome Biol. 2014;15(10):481.

Bell SP, Stillman B. ATP-dependent recognition of eukaryotic origins of DNA replication by a multiprotein complex. Nature. 1992 May 14;357(6374):128-34.

Bell SP. The origin recognition complex: from simple origins to complex functions.Genes Dev. 2002 Mar 15;16(6):659-72.

Belotserkovskaya R, Oh S, Bondarenko VA, Orphanides G, Studitsky VM, Reinberg D. FACT facilitates transcription-dependent nucleosome alteration. Science. 2003 Aug 22;301(5636):1090-3.

Bergmann JH, Rodríguez MG, Martins NM, Kimura H, Kelly DA, Masumoto H, Larionov V, Jansen LE, Earnshaw WC. Epigenetic engineering shows H3K4me2 is required for HJURP targeting and CENP-A assembly on a synthetic human kinetochore. EMBO J. 2011 Jan 19;30(2):328-40. doi: 10.1038/emboj.2010.329. Epub 2010 Dec 14.

Bernad R, Sánchez P, Rivera T, Rodríguez-Corsino M, Boyarchuk E, Vassias I, Ray-Gallet D, Arnaoutov A, Dasso M, Almouzni G, Losada A.Xenopus HJURP and condensin II are required for CENP-A assembly. J Cell Biol. 2011 Feb 21;192(4):569-82. doi: 10.1083/jcb.201005136. Epub 2011 Feb 14.

Bernard P, Maure JF, Partridge JF, Genier S, Javerzat JP, Allshire RC. Requirement of heterochromatin for cohesion at centromeres. Science. 2001 Dec 21;294(5551):2539-42. Epub 2001 Oct 11.

Bickmore WA, van Steensel B. Genome architecture: domain organization of interphase chromosomes. Cell. 2013 Mar 14;152(6):1270-84. doi: 10.1016/j.cell.2013.02.001.

Black BE, Jansen LE, Maddox PS, Foltz DR, Desai AB, Shah JV, Cleveland DW. Centromere identity maintained by nucleosomes assembled with histone H3 containing the CENP-A targeting domain. Mol Cell. 2007 Jan 26;25(2):309-22.

Black BE, Cleveland DW. Epigenetic centromere propagation and the nature of CENP-a nucleosomes. Cell. 2011 Feb 18;144(4):471-9. doi: 10.1016/j.cell.2011.02.002.

Bloom KS. Centromeric heterochromatin: the primordial segregation machine. Annu Rev Genet. 2014;48:457-84. doi: 10.1146/annurev-genet-120213-092033. Epub 2014 Sep 18.

Bøe CA, Knutsen JH, Boye E, Grallert B. Hpz1 modulates the G1-S transition in fission yeast. PLoS One. 2012;7(9):e44539. doi: 10.1371/journal.pone.0044539. Epub 2012 Sep 6.

Boeckmann L, Takahashi Y, Au WC, Mishra PK, Choy JS, Dawson AR, Szeto MY, Waybright TJ, Heger C, McAndrew C, Goldsmith PK, Veenstra TD, Baker RE, Basrai MA. Phosphorylation of centromeric histone H3 variant regulates chromosome segregation in Saccharomyces cerevisiae Mol Biol Cell. 2013 Jun;24(12):2034-44. doi: 10.1091/mbc.E12-12-0893. Epub 2013 May 1

Boltengagen M, Huang A, Boltengagen A, Trixl L, Lindner H, Kremser L, Offterdinger M, Lusser A. A novel role for the histone acetyltransferase Hat1 in the CENP-A/CID assembly pathway in Drosophila melanogaster. Nucleic Acids Res. 2016 Mar 18;44(5):2145-59. doi: 10.1093/nar/gkv1235. Epub 2015 Nov 19.

Bui M, Dimitriadis EK, Hoischen C, An E, Quenet D, Giebe S, NitaLazar A, Diekmann S, Dalal Y (2012) Cell-cycle-dependent structural transitions in the human CENP-A nucleosome in vivo. Cell 150:317–326

Bui M, Pitman M, Nuccio A, Roque S, Donlin-Asp PG, Nita-Lazar A, Papoian GA, Dalal Y (2017) Internal modifications in the CENP-A nucleosome modulate centromeric dynamics. Epigenetics Chromatin 10:17

Buscaino A, Lejeune E, Audergon P, Hamilton G, Pidoux A, Allshire RC. Distinct roles for Sir2 and RNAi in centromeric heterochromatin nucleation, spreading and maintenance. EMBO J. 2013 May 2;32(9):1250-64. doi: 10.1038/emboj.2013.72. Epub 2013 Apr 9.

Cai Y, Jin J, Yao T, Gottschalk AJ, Swanson SK, Wu S, Shi Y, Washburn MP, Florens L, Conaway RC, Conaway JW. YY1 functions with INO80 to activate transcription. Nat Struct Mol Biol. 2007 Sep;14(9):872-4. Epub 2007 Aug 26.

Canzonetta C, Vernarecci S, Iuliani M, Marracino C, Belloni C, Ballario P, Filetici P. SAGA DUB-Ubp8 Deubiquitylates Centromeric Histone Variant Cse4. G3 (Bethesda). 2015 Nov 27;6(2):287-98. doi: 10.1534/g3.115.024877.

Carone DM, Zhang C, Hall LE, Obergfell C, Carone BR, O'Neill MJ, O'Neill RJ (2013) Hypermorphic expression of centromeric retroelement-encoded small RNAs impairs CENP-A loading. Chromosome Res 21(1):49–62. doi: 10.1007/s10577-013-9337-0

Carroll CW, Silva MC, Godek KM, Jansen LE, Straight AF. Centromere assembly requires the direct recognition of CENP-A nucleosomes by CENP-N. Nat Cell Biol. 2009 Jul;11(7):896-902. doi: 10.1038/ncb1899. Epub 2009 Jun 21.

Carroll CW, Milks KJ, Straight AF. Dual recognition of CENP-A nucleosomes is required for centromere assembly. J Cell Biol. 2010 Jun 28;189(7):1143-55. doi: 10.1083/jcb.201001013. Epub 2010 Jun 21.

Castillo AG, Mellone BG, Partridge JF, Richardson W, Hamilton GL, Allshire RC, Pidoux AL. Plasticity of fission yeast CENP-A chromatin driven by relative levels of histone H3 and H4. PLoS Genet. 2007 Jul;3(7):e121. Epub 2007 Jun 7.

Castillo AG, Pidoux AL, Catania S, Durand-Dubief M, Choi ES, Hamilton G, Ekwall K, Allshire RC. Telomeric repeats facilitate CENP-A(Cnp1) incorporation via telomere binding proteins. PLoS One. 2013 Jul 31;8(7):e69673. doi: 10.1371/journal.pone.0069673. Print 2013.

Catania S, Pidoux AL, Allshire RC. Sequence features and transcriptional stalling within centromere DNA promote establishment of CENP-A chromatin. PLoS Genet. 2015 Mar 4;11(3):e1004986. doi: 10.1371/journal.pgen.1004986. eCollection 2015 Mar.

Chambers AL, Ormerod G, Durley SC, Sing TL, Brown GW, Kent NA, Downs JA. The INO80 chromatin remodeling complex prevents polyploidy and maintains normal chromatin structure at centromeres. Genes Dev. 2012 Dec 1;26(23):2590-603. doi: 10.1101/gad.199976.112.

Chan FL, Marshall OJ, Saffery R, Kim BW, Earle E, Choo KH, Wong LH. Active transcription and essential role of RNA polymerase II at the centromere during mitosis. Proc Natl Acad Sci U S A. 2012 Feb 7;109(6):1979-84. doi: 10.1073/pnas.1108705109. Epub 2012 Jan 20.

Cheeseman IM, Drubin DG, Barnes G. Simple centromere, complex kinetochore: linking spindle microtubules and centromeric DNA in budding yeast. J Cell Biol. 2002 Apr 15;157(2):199-203. Epub 2002 Apr 15.

Cheeseman IM, Chappie JS, Wilson-Kubalek EM, Desai A. The conserved KMN network constitutes the core microtubule-binding site of the kinetochore. Cell. 2006 Dec 1;127(5):983-97.

Chen CC, Dechassa ML, Bettini E, Ledoux MB, Belisario C, Heun P, Luger K, Mellone BG. CAL1 is the Drosophila CENP-A assembly factor. J Cell Biol. 2014 Feb 3;204(3):313-29. doi: 10.1083/jcb.201305036. Epub 2014 Jan 27.

Chen CC, Bowers S, Lipinszki Z, Palladino J, Trusiak S, Bettini E, Rosin L, Przewloka MR, Glover DM, O'Neill RJ, Mellone BG. Establishment of Centromeric Chromatin by the CENP-A Assembly Factor CAL1 Requires FACT-Mediated Transcription. Dev Cell. 2015 Jul 6;34(1):73-84. doi: 10.1016/j.devcel.2015.05.012.

Chen ES, Zhang K, Nicolas E, Cam HP, Zofall M, Grewal SI (2008) Cell cycle control of centromeric repeat transcription and heterochromatin assembly. Nature 451(7179):734–737. doi: 10.1038/nature06561

Chen L, Cai Y, Jin J, Florens L, Swanson SK, Washburn MP, Conaway JW, Conaway RC. Subunit organization of the human INO80 chromatin remodeling complex: an evolutionarily conserved core complex catalyzes ATP-dependent nucleosome remodeling. J Biol Chem. 2011 Apr 1;286(13):11283-9. doi: 10.1074/jbc.M111.222505. Epub 2011 Feb 8.

Chen ZA, Fischer L, Cox J, Rappsilber J\. Quantitative Cross-linking/Mass Spectrometry Using Isotope-labeled Cross-linkers and MaxQuant. Mol Cell Proteomics. 2016 Aug;15(8):2769-78. doi: 10.1074/mcp.M115.056481. Epub 2016 Jun 14.

Cheng H, Bao X, Rao H. The F-box Protein Rcy1 Is Involved in the Degradation of Histone H3 Variant Cse4 and Genome Maintenance. J Biol Chem. 2016 May 6;291(19):10372-7. doi: 10.1074/jbc.M115.701813. Epub 2016 Mar 14.

Cheng H, Bao X, Gan X, Luo S, Rao H. Multiple E3s promote the degradation of histone H3 variant Cse4. Sci Rep. 2017 Aug 17;7(1):8565. doi: 10.1038/s41598-017-08923-w.

Cheutin T, Gorski SA, May KM, Singh PB, Misteli T. In vivo dynamics of Swi6 in yeast: evidence for a stochastic model of heterochromatin. Mol Cell Biol. 2004 Apr;24(8):3157-67.

Choi ES, Shin JA, Kim HS, Jang YK. Dynamic regulation of replication independent deposition of histone H3 in fission yeast. Nucleic Acids Res. 2005 Dec 15;33(22):7102-10. Print 2005.

Choi ES, Strålfors A, Castillo AG, Durand-Dubief M, Ekwall K, Allshire RC. Identification of noncoding transcripts from within CENP-A chromatin at fission yeast centromeres. J Biol Chem. 2011 Jul 1;286(26):23600-7. doi: 10.1074/jbc.M111.228510. Epub 2011 Apr 28.

Choi ES, Strålfors A, Catania S, et al. Factors That Promote H3 Chromatin Integrity during Transcription Prevent Promiscuous Deposition of CENP-A^{Cnp}1 in Fission Yeast. Sullivan BA, ed. PLoS Genetics. 2012;8(9):e1002985. doi:10.1371/journal.pgen.1002985.

Choi ES, Cheon Y, Kang K, Lee D. The Ino80 complex mediates epigenetic centromere propagation via active removal of histone H3. Nat Commun. 2017 Sep 13;8(1):529. doi: 10.1038/s41467-017-00704-3.

Chu F, Thornton DT, Nguyen HT. Chemical cross-linking in the structural analysis of protein assemblies. Methods. 2018 Jul 15;144:53-63. doi: 10.1016/j.ymeth.2018.05.023. Epub 2018 May 30.

Chueh AC, Northrop EL, Brettingham-Moore KH, Choo KH, Wong LH (2009) LINE retrotransposon RNA is an essential structural and functional epigenetic component of a core neocentromeric chromatin. PLoS Genet 5(1):e1000354.

Clapier CR, Cairns BR. The biology of chromatin remodeling complexes. Annu Rev Biochem. 2009;78:273-304. doi: 10.1146/annurev.biochem.77.062706.153223.

Clapier CR, Iwasa J, Cairns BR, Peterson CL. Mechanisms of action and regulation of ATP-dependent chromatin-remodelling complexes. Nat Rev Mol Cell Biol. 2017 Jul;18(7):407-422. doi: 10.1038/nrm.2017.26. Epub 2017 May 17.

Clarke L, Carbon J. The structure and function of yeast centromeres. Annu Rev Genet. 1985;19:29-55.

Cleveland DW, Mao Y, Sullivan KF. Centromeres and kinetochores: from epigenetics to mitotic checkpoint signaling. Cell. 2003 Feb 21;112(4):407-21.

Coffman VC, Wu P, Parthun MR, Wu JQ. CENP-A exceeds microtubule attachment sites in centromere clusters of both budding and fission yeast. J Cell Biol. 2011 Nov 14;195(4):563-72. doi: 10.1083/jcb.201106078.

Collins KA, Furuyama S, Biggins S. Proteolysis contributes to the exclusive centromere localization of the yeast Cse4/CENP-A histone H3 variant. Curr Biol. 2004 Nov 9;14(21):1968-72.

Cooke CA, Bazett-Jones DP, Earnshaw WC, Rattner JB Mapping DNA within the mammalian kinetochore. Jcb 1993 , 1 March » 120 (5): 1083

Cottarel G, Shero JH, Hieter P, Hegemann JH. A 125-base-pair CEN6 DNA fragment is sufficient for complete meiotic and mitotic centromere functions in Saccharomyces cerevisiae. Mol Cell Biol. 1989 Aug;9(8):3342-9.

Cox J, and Mann M. MaxQuant enables high peptide identification rates, individualized p.p.b.-range mass accuracies and proteome-wide protein quantification. Nat. Biotechnol. 2008. 26:1367–1372.

Cox J, Neuhauser N, Michalski A, Scheltema RA, Olsen JV, and Mann M. Andromeda: a peptide search engine integrated into the MaxQuant environment. J. Proteome Res.2011. 10:1794–1805.

Cox J, Hein MY, Luber CA, Paron I, Nagaraj N, Mann M. Accurate proteome-wide label-free quantification by delayed normalization and maximal peptide ratio extraction, termed MaxLFQ. Mol.Cell Proteomics 2014. 13(9):2513-2.

Dawe RK, Henikoff S. Centromeres put epigenetics in the driver's seat. Trends Biochem Sci. 2006 Dec;31(12):662-9. Epub 2006 Oct 30.

DeLuca JG, Musacchio A. Structural organization of the kinetochore-microtubule interface. Curr Opin Cell Biol. 2012 Feb;24(1):48-56. doi: 10.1016/j.ceb.2011.11.003. Epub 2011 Dec 10.

Deyter GM, Biggins S. The FACT complex interacts with the E3 ubiquitin ligase Psh1 to prevent ectopic localization of CENP-A. Genes Dev. 2014 Aug 15;28(16):1815-26. doi: 10.1101/gad.243113.114.

Djupedal I, Portoso M, Spåhr H, Bonilla C, Gustafsson CM, Allshire RC, Ekwall K. RNA Pol II subunit Rpb7 promotes centromeric transcription and RNAi-directed chromatin silencing. Genes Dev. 2005 Oct 1;19(19):2301-6.

Dong Q, Yin FX, Gao F, Shen Y, Zhang F, Li Y, He H, Gonzalez M, Yang J, Zhang S, Su M, Chen YH, Li F1#. Ccp1 Homodimer Mediates Chromatin Integrity by Antagonizing CENP-A Loading. Mol Cell. 2016 Oct 6;64(1):79-91. doi: 10.1016/j.molcel.2016.08.022. Epub 2016 Sep 22.

Downey M, Johnson JR, Davey NE, Newton BW, Johnson TL, Galaang S, Seller CA, Krogan N, Toczyski DP Acetylome profiling reveals overlap in the regulation of diverse processes by sirtuins, gcn5, and esa1. Mol Cell Proteomics. 2015 Jan;14(1):162-76. doi: 10.1074/mcp.M114.043141. Epub 2014 Nov 7.

Drinnenberg IA, deYoung D, Henikoff S, Malik HS. Recurrent loss of CenH3 is associated with independent transitions to holocentricity in insects. Elife. 2014 Sep 23;3. doi: 10.7554/eLife.03676

Duda Z, Trusiak S, O'Neill R. Centromere Transcription: Means and Motive. Prog Mol Subcell Biol. 2017;56:257-281. doi: 10.1007/978-3-319-58592-5_11.

Dunleavy EM, Pidoux AL, Monet M, Bonilla C, Richardson W, Hamilton GL, Ekwall K, McLaughlin PJ, Allshire RC. A NASP (N1/N2)-related protein, Sim3, binds CENP-A and is required for its deposition at fission yeast centromeres. Mol Cell. 2007 Dec 28;28(6):1029-44.

Dunleavy EM, Roche D, Tagami H, Lacoste N, Ray-Gallet D, Nakamura Y, Daigo Y, Nakatani Y, Almouzni-Pettinotti G. HJURP is a cell-cycle-dependent maintenance and deposition factor of CENP-A at centromeres. Cell. 2009 May 1;137(3):485-97. doi: 10.1016/j.cell.2009.02.040.

Dunleavy EM, Almouzni G, Karpen GH. H3.3 is deposited at centromeres in S phase as a placeholder for newly assembled CENP-A in G_1 phase. Nucleus. 2011 Mar-Apr;2(2):146-57. doi: 10.4161/nucl.2.2.15211.

Dunleavy EM, Beier NL, Gorgescu W, Tang J, Costes SV, Karpen GH. The cell cycle timing of centromeric chromatin assembly in Drosophila meiosis is distinct from mitosis yet requires CAL1 and CENP-C. PLoS Biol. 2012;10(12):e1001460. doi: 10.1371/journal.pbio.1001460. Epub 2012 Dec 27.

Durand-Dubief M, Persson J, Norman U, Hartsuiker E, Ekwall K. Topoisomerase I regulates open chromatin and controls gene expression in vivo. EMBO J. 2010 Jul 7;29(13):2126-34. doi: 10.1038/emboj.2010.109. Epub 2010 Jun 4.

Earnshaw WC, Migeon BR. Three related centromere proteins are absent from the inactive centromere of a stable isodicentric chromosome. Chromosoma. 1985;92(4):290-6.

Earnshaw WC, Rothfield N. Identification of a family of human centromere proteins using autoimmune sera from patients with scleroderma. Chromosoma. 1985;91(3-4):313-21.

Earnshaw WC, Ratrie H 3rd, Stetten G. Visualization of centromere proteins CENP-B and CENP-C on a stable dicentric chromosome in cytological spreads. Chromosoma. 1989 Jun;98(1):1-12.

Eskat A, Deng W, Hofmeister A, Rudolphi S, Emmerth S, Hellwig D, Ulbricht T, Döring V, Bancroft JM, McAinsh AD, Cardoso MC, Meraldi P, Hoischen C, Leonhardt H, Diekmann S. Step-wise assembly, maturation and dynamic behavior of the human CENP-P/O/R/Q/U kinetochore sub-complex. PLoS One. 2012;7(9):e44717. doi: 10.1371/journal.pone.0044717. Epub 2012 Sep 18.

Fabre B, Lambour T, Bouyssié D, Menneteau T, Monsarrat B, Burlet-Schiltz O, Bousquet-Dubouch M-P. . Comparison of label-free quantification methods for the determination of protein complexes subunits stoichiometry. EuPA Open Proteomics 2014. 4:82–86.

Fachinetti D, Logsdon GA, Abdullah A, Selzer EB, Cleveland DW, Black BE. CENP-A Modifications on Ser68 and Lys124 Are Dispensable for Establishment, Maintenance, and Long-Term Function of Human Centromeres. Dev Cell. 2017 Jan 9;40(1):104-113. doi: 10.1016/j.devcel.2016.12.014.

Falk SJ, Guo LY, Sekulic N, Smoak EM, Mani T, Logsdon GA, Gupta K, Jansen LE, Van Duyne GD, Vinogradov SA, Lampson MA, Black BE. Chromosomes. CENP-C reshapes and stabilizes CENP-A nucleosomes at the centromere. Science. 2015 May 8;348(6235):699-703. doi: 10.1126/science.1259308.

Finley D, Ulrich HD, Sommer T, Kaiser P. The ubiquitin-proteasome system of Saccharomyces cerevisiae. Genetics. 2012 Oct;192(2):319-60. doi: 10.1534/genetics.112.140467.

Fleig U, Sen-Gupta M, Hegemann JH. Fission yeast mal2+ is required for chromosome segregation. Mol Cell Biol. 1996 Nov;16(11):6169-77.

Folco HD, Pidoux AL, Urano T, Allshire RC. Heterochromatin and RNAi are required to establish CENP-A chromatin at centromeres. Science. 2008 Jan 4;319(5859):94-7. doi: 10.1126/science.1150944.

Folco HD, Campbell CS, May KM, Espinoza CA, Oegema K, Hardwick KG, Grewal SIS, Desai A. The CENP-A N-tail confers epigenetic stability to centromeres via the CENP-T branch of the CCAN in fission yeast. Curr Biol. 2015 Feb 2;25(3):348-356. doi: 10.1016/j.cub.2014.11.060. Epub 2015 Jan 22.

Foltz DR, Jansen LE, Black BE, Bailey AO, Yates JR, Cleveland DW. The human CENP-A centromeric nucleosome-associated complex. Nat Cell Biol. 2006 May;8(5):458-69. Epub 2006 Apr 16.

Foltz DR, Jansen LE, Bailey AO, Yates JR 3rd, Bassett EA, Wood S, Black BE, Cleveland DW. Centromere-specific assembly of CENP-a nucleosomes is mediated by HJURP. Cell. 2009 May 1;137(3):472-84. doi: 10.1016/j.cell.2009.02.039.

Fujita Y, Hayashi T, Kiyomitsu T, Toyoda Y, Kokubu A, Obuse C, Yanagida M. Priming of centromere for CENP-A recruitment by human hMis18alpha, hMis18beta, and M18BP1. Dev Cell. 2007 Jan;12(1):17-30.

Fukagawa T, Pendon C, Morris J, Brown W. CENP-C is necessary but not sufficient to induce formation of a functional centromere. EMBO J. 1999 Aug 2;18(15):4196-209.

Fukagawa T, Mikami Y, Nishihashi A, Regnier V, Haraguchi T, Hiraoka Y, Sugata N, Todokoro K, Brown W, Ikemura T. CENP-H, a constitutive centromere component, is required for centromere targeting of CENP-C in vertebrate cells. EMBO J. 2001 Aug 15;20(16):4603-17.

Fukagawa T, Earnshaw WC. The centromere: chromatin foundation for the kinetochore machinery. Dev Cell. 2014 Sep 8;30(5):496-508. doi: 10.1016/j.devcel.2014.08.016.

Funabiki H, Hagan I, Uzawa S, Yanagida M Cell cycle-dependent specific positioning and clustering of centromeres and telomeres in fission yeast. J Cell Biol. 1993 Jun;121(5):961-76.

Fussner E, Ching RW, Bazett-Jones DP. Living without 30nm chromatin fibers. Trends Biochem Sci. 2011 Jan;36(1):1-6. doi: 10.1016/j.tibs.2010.09.002.

Gal C, Murton HE, Subramanian L, Whale AJ, Moore KM, Paszkiewicz K, Codlin S, Bähler J, Creamer KM, Partridge JF, Allshire RC, Kent NA, Whitehall SK. Abo1, a conserved bromodomain AAA-ATPase, maintains global nucleosome occupancy and organisation. EMBO Rep. 2016 Jan;17(1):79-93. doi: 10.15252/embr.201540476. Epub 2015 Nov 18.

Garavís M, Méndez-Lago M, Gabelica V, Whitehead SL, González C, Villasante A. The structure of an endogenous Drosophila centromere reveals the prevalence of tandemly repeated sequences able to form i-motifs. Sci Rep. 2015 Aug 20;5:13307. doi: 10.1038/srep13307.

Gascoigne KE, Takeuchi K, Suzuki A, Hori T, Fukagawa T, Cheeseman IM. Induced ectopic kinetochore assembly bypasses the requirement for CENP-A nucleosomes. Cell. 2011 Apr 29;145(3):410-22. doi: 10.1016/j.cell.2011.03.031.

Gassmann R, Rechtsteiner A, Yuen KW, Muroyama A, Egelhofer T, Gaydos L, Barron F, Maddox P, Essex A, Monen J, Ercan S, Lieb JD, Oegema K, Strome S, Desai A. An inverse relationship to germline transcription defines centromeric chromatin in C. elegans. Nature. 2012 Apr 8;484(7395):534-7. doi: 10.1038/nature10973.

Gerhold CB, Gasser SM. INO80 and SWR complexes: relating structure to function in chromatin remodeling. Trends Cell Biol. 2014 Nov;24(11):619-31. doi: 10.1016/j.tcb.2014.06.004. Epub 2014 Jul 31.

Gibcus JH, Dekker J. The hierarchy of the 3D genome. Mol Cell. 2013 Mar 7;49(5):773-82. doi: 10.1016/j.molcel.2013.02.011.

Gkikopoulos T, Singh V, Tsui K, Awad S, Renshaw MJ, Scholfield P, Barton GJ, Nislow C, Tanaka TU, Owen-Hughes T. The SWI/SNF complex acts to constrain distribution of the centromeric histone variant Cse4. EMBO J. 2011 May 18;30(10):1919-27. doi: 10.1038/emboj.2011.112. Epub 2011 Apr 19.

Gonen S, Akiyoshi B, Iadanza MG, Shi D, Duggan N, Biggins S, Gonen T. The structure of purified kinetochores reveals multiple microtubule-attachment sites. Nat Struct Mol Biol. 2012 Sep;19(9):925-9. doi: 10.1038/nsmb.2358. Epub 2012 Aug 12.

Gong Z, Wu Y, Koblízková A, Torres GA, Wang K, Iovene M, Neumann P, Zhang W, Novák P, Buell CR, Macas J, Jiang J. Repeatless and repeat-based centromeres in potato: implications for centromere evolution. Plant Cell. 2012 Sep;24(9):3559-74. doi: 10.1105/tpc.112.100511. Epub 2012 Sep 11.

Gonzalez M, He H, Dong Q, Sun S, Li F. Ectopic centromere nucleation by CENP--a in fission yeast. Genetics. 2014 Dec;198(4):1433-46. doi: 10.1534/genetics.114.171173. Epub 2014 Oct 7.

Grenfell AW, Heald R, Strzelecka M. Mitotic noncoding RNA processing promotes kinetochore and spindle assembly in Xenopus. J Cell Biol. 2016 Jul 18;214(2):133-41. doi: 10.1083/jcb.201604029. Epub 2016 Jul 11.

Grewal SI, Bonaduce MJ, Klar AJ. Histone deacetylase homologs regulate epigenetic inheritance of transcriptional silencing and chromosome segregation in fission yeast. Genetics. 1998 Oct;150(2):563-76.

Grewal SI, Jia S. Heterochromatin revisited.Nat Rev Genet. 2007 Jan;8(1):35-46.

Gribun A, Cheung KL, Huen J, Ortega J, Houry WA. Yeast Rvb1 and Rvb2 are ATP-dependent DNA helicases that form a heterohexameric complex. J Mol Biol. 2008 Mar 7;376(5):1320-33. doi: 10.1016/j.jmb.2007.12.049. Epub 2008 Jan 3.

Gross S, Catez F, Masumoto H, Lomonte P. Centromere architecture breakdown induced by the viral E3 ubiquitin ligase ICP0 protein of herpes simplex virus type 1. PLoS One. 2012;7(9):e44227. doi: 10.1371/journal.pone.0044227. Epub 2012 Sep 20.

Hahnenberger KM, Baum MP, Polizzi CM, Carbon J, Clarke L. Construction of functional artificial minichromosomes in the fission yeast Schizosaccharomyces pombe. Proc Natl Acad Sci U S A. 1989 Jan;86(2):577-81.

Harrington JJ, Van Bokkelen G, Mays RW, Gustashaw K, Willard HF. Formation of de novo centromeres and construction of first-generation human artificial microchromosomes. Nat Genet. 1997 Apr;15(4):345-55.

Hayashi A, Asakawa H, Haraguchi T, Hiraoka Y. Reconstruction of the kinetochore during meiosis in fission yeast Schizosaccharomyces pombe. Mol Biol Cell. 2006 Dec;17(12):5173-84. Epub 2006 Oct 11.

Hayashi M, Katou Y, Itoh T, Tazumi A, Yamada Y, Takahashi T, Nakagawa T, Shirahige K, Masukata H. Genome-wide localization of pre-RC sites and identification of replication origins in fission yeast. EMBO J. 2007 Mar 7;26(5):1327-39. Epub 2007 Feb 15.

Hayashi T, Fujita Y, Iwasaki O, Adachi Y, Takahashi K, Yanagida M. Mis16 and Mis18 are required for CENP-A loading and histone deacetylation at centromeres. Cell. 2004 Sep 17;118(6):715-29.

Hayashi T, Ebe M, Nagao K, Kokubu A, Sajiki K, Yanagida M. Schizosaccharomyces pombe centromere protein Mis19 links Mis16 and Mis18 to recruit CENP-A through interacting with NMD factors and the SWI/SNF complex. Genes Cells. 2014 Jul;19(7):541-54. doi: 10.1111/gtc.12152. Epub 2014 Apr 29.

He Q, Johnston J, Zeitlinger J. ChIP-nexus enables improved detection of in vivo transcription factor binding footprints. Nat Biotechnol. 2015 Apr;33(4):395-401. doi: 10.1038/nbt.3121. Epub 2015 Mar 9.

Henikoff S, Ahmad K, Malik HS. The centromere paradox: stable inheritance with rapidly evolving DNA. Science. 2001 Aug 10;293(5532):1098-102.

Henikoff S, Dalal Y. Centromeric chromatin: what makes it unique? Curr Opin Genet Dev. 2005 Apr;15(2):177-84.

Hennrich ML, Gavin AC. Quantitative mass spectrometry of posttranslational modifications: keys to confidence. Sci Signal. 2015 Apr 7;8(371):re5. doi: 10.1126/scisignal.aaa6466.

Hershko A. Ubiquitin: roles in protein modification and breakdown. Cell. 1983 Aug;34(1):11-2.

Heun P, Erhardt S, Blower MD, Weiss S, Skora AD, Karpen GH. Mislocalization of the Drosophila centromere-specific histone CID promotes formation of functional ectopic kinetochores. Dev Cell. 2006 Mar;10(3):303-15.

Hewawasam GS, Shivaraju M, Mattingly M, Venkatesh S, Martin-Brown S, Florens L, Workman JL, Gerton JL. Psh1 is an E3 ubiquitin ligase that targets the centromeric histone variant Cse4. Mol Cell. 2010 Nov 12;40(3):444-54. doi: 10.1016/j.molcel.2010.10.014.

Hewawasam GS, Mattingly M, Venkatesh S, Zhang Y, Florens L, Workman JL, Gerton JL. Phosphorylation by casein kinase 2 facilitates Psh1 protein-assisted degradation of Cse4 protein. J Biol Chem. 2014 Oct 17;289(42):29297-309. doi: 10.1074/jbc.M114.580589. Epub 2014 Sep 2.

Hildebrand EM, Biggins S. Regulation of Budding Yeast CENP-A levels Prevents Misincorporation at Promoter Nucleosomes and Transcriptional Defects. PLoS Genet. 2016 Mar 16;12(3):e1005930. doi: 10.1371/journal.pgen.1005930. eCollection 2016 Mar.

Hinshaw SM, Harrison SC. An Iml3-Chl4 heterodimer links the core centromere to factors required for accurate chromosome segregation. Cell Rep. 2013 Oct 17;5(1):29-36. doi: 10.1016/j.celrep.2013.08.036. Epub 2013 Sep 26.

Hochstrasser M Origin and function of ubiquitin-like proteins. Nature. 2009 Mar 26;458(7237):422-9. doi: 10.1038/nature07958.

Hogan CJ, Aligianni S, Durand-Dubief M, Persson J, Will WR, Webster J, Wheeler L, Mathews CK, Elderkin S, Oxley D, Ekwall K, Varga-Weisz PD. Fission yeast Iec1-ino80-mediated nucleosome eviction regulates nucleotide and phosphate metabolism. Mol Cell Biol. 2010 Feb;30(3):657-74. doi: 10.1128/MCB.01117-09. Epub 2009 Nov 23.

Hoischen C, Yavas S, Wohland T, Diekmann S. CENP-C/H/I/K/M/T/W/N/L and hMis12 but not CENP-S/X participate in complex formation in the nucleoplasm of living human interphase cells outside centromeres. PLoS One. 2018 Mar 6;13(3):e0192572. doi: 10.1371/journal.pone.0192572. eCollection 2018.

Holding AN. XL-MS: Protein cross-linking coupled with mass spectrometry. Methods. 2015 Nov 1;89:54-63. doi: 10.1016/j.ymeth.2015.06.010. Epub 2015 Jun 12.

Hori T, Amano M, Suzuki A, Backer CB, Welburn JP, Dong Y, McEwen BF, Shang WH, Suzuki E, Okawa K, Cheeseman IM, Fukagawa T. CCAN makes multiple contacts with centromeric DNA to provide distinct pathways to the outer kinetochore. Cell. 2008 Dec 12;135(6):1039-52. doi: 10.1016/j.cell.2008.10.019.

Hori T, Okada M, Maenaka K, Fukagawa T. CENP-O class proteins form a stable complex and are required for proper kinetochore function. Mol Biol Cell. 2008 Mar;19(3):843-54. Epub 2007 Dec 19.

Hori T, Shang WH, Takeuchi K, Fukagawa T. The CCAN recruits CENP-A to the centromere and forms the structural core for kinetochore assembly. J Cell Biol. 2013 Jan 7;200(1):45-60. doi: 10.1083/jcb.201210106. Epub 2012 Dec 31.

Howman EV, Fowler KJ, Newson AJ, Redward S, MacDonald AC, Kalitsis P, Choo KH. Early disruption of centromeric chromatin organization in centromere protein A (Cenpa) null mice. Proc Natl Acad Sci U S A. 2000 Feb 1;97(3):1148-53.

Hsieh TH, Weiner A, Lajoie B, Dekker J, Friedman N, Rando OJ. Mapping Nucleosome Resolution Chromosome Folding in Yeast by Micro-C. Cell. 2015 Jul 2;162(1):108-19. doi: 10.1016/j.cell.2015.05.048. Epub 2015 Jun 25.

Hsu JM, Huang J, Meluh PB, Laurent BC. The yeast RSC chromatin-remodeling complex is required for kinetochore function in chromosome segregation. Mol Cell Biol. 2003 May;23(9):3202-15.

Hua S, Wang Z, Jiang K, Huang Y, Ward T, Zhao L, Dou Z, Yao X. CENP-U cooperates with Hec1 to orchestrate kinetochore-microtubule attachment. J Biol Chem. 2011 Jan 14;286(2):1627-38. doi: 10.1074/jbc.M110.174946. Epub 2010 Nov 5.

Hübner, M. R., & Spector, D. L. (2010). Chromatin Dynamics. Annual Review of Biophysics, 39, 471–489. http://doi.org/10.1146/annurev.biophys.093008.131348

Huis in 't Veld, P.J.; Jeganathan, S.; Petrovic, A.; John, J.; Singh, P.; Weissmann, F.; Bange, T.; Musacchio, A. Molecular basis of outer kinetochore assembly on cenp-t. eLife 2016.

Ishihama, Y., J. Rappsilber, J.S. Andersen, and M. Mann. 2002. Microcolumns with self-assembled particle frits for proteomics. J. Chromatogr. A. 979:233–239

Ishii K, Ogiyama Y, Chikashige Y, Soejima S, Masuda F, Kakuma T, Hiraoka Y, Takahashi K. Heterochromatin integrity affects chromosome reorganization after centromere dysfunction. Science. 2008 Aug 22;321(5892):1088-91. doi: 10.1126/science.1158699.

Jae Yoo E, Kyu Jang Y, Ae Lee M, Bjerling P, Bum Kim J, Ekwall K, Hyun Seong R, Dai Park S. Hrp3, a chromodomain helicase/ATPase DNA binding protein, is required for heterochromatin silencing in fission yeast. Biochem Biophys Res Commun. 2002 Jul 26;295(4):970-4.

Jansen LE, Black BE, Foltz DR, Cleveland DW. Propagation of centromeric chromatin requires exit from mitosis. J Cell Biol. 2007 Mar 12;176(6):795-805. Epub 2007 Mar 5.

Jin QW, Pidoux AL, Decker C, Allshire RC, Fleig U. The mal2p protein is an essential component of the fission yeast centromere. Mol Cell Biol. 2002 Oct;22(20):7168-83.

Kagansky A, Folco HD, Almeida R, Pidoux AL, Boukaba A, Simmer F, Urano T, Hamilton GL, Allshire RC. Synthetic heterochromatin bypasses RNAi and centromeric repeats to establish functional centromeres. Science. 2009 Jun 26;324(5935):1716-9. doi: 10.1126/science.1172026.

Kapoor P, Chen M, Winkler DD, Luger K, Shen X. Evidence for monomeric actin function in INO80 chromatin remodeling. Nat Struct Mol Biol. 2013 Apr;20(4):426-32. doi: 10.1038/nsmb.2529. Epub 2013 Mar 24.

Karpen GH, Allshire RC. The case for epigenetic effects on centromere identity and function. Trends Genet. 1997 Dec;13(12):489-96.

Kasinathan S, Henikoff S. Non-B-Form DNA Is Enriched at Centromeres. Mol Biol Evol. 2018 Apr 1;35(4):949-962. doi: 10.1093/molbev/msy010.

Kato H, Jiang J, Zhou BR, Rozendaal M, Feng H, Ghirlando R, Xiao TS, Straight AF, Bai Y. A conserved mechanism for centromeric nucleosome recognition by centromere protein CENP-C.Science. 2013 May 31;340(6136):1110-3. doi: 10.1126/science.1235532.

Kato T1, Sato N, Hayama S, Yamabuki T, Ito T, Miyamoto M, Kondo S, Nakamura Y, Daigo Y. Activation of Holliday junction recognizing protein involved in the chromosomal stability and immortality of cancer cells. Cancer Res. 2007 Sep 15;67(18):8544-53. Epub 2007 Sep 6.

Keller C, Adaixo R, Stunnenberg R, Woolcock KJ, Hiller S, Bühler M. HP1(Swi6) mediates the recognition and destruction of heterochromatic RNA transcripts. Mol Cell. 2012 Jul 27;47(2):215-27. doi: 10.1016/j.molcel.2012.05.009. Epub 2012 Jun 7.

Ketel C, Wang HS, McClellan M, Bouchonville K, Selmecki A, Lahav T, Gerami-Nejad M, Berman J. Neocentromeres form efficiently at multiple possible loci in Candida albicans. PLoS Genet. 2009 Mar;5(3):e1000400. doi: 10.1371/journal.pgen.1000400. Epub 2009 Mar 6.

Kettenbach AN, Deng L, Wu Y, Baldissard S, Adamo ME, Gerber SA, Moseley JB. Quantitative phosphoproteomics reveals pathways for coordination of cell growth and division by the conserved fission yeast kinase pom1. Mol Cell Proteomics. 2015 May;14(5):1275-87. doi: 10.1074/mcp.M114.045245. Epub 2015 Feb 26.

Kim SM, Dubey DD, Huberman JA. Early-replicating heterochromatin. Genes Dev. 2003 Feb 1;17(3):330-5.

Klare K, Weir JR, Basilico F, Zimniak T, Massimiliano L, Ludwigs N, Herzog F, Musacchio A. CENP-C is a blueprint for constitutive centromere-associated network assembly within human kinetochores. J Cell Biol. 2015 Jul 6;210(1):11-22. doi: 10.1083/jcb.201412028. Epub 2015 Jun 29.

Kline SL, Cheeseman IM, Hori T, Fukagawa T, Desai A. The human Mis12 complex is required for kinetochore assembly and proper chromosome segregation. J Cell Biol. 2006 Apr 10;173(1):9-17. Epub 2006 Apr 3.

Koo DH, Zhao H, Jiang J. Chromosome Res. 2016 doi: 10.1007/s10577-016-9537-5

Kops GJ, Weaver BA, Cleveland DW. On the road to cancer: aneuploidy and the mitotic checkpoint. Nat Rev Cancer. 2005 Oct;5(10):773-85.

Kornberg, R. D. Chromatin structure: A repeating unit of histones and DNA. Science. 1974 184, 868–871

Kornberg, R. D. and Lorch Y. Chromatin Structure and Transcription. Annu. Rev. Cell Biol. 1992. 8:563-87

Koutelou E, Hirsch CL, Dent SY. Multiple faces of the SAGA complex. Curr Opin Cell Biol. 2010 Jun;22(3):374-82. doi: 10.1016/j.ceb.2010.03.005. Epub 2010 Apr 2.

Kouzarides T. Chromatin modifications and their function. Cell. 2007 Feb 23;128(4):693-705.

Kunitoku N, Sasayama T, Marumoto T, Zhang D, Honda S, Kobayashi O, Hatakeyama K, Ushio Y, Saya H, Hirota T. Kunitoku N1, Sasayama T, Marumoto T, Zhang D, Honda S, Kobayashi O, Hatakeyama K, Ushio Y, Saya H, Hirota T. Dev Cell. 2003 Dec;5(6):853-64.

Lando D, Endesfelder U, Berger H, Subramanian L, Dunne PD, McColl J, Klenerman D, Carr AM, Sauer M, Allshire RC, Heilemann M, Laue ED. Quantitative single-molecule microscopy reveals that CENP-

A(Cnp1) deposition occurs during G2 in fission yeast. Open Biol. 2012 Jul;2(7):120078. doi: 10.1098/rsob.120078.

Lechner J, Carbon J.A 240 kd multisubunit protein complex, CBF3, is a major component of the budding yeast centromere. Cell. 1991 Feb 22;64(4):717-25.

Lee SY, Rozenzhak S, Russell P. γH2A-Binding Protein Brc1 Affects Centromere Function in Fission Yeast. Molecular and Cellular Biology. 2013;33(7):1410-1416. doi:10.1128/MCB.01654-12.

Lermontova I, Schubert V, Fuchs J, Klatte S, Macas J, Schubert I. Loading of Arabidopsis centromeric histone CENH3 occurs mainly during G2 and requires the presence of the histone fold domain. Plant Cell. 2006 Oct;18(10):2443-51. Epub 2006 Oct 6.

Li B, Carey M, Workman JL. The role of chromatin during transcription. Cell. 2007 Feb 23;128(4):707-19.

Li G, Reinberg D. Chromatin higher-order structures and gene regulation. Curr Opin Genet Dev. 2011 Apr;21(2):175-86. doi: 10.1016/j.gde.2011.01.022. Epub 2011 Feb 20.

Lidsky PV, Sprenger F, Lehner CF. Distinct modes of centromere protein dynamics during cell cycle progression in Drosophila S2R+ cells. J Cell Sci. 2013 Oct 15;126(Pt 20):4782-93. doi: 10.1242/jcs.134122. Epub 2013 Aug 13.

Liu F, Heck AJ. Interrogating the architecture of protein assemblies and protein interaction networks by cross-linking mass spectrometry. Curr Opin Struct Biol. 2015 Dec;35:100-8. doi: 10.1016/j.sbi.2015.10.006. Epub 2015 Nov 23.

Liu X, McLeod I, Anderson S, Yates JR 3rd, He X. Molecular analysis of kinetochore architecture in fission yeast. EMBO J. 2005 Aug 17;24(16):2919-30. Epub 2005 Aug 4.

Locke DP, Hillier LW, Warren WC, Worley KC, Nazareth LV, Muzny DM, Yang SP, Wang Z, Chinwalla AT, Minx P, Mitreva M, Cook L, Delehaunty KD, Fronick C, Schmidt H, Fulton LA, Fulton RS, Nelson JO, Magrini V, Pohl C, Graves TA, Markovic C, Cree A, Dinh HH, Hume J, Kovar CL, Fowler GR, Lunter G, Meader S, Heger A, Ponting CP, Marques-Bonet T, Alkan C, Chen L, Cheng Z, Kidd JM, Eichler EE, White S, Searle S, Vilella AJ, Chen Y, Flicek P, Ma J, Raney B, Suh B, Burhans R, Herrero J, Haussler D, Faria R, Fernando O, Darré F, Farré D, Gazave E, Oliva M, Navarro A, Roberto R, Capozzi O, Archidiacono N, Della Valle G, Purgato S, Rocchi M, Konkel MK, Walker JA, Ullmer B, Batzer MA, Smit AF, Hubley R, Casola C, Schrider DR, Hahn MW, Quesada V, Puente XS, Ordoñez GR, López-Otín C, Vinar T, Brejova B, Ratan A, Harris RS, Miller W, Kosiol C, Lawson HA, Taliwal V, Martins AL, Siepel A, Roychoudhury A, Ma X, Degenhardt J, Bustamante CD, Gutenkunst RN, Mailund T, Dutheil JY, Hobolth A, Schierup MH, Ryder OA, Yoshinaga Y, de Jong PJ, Weinstock GM, Rogers J, Mardis ER, Gibbs RA, Wilson RK. Comparative and demographic analysis of orang-utan genomes. Nature. 2011 Jan 27;469(7331):529-33. doi: 10.1038/nature09687.

Lomonte P, Sullivan KF, Everett RD. Degradation of nucleosome-associated centromeric histone H3-like protein CENP-A induced by herpes simplex virus type 1 protein ICP0. J Biol Chem. 2001 Feb 23;276(8):5829-35. Epub 2000 Oct 26.

Lonskaya I, Potaman VN, Shlyakhtenko LS, Oussatcheva EA, Lyubchenko YL, Soldatenkov VA. Regulation of poly(ADP-ribose) polymerase-1 by DNA structure-specific binding. J Biol Chem. 2005 Apr 29;280(17):17076-83. Epub 2005 Feb 28.

Luger K, Mäder AW, Richmond RK, Sargent DF, Richmond TJ. Crystal structure of the nucleosome core particle at 2.8 A resolution. Nature. 1997 Sep 18;389(6648):251-60.

Luger K, Richmond TJ. DNA binding within the nucleosome core. Curr Opin Struct Biol. 1998 Feb;8(1):33-40.

Maine GT, Sinha P, Tye BK. Mutants of S. cerevisiae defective in the maintenance of minichromosomes. Genetics. 1984 Mar;106(3):365-85.

Malik HS, Henikoff S. Conflict begets complexity: the evolution of centromeres. Curr Opin Genet Dev. 2002 Dec;12(6):711-8.

Malik HS, Henikoff S. Major evolutionary transitions in centromere complexity. Cell. 2009 Sep 18;138(6):1067-82. doi: 10.1016/j.cell.2009.08.036.

Marti TM, Mansour AA, Lehmann E, Fleck O. Different frameshift mutation spectra in non-repetitive DNA of MutSalpha- and MutLalpha-deficient fission yeast cells. DNA Repair (Amst). 2003 May 13;2(5):571-80.

Matsuyama A, Arai R, Yashiroda Y, Shirai A, Kamata A, Sekido S, Kobayashi Y, Hashimoto A, Hamamoto M, Hiraoka Y, Horinouchi S, Yoshida M. ORFeome cloning and global analysis of protein localization in the fission yeast Schizosaccharomyces pombe. Nat Biotechnol. 2006 Jul;24(7):841-7. Epub 2006 Jun 25.

Maundrell K. nmt1 of fission yeast. A highly transcribed gene completely repressed by thiamine. J Biol Chem. 1990 Jul 5;265(19):10857-64.

McGrew J, Diehl B, Fitzgerald-Hayes M. Single base-pair mutations in centromere element III cause aberrant chromosome segregation in Saccharomyces cerevisiae. Mol Cell Biol. 1986 Feb;6(2):530-8.

McKinley KL, Cheeseman IM. Polo-like kinase 1 licenses CENP-A deposition at centromeres. Cell. 2014 Jul 17;158(2):397-411. doi: 10.1016/j.cell.2014.06.016.

McKinley KL, Sekulic N2, Guo LY2, Tsinman T3, Black BE2, Cheeseman IM4. The CENP-L-N Complex Forms a Critical Node in an Integrated Meshwork of Interactions at the Centromere-Kinetochore Interface. Mol Cell. 2015 Dec 17;60(6):886-98. doi: 10.1016/j.molcel.2015.10.027. Epub 2015 Nov 19.

McKinley KL, Cheeseman IM. The molecular basis for centromere identity and function. Nat Rev Mol Cell Biol. 2016 Jan;17(1):16-29. doi: 10.1038/nrm.2015.5. Epub 2015 Nov 25.

McNulty SM, Sullivan LL, Sullivan BA. Human Centromeres Produce Chromosome-Specific and Array-Specific Alpha Satellite Transcripts that Are Complexed with CENP-A and CENP-C. Dev Cell. 2017 Aug 7;42(3):226-240.e6. doi: 10.1016/j.devcel.2017.07.001.

Mellone BG, Allshire RC. Stretching it: putting the CENP-A in centromere. Curr Opin Genet Dev. 2003 Apr;13(2):191-8.

Mellone BG, Grive KJ, Shteyn V, Bowers SR, Oderberg I, Karpen GH. Assembly of Drosophila centromeric chromatin proteins during mitosis. PLoS Genet. 2011 May;7(5):e1002068. doi: 10.1371/journal.pgen.1002068. Epub 2011 May 12.

Melters DP, Paliulis LV, Korf IF, Chan SW. Holocentric chromosomes: convergent evolution, meiotic adaptations, and genomic analysis. Chromosome Res. 2012 Jul;20(5):579-93. doi: 10.1007/s10577-012-9292-1.

Mendiburo MJ, Padeken J, Fülöp S, Schepers A, Heun P. Drosophila CENH3 is sufficient for centromere formation. Science. 2011 Nov 4;334(6056):686-90. doi: 10.1126/science.1206880.

Merkley ED, Rysavy S, Kahraman A, Hafen RP, Daggett V, Adkins JN. Distance restraints from crosslinking mass spectrometry: mining a molecular dynamics simulation database to evaluate lysine-lysine distances. Protein Sci. 2014 Jun;23(6):747-59. doi: 10.1002/pro.2458. Epub 2014 Apr 3.

Metzger MB, Scales JL, Dunklebarger MF, Weissman AM. The Ubiquitin Ligase (E3) Psh1p Is Required for Proper Segregation of both Centromeric and Two-Micron Plasmids in Saccharomyces cerevisiae. G3 (Bethesda). 2017 Nov 6;7(11):3731-3743. doi: 10.1534/g3.117.300227.

Milks KJ, Moree B, Straight AF. Dissection of CENP-C-directed centromere and kinetochore assembly. Mol Biol Cell. 2009 Oct;20(19):4246-55. doi: 10.1091/mbc.E09-05-0378. Epub 2009 Jul 29.

Mills WE, Spence JM, Fukagawa T, Farr CJ. Site-Specific Cleavage by Topoisomerase 2: A Mark of the Core Centromere. Int J Mol Sci. 2018 Feb 10;19(2). pii: E534. doi: 10.3390/ijms19020534.

Molina O, Vargiu G, Abad MA, Zhiteneva A, Jeyaprakash AA, Masumoto H, Kouprina N, Larionov V, Earnshaw WC.Epigenetic engineering reveals a balance between histone modifications and transcription in kinetochore maintenance. Nat Commun. 2016 Nov 14;7:13334. doi: 10.1038/ncomms13334.

Monahan BJ, Villén J, Marguerat S, Bähler J, Gygi SP, Winston F. Fission yeast SWI/SNF and RSC complexes show compositional and functional differences from budding yeast. Nat Struct Mol Biol. 2008 Aug;15(8):873-80. doi: 10.1038/nsmb.1452. Epub 2008 Jul 11.

Moree B, Meyer CB, Fuller CJ, Straight AF. CENP-C recruits M18BP1 to centromeres to promote CENP-A chromatin assembly. J Cell Biol. 2011 Sep 19;194(6):855-71. doi: 10.1083/jcb.201106079. Epub 2011 Sep 12.

Moreno-Moreno O, Torras-Llort M, Azorín F. Proteolysis restricts localization of CID, the centromere-specific histone H3 variant of Drosophila, to centromeres. Nucleic Acids Res. 2006;34(21):6247-55. Epub 2006 Nov 7.

Moreno-Moreno O, Medina-Giró S, Torras-Llort M, Azorín F. The F box protein partner of paired regulates stability of Drosophila centromeric histone H3, CenH3(CID). Curr Biol. 2011 Sep 13;21(17):1488-93. doi: 10.1016/j.cub.2011.07.041. Epub 2011 Aug 25.

Moroi Y, Peebles C, Fritzler MJ, Steigerwald J, Tan EM. Autoantibody to centromere (kinetochore) in scleroderma sera. Proc Natl Acad Sci U S A. 1980 Mar;77(3):1627-31.

Moroi Y, Hartman AL, Nakane PK, Tan EM. Distribution of kinetochore (centromere) antigen in mammalian cell nuclei. J Cell Biol. 1981 Jul;90(1):254-9.

Musacchio A, Desai A. A Molecular View of Kinetochore Assembly and Function. Biology (Basel). 2017 Jan 24;6(1). pii: E5. doi: 10.3390/biology6010005.

Nakagawa H, Lee JK, Hurwitz J, Allshire RC, Nakayama J, Grewal SI, Tanaka K, Murakami Y. Fission yeast CENP-B homologs nucleate centromeric heterochromatin by promoting heterochromatin-specific histone tail modifications. Genes Dev. 2002 Jul 15;16(14):1766-78.

Nakano M, Cardinale S, Noskov VN, Gassmann R, Vagnarelli P, Kandels-Lewis S, Larionov V, Earnshaw WC, Masumoto H. Inactivation of a human kinetochore by specific targeting of chromatin modifiers. Dev Cell. 2008 Apr;14(4):507-22. doi: 10.1016/j.devcel.2008.02.001.

Nakayama KI, Nakayama K. Ubiquitin ligases: cell-cycle control and cancer. Nat Rev Cancer. 2006 May;6(5):369-81.

Nardi IK, Zasadzińska E, Stellfox ME, Knippler CM, Foltz DR. Licensing of Centromeric Chromatin Assembly through the Mis18α-Mis18β Heterotetramer. Mol Cell. 2016 Mar 3;61(5):774-787. doi: 10.1016/j.molcel.2016.02.014.

Natsume T, Tsutsui Y, Sutani T, Dunleavy EM, Pidoux AL, Iwasaki H, Shirahige K, Allshire RC, Yamao F. A DNA polymerase alpha accessory protein, Mcl1, is required for propagation of centromere structures in fission yeast. PLoS One. 2008 May 21;3(5):e2221. doi: 10.1371/journal.pone.0002221.

Niikura Y, Kitagawa R, Ogi H, Abdulle R, Pagala V, Kitagawa K. CENP-A K124 Ubiquitylation Is Required for CENP-A Deposition at the Centromere. Dev Cell. 2015 Mar 9;32(5):589-603. doi: 10.1016/j.devcel.2015.01.024. Epub 2015 Feb 26.

Nishihashi A, Haraguchi T, Hiraoka Y, Ikemura T, Regnier V, Dodson H, Earnshaw WC, Fukagawa T. CENP-I is essential for centromere function in vertebrate cells. Dev Cell. 2002 Apr;2(4):463-76.

Nishino T, Takeuchi K, Gascoigne KE, Suzuki A, Hori T, Oyama T, Morikawa K, Cheeseman IM, Fukagawa T. CENP-T-W-S-X forms a unique centromeric chromatin structure with a histone-like fold. Cell. 2012 Feb 3;148(3):487-501. doi: 10.1016/j.cell.2011.11.061.

Nonaka N, Kitajima T, Yokobayashi S, Xiao G, Yamamoto M, Grewal SI, Watanabe Y. Recruitment of cohesin to heterochromatic regions by Swi6/HP1 in fission yeast. Nat Cell Biol. 2002 Jan;4(1):89-93

Norman-Axelsson U, Durand-Dubief M, Prasad P, Ekwall K. DNA topoisomerase III localizes to centromeres and affects centromeric CENP-A levels in fission yeast. PLoS Genet. 2013;9(3):e1003371. doi: 10.1371/journal.pgen.1003371. Epub 2013 Mar 14.

Obuse C, Yang H, Nozaki N, Goto S, Okazaki T, Yoda K. Proteomics analysis of the centromere complex from HeLa interphase cells: UV-damaged DNA binding protein 1 (DDB-1) is a component of the CEN-complex, while BMI-1 is transiently co-localized with the centromeric region in interphase. Genes Cells. 2004 Feb;9(2):105-20.

Ogbadoyi E, Ersfeld K, Robinson D, Sherwin T, Gull K. Architecture of the Trypanosoma brucei nucleus during interphase and mitosis. Chromosoma. 2000 Mar;108(8):501-13.

Ohkuni K, Kitagawa K. Endogenous transcription at the centromere facilitates centromere activity in budding yeast. Curr Biol. 2011 Oct 25;21(20):1695-703. doi: 10.1016/j.cub.2011.08.056. Epub 2011 Oct 13. In fact, chromosome instability of cbf1Δ cells is suppressed by transcription driven from an artificial promoter suggesting that although not essential, transcription may be involved in ensuring proper centromere function

Ohkuni K, Abdulle R, Kitagawa K. Degradation of centromeric histone H3 variant Cse4 requires the Fpr3 peptidyl-prolyl Cis-Trans isomerase. Genetics. 2014 Apr;196(4):1041-5. doi: 10.1534/genetics.114.161224. Epub 2014 Feb 10.

Ohkuni K, Takahashi Y, Fulp A, Lawrimore J, Au WC, Pasupala N, Levy-Myers R, Warren J, Strunnikov A, Baker RE, Kerscher O, Bloom K, Basrai MA. SUMO-Targeted Ubiquitin Ligase (STUbL) Slx5 regulates proteolysis of centromeric histone H3 variant Cse4 and prevents its mislocalization to euchromatin. Mol Biol Cell. 2016 Mar 9. pii: mbc.E15-12-0827. [Epub ahead of print]

Ohkuni K, Levy-Myers R, Warren J, Au WC, Takahashi Y, Baker RE, Basrai MA. N-terminal Sumoylation of Centromeric Histone H3 Variant Cse4 Regulates Its Proteolysis To Prevent Mislocalization to Non-centromeric Chromatin. G3 (Bethesda). 2018 Mar 28;8(4):1215-1223. doi: 10.1534/g3.117.300419.

Ohzeki J, Shono N, Otake K, Martins NM, Kugou K, Kimura H, Nagase T, Larionov V, Earnshaw WC, Masumoto H. KAT7/HBO1/MYST2 Regulates CENP-A Chromatin Assembly by Antagonizing Suv39h1-Mediated Centromere Inactivation. Dev Cell. 2016 Jun 6;37(5):413-27. doi: 10.1016/j.devcel.2016.05.006.

Okada M, Cheeseman IM, Hori T, Okawa K, McLeod IX, Yates JR 3rd, Desai A, Fukagawa T. The CENP-H-I complex is required for the efficient incorporation of newly synthesized CENP-A into centromeres. Nat Cell Biol. 2006 May;8(5):446-57. Epub 2006 Apr 16.

Okada M, Okawa K, Isobe T, Fukagawa T. CENP-H-containing complex facilitates centromere deposition of CENP-A in cooperation with FACT and CHD1. Mol Biol Cell. 2009 Sep;20(18):3986-95. doi: 10.1091/mbc.E09-01-0065. Epub 2009 Jul 22.

Okada T, Ohzeki J, Nakano M, Yoda K, Brinkley WR, Larionov V, Masumoto H. CENP-B controls centromere formation depending on the chromatin context. Cell. 2007 Dec 28;131(7):1287-300.

Olsen, J.V., B. Macek, O. Lange, A. Makarov, S. Horning, and M. Mann. 2007. Higher-energy C-trap dissociation for peptide modification analysis. Nat.Methods. 4:709–712.

Olszak AM, van Essen D, Pereira AJ, Diehl S, Manke T, Maiato H, Saccani S, Heun P. Heterochromatin boundaries are hotspots for de novo kinetochore formation. Nat Cell Biol. 2011 Jun 19;13(7):799-808. doi: 10.1038/ncb2272.

Pak DT, Pflumm M, Chesnokov I, Huang DW, Kellum R, Marr J, Romanowski P, Botchan MR. Association of the origin recognition complex with heterochromatin and HP1 in higher eukaryotes. Cell. 1997 Oct 31;91(3):311-23.

Palmer DK, O'Day K, Trong HL, Charbonneau H, Margolis RL. Purification of the centromere-specific protein CENP-A and demonstration that it is a distinctive histone. Proc Natl Acad Sci U S A. 1991 May 1;88(9):3734-8.

Papamichos-Chronakis M, Watanabe S, Rando OJ, Peterson CL. Global regulation of H2A.Z localization by the INO80 chromatin-remodeling enzyme is essential for genome integrity. Cell. 2011 Jan 21;144(2):200-13. doi: 10.1016/j.cell.2010.12.021.

Papamichos-Chronakis M, Peterson CL. Chromatin and the genome integrity network. Nat Rev Genet. 2013 Jan;14(1):62-75. doi: 10.1038/nrg3345.

Partridge JF, Borgstrøm B, Allshire RC. Distinct protein interaction domains and protein spreading in a complex centromere. Genes Dev. 2000 Apr 1;14(7):783-91.

Perpelescu M, Nozaki N, Obuse C, Yang H, Yoda K. Active establishment of centromeric CENP-A chromatin by RSF complex. J Cell Biol. 2009 May 4;185(3):397-407. doi: 10.1083/jcb.200903088. Epub 2009 Apr 27.

Perpelescu M, Fukagawa T. The ABCs of CENPs. Chromosoma. 2011 Oct;120(5):425-46. doi: 10.1007/s00412-011-0330-0. Epub 2011 Jul 13.

Pesenti ME, Prumbaum D, Auckland P, Smith CM, Faesen AC, Petrovic A, Erent M, Maffini S, Pentakota S, Weir JR, Lin YC, Raunser S, McAinsh AD, Musacchio A. Reconstitution of a 26-Subunit Human Kinetochore Reveals Cooperative Microtubule Binding by CENP-OPQUR and NDC80. Mol Cell. 2018 Sep 20;71(6):923-939.e10. doi: 10.1016/j.molcel.2018.07.038. Epub 2018 Aug 30.

Petrovic A, Pasqualato S, Dube P, Krenn V, Santaguida S, Cittaro D, Monzani S, Massimiliano L, Keller J, Tarricone A, Maiolica A, Stark H, Musacchio A. The MIS12 complex is a protein interaction hub for outer kinetochore assembly. J Cell Biol. 2010 Sep 6;190(5):835-52. doi: 10.1083/jcb.201002070.

Pidoux AL, Allshire RC. Centromeres: getting a grip of chromosomes. Curr Opin Cell Biol. 2000 Jun;12(3):308-19.

Pidoux AL, Richardson W, Allshire RC. Sim4: a novel fission yeast kinetochore protein required for centromeric silencing and chromosome segregation. J Cell Biol. 2003 Apr 28;161(2):295-307.

Pidoux AL, Allshire RC. Kinetochore and heterochromatin domains of the fission yeast centromere. Chromosome Res. 2004;12(6):521-34.

Pidoux AL, Choi ES, Abbott JK, Liu X, Kagansky A, Castillo AG, Hamilton GL, Richardson W, Rappsilber J, He X, Allshire RC. Fission yeast Scm3: A CENP-A receptor required for integrity of subkinetochore chromatin. Mol Cell. 2009 Feb 13;33(3):299-311. doi: 10.1016/j.molcel.2009.01.019.

Pinsky BA, Tatsutani SY, Collins KA, Biggins S. An Mtw1 complex promotes kinetochore biorientation that is monitored by the Ipl1/Aurora protein kinase. Dev Cell. 2003 Nov;5(5):735-45.

Pommier Y, Sun Y, Huang SN, Nitiss JL. Roles of eukaryotic topoisomerases in transcription, replication and genomic stability. Nat Rev Mol Cell Biol. 2016 Nov;17(11):703-721. doi: 10.1038/nrm.2016.111. Epub 2016 Sep 21.

Prasad P, Ekwall K. New insights into how chromatin remodellers direct CENP-A to centromeres. EMBO J. 2011 May 18;30(10):1875-6. doi: 10.1038/emboj.2011.131.

Prasanth SG, Prasanth KV, Siddiqui K, Spector DL, Stillman B. Human Orc2 localizes to centrosomes, centromeres and heterochromatin during chromosome inheritance. EMBO J. 2004 Jul 7;23(13):2651-63. Epub 2004 Jun 24.

Prasanth SG, Shen Z, Prasanth KV, Stillman B. Human origin recognition complex is essential for HP1 binding to chromatin and heterochromatin organization. Proc Natl Acad Sci U S A. 2010 Aug 24;107(34):15093-8. doi: 10.1073/pnas.1009945107. Epub 2010 Aug 5.

Probst AV, Dunleavy E, Almouzni G. Epigenetic inheritance during the cell cycle. Nat Rev Mol Cell Biol. 2009 Mar;10(3):192-206. doi: 10.1038/nrm2640.

Przewloka MR, Venkei Z, Bolanos-Garcia VM, Debski J, Dadlez M, Glover DM. CENP-C is a structural platform for kinetochore assembly. Curr Biol. 2011 Mar 8;21(5):399-405. doi: 10.1016/j.cub.2011.02.005. Epub 2011 Feb 25.

Quenet D, Dalal Y (2014) A long non-coding RNA is required for targeting centromeric protein A to the human centromere. eLife 3:e03254.

Rago F, Gascoigne KE, Cheeseman IM. Distinct organization and regulation of the outer kinetochore KMN network downstream of CENP-C and CENP-T. Curr Biol. 2015 Mar 2;25(5):671-7. doi: 10.1016/j.cub.2015.01.059. Epub 2015 Feb 5.

Ranjitkar P, Press MO, Yi X, Baker R, MacCoss MJ, Biggins S. An E3 ubiquitin ligase prevents ectopic localization of the centromeric histone H3 variant via the centromere targeting domain. Mol Cell. 2010 Nov 12;40(3):455-64. doi: 10.1016/j.molcel.2010.09.025.

Ray-Gallet D, Woolfe A, Vassias I, Pellentz C, Lacoste N, Puri A, Schultz DC, Pchelintsev NA, Adams PD, Jansen LE, Almouzni G. Dynamics of histone H3 deposition in vivo reveal a nucleosome gap-filling mechanism for H3.3 to maintain chromatin integrity. Mol Cell. 2011 Dec 23;44(6):928-41. doi: 10.1016/j.molcel.2011.12.006

Rischitor PE, May KM, Hardwick KG. Bub1 is a fission yeast kinetochore scaffold protein, and is sufficient to recruit other spindle checkpoint proteins to ectopic sites on chromosomes. PLoS One. 2007 Dec 19;2(12):e1342.

Rosic S, Kohler F, Erhardt S (2014) Repetitive centromeric satellite RNA is essential for kinetochore formation and cell division. J Cell Biol 207(3):335–349. doi: 10.1083/jcb.201404097

Saffery R, Sumer H, Hassan S, Wong LH, Craig JM, Todokoro K, Anderson M, Stafford A, Choo KH. Transcription within a functional human centromere. Mol Cell. 2003 Aug;12(2):509-16

Saitoh H, Tomkiel J, Cooke CA, Ratrie H 3rd, Maurer M, Rothfield NF, Earnshaw WC. CENP-C, an autoantigen in scleroderma, is a component of the human inner kinetochore plate. Cell. 1992 Jul 10;70(1):115-25.

Saitoh S, Takahashi K, Yanagida M. Mis6, a fission yeast inner centromere protein, acts during G1/S and forms specialized chromatin required for equal segregation. Cell. 1997 Jul 11;90(1):131-43.

Sanchez JP, Murakami Y, Huberman JA, Hurwitz J. Isolation, characterization, and molecular cloning of a protein (Abp2) that binds to a Schizosaccharomyces pombe origin of replication (ars3002). Mol Cell Biol. 1998 Mar;18(3):1670-81.

Sasaki T, Gilbert DM. The many faces of the origin recognition complex. Curr Opin Cell Biol. 2007 Jun;19(3):337-43. Epub 2007 Apr 26.

Sathyan KM, Fachinetti D, Foltz DR α-amino trimethylation of CENP-A by NRMT is required for full recruitment of the centromere. Nat Commun. 2017 Mar 7;8:14678. doi: 10.1038/ncomms14678.

Sato H, Masuda F, Takayama Y, Takahashi K, Saitoh S. Epigenetic inactivation and subsequent heterochromatinization of a centromere stabilize dicentric chromosomes. Curr Biol. 2012 Apr 24;22(8):658-67. doi: 10.1016/j.cub.2012.02.062. Epub 2012 Mar 29.

Schuh M, Lehner CF, Heidmann S. Incorporation of Drosophila CID/CENP-A and CENP-C into centromeres during early embryonic anaphase. Curr Biol. 2007 Feb 6;17(3):237-43. Epub 2007 Jan 11.

Schwanhäusser B, Busse D, Li N, Dittmar G, Schuchhardt J, Wolf J, Chen W, Selbach M.2011. Global quantification of mammalian gene expression control. Nature. 2011 May 19;473(7347):337-42.

Scott KC, Merrett SL, Willard HF. A heterochromatin barrier partitions the fission yeast centromere into discrete chromatin domains. Curr Biol. 2006 Jan 24;16(2):119-29.

Scott KC, Sullivan BA. Neocentromeres: a place for everything and everything in its place. Trends Genet. 2014 Feb;30(2):66-74. doi: 10.1016/j.tig.2013.11.003. Epub 2013 Dec 13.

Screpanti E, De Antoni A, Alushin GM, Petrovic A, Melis T, Nogales E, Musacchio A. Direct binding of Cenp-C to the Mis12 complex joins the inner and outer kinetochore. Curr Biol. 2011 Mar 8;21(5):391-8. doi: 10.1016/j.cub.2010.12.039. Epub 2011 Feb 25.

Shang WH, Hori T, Toyoda A, Kato J, Popendorf K, Sakakibara Y, Fujiyama A, Fukagawa T. Chickens possess centromeres with both extended tandem repeats and short non-tandem-repetitive sequences. Genome Res. 2010 Sep;20(9):1219-28. doi: 10.1101/gr.106245.110. Epub 2010 Jun 9.

Shelby RD, Monier K, Sullivan KF. Chromatin assembly at kinetochores is uncoupled from DNA replication. J Cell Biol. 2000 Nov 27;151(5):1113-8.

Shen X, Mizuguchi G, Hamiche A, Wu C. A chromatin remodelling complex involved in transcription and DNA processing. Nature. 2000 Aug 3;406(6795):541-4.

Shen X, Ranallo R, Choi E, Wu C. Involvement of actin-related proteins in ATP-dependent chromatin remodeling. Mol Cell. 2003 Jul;12(1):147-55.

Shevchenko A, Roguev A, Schaft D, Buchanan L, Habermann B, Sakalar C, Thomas H, Krogan NJ, Shevchenko A, Stewart AF. Chromatin Central: towards the comparative proteome by accurate mapping of the yeast proteomic environment. Genome Biol. 2008;9(11):R167. doi: 10.1186/gb-2008-9-11-r167. Epub 2008 Nov 28.

Shin JA, Choi ES, Kim HS, Ho JC, Watts FZ, Park SD, Jang YK. SUMO modification is involved in the maintenance of heterochromatin stability in fission yeast.Mol Cell. 2005 Sep 16;19(6):817-28.

Shiroiwa Y, Hayashi T, Fujita Y, Villar-Briones A, Ikai N, Takeda K, Ebe M, Yanagida M. Mis17 is a regulatory module of the Mis6-Mal2-Sim4 centromere complex that is required for the recruitment of CenH3/CENP-A in fission yeast. PLoS One. 2011 Mar 21;6(3):e17761. doi: 10.1371/journal.pone.0017761.

Shukla, M., Tong, P., White, S.A., Singh, P.P., Reid, A.M., Catania, S., Pidoux, A.L., andAllshire, R.C. Centromeric DNA destabilizes H3 nucleosomes to promote CENP-Adeposition during the cell cycle. bioRxiv. 2017 doi: https://doi.org/10.1101/215624

Silva MC, Bodor DL, Stellfox ME, Martins NM, Hochegger H, Foltz DR, Jansen LE. Cdk activity couples epigenetic centromere inheritance to cell cycle progression.

Sinz A, Arlt C, Chorev D, Sharon M. Chemical cross-linking and native mass spectrometry: A fruitful combination for structural biology. Protein Sci. 2015 Aug;24(8):1193-209. doi: 10.1002/pro.2696. Epub 2015 May 27.

Spence JM, Fournier RE, Oshimura M, Regnier V, Farr CJ. Topoisomerase II cleavage activity within the human D11Z1 and DXZ1 alpha-satellite arrays. Chromosome Res. 2005;13(6):637-48. Epub 2005 Sep 21.

Spencer F, Gerring SL, Connelly C, Hieter P. Mitotic chromosome transmission fidelity mutants in Saccharomyces cerevisiae. Genetics. 1990 Feb;124(2):237-49.

Srivastava S, Foltz DR. Posttranslational modifications of CENP-A: marks of distinction. Chromosoma. 2018 Mar 22. doi: 10.1007/s00412-018-0665-x. [Epub ahead of print]

Srivastava S, Zasadzińska E, Foltz DR. Posttranslational mechanisms controlling centromere function and assembly. Curr Opin Cell Biol. 2018 Jun;52:126-135. doi: 10.1016/j.ceb.2018.03.003. Epub 2018 Apr 2.

Steiner FA, Henikoff S. Diversity in the organization of centromeric chromatin. Curr Opin Genet Dev. 2015 Apr;31:28-35. doi: 10.1016/j.gde.2015.03.010. Epub 2015 May 16.

Steiner NC, Clarke L. A novel epigenetic effect can alter centromere function in fission yeast. Cell. 1994 Dec 2;79(5):865-74.

Stoler S, Keith KC, Curnick KE, Fitzgerald-Hayes M. A mutation in CSE4, an essential gene encoding a novel chromatin-associated protein in yeast, causes chromosome nondisjunction and cell cycle arrest at mitosis. Genes Dev. 1995 Mar 1;9(5):573-86.

Strålfors A, Walfridsson J, Bhuiyan H, Ekwall K. The FUN30 chromatin remodeler, Fft3, protects centromeric and subtelomeric domains from euchromatin formation. PLoS Genet. 2011 Mar;7(3):e1001334. doi: 10.1371/journal.pgen.1001334. Epub 2011 Mar 17.

Subramanian L, Toda NR, Rappsilber J, Allshire RC. Eic1 links Mis18 with the CCAN/Mis6/Ctf19 complex to promote CENP-A assembly. Open Biol. 2014 Apr 30;4:140043. doi: 10.1098/rsob.140043.

Sugata N, Li S, Earnshaw WC, Yen TJ, Yoda K, Masumoto H, Munekata E, Warburton PE, Todokoro K. Human CENP-H multimers colocalize with CENP-A and CENP-C at active centromere--kinetochore complexes. Hum Mol Genet. 2000 Nov 22;9(19):2919-26.

Sugimoto K, Yata H, Muro Y, Himeno M. Human centromere protein C (CENP-C) is a DNA-binding protein which possesses a novel DNA-binding motif. J Biochem. 1994 Oct;116(4):877-81.

Suh KS, Tanaka T, Sarojini S, Nightingale G, Gharbaran R, Pecora A, Goy A. The role of the ubiquitin proteasome system in lymphoma. Crit Rev Oncol Hematol. 2013 Sep;87(3):306-22. doi: 10.1016/j.critrevonc.2013.02.005. Epub 2013 Mar 27.

Sullivan KF, Hechenberger M, Masri K. Human CENP-A contains a histone H3 related histone fold domain that is required for targeting to the centromere. J Cell Biol. 1994 Nov;127(3):581-92.

Sullivan KF. A solid foundation: functional specialization of centromeric chromatin. Curr Opin Genet Dev. 2001 Apr;11(2):182-8.

Sullivan B, Karpen G. Centromere identity in Drosophila is not determined in vivo by replication timing. J Cell Biol. 2001 Aug 20;154(4):683-90.

Sun X, Wahlstrom J, Karpen G. Molecular structure of a functional Drosophila centromere. Cell. 1997 Dec 26;91(7):1007-19.

Suzuki A, Badger BL, Salmon ED. A quantitative description of Ndc80 complex linkage to human kinetochores. Nat Commun. 2015 Sep 8;6:8161. doi: 10.1038/ncomms9161.

Svensson JP, Shukla M, Menendez-Benito V, Norman-Axelsson U, Audergon P, Sinha I, Tanny JC, Allshire RC, Ekwall K. A nucleosome turnover map reveals that the stability of histone H4 Lys20 methylation depends on histone recycling in transcribed chromatin. Genome Res. 2015 Jun;25(6):872-83. doi: 10.1101/gr.188870.114. Epub 2015 Mar 16.

Swaney DL, Wenger CD, Coon JJ. Value of using multiple proteases for large-scale mass spectrometry-based proteomics. J Proteome Res. 2010 Mar 5;9(3):1323-9. doi: 10.1021/pr900863u.

Szklarczyk D, Morris JH, Cook H, Kuhn M, Wyder S, Simonovic M, Santos A, Doncheva NT, Roth A, Bork P, Jensen LJ, von Mering C. The STRING database in 2017: quality-controlled protein-protein association networks, made broadly accessible. Nucleic Acids Res. 2017 Jan 4;45(D1):D362-D368. doi: 10.1093/nar/gkw937. Epub 2016 Oct 18.

Tachiwana H, Müller S, Blümer J, Klare K, Musacchio A, Almouzni G. HJURP involvement in de novo CenH3(CENP-A) and CENP-C recruitment. Cell Rep. 2015 Apr 7;11(1):22-32. doi: 10.1016/j.celrep.2015.03.013. Epub 2015 Apr 2.

Takada M, Zhang W, Suzuki A, Kuroda TS, Yu Z, Inuzuka H, Gao D, Wan L, Zhuang M, Hu L, Zhai B, Fry CJ, Bloom K, Li G, Karpen GH, Wei W, Zhang Q. FBW7 Loss Promotes Chromosomal Instability and Tumorigenesis via Cyclin E1/CDK2-Mediated Phosphorylation of CENP-A. Cancer Res. 2017 Sep 15;77(18):4881-4893. doi: 10.1158/0008-5472.CAN-17-1240. Epub 2017 Jul 31.

Takahashi K, Murakami S, Chikashige Y, Niwa O, Yanagida M. A large number of tRNA genes are symmetrically located in fission yeast centromeres. J Mol Biol. 1991 Mar 5;218(1):13-7.

Takahashi K, Yamada H, Yanagida M. Fission yeast minichromosome loss mutants mis cause lethal aneuploidy and replication abnormality. Mol Biol Cell. 1994 Oct;5(10):1145-58.

Takahashi K, Chen ES, Yanagida M. Requirement of Mis6 centromere connector for localizing a CENP-A-like protein in fission yeast. Science. 2000 Jun 23;288(5474):2215-9.

Takayama Y, Shirai M, Masuda F. Characterisation of functional domains in fission yeast Ams2 that are required for core histone gene transcription. Sci Rep. 2016 Nov 30;6:38111. doi: 10.1038/srep38111.

Takeuchi K, Nishino T, Mayanagi K, Horikoshi N, Osakabe A, Tachiwana H, Hori T, Kurumizaka H, Fukagawa T. The centromeric nucleosome-like CENP-T-W-S-X complex induces positive supercoils into DNA. Nucleic Acids Res. 2014 Feb;42(3):1644-55. doi: 10.1093/nar/gkt1124. Epub 2013 Nov 14.

Tanaka K, Nishide J, Okazaki K, Kato H, Niwa O, Nakagawa T, Matsuda H, Kawamukai M, Murakami Y. Characterization of a fission yeast SUMO-1 homologue, pmt3p, required for multiple nuclear events, including the control of telomere length and chromosome segregation. Mol Cell Biol. 1999 Dec;19(12):8660-72.

Tanaka K, Chang HL, Kagami A, Watanabe Y. CENP-C functions as a scaffold for effectors with essential kinetochore functions in mitosis and meiosis. Dev Cell. 2009 Sep;17(3):334-43. doi: 10.1016/j.devcel.2009.08.004.

Tang MY, Guo H, Nguyen TT, Low LS, Jackson RA, Yamada T, Chen ES. Two fission yeast high mobility group box proteins in the maintenance of genomic integrity following doxorubicin insult. Gene. 2015 May 10;562(1):70-5. doi: 10.1016/j.gene.2015.02.041. Epub 2015 Feb 17.

Tange Y, Niwa O. Schizosaccharomyces pombe Bub3 is dispensable for mitotic arrest following perturbed spindle formation. Genetics. 2008 Jun;179(2):785-92. doi: 10.1534/genetics.107.081695. Epub 2008 May 27.

Tong P, Pidous AL, Toda NRT, Ard R, Berger H, Shukla M, Torres-Garcia J, Mueller CA, Nieduszynski CA and Allshire RC. Inter-species conservation of organisation and function between non-homologous regional centromeres. 2018. bioRxiv 309815; doi: https://doi.org/10.1101/309815

Topp CN, Zhong CX, Dawe RK. Centromere-encoded RNAs are integral components of the maize kinetochore. Proc Natl Acad Sci U S A. 2004 Nov 9;101(45):15986-91. Epub 2004 Oct 28.

Tornier C, Bessone S, Varlet I, Rudolph C, Darmon M, Fleck O. Requirement for Msh6, but not for Swi4 (Msh3), in Msh2-dependent repair of base-base mismatches and mononucleotide loops in Schizosaccharomyces pombe. Genetics. 2001 May;158(1):65-75.

Tosi A, Haas C, Herzog F, Gilmozzi A, Berninghausen O, Ungewickell C, Gerhold CB, Lakomek K, Aebersold R, Beckmann R, Hopfner KP. Structure and subunit topology of the INO80 chromatin remodeler and its nucleosome complex. Cell. 2013 Sep 12;154(6):1207-19. doi: 10.1016/j.cell.2013.08.016.

Trewick SC, Minc E, Antonelli R, Urano T, Allshire RC. The JmjC domain protein Epe1 prevents unregulated assembly and disassembly of heterochromatin. EMBO J. 2007 Nov 14;26(22):4670-82. Epub 2007 Oct 18.

Tyanova S, Temu T, Sinitcyn P, Carlson A, Hein MY, Geiger T, Mann M, Cox J. The Perseus computational platform for comprehensive analysis of (prote)omics data. Nat Methods. 2016 Sep;13(9):731-40. doi: 10.1038/nmeth.3901. Epub 2016 Jun 27.

Uemura T, Yanagida M. Isolation of type I and II DNA topoisomerase mutants from fission yeast: single and double mutants show different phenotypes in cell growth and chromatin. organization. EMBO J. 1984 Aug;3(8):1737-44.

Van Hooser AA, Ouspenski II, Gregson HC, Starr DA, Yen TJ, Goldberg ML, Yokomori K, Earnshaw WC, Sullivan KF, Brinkley BR. Specification of kinetochore-forming chromatin by the histone H3 variant CENP-A. J Cell Sci. 2001 Oct;114(Pt 19):3529-42.

Varshavsky A. Regulated protein degradation. Trends Biochem Sci. 2005 Jun;30(6):283-6.

Venkei Z, Przewloka MR, Glover DM. Drosophila Mis12 complex acts as a single functional unit essential for anaphase chromosome movement and a robust spindle assembly checkpoint. Genetics. 2011 Jan;187(1):131-40. doi: 10.1534/genetics.110.119628. Epub 2010 Oct 26.

Villahermosa D, Christensen O, Knapp K, Fleck O. Schizosaccharomyces pombe MutSα and MutLα Maintain Stability of Tetra-Nucleotide Repeats and Msh3 of Hepta-Nucleotide Repeats. G3 (Bethesda). 2017 May 5;7(5):1463-1473. doi: 10.1534/g3.117.040816

Vo TV, Das J, Meye MJ, Cordero NA, Akturk N, Wei X, Fair BJ, Degatano AG, Fragoza R, Liu LG, Matsuyama A, Trickey M, Horibata S, Grimson A, Yamano H, Yoshida M, Roth FP, Pleiss JA, Xia Y, Yu H. A Proteome-wide Fission Yeast Interactome Reveals Network Evolution Principles from Yeasts to Human. Cell. 2016 Jan 14;164(1-2):310-323. doi: 10.1016/j.cell.2015.11.037.

Volpe TA, Kidner C, Hall IM, Teng G, Grewal SI, Martienssen RA. Regulation of heterochromatic silencing and histone H3 lysine-9 methylation by RNAi. Science. 2002 Sep 13;297(5588):1833-7. Epub 2002 Aug 22.

Voullaire LE, Slater HR, Petrovic V, Choo KH. A functional marker centromere with no detectable alpha-satellite, satellite III, or CENP-B protein: activation of a latent centromere? Am J Hum Genet. 1993 Jun;52(6):1153-63.

Wade CM, Giulotto E, Sigurdsson S, Zoli M, Gnerre S, Imsland F, Lear TL, Adelson DL, Bailey E, Bellone RR, Blöcker H, Distl O, Edgar RC, Garber M, Leeb T, Mauceli E, MacLeod JN, Penedo MC, Raison JM, Sharpe T, Vogel J, Andersson L, Antczak DF, Biagi T, Binns MM, Chowdhary BP, Coleman SJ, Della Valle G, Fryc S, Guérin G, Hasegawa T, Hill EW, Jurka J, Kiialainen A, Lindgren G, Liu J, Magnani E, Mickelson JR, Murray J, Nergadze SG, Onofrio R, Pedroni S, Piras MF, Raudsepp T, Rocchi M, Røed KH, Ryder OA, Searle S, Skow L, Swinburne JE, Syvänen AC, Tozaki T, Valberg SJ, Vaudin M, White JR, Zody MC; Broad Institute Genome Sequencing Platform; Broad Institute Whole Genome Assembly Team, Lander ES, Lindblad-Toh K. Genome sequence, comparative analysis, and population genetics of the domestic horse. Science. 2009 Nov 6;326(5954):865-7. doi: 10.1126/science.1178158.

Walfridsson J, Bjerling P, Thalen M, Yoo EJ, Park SD, Ekwall K. The CHD remodeling factor Hrp1 stimulates CENP-A loading to centromeres. Nucleic Acids Res. 2005 May 20;33(9):2868-79. Print 2005

Wang J, Tadeo X, Hou H, Tu PG, Thompson J, Yates JR 3rd, Jia S. Epe1 recruits BET family bromodomain protein Bdf2 to establish heterochromatin boundaries. Genes Dev. 2013 Sep 1;27(17):1886-902. doi: 10.1101/gad.221010.113.

Warburton PE, Cooke CA, Bourassa S, Vafa O, Sullivan BA, Stetten G, Gimelli G, Warburton D, Tyler-Smith C, Sullivan KF, Poirier GG, Earnshaw WC. Immunolocalization of CENP-A suggests a distinct nucleosome structure at the inner kinetochore plate of active centromeres. Curr Biol. 1997 Nov 1;7(11):901-4.

Weir JR, Faesen AC, Klare K, Petrovic A, Basilico F, Fischböck J, Pentakota S, Keller J, Pesenti ME, Pan D, Vogt D, Wohlgemuth S, Herzog F, Musacchio A. Insights from biochemical reconstitution into the architecture of human kinetochores. Nature. 2016 Sep 8;537(7619):249-253. doi: 10.1038/nature19333. Epub 2016 Aug 31.

Westermann S, Drubin DG, Barnes G. Structures and functions of yeast kinetochore complexes. Annu Rev Biochem. 2007;76:563-91.

Westhorpe FG, Straight AF. The centromere: epigenetic control of chromosome segregation during mitosis. Cold Spring Harb Perspect Biol. 2014 Nov 20;7(1):a015818. doi: 10.1101/cshperspect.a015818.

Williams JS, Hayashi T, Yanagida M, Russell P. Fission yeast Scm3 mediates stable assembly of Cnp1/CENP-A into centromeric chromatin. Mol Cell. 2009 Feb 13;33(3):287-98. doi: 10.1016/j.molcel.2009.01.017.

Winkler GS, Kristjuhan A, Erdjument-Bromage H, Tempst P, Svejstrup JQ. Elongator is a histone H3 and H4 acetyltransferase important for normal histone acetylation levels in vivo. Proc Natl Acad Sci U S A. 2002 Mar 19;99(6):3517-22.

Wisniewski J, Hajj B, Chen J, Mizuguchi G, Xiao H, Wei D, Dahan M, Wu C. Imaging the fate of histone Cse4 reveals de novo replacement in S phase and subsequent stable residence at centromeres. Elife. 2014 May 20;3:e02203. doi: 10.7554/eLife.02203.

Wisniewski, J. R., Zougman, A., Nagaraj, N., & Mann, M. (2009). Universal sample preparation method for proteome analysis. Nature Methods, 6(5), 359-362.

Woodcock CL, Ghosh RP. Chromatin higher-order structure and dynamics. Cold Spring Harb Perspect Biol. 2010 May;2(5):a000596. doi: 10.1101/cshperspect.a000596. Epub 2010 Apr 7.

Xu YM, Du JY, Lau AT. Posttranslational modifications of human histone H3: an update. Proteomics. 2014 Sep;14(17-18):2047-60. doi: 10.1002/pmic.201300435. Epub 2014 Aug 8

Yamagishi Y, Sakuno T, Goto Y, Watanabe Y. Kinetochore composition and its function: lessons from yeasts. FEMS Microbiol Rev. 2014 Mar;38(2):185-200.

Yang CH, Tomkiel J, Saitoh H, Johnson DH, Earnshaw WC. Identification of overlapping DNA-binding and centromere-targeting domains in the human kinetochore protein CENP-C. Mol Cell Biol. 1996 Jul;16(7):3576-86.

Young MM, Tang N, Hempel JC, Oshiro CM, Taylor EW, Kuntz ID, Gibson BW, Dollinger G. High throughput protein fold identification by using experimental constraints derived from intramolecular cross-links and mass spectrometry. Proc Natl Acad Sci U S A. 2000 May 23;97(11):5802-6.

Yu Y, Ren JY, Zhang JM, Suo F, Fang XF, Wu F, Du LL. A proteome-wide visual screen identifies fission yeast proteins localizing to DNA double-strand breaks. DNA Repair (Amst). 2013 Jun 1;12(6):433-43. doi: 10.1016/j.dnarep.2013.04.001. Epub 2013 Apr 28.

Yu Z, Zhou X, Wang W, Deng W, Fang J, Hu H, Wang Z, Li S, Cui L, Shen J, Zhai L, Peng S, Wong J, Dong S, Yuan Z, Ou G, Zhang X, Xu P, Lou J, Yang N, Chen P, Xu RM, Li G. Dynamic phosphorylation of CENP-A at Ser68 orchestrates its cell-cycle-dependent deposition at centromeres. Dev Cell. 2015 Jan 12;32(1):68-81. doi: 10.1016/j.devcel.2014.11.030. Epub 2014 Dec 31.

Yuen KW, Nabeshima K, Oegema K, Desai A. Rapid de novo centromere formation occurs independently of heterochromatin protein 1 in C. elegans embryos. Curr Biol. 2011 Nov 8;21(21):1800-7. doi: 10.1016/j.cub.2011.09.016. Epub 2011 Oct 20.

Zeitlin SG, Shelby RD, Sullivan KF. CENP-A is phosphorylated by Aurora B kinase and plays an unexpected role in completion of cytokinesis. J Cell Biol. 2001 Dec 24;155(7):1147-57. Epub 2001 Dec 24.

Zhu P, Li G. Higher-order structure of the 30-nm chromatin fiber revealed by cryo-EM. IUBMB Life. 2016 Nov;68(11):873-878. doi: 10.1002/iub.1568. Epub 2016 Oct 5.

Appendix 1: List if 199 proteins showing their enrichment in GFP-CENP-A^{Cnp1} chromatin relative to untagged and histone H3 control.

Protein IDs	-LOG$_2$(P-value) (cnp1/ untagged)	Difference (cnp1/ untagged)	-LOG$_{10}$(P-value) (cnp1/ H3)	Difference (cnp1/H3)
SPAC25B8.14|mal2|I|kinetochore	5.74	12.14	3.42	5.93
SPAC1783.03|fta2|I|kinetochore	5.99	11.72	3.69	6.36
SPBP22H7.09c|mis15|II|kinetochore	5.7	11.66	3.56	6.73
SPAC1687.20c|mis6|I|kinetochore	4.18	11.48	2.05	6.1
SPBC800.13|cnp20|II|histone	5.75	11.41	3.8	6.92
SPCC1393.04|fta4|III|Mis6-Sim4	5.71	11.09	3.35	5.08
SPBC21.01|mis17|II|kinetochore	5.82	10.99	3.24	6.73
SPBC18E5.03c|sim4|II|kinetochore	5.65	10.98	3.38	6
SPBC1703.14c|top1|II|DNA	4.97	10.9	0.2	0.38
SPAC23H4.11c|cnl2|I|centromere	4.42	10.5	3.43	6.2
SPCC1919.14c|bdp1|III|transcription	6.06	10.3	1.23	3.01
SPCC1235.07|fta7|III|kinetochore	6.25	10.03	3.35	5.08
SPBC2D10.16|mhf1|II|kinetochore	5.66	10.01	2.36	5.21
SPBP8B7.12c|fta3|II|kinetochore	5.06	9.89	3.24	5.43
SPBC1861.01c|cnp3|II|kinetochore	4.89	9.81	2.56	7.7
SPAC4F10.12|fta1|I|kinetochore	5.24	9.79	3.19	5.35
SPBP8B7.19|spt16|II|FACT	6.11	9.78	1.43	2.19
SPBC557.03c|pim1|II|RCC1	3.29	9.59	-	-
SPCC548.05c|dbl5|III|	5.14	9.52	0.68	1.07
SPAC31G5.19|abo1|I|ATPase	5.31	9.37	0.37	-0.49
SPBC1105.17|cnp1|II|	2.09	9.17	3.29	7.36
SPBC609.05|pob3|II|FACT	6.8	9.16	1.34	2.19
SPAC1F7.01c|spt6|I|nucleosome	6.85	9.06	2.77	-2.07
SPAC17G8.15|wip1|I|Cenp-W	5.97	9.04	2.51	3.01
SPAC16A10.05c|dad1|I|DASH	4.42	8.89	1.86	3.6
SPAC664.01c|swi6|I|HP1	4.78	8.87	3.23	5.77
SPBC13E7.10c|brf1|II|transcription	5.71	8.57	1.35	2.43
SPAC29E6.08|tbp1|I|TATA-binding	3.94	8.5	0.03	-0.06
SPBP23A10.13|orc4|II|origin	3.9	8.46	2.8	-0.83
SPCC576.12c|mhf2|III|kinetochore	4.83	8.45	2.25	3.15
SPAPB1E7.10|rpc17|I|DNA-directed	4.52	8.27	0.36	0.79
SPCC330.01c|rhp16|III|Rad16	5.24	8.25	0.04	0.2
SPCC290.02|rpc34|III|DNA-directed	4.73	8.19	-	-
SPBC1A4.03c|top2|II|DNA	4.14	8.06	1.22	-1.51
SPAC25B8.20|SPAC25B8.20|I|	4.6	7.66	0.68	2.27
SPAC23E2.02|lsd2|I|histone	3.88	7.59	2.4	2.99
SPAC6B12.05c|ies2|I|Ino80	3.83	7.47	2.01	-1.53
SPBC146.09c|lsd1|II|histone	4.46	7.42	2.79	2.83
SPAC664.02c|arp8|I|actin-like	2.77	7.3	0.93	-0.7
SPCC18.07|rpc53|III|DNA-directed	3.77	7.22	1.51	2.7
SPBP22H7.05c|abo2|II|ATPase	3.29	7.16	-	-
SPCC622.08c|hta1|III|histone	6.23	7.12	-	-

SPBC336.07|sfc3|II|transcription	2.76	7.01	0.98	2.3
SPAC11H11.05c|fta6|I|Mis6-Sim4	4.12	6.82	1.3	2.31
SPBC839.12|rpc31|II|DNA-directed	3.59	6.8	0.53	0.83
SPAC10F6.08c|nht1|I|Ino80	1.91	6.8	-	-
SPBC29A10.15|orc1|II|origin	2.84	6.74	0.15	0.51
SPAC23G3.04|ies4|I|Ino80	3.57	6.4	1.13	-0.76
SPAC222.04c|ies6|I|Ino80	3.41	6.34	0.98	-0.72
SPAC2F7.07c|cph2|I|Clr6	4.1	6.28	-	-
SPAC29B12.01|ino80|I|SNF2	3.29	6.27	1.49	-1.04
SPAC23C11.15|pst2|I|Clr6	4.05	6.26	2.25	-4.96
SPBC2A9.07c|hpz1|II|zf-PARP	4.21	6.25	0.44	0.72
SPBC365.10|arp5|II|actin-like	3.15	6.14	1.13	-0.78
SPAC1783.05|hrp1|I|ATP-dependent	3.18	6.12	0.03	0.01
SPBC365.06|pmt3|II|SUMO	5.51	6.12	2.57	2.9
SPBC11C11.03|ndc80|II|NMS	2.24	6.02	0.26	0.81
SPAPB1E7.03|rpc82|I|DNA-directed	4.31	6	0.97	1.66
SPAC16C9.05|cph1|I|Clr6	3.88	5.94	1.36	-5.67
SPCC553.11c|toa2|III|transcription	4.72	5.91	0.17	-0.23
SPBC646.14c|orc5|II|origin	2.71	5.9	0.46	-0.48
SPBC8D2.07c|sfc9|II|transcription	3.14	5.88	1.18	1.94
SPAC17G8.03c|dpb3|I|DNA	2.25	5.86	0.39	-0.67
SPAC3H1.01c|orc3|I|origin	2.81	5.85	0.87	-0.58
SPBC651.08c|rpc1|II|DNA-directed	4.05	5.84	0.87	1.26
SPBC947.12|kms2|II|spindle	3.49	5.75	-	-
SPBC28F2.11|hmo1|II|HMG	1.86	5.64	-	-
SPCC330.02|rhp7|III|Rad7	2.98	5.62	0.5	1.1
SPAPB1E7.14|iec5|I|Ino80	1.93	5.61	0.79	-0.98
SPAC23H4.12|alp13|I|MRG	3.7	5.58	2.5	-4.18
SPCC16C4.14c|sfc4|III|transcription	2.34	5.54	0.55	1.27
SPCC4G3.07c|phf1|III|PHD	3.26	5.46	2.72	2.75
SPBC685.09|orc2|II|origin	2.58	5.37	0.47	-1.55
SPAC30D11.08c|phf2|I|Lsd1/2	3.69	5.34	2.7	2.54
SPBC31F10.14c|hip3|II|HIRA	1.99	5.33	2.82	-6.95
SPCC126.02c|pku70|III|Ku	4.45	5.23	-	-
SPCC1322.12c|bub1|III|mitotic	2.1	5.21	0.56	-1.03
SPCC1020.04c|rpb6|III|DNA-directed	2.96	5.19	0.61	1.22
SPAC6G9.06c|pcp1|I|pericentrin	1.27	5.18	-	-
SPCC330.13|rpc37|III|DNA-directed	4.42	5.16	0.72	1.05
SPBC947.08c|hip4|II|histone	2.22	5.15	-	-
SPBC2G5.07c|rpc25|II|DNA-directed	2.25	5.11	0.89	1.3
SPAC27F1.04c|nuf2|I|NMS	2.1	5.11	0.04	0.05
SPBC30D10.02|ncb2|II|transcription	2.42	5.1	0.12	-0.28
SPCC285.16c|msh6|III|MutS	2.92	5.08	1.64	1.66
SPBC21H7.05|sfc6|II|transcription	2.01	5.07	0.13	0.42
SPBC19C7.09c|uve1|II|endonuclease	2.8	5.06	0.46	2.29
SPBC19C2.03|rpc10|II|DNA-directed	2.96	5.03	1.41	2.7
SPBC543.03c|pku80|II|Ku	4.23	5.01	0.65	-1.69
SPBC31F10.13c|hip1|II|hira	2	5.01	2.86	-5.96

SPBC2A9.12|orc6|II|origin	2.42	4.98	0.17	-0.2
SPAC22H12.02|tfg3|I|transcription	5.71	4.9	1.7	-1.22
SPCC417.07c|mto1|III|MT	1.52	4.83	-	-
SPBP23A10.08|alp5|II|actin-like	3.3	4.79	1.15	-0.85
SPAC1783.07c|pap1|I|transcription	2.85	4.78	0.16	-0.17
SPAC22A12.05|rpc11|I|DNA-directed	2.93	4.77	1.41	2.7
SPAC6F12.11c|sfc1|I|transcription	2.29	4.75	0.62	1.53
SPCC16C4.20c|hap2|III|HMG	1.55	4.74	1.32	1.89
SPCC1672.02c|sap1|III|	2.42	4.69	0.6	-1.44
SPBC11B10.10c|pht1|II|histone	2.56	4.67	3.3	-2.13
SPAC4H3.11c|ppc89|I|spindle	1.18	4.65	-	-
SPCC1020.02|spc7|III|NMS	1.41	4.65	0.16	0.28
SPBC409.09c|mis13|II|NMS	1.92	4.64	0.24	-0.85
SPAC17G8.13c|mst2|I|histone	3.46	4.58	3.62	-5.26
SPBC83.03c|tas3|II|RITS	2.15	4.57	-	-
SPCC188.04c|spc25|III|NMS	1.46	4.56	-	-
SPAC23H3.08c|bub3|I|mitotic	3.08	4.52	0.39	-0.77
SPCC622.16c|epe1|III|Jmjc	2.5	4.43	-	-
SPBC577.15c|sim3|II|NASP	1.84	4.43	3.8	-2.62
SPAC6G9.03c|mug183|I|histone	3.64	4.42	2.01	-1.68
SPAC144.02|iec1|I|Ino80	1.83	4.32	0.8	-0.87
SPAC4G9.08c|rpc2|I|DNA-directed	3.52	4.25	0.9	1.28
SPBC15D4.03|slm9|II|hira	2.11	4.24	3.01	1.12
SPAC3G6.01|hrp3|I|ATP-dependent	3.08	4.18	1.05	-0.63
SPBC29A10.04|psm1|II|mitotic	1.76	4.12	0.15	-0.56
SPAC688.02c|mis14|I|NMS	1.46	4.1	-	-
SPBC83.08|rvb2|II|AAA	3.56	4.09	0.96	-0.68
SPAC18G6.02c|chp1|I|chromodomain	1.47	4.08	0.99	1.09
SPCC1259.04|iec3|III|Ino80	1.73	4.08	1.1	-1.14
SPBC336.08|spc24|II|NMS	1.83	4.07	-	-
SPAPB17E12.06|sos7|I|NMS	1.75	4.06	-	-
SPBC12D12.01|sad1|II|spindle	1.14	3.95	5.33	3
SPCC1450.02|bdf1|III|Swr1	2.7	3.95	1.83	-2.17
SPAPB8E5.09|rvb1|I|AAA	3.45	3.95	0.99	-0.7
SPAPYUG7.04c|rpb9|I|DNA-directed	2.34	3.8	0.2	-0.64
SPBC3H7.18|tam8|II|	2	3.8	-	-
SPCC338.17c|rad21|III|mitotic	1.76	3.76	-	-
SPBC244.01c|sid4|II|SIN	0.92	3.72	-	-
SPAC2E12.02|hsf1|I|transcription	2.47	3.68	0.72	-1.76
SPAC29E6.04|nnf1|I|NMS	1.58	3.66	-	-
SPAC1687.01|rpc19|I|DNA-directed	2.9	3.59	0.41	0.92
SPBC409.04c|mis12|II|NMS	1.67	3.58	-	-
SPCC24B10.22|pog1|III|	2.24	3.57	-	-
SPCC970.12|mis18|III|kinetochore	2.14	3.54	-	-
SPBC685.08|SPBC685.08|II|	3.85	3.53	-	-
SPAC4A8.05c|myp2|I|myosin	1.01	3.51	-	-
SPCC1682.04|cdc31|III|centrin	1.02	3.51	-	-
SPBC649.05|cut12|II|spindle	1.13	3.5	-	-

SPCC285.17|spp27|III|RNA	1.8	3.48	0.02	0.04
SPBC428.20c|alp6|II|gamma	1.14	3.47	-	-
SPBC1289.07c|rpc40|II|DNA-directed	3.65	3.45	0.39	0.51
SPBC1861.07|SPBC1861.07|II|	2.82	3.43	0.21	0.33
SPAC23C4.15|rpb5|I|DNA-directed	4.48	3.41	0.27	-0.34
SPAC23D3.01|pdp3|I|PWWP	2.33	3.34	3.41	-8.11
SPAPB1A10.02|scm3|I|CENP-A	3.25	3.31	-	-
SPACUNK4.06c|rpb7|I|DNA-directed	4.91	3.28	1.12	-1.24
SPBC28F2.09|toa1|II|transcription	3.46	3.14	-	-
SPBC582.05c|brc1|II|BRCT	1.05	3.09	0.07	-0.15
SPBC14C8.12|rpb8|II|DNA-directed	2.95	3.08	0.22	-0.29
SPAC1250.07|sfc7|I|TFIIIC	2.04	3.08	-	-
SPBC1685.08|cti6|II|histone	1.98	3.06	-	-
SPBC19G7.01c|msh2|II|MutS	2.93	3	1.79	1.84
SPAC4D7.07c|csi2|I|mitotic	1.17	2.94	-	-
SPAC6F6.09|eaf6|I|Mst2/NuA4	2.03	2.88	3.73	-4.09
SPAC1B3.12c|rpb10|I|DNA-directed	3.18	2.83	0.02	-0.02
SPCC1739.11c|cdc11|III|SIN	0.66	2.83	-	-
SPAC10F6.09c|psm3|I|mitotic	2.27	2.79	0.02	0.06
SPBC4B4.03|rsc1|II|RSC	1.75	2.78	0.44	-0.15
SPAC3A12.07|rpb11|I|RNA	3.39	2.77	0.71	-2.66
SPBC8D2.05c|sfi1|II|spindle	0.97	2.75	3.64	-6.92
SPAC823.14|ptf1|I|Mst2	1.83	2.74	-	-
SPBC28F2.12|rpb1|II|RNA	4.67	2.74	2.06	-1.76
SPBC27B12.02|mis19|II|centromere	2.39	2.72	-	-
SPBC16A3.19|eaf7|II|histone	1.85	2.71	3.27	-5.47
SPBC337.14|rpb4|II|DNA-directed	4.38	2.7	1.56	-1.53
SPAC1F3.07c|rsc58|I|RSC	1.88	2.67	0.33	-0.1
SPCC550.12|arp6|III|actin-like	1.01	2.66	1.92	-2.51
SPBC32F12.04|gtb1|II|gamma-tubulin	1.42	2.65	1.98	1.67
SPBC4.04c|mcm2|II|MCM	1.47	2.64	0.36	-0.68
SPBC1703.02|rsc9|II|RSC	1.84	2.63	0.63	0.16
SPAC110.02|pds5|I|mitotic	1.5	2.57	-	-
SPAC15E1.05c|ect1|I|	0.85	2.57	0.25	1.12
SPAC1250.01|snf21|I|ATP-dependent	1.71	2.53	0.28	-0.09
SPBC27B12.11c|pho7|II|transcription	2.53	2.52	-	-
SPBC1734.15|rsc4|II|RSC	1.71	2.51	0.2	-0.08
SPCC1281.05|rsc7|III|RSC	1.68	2.49	0.12	-0.05
SPAC17G8.07|yaf9|I|YEATS	1.52	2.48	3.1	-1.8
SPAC8C9.14|prr1|I|transcription	1.29	2.44	0.01	0.03
SPCC16A11.14|sfh1|III|RSC	1.65	2.41	0.36	-0.14
SPAC23H3.10|ssr2|I|SWI/SNF	1.89	2.39	0.04	-0.02
SPAC637.12c|mst1|I|KAT5	1.55	2.39	1.5	-3.86
SPAC23G3.01|rpb2|I|RNA	4.68	2.37	2.05	-1.65
SPAC1805.08|dlc1|I|dynein	1.75	2.37	-	-
SPBC36.05c|clr6|II|histone	3.13	2.34	1.87	-3.99
SPAC23D3.09|arp42|I|SWI/SNF	1.44	2.33	0.1	0.05
SPAC1071.06|arp9|I|SWI/SNF	1.61	2.31	0.38	-0.12

SPCC1442.10c|rpb3|III|RNA	3.85	2.28	1.79	-1.9
SPAC26H5.12|rpo41|I|mitochondrial	1.13	2.27	-	-
SPAC23G3.10c|ssr3|I|SWI/SNF	1.61	2.24	0.01	0.01
SPBP23A10.05|ssr4|II|SWI/SNF	1.58	2.23	0.31	0.1
SPAC29A4.18|prw1|I|Clr6	2.48	2.22	2.49	-3.57
SPAPB24D3.01|toe3|I|transcription	1.51	2.13	-	-
SPCC965.10|SPCC965.10|III|	2.17	2.1	-	-
SPCC1393.06c|ipi1|III|rRNA	1.47	2.06	1.56	1.3
SPBC3E7.02c|hsp16|II|heat	1.58	2.06	0.45	-3.66
SPAC17G6.10|ssr1|I|SWI/SNF	1.55	2.05	0.32	-0.09
SPBC19G7.16|iws1|II|transcription	3.83	2.05	2.29	-1.87
SPBC16G5.13|ptf2|II|Mst2	2.28	2.02	4.23	-5.57
SPCC1393.02c|spt2|III|non-specific	3.79	1.92	-	-